



HAL
open science

Evaluation of physico-chemical properties of biorefinery-derived amphiphilic molecules and their effects on multi-scale biological models

Biao Lu

► **To cite this version:**

Biao Lu. Evaluation of physico-chemical properties of biorefinery-derived amphiphilic molecules and their effects on multi-scale biological models. Biomechanics [physics.med-ph]. Université de Technologie de Compiègne, 2015. English. NNT : 2015COMP2218 . tel-01299523

HAL Id: tel-01299523

<https://theses.hal.science/tel-01299523v1>

Submitted on 7 Apr 2016

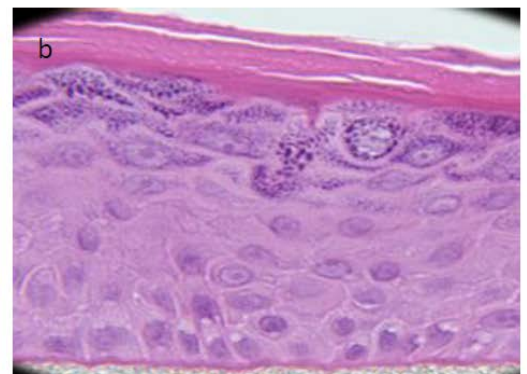
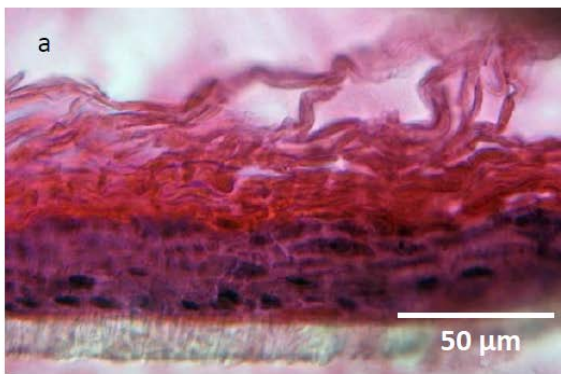
HAL is a multi-disciplinary open access archive for the deposit and dissemination of scientific research documents, whether they are published or not. The documents may come from teaching and research institutions in France or abroad, or from public or private research centers.

L'archive ouverte pluridisciplinaire **HAL**, est destinée au dépôt et à la diffusion de documents scientifiques de niveau recherche, publiés ou non, émanant des établissements d'enseignement et de recherche français ou étrangers, des laboratoires publics ou privés.

Par **Biao LU**

Évaluation of physico-chemical properties of biorefinery-derived amphiphilic molecules and their effects on multi-scale biological models

Thèse présentée
pour l'obtention du grade
de Docteur de l'UTC



Soutenue le 16 octobre 2015
Spécialité : Biomécanique, Bio-ingénierie

D2218



Université de Technologie de Compiègne

Ecole Doctorale

Laboratoire Biomécanique et Bioingénierie, UMR CNRS 7388
Laboratoire Transformations Intégrées de la Matière Renouvelable, EA 4297

Thèse par **Biao Lu**

En vue de l'obtention du grade de

Docteur de L'Université de Technologie de Compiègne

**Evaluation of Physico-chemical Properties of
Biorefinery-derived Amphiphilic Molecules and
Their Effects on Multi-scale Biological Models**

Vendredi 16 Octobre 2015

Composition du jury

Mme. Sophie Gangloff	Professeur, Université de Reims Champagne-Ardenne
M. Vladimir Hlady	Professeur, University of Utah
Mme. Anne Wadouachi	Professeur, Université de Picardie Jules Verne
M. Hervé Ficheux	Docteur, THOR Personal Care SAS
M. André Pauss	Professeur, Université de Technologie de Compiègne
Mme. Muriel Vayssade	Professeur, Université de Technologie de Compiègne
Mme. Isabelle Pezron	Professeur, Université de Technologie de Compiègne
M. Christophe Egles	Professeur, Université de Technologie de Compiègne

Acknowledgements

This PhD work was performed, in partnership with the **SAS PIVERT**, within the frame of the French Institute for the Energy Transition (Institut pour la Transition Energétique (ITE) P.I.V.E.R.T. (www.institut-pivert.com) selected as an Investment for the Future (“Investissements d’Avenir”). This work was supported, as part of the Investments for the Future, by the French Government under the reference ANR-001-01. In the meantime, **Chinese Scholarship Council** provided final support for my PhD grant during my study in UTC. I would like to thank them all.

I would like to express my sincere appreciation to jury members of the thesis, who have agreed to bring their knowledgeable judgements to the work. Thanks to my reviewers: Professor **Vladimir Hlady** and Professor **Sophie Gangloff** for your work of reviewing the manuscript. I thank Professor **Anne Wadouachi**, Professor **André Pauss** and Doctor **Hervé Ficheux** for examining my thesis.

It is with immense gratitude that I acknowledge my supervisors: Professor **Muriel Vayssade**, Professor **Isabelle Pezron** and Professor **Christophe Egles**. Without your guidance and support, it would have been impossible to complete this thesis. Muriel, you welcomed me on my first day entering the C2B (Cellules Biomatériaux Bioréacteur) team, BMBI (Biomécanique et Bioingénierie) laboratory. You taught me all the basic experimental skills with great patience and led me to explore the domain of cells related biological analysis. I have learned a lot from your meticulous attitude to knowledge, which has become valuable asset for my future career. Isabelle, during my 5 years stay in UTC, you were always there to help me as responsible person of my master studies and my PhD supervisor, both personally and scientifically. In IMID (Interfaces et Milieux Divisés) team, TIMR (Transformations Intégrées de la Matière Renouvelable) laboratory, I developed my knowledge under your instruction. You encouraged me and kindled my enthusiasm to further step into the multidisciplinary research area of physico-chemical and biological analysis. Thank you for all of these. Christophe, I am so honored and happy to be your PhD student. You always managed to make time from your very busy schedule and discuss with me, giving me suggestions and teaching me how to do research. Your optimism and humorous (although sometimes I didn’t get it) made my stay in C2B team a very pleasant experience.

The work presented in the thesis was completed with the help of many people. The program was realized in partnership with Laboratoire LG2A, Université de Picardie Jules Verne. **Yong Miao**, **Vincent Chagnault**, **Eric Grand**, **Anne Wadouachi** and **Denis Postel** have provided synthesized molecules for tests and we exchanged ideas regularly for the advance of program. Analysis work on the SAXS platform was performed by **Mélanie Emo** and **Marie-José Stébé** from the Laboratoire SRSMC, Université de Lorraine. I hereby thank you for your contributions. Besides, I am indebted to my colleagues who supported me during the period. **Pascale Vigneron** and **Vanessa Bleicher**, without you I could not even commence my work. You know everything about our laboratory! You were always so patient whenever I came to you to demand assistance, your experiences and knowledge are indispensable part of my successful experiments. **Jean-Luc Duval**, I really cherish the time I spent in laboratory with you, thank

you for your many magical tiny tools and your instructions, they helped me a lot. **Julie Follet**, you were there to support me of my first year PhD, your advices were fruitful for my research as well as career developments. There are still many other people who helped with my thesis but I didn't manage to mention here, I owe my deepest gratitude to all of you.

Working in C2B team and IMID teams gave me the chances to meet various outstanding fellows and students. For those that are not mentioned above, I would like to list your names here. We shared happiness moments together and supported each other, working with you was such an unforgettable experience. These names include but not limited to: **Guillaume Vidal, Tony Dinis, Laetitia Nowacki, Laura Rotellini, Kamélia Ghazi-Naiji, Olfat Gsib, Kayla Belanger, Florian Lombart and Huiling Lu...**

I also want to thank my old friends, either in France or in China: **Bing Meng, Bin Gao, Shaojuan Huang, Ming Li, Bihao Wang, Kang Yang...** for helping me to overcome any obstacles during this period.

Most importantly, none of this would have been possible without the support from my family. My mother **Aizhen Yang**, my father **Jiangming Lu** and my older brother **Xun Lu**. For all the 27 years, I have been surrounded by your endless love. You were standing by my side for any achievement that I may have accomplished. You supported me for every decision that I made no matter how hard it was for you to understand. I would like to express my heart-felt gratitude to you!

Contents

Abstract	7
Abbreviations.....	8
List of Figures	9
List of Tables	13
General Introduction.....	15
Chapter I: Scientific Context	17
A) General introduction of surfactants.....	19
1. Definition and classification of surfactants.....	19
2. Surface-active properties of surfactants.....	20
3. Critical Micellar Concentration (CMC)	21
4. Krafft point.....	23
5. Hydrophilic-Lipophilic Balance (HLB)	25
6. Surfactant applications	26
7. Marketing.....	29
8. Sugar-based surfactants.....	32
B) Surfactants and human health.....	37
1. Possible hazard to human health.....	37
2. Skin irritation — an important endpoint to assess surfactant toxicity	40
3. Cytotoxicity.....	47
4. <i>In vitro</i> models for skin related cytotoxicity or irritation tests	56
C) Objectives.....	63
Chapter II: Materials and Methods	65
A) Materials	67
B) Sugar-based surfactants and their physico-chemical properties, pre-selection of surfactants for biological tests	69
1. Synthesis of sugar-based surfactants.....	69
2. Selection of standard surfactants	73
3. HLB of surfactants	74

4.	Solubility of surfactants.....	74
5.	Measurement of Krafft point	75
6.	Surface active properties of surfactants	76
7.	Adsorption of surfactant molecules at air/water interface	77
8.	Determination of Critical Micellar Concentrations (CMC)	77
9.	Self-assembling properties of surfactants	79
C)	Establishment of cell/ tissue models and cytotoxicity/ irritancy tests	81
1.	Cells/ tissues used in tests.....	81
2.	2D cell models	81
3.	3D cell model.....	84
4.	3D tissue model.....	86
5.	Statistical analysis	91
Chapter III: Results and Discussions		93
A)	Reception of synthesized molecules.....	95
B)	Physico-chemical properties of surfactants.....	97
1.	HLB of synthesized and standard surfactants	97
2.	Preliminary tests – estimation of water solubility of surfactants from batch 1 and their ability to lower surface tension of water.....	98
3.	Solubility of standard surfactants and pre-selected surfactants in batch 2	100
4.	Comparison between batch 1 and batch 2	101
5.	Krafft point determination.....	101
6.	Surface-active properties of surfactants and their CMCs in water.....	102
9.	Surface tensions of surfactants in complete DMEM without Fetal Bovine Serum	110
10.	Surface tensions of surfactants in complete DMEM (with Fetal Bovine Serum)	111
C)	Cytotoxic/ irritant effects of synthesized surfactants on multi-scale cell/ tissue models.....	115
1.	Selection of 2D cell culture models for cytotoxicity tests.....	115
2.	Influence of surfactant on cell morphology in Model 2 (monolayer model).....	116
3.	Cytotoxicity of surfactants on monolayer cell culture models	118
4.	Establishment and characterization of L929 cells in 3D cell culture model.....	124
5.	Cytotoxicity of surfactants on 3D cell culture models	125
6.	Morphology of 3D tissue model: Reconstituted Human Epidermis	132

7. Cytotoxicity of surfactants on EpiDerm™ tissues	135
8. Irritancy potential of surfactants tested on EpiDerm™ tissue	137
9. Number of proliferating keratinocytes in EpiDerm™ tissues after exposure to surfactants	138
D) Physico-chemical properties/ Chemical structures of surfactants and their cytotoxicity	143
1. Relationship between CMC and cytotoxicity	143
2. Influence of structural features	144
Conclusions and Perspectives	151
References	155
Appendix.....	175

Abstract

Evaluation of Physico-chemical Properties of Biorefinery-derived Amphiphilic Molecules and Their Effects on Multi-scale Biological Models

Nowadays, a wide variety of new molecules can derive from biomass. Among them, the family of sugar-based surfactants, which are considered as alternatives to fossil-based surfactants, due to their relatively high biodegradability and biocompatibility, exhibit interesting properties both in terms of their self-assembly and their ability to induce biological responses. In the study, for the purpose to analyse these properties, different methodologies have been established. In this work, physico-chemistry and cellular biology methodologies are associated to analyse the properties of pre-selected molecules characterized by gradual structure modifications.

Firstly, we have screened synthesized sugar-based surfactants according to their solubility and their ability to reduce surface tension of water. Four pre-selected molecules, with a C8 chain linked to a glucose or maltose head through an amide functional group, either under the form of carbamoyl (carbohydrate scaffold bearing the carbonyl) or alkylcarboxamide (the alkyl chain bearing the carbonyl), were then dissolved in water/ cell culture media for surface tension measurements. Their behaviors in solutions were characterized by Krafft points, Critical Micellar Concentrations or self-assembling properties through different methods.

To evaluate the cytotoxic/ irritant effects of these molecules on cells and tissues, 3 *in-vitro* models were established: I) 2D cell culture model (L929 cell monolayer) II) 3D cell culture model (L929 cells embedded in collagen gel) and III) Reconstituted human epidermis (differentiated human keratinocytes). Corresponding experiments were carried out on these models with increasing complexity.

Results show that the synthesized sugar-based surfactants, Glu1amideC8, Glu6amideC8, Glu6amideC8' and Mal1amideC8 can reduce the surface tension of water solution to the same level as standard surfactants (Tween 20 and Hecameg). In the meantime, Glu1amideC8, Glu6amideC8' and Mal1amideC8 present less cytotoxicity effects on L929 cells both in the monolayer model and the 3D model than Tween 20 and Hecameg. All synthesized and standard surfactants (Glu1amideC8, Glu6amideC8, Gu6amideC8', Mal1amideC8, Tween 20 and Hecameg) have no significant cytotoxic/ irritant effects on reconstituted human epidermis at 1000 µg/mL after 48 h of topical application. Discussions have been made according to the results of experiments to establish possible structures/ physico-chemical properties – cytotoxicity relationships of these surfactants.

Abbreviations

APG: Alkyl Polyglycoside

CMC: Critical Micellar Concentration

CTAB: Cetyltrimethylammonium Bromide

DAPI: 4',6-diamidino-2-phenylindole

RHE: Reconstituted Human Epidermis

DMEM: Dulbecco's Modified Eagle's Medium

DSC: Differential Scanning Calorimeter

ECM: Extracellular Matrix

EdU: 5-ethynyl-2'-deoxyuridine

ELISA: Enzyme Linked Immunosorbent Assay

FBS: Fetal Bovine Serum

HBSS: Hank's Balanced Salt Solution

HLB: Hydrophile-Lipophile Balance

IL-1 α : Interleukin 1 α

LDH: Lactate Dehydrogenase

MEM: Modified Eagle Medium

MTS: 3-(4,5-dimethylthiazol-2-yl)-5-(3-carboxymethoxyphenyl)-2-(4-sulfophenyl)-2H tetrazolium

NRU: Neutral Red Uptake

PBS: Phosphate-Buffered Saline

RHE: Reconstituted Human Epidermis

SAXS: Small angle X-Ray scattering

SDS: Sodium Dodecyl Sulfate

List of Figures

Figure 1: Schematic of a surfactant molecule.	19
Figure 2: Schematic of forces on molecules in air-water system.	21
Figure 3: Schematic of surfactant molecules absorbed at air-water interface.	21
Figure 4: Geometrical shapes of surfactant micelles in aqueous solutions.	22
Figure 5: Schematic representation of the concentration dependence of some physico-chemical properties for solutions of a micelle-forming surfactant.	22
Figure 6: Phase diagram close to the Krafft point.	24
Figure 7: Some important, high impact areas of surfactant applications.	27
Figure 8: World surfactant consumption by region %.	29
Figure 9: Surfactants production EU 1994-2013.	30
Figure 10: Global surfactant market: end-user-wise.	31
Figure 11: Bio-surfactant market projection.	32
Figure 12: Examples for the most frequent linkages between the hydrophilic and the hydrophobic moiety in sugar surfactants.	33
Figure 13: Structure of alkyl polyglycoside.	33
Figure 14: Human skin diagram.	41
Figure 15: Structure of epidermis.	42
Figure 16: Skin irritation induced by surfactants.	45
Figure 17: Sequence of events after application of skin irritan.	46
Figure 18: Anatomy of animal cell.	48
Figure 19: Schema of human cell cycle.	50
Figure 20: Structure changes of cells undergoing apoptosis or necrosis.	52
Figure 21: Schema of macro-autophagy process.	53
Figure 22: Schematic representation of the sequence of events arising on exposure of a bio-membrane to increasing amounts of surfactant.	55

of the micelle.	109
Figure 44: a) Experimental SAXS spectrum of 50 g/L Hecameg in water at 25°C, b) Pair-distance distribution function obtained by GIFT analysis showing the characteristic dimensions of the micelle.	110
Figure 45: Surface tensions of surfactant in water and in complete DMEM (no FBS)	110
Figure 46: Surface tensions of surfactant in complete DMEM and in complete DMEM (no FBS)	112
Figure 47: Displacement of macromolecule by small surfactant molecule at fixed concentration of macromolecule	114
Figure 48: Proliferative index of L929 cells cultured in Model 1 and Model 2 treated with Tween 20 for 48 h (Model 1: Tween 20 was added right after seeding of cells; Model 2: Tween 20 was added after 24 h of cell culture in spread cells), results were normalized according to cell culture models without treatment.	116
Figure 49: Morphology of L929 cells cultured in Model 2 (monolayer model) treated with surfactants for 48 h.	117
Figure 50: Normalized proliferative index and metabolic activity of L929 cells cultured in monolayer model for 24 h and then treated with synthesized surfactants for 48 h.....	119
Figure 51: Normalized proliferative index and metabolic activity of L929 cells cultured in monolayer model for 24 h and then treated with standard surfactants for 48 h	121
Figure 52: H&E stained paraffin section of L929 cells cultured in 3D cell culture model.	124
Figure 53: Normalized proliferative index and metabolic activity of L929 cells cultured for 96 h in 3D cell culture model and then treated with synthesized surfactants for 48 h	125
Figure 54: Normalized proliferative index and metabolic activity of L929 cells cultured for 96 h in 3D cell culture model and then treated with standard surfactants for 48 h.....	127
Figure 55: L929 cell growth curve in 3D cell culture model	132
Figure 56: a) H&E stained paraffin section of EpiDerm™ tissue model after conditioning and 48 h of PBS treatment (negative control); b) cross-section of EpiDerm™ tissue model provided by MATTEK (no available scale).....	133
Figure 57: Hematoxylin and Eosin staining of paraffin section of EpiDerm™ tissues treated with PBS or surfactants in PBS solutions (48h).	134
Figure 58: Metabolic activity of human keratinocyte in EpiDerm™ tissue treated with 30 µL PBS or 30 µL surfactant in PBS solutions	136
Figure 59: IL-1α concentration in culture medium for EpiDerm™ tissue treated with topical	

exposure of 30 μ L PBS or 30 μ L surfactant in PBS solutions	138
Figure 60: EdU-DAPI co-staining of cryostat section of EpiDerm™ tissues treated with surfactants (48h).....	140
Figure 61: Linear relationship between IC50s and CMCs of observed for tested surfactants in 2D cell culture model	144
Figure 62: Structure of Glu6amideC8 and Glu6amideC8'	145
Figure 63: Structure of Octyl glucuronate and Glucose octanoate	145
Figure 64: Structure of Alkyl-D-glucopyranosides and their analog Alkl galactopyranosides. Their corresponding EC50s.....	147
Figure 65: Structure of PEO-ester surfactants.....	148
Figure 66: Structure of Glu1amidec8 and Mal1amideC8.....	148
Figure 67: Structures of hydrocarbon alkyl β -D-xylopyranoside	149
Figure 68: Structures of perfluorinated carboxylic acids	149

List of Tables

Table 1: Classification of surfactants	20
Table 2: Some common CMC methods	23
Table 3: Surfactants' properties classified by their HLB	25
Table 4: HLB group number to be used in HLB equation of Davies.....	26
Table 5: Functions of the skin.....	43
Table 6: Eukaryotic cell organelles and their functions.....	49
Table 7: Reconstituted human epidermis by different companies and research groups.....	61
Table 8: Materials used in experiments and their origins.	67
Table 9: Families of synthesized glycolipids.....	70
Table 10: Structures of synthesized surfactants with C8 hydrocarbon chain.....	95
Table 11: Structures of synthesized surfactants with C10 hydrocarbon chain.....	96
Table 12: HLB values of synthesized and standards surfactant calculated by Griffin's method.....	97
Table 13: solubility synthesized surfactants and minimum surface tension of saturated surfactant water solutions (room temperature).	99
Table 14: a) solubility of synthesized molecules from batch 2 and b) solubility of standard surfactants.....	100
Table 15: CMCs of surfactants determined by surface tension measurement.	104
Table 16: CMC of surfactant in water solution determined by surface tension and dye solubilization, T=37°C.	107
Table 17: Calculated surface excess concentration and surface area occupied by molecule.	107
Table 18: IC50 of surfactant against L929 cells determined by cell proliferative index or cell metabolic activity in monolayer model.....	122
Table 19: Cell viability after 24 h of growth followed by 48 h of surfactant treatment and their corresponding proliferative index in 2D cell culture model.	122
Table 20: Non-normalized cell proliferative index after 24 h of growth and then 48 h of surfactant treatment in 2D cell culture models.	123

Table 21: Comparison of cytotoxicity of surfactants against L929 cells culture in 2D and 3D models.	128
Table 22: Cell viability after 96 h of growth followed by 48 h of surfactant treatment and their corresponding proliferative index in 3D cell culture model.	130
Table 23: Non-normalized cell proliferative index after 96 h of growth and then 48 h of surfactant treatment in 3D cell culture models.	131
Table 24: Highest surfactant concentrations used in different models and corresponding cell metabolic activity.	136
Table 25: Amount of proliferating cells in basal layer of EpiDerm™ tissues treated with surfactants.	141
Table 26: CMCs in complete DMEM solutions and IC50s against L929 cells culture in 2D models of surfactants.	143

General Introduction

Take into account of limited fossil resources, increasing price of petroleum-based products and increasing environmental impact of human activities, it is necessary to reconsider our current economic model based on the exclusive exploitation of oil resources. It was under this circumstance that the ITE P.I.V.E.R.T. project (Picardie Plant Innovations Teaching and Technological Research) was funded by the French Government in 2011 within the context of “Programme Investissements d’Avenir”. The main purpose of the project is to develop a renewable chemistry, using agricultural raw materials to substitute to fossil-based ones and apply the products in applications like food and health ingredients, active molecules and primary products for cosmetics, new polymers, building materials...

Within the ITE P.I.V.E.R.T. project, the precompetitive research program GENESYS aims at determining the fundamentals of the oilseed biorefinery of the future, more precisely, the production, fractionation and transformation and the delivery of industrial bio-products. The GENESYS program is divided into 7 work packages. My thesis work was carried out within the AMPHISKIN project of the work package 5: “Structure/ functionality relationships and formulation of biomolecules”. Objectives of the work are to establish the link between the new biomolecules and their use and find out new formulation based on biomolecules or products produced by biorefinery.

Among the new molecules obtained from work packages 3 (catalysis and biocatalysis) and 4 (microbial production of lipids and derivatives) of GENESYS program, the family of sugar-based molecules, mostly surfactants, which can be synthesized from natural resources, presents interesting properties. More specifically, some sugar-based surfactants have been reported to have higher biodegradability and biocompatibility compared to petroleum derived surfactants. They also possess self-assembling properties and can induce interesting biological responses. Therefore, these sugar-based surfactants are excellent candidates as alternatives to currently-used commercially available surfactants. Considering their great potential in various sectors and corresponding economic benefits, research work to enrich current knowledge about the synthesis, characterization and applications of these types of surfactants is becoming increasingly important.

In this context, several goals and strategies have been defined for my thesis work.

1) Screening of synthesized sugar-based surfactants with tailor-made structures.

Different molecules, containing a hydrocarbon chain linked to a glucose or maltose head through an amide functional group have been synthesized. Several factors can influence their structures (the number of glucose units in the hydrophilic head group, the orientation of amide linker between head group and tail, the chain length of hydrophobic tail and the position on linker on sugar unit). Preliminary tests were firstly carried out on these molecules to identify sugar-based surfactants with relatively higher solubility and stronger surface-active

properties. Pre-selected sugar-based surfactants were then used for more in-depth tests.

II) Characterization of physico-chemical properties of synthesized surfactants.

Physico-chemical properties of surfactants are essential for their applications. Therefore, we have evaluated the ability of surfactants to reduce surface tension in solutions with water. Their Critical Micellar Concentration, Krafft points and self-assembling properties were also measured. Since these sugar-based surfactants were to be tested in biological models, their behaviors in cell culture media have also been investigated by surface tension methods.

III) Cytotoxic/ irritant effects of sugar-based surfactants on multi-scale biological models.

Surfactants are widely used in our daily lives. Direct contacts between human and surfactants-derived products are inevitable. Therefore, the potential hazard of sugar-based surfactants on human skin needs to be evaluated. To this aim, we have developed three *in vitro* models with increasing complexity (2D cell model: L929 cells monolayer, 3D cell model: L929 cells embedded in collagen gel, 3D tissue model: reconstituted human epidermis with human keratinocytes). Different cytotoxicity and irritancy tests were carried out on the 3 models and the potential hazard induced by synthesized sugar-based surfactants were discussed.

IV) Relationship between structure of sugar-surfactants and their cytotoxicity.

Results from experiments and from other researchers have been compared to interpret the structure-cytotoxicity relationship of synthesized surfactants. As preliminary conclusions, these relationships can be used to guide the synthesis of new sugar-based surfactants with desired properties.

The first part of this dissertation presents the scientific context of surfactants and their potential hazard to human health. Then, we described the methodologies used to evaluate the physico-chemical properties and cytotoxicity/ irritancy of surfactants. Later on, the results of experiments are presented and discussed. Finally, several synthesized sugar-based surfactants, characterized by gradual structure modifications, and standard surfactants are compared. Conclusions are drawn and perspectives are proposed in the end of the dissertation.

Chapter I: Scientific Context

A) General introduction of surfactants

1. Definition and classification of surfactants

A surfactant (or surface-active molecule) is an organic compound including in its structure at least one lyophilic (affinity with solvent) and one lyophobic (no affinity with solvent) group. (Figure 1).

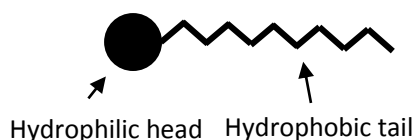


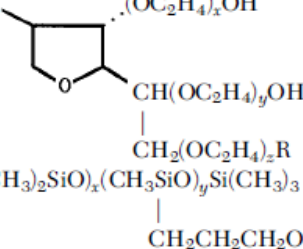
Figure 1: Schematic of a surfactant molecule (solvent: water).

Since the hydrophobic tails of most surfactants consisting of one or several hydrocarbon chains are similar to each other, surfactants are classified into 4 types according to the nature of their head group: anionic surfactant, cationic surfactant, non-ionic surfactant and zwitterionic surfactant (Table 1):

- I) Anionic surfactants contain anionic functional groups at their head such as sulfate, sulfonate, phosphate and carboxylate.
- II) Cationic surfactants usually have primary, secondary, tertiary or quaternary ammonium as the polar ends which are positively charged.
- III) Non-ionic surfactant usually includes highly polar (non-charged) moiety like polyglucoside, polyoxyethylene, acetylenic or polyol groups, its relatively high solubility is a result of affinity between its polar groups and water.
- IV) Zwitterionic (amphoteric) surfactant's head is composed both by a positive and a negative group such as amine oxide, betaine and aminocarboxylates (Farn, R.J. 2008).

It should be noticed that the charge of some surfactants can change according to pH of their solutions. Some zwitterionic surfactant with a primary, secondary or tertiary ammonium will change from net cationic to zwitterionic and finally to net anionic as the pH increased. For example, surfactant like N-alkyl derivatives of simple amino acids ($\text{NH}_2\text{CH}_2\text{COOH}$) and aminopropionic acid ($\text{NH}_2\text{CH}_2\text{CH}_2\text{COOH}$), at the isoelectric point, both charged groups will be fully ionized and the molecule will have properties similar to non-ionic surfactants. As the pH shifts away from the isoelectric point, the molecule will gradually assume the properties of either a cationic or anionic surfactant (Attwood, D., & Florence, A. T. 2012).

Table 1: Classification of surfactants (Shramm, L.L. 2000).

Class	Examples	Structures
Anionic	Na stearate Na dodecyl sulfate Na dodecyl benzene sulfonate	$\text{CH}_3(\text{CH}_2)_{16}\text{COO}^- \text{Na}^+$ $\text{CH}_3(\text{CH}_2)_{11}\text{SO}_4^- \text{Na}^+$ $\text{CH}_3(\text{CH}_2)_{11}\text{C}_6\text{H}_4\text{SO}_3^- \text{Na}^+$
Cationic	Laurylamine hydrochloride Trimethyl dodecylammonium chloride Cetyl trimethylammonium bromide	$\text{CH}_3(\text{CH}_2)_{11}\text{NH}_3^+ \text{Cl}^-$ $\text{C}_{12}\text{H}_{25}\text{N}^+(\text{CH}_3)_3 \text{Cl}^-$ $\text{CH}_3(\text{CH}_2)_{15}\text{N}^+(\text{CH}_3)_3 \text{Br}^-$
Nonionic	Polyoxyethylene alcohol Alkylphenol ethoxylate Polysorbate 80 $w + x + y + z = 20$, $\text{R} = (\text{C}_{17}\text{H}_{33})\text{COO}$	$\text{C}_n\text{H}_{2n+1}(\text{OCH}_2\text{CH}_2)_m\text{OH}$ $\text{C}_9\text{H}_{19}-\text{C}_6\text{H}_4-(\text{OCH}_2\text{CH}_2)_n\text{OH}$ $\text{HO}(\text{C}_2\text{H}_4\text{O})_w$ 
Zwitterionic	Propylene oxide-modified polymethylsiloxane EO = ethyleneoxy PO = propyleneoxy Dodecyl betaine Lauramidopropyl betaine Cocoamido-2-hydroxy-propyl sulfobetaine	$(\text{CH}_3)_3\text{SiO}((\text{CH}_3)_2\text{SiO})_x(\text{CH}_3\text{SiO})_y\text{Si}(\text{CH}_3)_3$ $\text{C}_{12}\text{H}_{25}\text{N}^+(\text{CH}_3)_2\text{CH}_2\text{COO}^-$ $\text{C}_{11}\text{H}_{23}\text{CONH}(\text{CH}_2)_3\text{N}^+(\text{CH}_3)_2\text{CH}_2\text{COO}^-$ $\text{C}_n\text{H}_{2n+1}\text{CONH}(\text{CH}_2)_3\text{N}^+(\text{CH}_3)_2\text{CH}_2\text{CH}(\text{OH})\text{CH}_2\text{SO}_3^-$

2. Surface-active properties of surfactants

The ability of surfactant to reduce the surface tension of its solvent or interfacial tension between two phases is defined as surface-active property. In a two phases system (water-air system for example), the attractive forces that water molecules exert on one another at the bulk and at surface regions are not equal. As can be seen from Figure 2, a water molecule in the bulk is pulled in every direction which results in a zero net force. However, if it is located at air-water interface, the water molecule will be pulled solely inwards due to lack of forces from exterior. The attraction force created here drives the liquid surface to contract towards interior and is termed as surface tension γ_0 , the unit of surface tension is N/m. Alternatively, surface tension can also be defined as the minimum amount of work (W_{min}) required to create new unit area of the interface (ΔA), so $W_{min} = \gamma_0 \times \Delta A$, where the unit of γ_0 is J/m² (Eastoe, J. 2002).

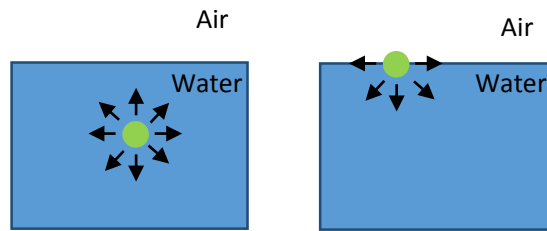


Figure 2: Schematic of forces on molecules in air-water system.

When surfactant molecules are dissolved in water, they tend to migrate to the water-air interface as a result of their amphiphilic properties (Figure 3). To maintain a minimal potential energy of water-air system, hydrophilic head of surfactant molecule stays in water, whereas its hydrophobic tail stretches into air due to its affinity to non-polar phase and limit its contact with water. Adsorption of surfactant molecules at interface can reduce the surface tension of solution (γ). The surface pressure is defined as $\pi = \gamma_0 - \gamma$, γ_0 is the surface tension of pure water (Eastoe, J. 2002).

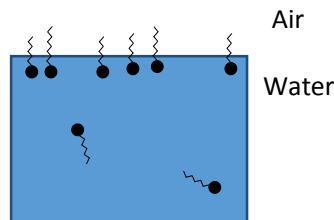


Figure 3: Schematic of surfactant molecules absorbed at air-water interface.

3. Critical Micellar Concentration (CMC)

The surface tension of solution decreases with addition of surfactant since they will automatically adsorb at the water-air interface. When the concentration of surfactant molecules at interface reaches a certain value, the energy required to insert more surfactant molecules into this monolayer will be higher than the energy for surfactant molecules to form “micelles” in the bulk solution. More precisely, with addition of surfactants, to minimize further free energy of the system, surfactant molecules will aggregate with their hydrophilic heads oriented towards water phase and form “micelles”. The spontaneous process to form micelles in surfactant solution is called micellization and this concentration is defined as Critical Micellar Concentration. In most cases, the shape of micelles are sphere. However, depending on the structure of surfactant molecules, solution composition, temperature and surfactant concentrations, micelles shapes can be spherical, rod-like, hexagonal, cubic or lamellar (Figure 4).

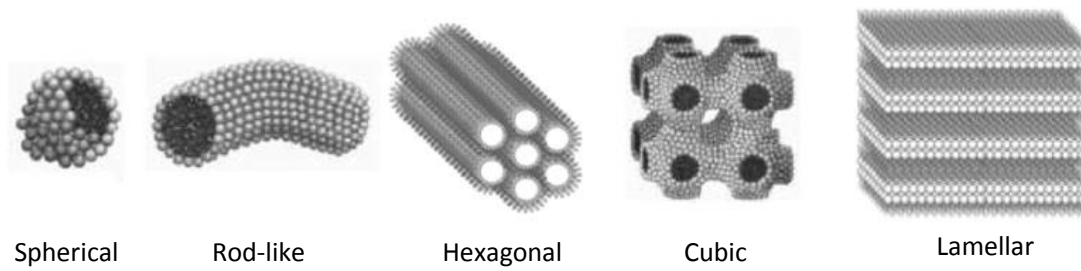


Figure 4: Geometrical shapes of surfactant micelles in aqueous solutions (Fayed, T. A. 2014).

CMC is a concentration where physico-chemical properties of surfactant solutions were found to change dramatically. These properties including self-diffusion coefficients, turbidity, conductance, surface tension, osmotic pressure etc... (Figure 5).

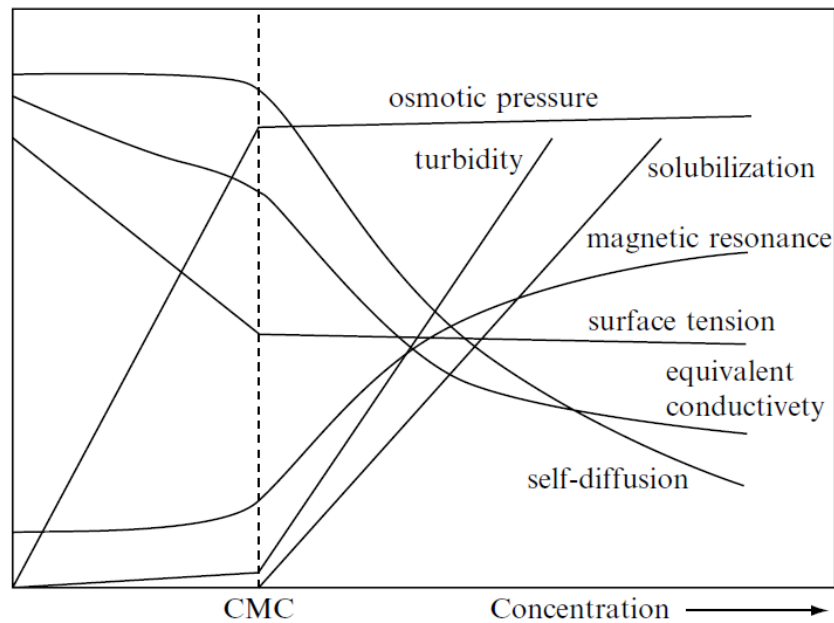


Figure 5: Schematic representation of the concentration dependence of some physico-chemical properties for solutions of a micelle-forming surfactant (Lindman, B., & Wennerström, H. 1980).

According to Figure 5, corresponding measurements can be used to determine the CMC of surfactant. Table 2 presents some common methods to determine CMC. By plotting the physico-chemical property against surfactant concentration, CMC value is obtained at the break point of curve. Values from those methods may be slightly different from each other, but for a single surfactant system, they are usually in good agreements and reliable (Mukerjee, p., & Mysels, K.J. 1971).

Table 2: Some common CMC methods (Adapted from Schramm, L.L. 2000).

UV/Vis, IR spectroscopy
Fluorescence spectroscopy
Nuclear magnetic resonance spectroscopy
Electrode potential/ conductivity
Voltammetry
Scattering techniques
Calorimetry
Surface tension
Foaming

One key factor that influences the CMC of surfactant is its chemical structure (Lindman, B., & Wennerström, H. 1980).

- I) Increase of surfactant's alkyl chain length will strongly decrease the CMC. A relationship between CMC and number of carbon atoms in hydrophobic chain is established:

$$\log(CMC) = a - (b \times (\text{number of carbon atoms}))$$

For ionic surfactants, the factor b is near 0.5; for non-ionic surfactants, b=0.29-0.30.

- II) Presence of instauration or ramification in the carbon chain of surfactant have an effect to increase the CMC.
- III) Generally, non-ionic surfactants have lower CMCs than ionic surfactants if they possess same hydrophobic chain.
- IV) Cationic surfactants typically have slightly higher CMCs than anionic surfactants.
- V) Counterions are reported to alter the CMC of surfactant solution (Mukerjee, p., Mysels, K.J., et, al. 1967; Emerson, M.F., & Holtzer, A. 1967), but no general rules have yet been established.

Besides the structure, addition of electrolyte to ionic surfactant solution will reduce electrical repulsion and allow formation of micelles at lower concentration. Temperature and pressure generally have little influence on CMCs, however, for some surfactants (some carboxyl-betaine or sulfo-betaine), their CMCs were found to decrease to a minimum with increasing temperature and then sharply increase, most markedly over 100°C (Stasiuk, E.N., & Schramm, L.L. 1996).

4. Krafft point

The temperature above which the solubility of a surfactant rises sharply is defined as Krafft point (known as Krafft temperature or critical micelle temperature). It is also the minimum

temperature that allows surfactant to form micelles in solutions. A usual way to determine the Krafft point is to find out the intersection of the solubility and the CMC curves of surfactant in solution (Figure 6). Krafft points have been observed for most ionic surfactants above 0°C, while only few nonionic surfactants were reported to have measurable Krafft point (for example, Brij 56 (polyoxyethylene cetyl alcohol) has a Krafft point of 34°C at concentration of 1% w/w. Brij 76 (polyoxyethylene stearyl alcohol) possess a Krafft point of 46°C at 1% w/w.) (Schick, M.J (Ed.). 1987; Schott, H., & Han, S. K. 1976).

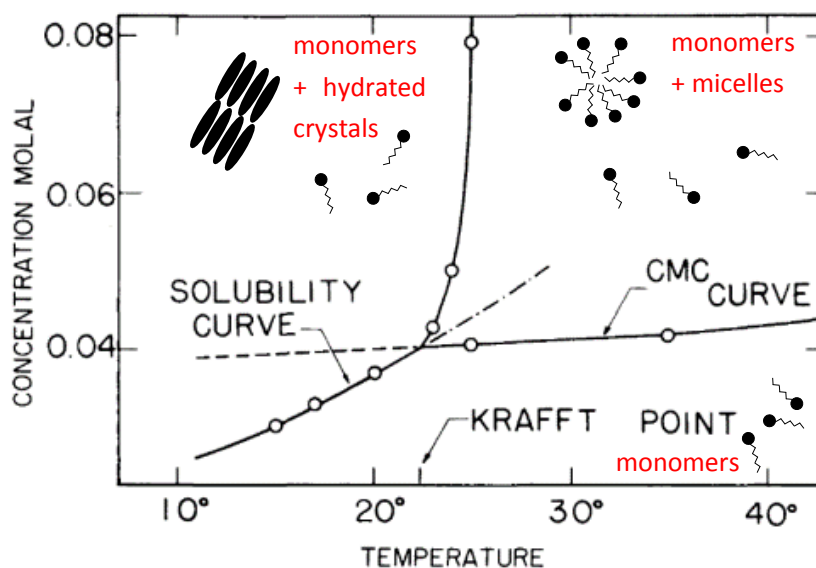


Figure 6: Phase diagram close to the Krafft point (Adapted from Shinoda, K., Nakagawa, T., & Tamamushi, B. I. 2013).

The Krafft point of surfactant is important in many applications since surfactant can act efficiently only above this temperature (for example, form micelles in solution...). Efforts have been devoted to reveal the factors influencing the Krafft point or to monitor the Krafft point of surfactant solution system. Some research have found that the type of counterion, alkyl chain length, chain structure or pressure can influence the Krafft points of surfactant solutions (Hato M., & Shinoda, K. 1973; Nishikido, N., Kobayashi, H., & Tanaka, M. 1982), these properties are used to bring down the Krafft point and prevent crystallization of surfactant even at low temperature.

For ethoxylated surfactant specifically, when the temperature of surfactant aqueous solution increases, the molecular motions of system increase and therefore inhibit the hydrogen bonding between surfactants and water molecules, their solubility decreases accordingly. The reduction of surfactant solubility will result in turbid of solution. The temperature at which the ethoxylated surfactant solution becomes turbid is called the cloud point. Cloud point is an important temperature to indicate the stability of surfactant solutions. The maximal effectiveness of surfactant will be obtained only when they are used near or below this temperature.

5. Hydrophilic-Lipophilic Balance (HLB)

HLB was firstly introduced by Griffin in 1949 for the purpose to establish a structure-property relationship of surfactant. It is defined as the balance of size and strength of surfactant's hydrophilic head and hydrophobic tails. After that, to estimate HLB values for surfactants, experimental or mathematical models have been suggested by various research groups. One common sense was developed that HLB value is linked to surfactant solubility and can be used to predict their potential domain of applications, especially for oil/water emulsification (Table 3).

Table 3: Surfactants' properties classified by their HLB (Adapted from Dominique, C. 1994).

Solubility	HLB range	Use
Oil soluble	1.5-3	Antifoaming agents
Oil soluble	3-6	Water/Oil Emulsifying agents
Water dispersible	7-9	Foaming agents
Water dispersible/ soluble	8-13	Oil/Water Emulsifying agents
Water soluble	13-15	Detergents
Water soluble	15-20	Solubilizing agents

Concerning the HLB estimated by calculation for non-ionic surfactants, Griffin firstly proposed the equation:

$$HLB = 20 \times \frac{M_h}{M}$$

M_h is the molecular mass of the hydrophilic part of surfactant and M is the molecular mass of the whole surfactant.

Another equation suggested by Davies, J.T. (1957) has counted in the effect of different groups by defining a number for each of them, according to Davies method, HLB of surfactants can be higher than 20:

$$HLB = \sum (\text{hydrophilic groups numbers}) - n(\text{group number per } CH_2 \text{ group}) + 7$$

The HLB group numbers are listed in Table 4.

Table 4: HLB group number to be used in HLB equation of Davies (Adapted from Davies, J.T. 1957).

Hydrophilic groups	Group Number
-SO ₄ ⁻ Na ⁺	38.7
-COO ⁻ K ⁺	21.1
-COO ⁻ Na ⁺	19.1
N (tertiary amine)	9.4
Ester (sorbitan ring)	6.8
Ester (free)	2.4
-COOH	2.1
Hydroxyl (free)	1.9
-O-	1.3
Hydroxyl (sorbitan ring)	0.5
Lipophilic groups	
-CH-	
-CH ₂ -	-4.75
CH ₃ -	
=CH-	
Derived groups	
-(CH ₂ -CH ₂ -O)-	+0.33
-(CH ₂ -CH ₂ -CH ₂ -O)-	-0.15

6. Surfactant applications

As a result of their amphiphilic properties and affinity to two immiscible phases, surfactant can interact strongly in liquid/liquid, gas/liquid or solid/liquid interfaces and help to stabilize composites with different polarity so as to form stable mixtures. Nowadays, surfactant are being applied widely in different sectors from scientific research to industrial production. Actually, a vast number of names of surfactants are created according to the area in which they are used, those names include but not limited to detergents, wetting agents, dispersing agents, adhesive agents, foaming/ antifoaming agents, emulsifier, collecting agents. Figure 7 gives out some major applications of surfactants.

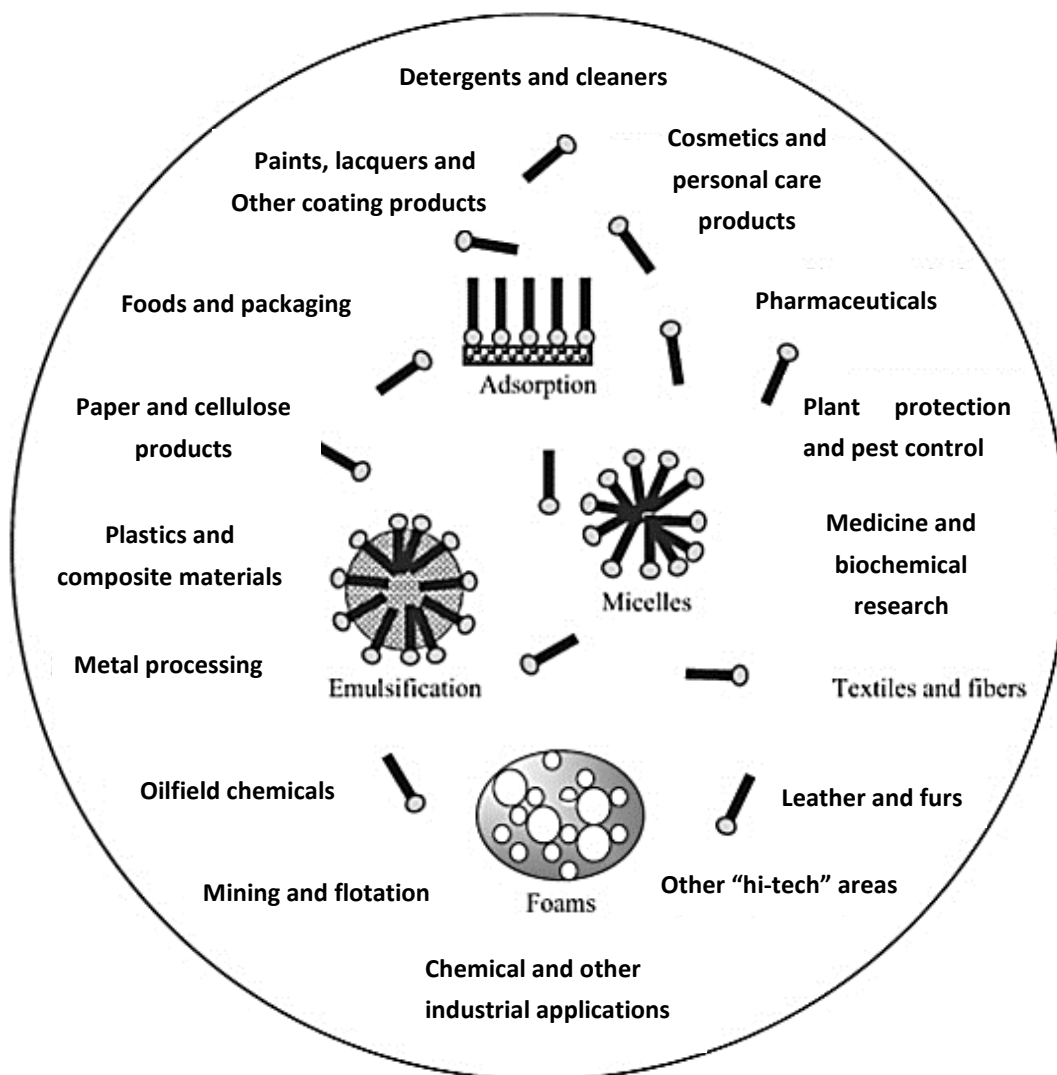


Figure 7: Some important, high impact areas of surfactant applications (Adapted from Myers, D. 2005).

6.1. Detergent and cleaning agents

One traditional area of surfactant application is to use them as detergent or cleaning agents. The cleaning effect of surfactant is based upon its ability to wet the hydrophobic substances (unwanted dirt) and enclose them into surfactant micelles. Anionic surfactants are most widely used in this sector. Some major types of anionics include alkylbenzene sulfonates, alkyl sulfates, alkyl ether sulfates and soaps (Simion, F. A., et al. 1990; Parris, N., et al. 1973).

6.2. Coating products

Surfactant are known to be used in different process for production of paint. They can help with grinding process of paint's pigments by reducing the surface energy of particles. The adsorption of surfactant molecules at particles' surfaces also help to create barriers that prevent the aggregation of pigments. Study has found that addition of surfactant greatly

reduce the energy consumption up to 75% during the grinding process. Another important role of surfactant in paint industry is that they help to stabilize pigment particles in final paint products. This will facilitate the storage of paints for an extend period of time (Myers, D. 2005).

6.3. Petroleum industry

Dispersant and emulsifying surfactants are essential for drilling mud used in prospecting for petroleum. Drilling mud is composed of water, clay, salts of heavy metals which cannot be homogeneously mixed under normal conditions. Addition of surfactant helps to stabilize this mixture. Surfactants also enhance the recovery of remaining petroleum trapped in the reservoir's porous media by capillary and viscous forces in depleted well (Kanicky, J. R., Lopez-Montilla, J. C., Pandey, S., & Shah, D. 2001). Techniques such as injecting high pressure steam into the oil-bearing rock need the participation of surfactant so as to alter the wetting characteristics of water-oil-rock system and thus raise the successful rate of petroleum recovery (Myers, D. 2005). Other possible applications of surfactant in petroleum industry such as corrosion inhibitors, water flooding agents have also been described by different authors (Migahed, M. A., & Al-Sabagh, A. M. 2009; Bhardwaj, A., & Hartland, S. 1993).

6.4. Personal care products

Surfactant is one of the key ingredients for most of current personal care products such as shampoo, hand/ face cream, facial cleaner. One reason is that those products are always mixture of various substances with different polarity, surfactant increases their mixability and stability. In some other cases, surfactants help active ingredients to penetrate into skin layer. Surfactants (emulsifiers, wetting agents and foaming agents) in cosmetic products also modify the sensorial experiences of customers. Monitoring the phase behavior of cosmetic products when it is applied onto human body by surfactants creates desired products (Schramm, L. L., Stasiuk, E. N., & Marangoni, D. G. 2003).

6.5. Food industry

Surfactants with low toxicity and good surface-active properties are of great interests for the food industry. Almost infinite combination of ingredients can be developed in food and their microstructures need to be monitored. For example, surfactant serves to form stable dispersions, emulsions, gels, foams in those products (Kralova, I., & Sjöblom, J. 2009). It can help with the rheological characteristic of flour (Fiechter, A. 1992), some can substitute fat in products to reduce total calories and maintain food texture (Dobson, K. S., Williams, K. D., & Boriack, C. J. 1993).

6.6. Pharmaceutical research

Surfactants have great potential as drug carrier or targeting systems as a result of its unique phase structure under different conditions. The capability of surfactant to form micelles in aqueous solutions allow them to encapsulate poor water-soluble drugs, it can create a stable

solution for intravenous or oral administration (Lawrence, M. J. 1994). Furthermore, the possibility of surfactant to act in targeting system of drugs has drawn attention of different research groups. Some suggested that use of surfactant micelles as micro-containers can increase the efficiency of neuroleptic targeting from blood flow into the brain (Kabanov, a. V. & et, al. 1989), others used the nonionic surfactant based vesicles for anti-cancer drug targeting (Rogerson, A. & et, al. 1998; Uchegbu, I. F. 1995), which exploits the specific vascular architecture of tumor tissue.

6.7. Others

Surfactants can also be applied on industries of textiles, fibers, leather and furs, paper, cellulose products, mining, metal processing industries, plant protection, plastics and composite materials. They have already become an indispensable part in every aspect of daily lives.

7. Marketing

Surfactants are produced in a range of millions of tons per year. In 2014, a global turnover of 33.2 billion US\$ was achieved with surfactants (Ceresana Market Study: surfactant (2nd edition), <http://www.ceresana.com>). The distribution of world's consumption by major regions in 1994 is presented in Figure 8. Asia, North America and Europe together occupy 83% of world's total consumption, presumably due to its high demand of surfactants in industry use and consumer products.

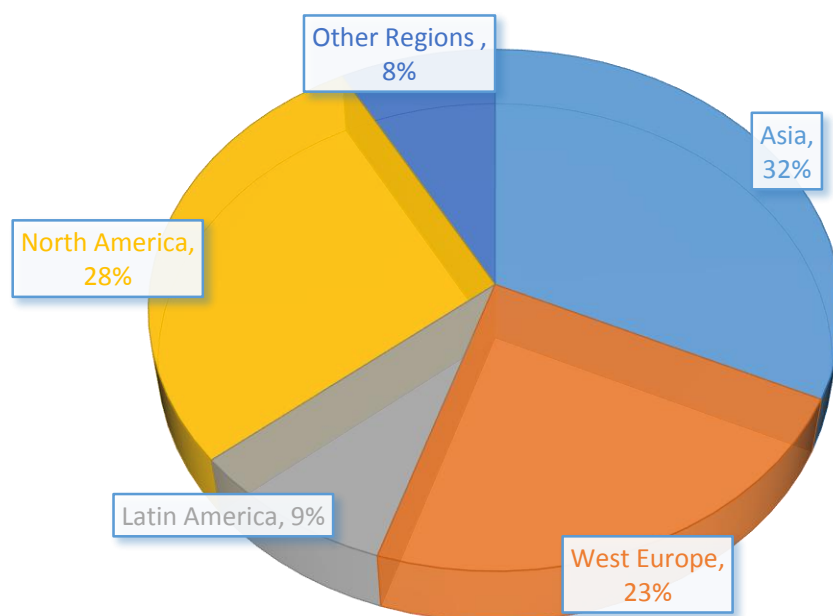


Figure 8: World surfactant consumption by region % (Adapted from Colin A. Houston (CAH) report, 1997).

The market of surfactants continues to grow, as for the case of Europe, according to statistics

by European Committee of Organic Surfactants and their Intermediates (CESIO), the surfactant production in Europe from 1994 to 2013 rises gradually (Figure 9). Among them, Ethoxylates derived surfactants are the most important type in markets, their production rises from approximately 1000 kT/ year to 1300 kT/ year. Anionic surfactants are also produced in large quantity due to their wide applications in different sectors. Other classes of surfactant, the cationic, non-ionic (except for Ethoxylates) and amphoteric are relatively fabricated in lower quantity, their production didn't increase too much during these years.

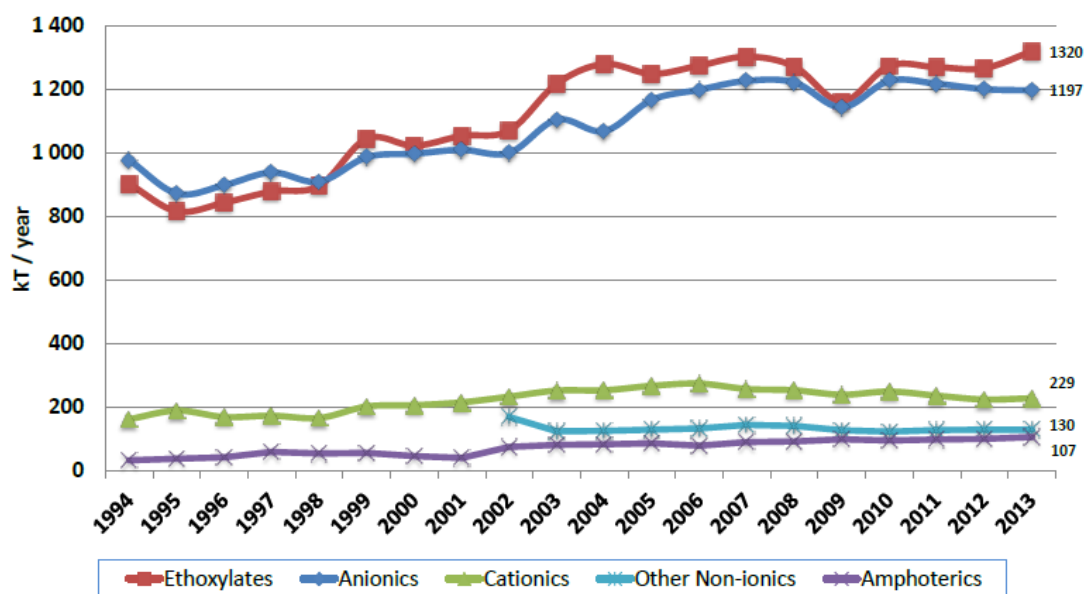


Figure 9: Surfactants production EU 1994-2013 (European Committee of Organic Surfactants and their Intermediates. <http://www.cefic.org>).

The end-use of surfactant can be divided into 6 groups (Figure 10), among them, most of produced surfactants goes to cleaning sectors. Other applications sectors, such as textile auxiliaries, personal care, industrial and institutional cleaning and oilfield share 30% of global surfactant market.

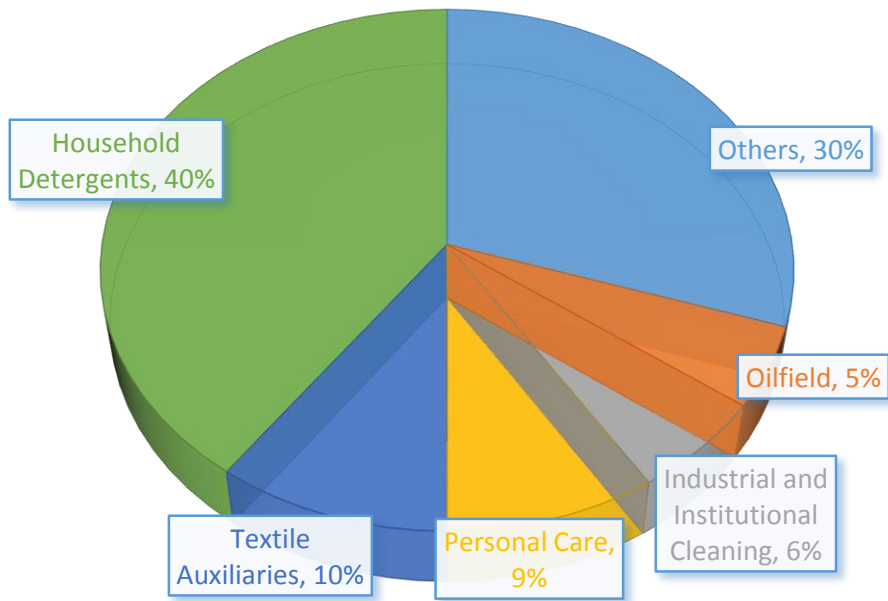


Figure 10: Global surfactant market: end-user-wise (Adapted from Khandal, R.K. 2003).

As a result of environmental awareness and the trend to produce more biocompatible/biodegradable surfactants, there is a trend to develop bio-based surfactant as promising substitutes for conventional ones. The process of industrialization of bio-based surfactants is just starting. But they are believed to have a higher growth rate than chemical - based surfactants in the coming years (Markets and Markets report. <http://marketsandmarkets.com>). For example, the consumption of bio-surfactants totaled 1.52 Million tons in the EU in 2008. Annual growth potential is estimated to be 3.5%, and bio-surfactant potential 2.3 Mt in 2020 (Biochem. <http://www.biochem-project.eu>). Another projection made by BIO-TIC (2014) is presented in Figure 11. With an estimated demand of 679 Million EUR in 2013 corresponding to half of the global demand. The market growth rate is believed to maintain at approximately 3% per annum. By the year 2030, the bio-based surfactants market in Europe could have a value of between 0.8 Million EUR (low scenario) and 1.8 Million EUR (high scenario).

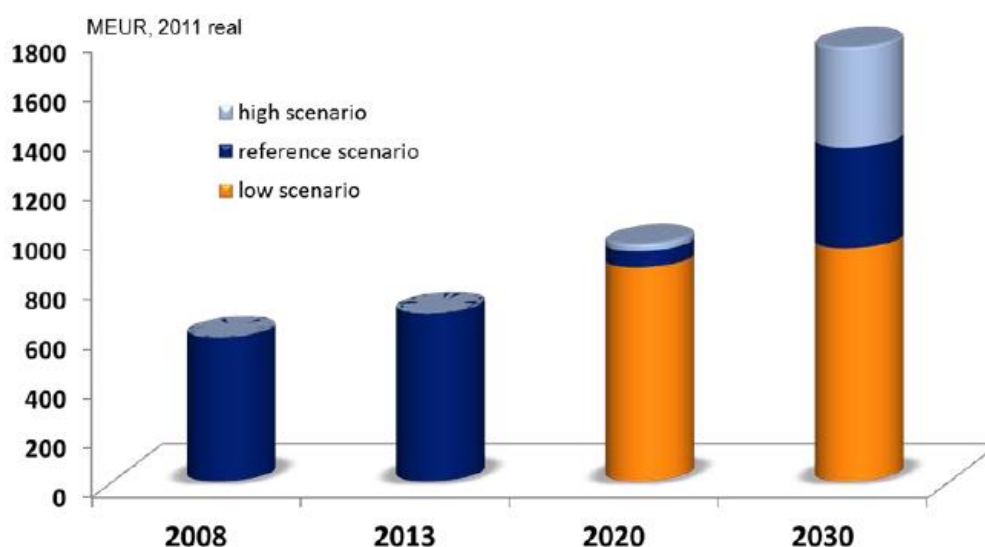


Figure 11: Bio-surfactant market projection (BIO-TIC. 2014).

8. Sugar-based surfactants

The large scale of production of synthetic surfactants from non-renewable resources have induced a series of environmental problems. After use, residual surfactants are normally washed away and dispersed into different systems such as water, soil or sediment. The possible toxicity of some surfactants to different organisms: bacteria, aquatic plants, invertebrates, vertebrate, terrestrial plants have been reviewed by Ivanković, T., & Hrenović, J. (2010). A number of surfactants are classified to have relatively low biodegradability compared to sugar-based surfactant, for example, a linear primary alcohol ethoxylate ($C_{12-15}AE-7$, Carbon number in the alky chain = 12-15, with 7 moles of ethylene oxide) was found to be less biodegradable than a linear alkyl polyglycoside ($C_{12-14}APG$, Carbon number = 12-14, average degree of polymerization=1.4) in anaerobic degradability tests (Anaerobic mineralization: $C_{12-15}AE-7$: less than 50% at day 50; $C_{12-14}APG$: more than 50% at day 50) (Madsen, T., et al. 1996).

With the increasing of environmental awareness, there is a great trend to replace conventional surfactants by surfactants with natural building blocks. Synthesis of these types of surfactants through renewable natural resources can greatly reduce the use of hazardous substances, which is referred as 'green chemistry'. Furthermore, surfactant with natural blocks are usually found to be less toxic and more biodegradable than traditional ones (Steber, J. 2008; Negm, N. A., & Tawfik, S. M. 2013; Holmberg, K. 2001; Porter, M. R. 1995).

Sugar based surfactant, with a sugar derived moiety as its hydrophilic head, is one major type of natural surfactant. They can present strong surface-active properties, high biocompatibility, low toxicity and other interesting physico-chemical or biological activity by varying their structures (Negm, N. A., & Tawfik, S. M. 2013). According to the linkage between surfactant head unit (glucose, maltose etc...) and its hydrophobic carbon chains, 4 major types of sugar based surfactant were listed below (Figure 12).

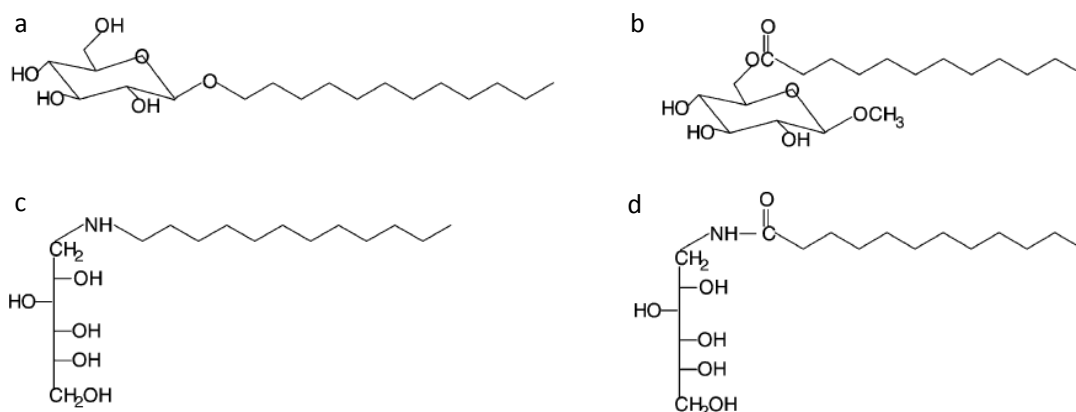


Figure 12: Examples for the most frequent linkages between the hydrophilic and the hydrophobic moiety in sugar surfactants: a. ether bond, dodecyl- β -glucoside; b. ester bond, β -methyl6-O-dodecanoyl-D-glucoside; c. amine bond, N-dodecyl-glucamine; and d. amide bond, dodecyl-glucamide (N-dodecanoyl-glucamine) (Adapted from Stubenrauch, C. 2001).

8.1. Sugar-based surfactant with ether bond-Alkyl polyglycoside

A typical and most commonly used sugar-based surfactant with an ether linkage is alkyl polyglycoside, known as APG (Figure 13). APG was firstly synthesized by Emil Fischer more than 100 years ago, but it is until recently that this type of surfactant was considered as proper agents for personal care products, laundry detergent and hard surface cleaners. As natural surfactants derived from renewable resources, APG are characterized as readily biodegradable and cause no mutations (Willing, A., Messinger, H., & Aulumann, W. 2004). Kristin, K. (2000) has reviewed the industry data of APG and concluded that it has low acute oral/ dermal toxicity and is not skin sensitizer. Methods were used to synthesis APG with chain lengths from C4 to C22 (Weuthen, M., Kawa, R., Hill, K., & Ansmann, A. 1995), results showed that only APG with longer hydrophobic chains can act efficiently as emulsifier. A study of the cleaning effect and surfactant properties of a series of APG revealed that with increasing chain length, the CMC decreases and the adsorption increases (Matsson, M. K., Kronberg, B., & Claesson, P. M. 2004).

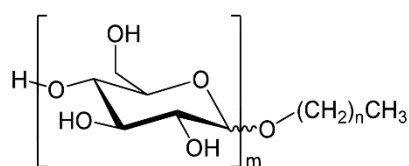


Figure 13: Structure of alkyl polyglycoside.

8.2. Sugar-based surfactant with ester bond

Sugar ester is surfactant containing sugar head and fatty acids. It can be produced in a wide range of HLB (from 1 to 16), which guarantees its applications in various sectors. Sugar esters are mostly used in food industry as a result of their tasteless, odorless and nontoxic properties.

The interfacial and emulsifying properties of sucrose monostearate have been investigated by Ariyaprakai, S., et al. (2013), they found that sucrose monostearate has a slightly better ability to lower interfacial tension at coconut oil-water interface than Tween 60 and it can form stable coconut milk emulsions regardless of temperature change. According to Farooq, K., & Haque, Z. U. (1992), addition of sugar esters with different HLBs in yogurts help to improve their body, texture and mouthfeel. Besides their favorable roles as food additives, their biodegradability are also studied. Some types of sugar esters, mainly the sucrose fatty acid esters are rapidly biodegradable (Isaac, P. C. G., & Jenkins, D. 1958). Research of an array of sugar ester surfactants revealed that the variations in sugar head groups' size or in alkyl chain length and number do not significantly affect their biodegradability, on the contrary, sugar esters with α -sulfonyl or α -alkyl groups, showed much lower biodegradability compared to non-substituted sugar esters. This study helped to understand the relationship between structures and biodegradability of sugar esters.

8.3. Sugar-based surfactant with amine bond

Amine based surfactants with sugar moiety have not yet been used in large quantity, but they are considered potential to replace traditional amine-based nonionic surfactants which are used for acid thickening, microemulsification, textile processing aid and detergent booster such as ethoxylated amines (Van Os, N. M. (Ed.). 1997). It is anticipated that addition of natural blocks will help to reduce the toxicity and increase biodegradability of amine based surfactants. Researches on pH-dependent aggregation behavior of a sugar amine gemini surfactant have discovered that, when pH changes from 7.5 to below 4, the conformation of hexane-1,6-bis(hexadecyl-1'-deoxyglucitylamine) molecules will alter from bilayer vesicles to micelles (Bergsma, M., Fielden, M. L., & Engberts, J. B. 2001). Another interesting pH dependent property of a set of sugar amine surfactants was reported, they can turn from cationics to nonionics when pH value arises (Egan, P. A. 1989).

8.4. Sugar-based surfactant with amide bond

There are actually two types of sugar surfactants according to the orientation of amide groups bonding the hydrophilic head and hydrophobic tail. The form of alkylcarboxamide where the hydrocarbon chain carries the amide carbon or the form of carbamoyl where the sugar head carries the amide carbon. Some examples concerning this type of surfactants are described below.

N-Octanoyl- β -D-glucosylamine was synthesized and characterized by Brennerhenaff. C., et al. (1993), this non-ionic sugar-based surfactant presents temperature dependent solubility. Its extraction efficacy and mildness toward protein structure and activity make it an idea candidate for membrane studies. The surface active properties of D-glucuronamide, N-Octyl have been estimated together with a series of similar sugar-based surfactants (Laurent, P., et al. 2011), it showed relatively strong ability to reduce surface tension of water solution. 6-O-(N-Heptylcarbamoyl)-methyl- α -D-glucopyranoside, also known as Hecameg, is a commercially available amide surfactant with sugar head. An assessment of its application especially for biomedical use has been made by Ruiz, M. B., et al. (1994), it is suitable for reconstitution

procedures and is considered as effective lipid-solubilizing agent. As for other sugar amide surfactants which are not listed above, a range of D-gluconamides compounds were synthesized, evaluation of their physico-chemical properties indicate that they are effectiveness as foaming agents, dispersion agents and emulsification agents, but these types of surfactants presented different level of biodegradability and toxicity (Negm, N. A., & Tawfik, S. M. 2013).

The properties of sugar-based surfactants can vary greatly based on their structures. Their physico-chemical properties, such as surface-active properties, critical micellar concentrations, self-assembling properties are in need of study to identify their potential applications in different sectors. Furthermore, understanding of their effects on biological systems, especially cells and skins, are of great importance if those surfactants are to be used in household, cosmetic, food or pharmaceutical products where they will contact directly with human body.

B) Surfactants and human health

1. Possible hazard to human health

Millions of tons of surfactants are produced each year. Some of them are ingredients of household, cosmetic or food products, which, after use, will subsequently go into water or soil and result in possible human/ environmental exposure. Potential toxic effects on human health by surfactants through direct or indirect contact has drawn attention of scientists. In guidance on information requirements and chemical safety assessment compiled by European Chemicals Agency (ECHA), several typical endpoints to assess human hazard by chemical exposure have been listed as detailed below (European Chemicals Agency. <http://echa.europa.eu>).

1.1. Irritation and corrosion

Irritation and corrosion refer to local effects on the skin, in the eyes or in the respiratory system. Corrosion causes irreversible damage of the tissues whereas dermal, eye or respiratory irritations are considered to be reversible and usually less severe (European Chemicals Agency. <http://echa.europa.eu>). Routine activities of human can result in relatively high level of skin, eye exposure to surfactants (dish washing, use of shampoos, body lotions, make ups...). To ensure safety, irritation and corrosion effects of surfactant are in need of comprehensive studies.

A dose-response study has revealed the susceptibility of Sodium Dodecyl Sulfate (SDS) induced irritation on forearm skin of patient with history of seborrhoeic dermatitis and atopic eczema compared to normal subjects (Cowley, N. C., & Farr, P. M. 1992). The effects of a mixed surfactant system on human cutaneous response has been investigated and revealed that SDS can induce erythema by a 21-day cumulative irritation patch test, but addition of 7-ethoxy sulfate (AEOS-7EO) to a constant dose of SDS results in a significant reduction in erythema (Rhein, L.D., et al. 1990).

Effort has also been made to predict surfactant irritation effect by different models. For example, the correlation between swelling response of a collagen film model (prepared from bovine deep flexor tendon) and the *in vivo* irritation potential (tested on human skin) of anionic surfactant (SDS) were reported (Blake-Haskins, J. C., et al. 1986). Moreover, a unilamellar liposome system produced by the petroleum ether evaporation technique can be used to screen surfactants according to their mildness. More precisely, the relative tendency of anionic surfactants or surfactant blends (SDS, di-Na lauryl ether sulfosuccinate etc...) to form mixed micelles with liposome membrane components determines aggressivity factors and these factors are believed to correlate to *in vivo* surfactant irritation responses obtained from *in vivo* human skin tests. Three established cell lines (SIRC rabbit corneal cells, Balb/c 3T3 and L929 mouse fibroblasts) have been used to test cytotoxicity of different surfactants (Span 20, Triton X155, Tween 20, CTAB...): *in vivo* irritation results (MTT test, Neutral red uptake assay)

and *in vitro* data (rabbit eye irritation assay) were compared after these tests, however, no evident correlations were found (Vian, L., et al. 1995).

1.2. Sensitization

Skin sensitizer is defined as a substance that will induce an allergic response following skin contact (United Nations. Economic Commission for Europe. <http://www.unece.org>). A respiratory sensitizer is a substance that will induce hypersensitivity of the airways following inhalation of the substance (International Labour Organization. <http://www.ilo.org>). Since the main sensitization effect caused by surfactants are through skin contact, identifying surfactants that are skin sensitizers becomes important.

Up to now, many *in vivo* methods to identify a skin sensitizer are accepted. Some tests are used widely such as Guinea Pig Maximization Test and Local Lymph Node Assay. By these two methods, Garcia, C., Ball, N., et al. (2010) tested 10 surfactants composed of glucose/ xylose sugar moiety and a fatty alcohol linked through ether group: the molecules were all classified as non-sensitizers and it was confirmed by test result from human volunteers. Karlberg, A. T., et al. (2003) emphasized the importance of storage control of ethoxylated alcohols, which, at autoxidation, can become skin sensitizer. In the same time, efforts have been made to promote the use of *in vitro* experiments as alternatives of *in vivo* sensitization tests. Ball, N., et al. (2011) compared skin sensitization effect of several surfactants (Isononyl glucoside, thioglucopyranoside, nonane sulfate etc...) between *in vitro* and *in vivo* models. The results obtained in the two methods were not corresponded. Hence, they highlighted the importance of careful choosing *in vitro* skin sensitization models for research.

1.3. Acute toxicity

The term acute toxicity is used to describe the adverse effects, which may result from a single exposure (for example, a single exposure or multiple exposures within 24 hours) to a substance (European Chemicals Agency. <http://echa.europa.eu/>).

Data of acute toxicity on human body are limited, mainly because their low availability and unclear level of exposure. Alternatively, an evaluation of the data dealing with various measures of mammalian toxicity as indicators of potential human toxicity as well as acute toxicity can be applied to determine the influence of surfactants on human health (Talmage, S. S. 1994). Multiple research groups have evaluated in laboratory animals, the acute toxicity of alcohol ethoxylates exposed by the oral, dermal and inhalation routes (Talmage, S. S. 1994). Study of the acute toxicity of nonylphenol ethoxylate and alcohol alkoxylate to six types of frogs has been made, and all the six species exhibited nonspecific narcosis following exposure the both surfactants (Mann, R. M., & Bidwell, J. R. 2001). Besides that, a number of studies were carried out with marine animals such as fish and water flea. Sandbacka, M., et al. (2000) replaced normal *in vivo* acute toxicity tests on fish with more effective *in vitro* assays. The acute toxicity of 10 synthetic surfactants (SDS, dodecyl trimethylammonium bromide, Zwittergent® 3-10 etc...) were determined *in vitro* on hepatocytes and gill epithelial cells

(rainbow trout) and *in vivo* on daphnia magna (water flea) and on rainbow trout (fish). Results indicated that a combination of the toxicity values for daphnia magna and freshly isolated gill epithelial cells in suspension correspond with acute toxicity on *in vivo* values. Acute toxicity of surfactants to rainbow trout were also reported by Buhl, K. J., et al. (2000): they found that Linear Alkylbenzene Sulfonate (LAS) is intermediate in toxicity and SDS is less toxic to rainbow trout when compared with a series of surfactant-based fire suppressant foams (Firefoam 103B, FireFoam 104 ...).

1.4. Repeated dose toxicity

The term repeated dose toxicity comprises the general toxicological effects occurring as a result of repeated daily dosing with, or exposure to, a substance for a part of the expected life span (sub-acute or sub-chronic exposure) or for the major part of the lifespan, in case of chronic exposure (European Chemicals Agency. <http://echa.europa.eu/>).

For a few surfactants, their chronic toxicity was tested in rats. Isomaa, B., et al. (1976) gave Cetyltrimethylammonium Bromide (CTAB), a cationic surfactant to Sprague Dawley rats through drinking water in dosages of 10, 20 and 45 mg/kg-d for 1 year. They found that the surfactant was well tolerated at the two lowest dose levels. At the highest dose level, a significant loss of body weight was observed. Two synthetic lipids, 1,2-dioleoyl-rac-glycerol-3-dodecaethylene glycol and 1,2-distearoyl-rac-glycerol-3-dodecaethylene glycol were studied: the two novel surfactants seemed to have no evident sub-chronic toxicity against Sprague-Dawley rats at concentration of 250, 500 and 1000 mg/kg-d for 28 days (by Bidhe, R. M., & Ghosh, S. 2004). More repeated dose toxicity results of surfactant come from tests in aquatic organisms. For example, the chronic toxicities of surfactants and detergent builders to algae were reviewed: the reported toxicities of surfactants have varied widely over several orders of magnitude and the effect levels are compound and species-specific (Lewis, M. A. 1990). Generally speaking, anionic/ nonionic surfactants and detergent builders are relatively non-toxic when compared to various cationic monoalkyl and dialkyl quaternary ammonium salts, but toxicity of surfactants needs to be evaluated for each unique case.

1.5. Reproductive and developmental toxicity

Reproductive toxicity refers to effects such as reduced fertility, effects on gonads and disturbance of spermatogenesis and also covers developmental toxicity. Developmental effects refer to growth and developmental retardation, malformations and functional deficits in the offspring... (United Nations. Economic Commission for Europe. <http://www.unece.org>).

Reproductive and developmental toxicity of surfactants are studied in animal tests as references of human health risk analysis. A C₉₋₁₁ linear primary alcohol 6-mole ethoxylate, which is used in cleaning formulations, was studied by Gingell, R., & Lu, C. C. (1991). At concentrations from 1% w/v to 25% w/v in aqueous solutions, rat dermal exposure causes no compound-related effect on the reproductive performance or the growth and development of the offsprings. Butenhoff, J. L., et al. (2009) reported that potassium perfluorohexanesulfonate

presents no reproductive or developmental toxicity at dosages from 0.3 mg/kg-d to 10 mg/kg-d in Sprague-Dawley rats. A commercial fluorotelomer-based urethane polymeric dispersion, consisting of polymer, surfactant and water was evaluated (Stadler, J. C. 2008). The product was characterized to produce no specific developmental or reproductive toxicity at 1000 mg /kg-d. Generally speaking, surfactants that can cause reproductive or developmental toxicity in animal tests are barely reported.

1.6. Mutagenicity and carcinogenicity

Mutagenicity refers to the capacity of substances to induce mutations. Carcinogenicity describes the ability of tendency to produce cancer. These two classes of toxicity are of major concerns when evaluating chemicals' potential hazard to human health.

A series of toxicity evaluation has been carried out to investigate mutagenicity and carcinogenicity of surfactants. No skin tumors were observed in female Swiss mice following twice weekly percutaneous applications with 5% aqueous solutions of alcohol ethoxylate sulfate (C₁₂AE₃S) for two years (Tusting, R.F., et al. 1962, reviewed by Talmage, S. S. 1994). Ten surfactants, including linear alkylbenzene sulphonate (LAS), Alcohol ethoxylate sulfate (AES), cetyltrimethylammonium chloride (CTAC), cetyldimethylbenzylammonium chloride (CDBAC), N,N-Bis(2-hydroxyethyl) lauramide and N,N-Dimethyldodecyl-amine oxide were tested and they neither cause morphological transformation of Syrian golden hamster embryo cells (carcinogenicity) nor induce increase of revertant colonies of cultured auxotrophic bacteria - *S. typhimurium* (mutagenicity) (Inoue, k., et al. 1980). Actually, a comprehensive review concerning the short term genotoxicity of 200 common surfactants revealed that all four major classes of surfactants (anionic, cationic, nonionic and zwitterionic) have negligible potential to cause genetic damage (mutagenicity or carcinogenicity) (Yam, J. 1984).

2. Skin irritation — an important endpoint to assess surfactant toxicity

Among all the possible hazard to human health, surfactant's adverse effects on human skin have attracted attention. There are two main reasons:

- I) High exposure level of human skin to surfactants in daily life. Surfactants are widely used in cosmetic formulation, food, household products or pharmaceutical products, frequent cutaneous contacts with surfactants are inevitable. Therefore, understanding the toxicity of surfactants against human skin ensures their safe use.
- II) Most surfactants are mild chemicals, they won't induce severe damage to human health. Skin irritation is one of the most observable endpoints to evaluate surfactant's toxicity.

2.1. Structure of the skin

The skin is the largest organ of the body, for average adult human, skin has a surface area of about 1.5-2.0 m². It is a complex, multilayered organ, which produces several specialized

derivative structures called appendages (hair follicles, eccrine sweat glands, sebaceous glands, apocrine glands) and consists of heterogeneous cell types and extracellular components (Freinkel, R. K., & Woodley, D. T. (Eds.). 2001). The skin is composed of 3 layers: epidermis, dermis and hypodermis /subcutaneous layer (Figure 14).

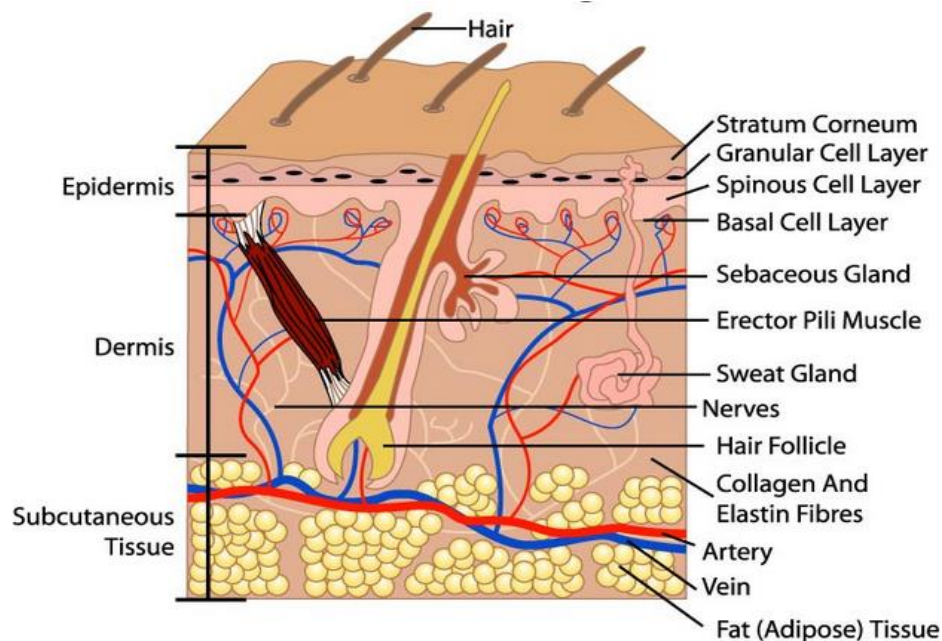


Figure 14: Human skin diagram (<http://seabuckthorn.com>).

1) Epidermis

The epidermis is the outmost layer of human skin. It consists of 4 main types of cells: keratinocytes, melanocytes, Langerhans cells and Merkel cells. Among them, the keratinocytes represent 90% to 95% of total epidermal cells. According to the position and differentiation state of keratinocytes, epidermis can be further divided into 4 layers or 5 layers (only for palms and soles) from inside out (Figure 15). Basal layer/ stratum basal is organized with one single (sometimes 2 or 3) layers of non-differentiated basal keratinocyte cells, also recognized as stem cells of epidermis. The basal keratinocytes are constantly undergoing cell division and form new keratinocytes which migrate superficially and build the spinous layer/ stratum spinosum. At spinous layer, the keratinocytes were connected together by specialized cells known as desmosomes and they start to synthesize keratins (Wiles, M. 2010). The cells continue to flatten and become granular cells, in granular layer/ stratum granulosum, cells accumulate dense, basophilic granules (keratohyalin granules—precursors of keratin) in the cytoplasm. At the same time, the nucleus and cytoplasmic organelles disappear, the keratinocyte is reducing to a flat square of keratin. The cells finally die when they reach the stratum corneum layer, where the keratinocytes (also called corneocytes) containing keratin form thick barrier and prevent loss of water and entry of bacteria. In the case of palms and soles, lucidum layer/ stratum lucidum lays between granular layer and stratum corneum, it

consists mainly of transparent dead cells and function as a barrier.

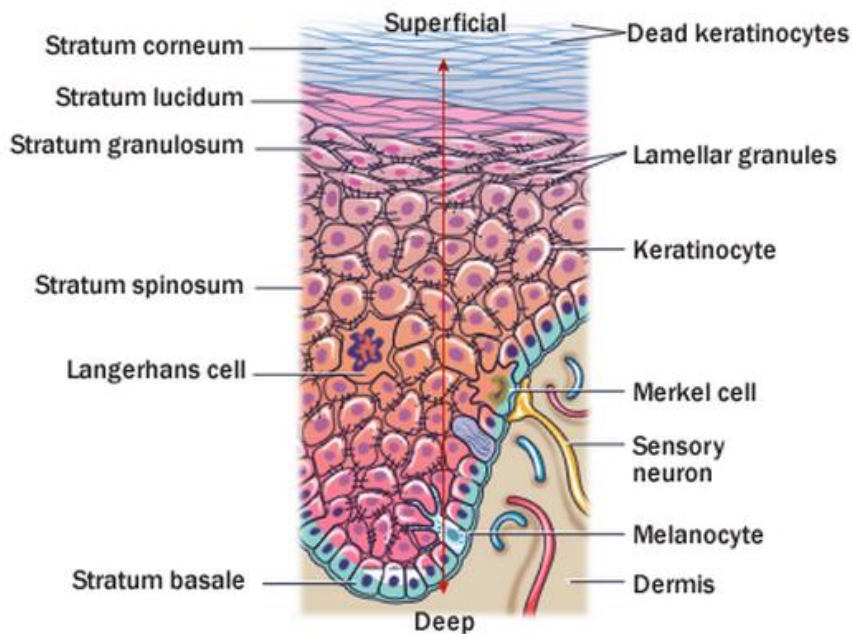


Figure 15: Structure of epidermis (<http://kreativestudios.com>).

Concerning other cells in epidermis, each of them have its unique function. Melanocytes are located at basal layer, they produce melanin which is responsible for skin color and protect inner skin cells from UV light. Merkel cells, also found in the basal layer, are believed to be involved in sensory perception (Alexandre, B. S. <http://www.icsmsu.com>). Langerhans cells in the middle layer of the epidermis serve as antigen-presenting cells in skin infections.

II) Dermis

The dermis is the structure foundation of epidermis, it supplies nutrition for the epidermis and provides its pliability, elasticity and tensile strength for the skin (Freinkel, R. K., & Woodley, D. T. (Eds.). 2001). Collagen, elastic fibres and microfibrillar components are major protein fibres in dermis. Together, they form supporting matrix/ ground substance of dermis in which cellular elements (fibroblasts, mast cells, histocytes, Langerhans cells, lymphocytes, eosinophils), hair follicles, sebaceous glands, apocrine glands, sweat glands, lymphatic vessels and blood vessels are embedded (Shimizu, H. 2007) (Figure 14). Dermis can be separated into two regions, the one adjacent to epidermis is papillary region. The papillary region is thin layer containing a lot of fibroblasts, irregular collagen fibres and delicate elastic fibres. The reticular region underlies the papillary region. This region is thicker and makes up the bulk of the dermis. It has dense connective tissue comprising fibre component (Shimizu, H. 2007).

The major component of matrix in dermis is collagen, it accounts for approximately 75% of the skin's dry weight. Up to now, more than 20 different collagens have been identified, these molecules are composed of 3 chains that may be same or distinct from each other depending on their types (Freinkel, R. K., & Woodley, D. T. (Eds.). 2001). The most found collagen in human

dermis is collagen type I (accounts for 80%-90% of the total collagen). It is produced by fibroblasts and self-assemble into irregular overlapping staggered fibres in the extracellular space (Introduction to the skin, <http://www.icsmsu.com>).

Fibroblasts are the most numerous cells in the dermis. They are responsible for synthesizing and degradation of collagen and elastin proteins. The study of fibroblasts activity is of great interest. Their proliferative rate and response to immune mediators are always used as references of toxicity tests or wound healing evaluation in different models (Welss, T., et al. 2004; Carlson, M. A., & Longaker, M. T. 2004).

III) Hypodermis/ subcutaneous tissue

The tissue of the hypodermis insulates the body, serves as a reserve energy supply, cushion and protects the skin, and allows for its mobility over underlying structures (Freinkel, R. K., & Woodley, D. T. (Eds.). 2001). The main cells in hypodermis are adipocytes, functioning to accumulate and store fats. Blood vessels and lymphatic vessels go through the tissue to the dermis. Cutaneous nerves, hair follicle roots are also located in the hypodermis.

2.2. Functions of the skin

Functions of the skin are listed in Table 5.

Table 5: Functions of the skin (Bensouillah. Aromadermatology. <http://courses.washington.edu>).

-
- Provides a protective barrier against mechanical, thermal and physical injury and noxious agents.
 - Prevents loss of moisture.
 - Reduces the harmful effects of UV radiation.
 - Acts as a sensory organ.
 - Helps regulate temperature control.
 - Plays a role in immunological surveillance.
 - Synthesizes vitamin D3 (cholecalciferol)
 - Has cosmetic, social and sexual associations.
-

Skin serves as an important organ of human body with multiple essential functions. Skin defection caused by chemical exposure will possibly reduce its efficiency as an outmost barrier against hazard or disrupt its self-regulation. Studies concerning subject like chemical toxicity against skin are of great interest for human health.

2.3. Skin irritation

Skin irritation refers to the production of reversible damage of the skin following the application of a test substance for up to 4 hours (Organization for Economic Co-operation and Development - OECD guideline for the testing of chemicals. <http://oecd-ilibrary.org>The presence of erythema, oedema, dryness of the skin, fissures, desquamation, itching and pain

characterizes both irritant contact dermatitis and allergic contact dermatitis (Welss, T., et al. 2004). The difference between skin irritation and allergic contact dermatitis is that the former one is initiated through a direct inflammatory effect on the skin, excluding mechanisms of causation involving sensitization (Basketter, D. 1999). According to Corsini, E., & Galli, C. L. (1998), skin irritation can be divided into 2 subtypes, acute skin irritation and chronic skin irritation. Acute skin irritation is often characterized by skin inflammation. Chronic skin irritation, on the contrary, is characterized predominantly by hyperproliferation and transient hyperkeratosis after long time exposure.

Considering the tremendous structure variations of chemicals and their different physico-chemical/ biological properties, it is generally believed that there are at least two major pathways involved to initiate and modulate skin irritation (Welss, T., et al. 2004) and the two pathways can either function alone or together.

The first one is damage of chemicals to stratum corneum, causing loss of barrier integrity through the process known as stratum corneum hydration, delipidation or protein denaturation. Wilhelm, K. P., et al. (1993) have demonstrated that anionic surfactants increase *in vivo* stratum corneum hydration and the mechanism is related to irritation properties of these compounds. The importance of stratum corneum lipids for the cutaneous barrier function has been recently reviewed (Van Smeden, J., et al. 2014). In granular layer, the keratinocytes store precursors of stratum corneum lipids such as glucosylceramides, sphingomyelin and phospholipids, they are enzymatically processed in to their final constituents: ceramides and free fatty acids. Ceramides and free fatty acids, together with cholesterol form the so called “mortar” of stratum corneum in which the corneocytes are embedded like “bricks”. This structure serves as the main barrier for diffusion of substances through the skin. Moreover, the process of delipidation is described (Ponec, M. 1992), where different lipids in stratum corneum were disturbed, resulting in altered “lipid cement” and loss of the barrier function. As for protein denaturation, Harding, C. R. (2004) concluded that surfactants which can strongly bind to protein in stratum corneum may lead to significant proteins denaturation, resulting in barrier damage. Stratum corneum hydration, delipidation and protein denaturation can all induce barrier deficiency. The permeability of substance into inner epidermis increases, potential irritants can thus contact directly with living keratinocytes. In some cases, irritants may penetrate deeper and reach dermis layer, where fibroblasts are exposed to chemical stimulation.

The second pathway to cause skin irritation is the direct effects of substances on living cells of the skin. Among them, several mechanisms have been reported.

1) Welss, T., et al. (2004) have reviewed a well-described mechanism of surfactant-induced irritation (Figure 16). Firstly, irritants interact with keratinocyte membrane, cause disruption of membrane integrity and release keratinocyte cytoplasm. The keratinocyte cytoplasm contains the pro-inflammatory cytokine IL-1 α , known as the switch to inflammatory cascade. IL-1 α further induces the secretion of other cytokines such as IL-6, IL-8, TNF- α and PLA₂ (phospholipase 2), causing a series of morphological alteration and finally create typical

symptoms of contact dermatitis. II) Another possible mechanism for chemical induced skin irritation is known as oxidative stress. When skin is exposed to endogenous and environmental pro-oxidant agents, Reactive Oxygen Species (ROS) can be produced. The imbalance between ROS and antioxidants can lead to an elevated oxidative stress level (Okayama, Y. 2005) which will damage cell membranes, DNA, sulphur-containing enzymes and proteins. Following process includes promotion of IL-1 α synthesis and inflammatory cascade. This process was confirmed by Zhao, J., et al. (2000), who found that a flavonoid antioxidant, silymarin can inhibit benzoyl peroxide (BPO)-induced skin edema, myeloperoxidase activity and IL-1 α level in epidermis, suggesting that the skin inflammation is caused by oxidative stress. Another evidence was given by Nakamura, Y. et al (1998), in their experiments, superoxide generation inhibitor 1'-Acetoxychavicol Acetate was proven to inhibit oxidative stress and inflammatory responses in mouse skin. III) Furthermore, in some cases, interaction between irritants and the cell membrane can modify the membrane fluidity, impact receptor-mediated signal transition and lead to skin irritation (Wells, T., et al. 2004; Zavodnik, I. B. 1997; Rosette, C., & Karin, M. 1996). Other examples such as alteration of the epidermal environment, modification of trans-membranous receptors by non-specific affinity of irritants might also result in an altered signal transduction leading to irritant response (Wells, T., et al. 2004; Chou, C. C., et al. 2003).

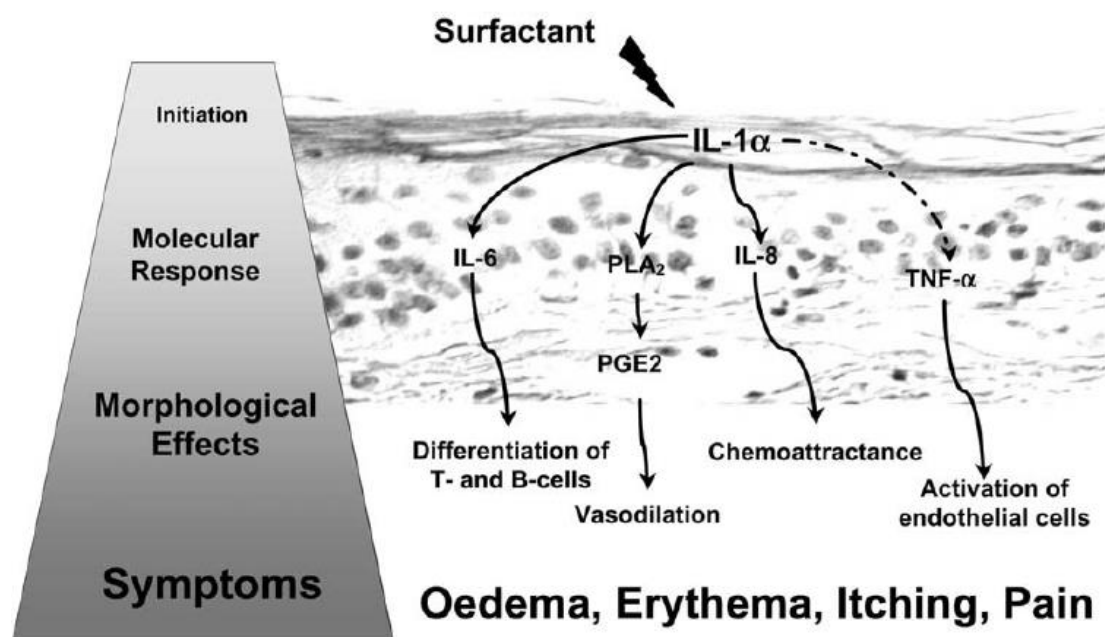


Figure 16: Skin irritation induced by surfactants. Proposed mechanism of the pathway: surfactants initiated the release of IL-1 α , subsequently leading to the induction of secondary mediators (molecular responses), followed by morphological alterations and, finally, the onset of typical symptoms of contact dermatitis (Wells, T., et al. 2004).

Mechanisms of irritation induce by direct effects of substances on skin cells can be summarized in Figure 17. Either by doing damage to epidermal cells or activating them, irritants can promote the release or formation of inflammatory mediators. Different inflammatory processes are therefore triggered (Corsini, E., & Galli, C. L. 1998).

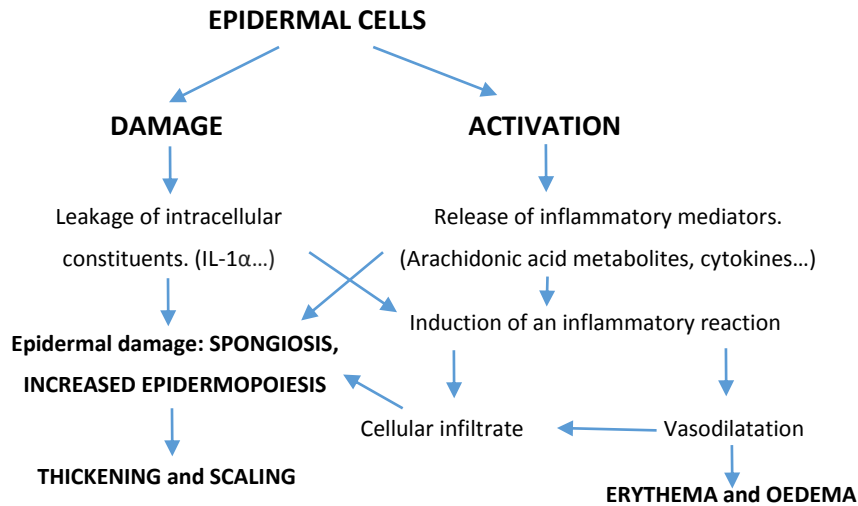


Figure 17: Sequence of events after application of skin irritant (Adapted from Corsini, E., & Galli, C. L. 1998).

2.4. Surfactant-induced skin irritation

The surfactant-induced irritation has been extensively studied. The physico-chemical properties of surfactants are believed to be the main factor to elicit skin irritation. It is suggested that binding of surfactants to keratin, concomitant protein denaturation and disruption of lipids resulting in swelling of the membrane are all directly related to induction of irritation (Effendy, I., & Maibach, H. I. 1995; Froebe, C. L. 1990). In general, a few anionic and cationic surfactants are believed to be potential irritants to the skin, whereas non-ionic surfactants are considered to have much less irritancy potential.

One typical anionic surfactant known as irritant is SDS. After 5% SDS patch test on upper back skin of healthy volunteers during 4 h, disturbances of barrier function, upregulation of epidermal fatty acid binding protein (E-FABP), increasing of cellular proliferation in the basal layer were observed in the followed 14 days, which indicates an irritation effects of SDS (Le, M., et al. 1995). Besides, SDS has been applied *in vivo* on human skin by 24 h patch test, the irritant responses were quantified by erythema and transepidermal water loss, results confirm the capacity of SDS to cause skin irritation (Wilhelm, K.P., et al. 1993). Actually, for its fast-acting, non-allergenic and consistent in its toxicity, SDS has already been recommended as reference irritant (Effendy, I., & Maibach, H. I. 1995). Concerning other types of anionic surfactant, Blake-Haskins, J. (1986) suggested that Linear Alkylbenzene Sulfonate (LAS) has an irritation potential with regards to its strong ability to swell collagen film. Sodium laurate was found to provoke erythema after 24h of skin application (Prottey, C., & Ferguson, T. 1975).

Several cationic surfactants have been identified to have potential irritation effect. Cetrimide is an antiseptic by mixture of different quaternary ammonium. Normally, 0.1%-1% cetrimide solutions are used for skin cleaning. However, a few cases were reported that cetrimide can cause contact dermatitis (Cruickshank, C. N. D., & Squire, J. R. 1949). In related studies,

Lansdown, A. B. G., & Grasso, P. (1972) observed severe mice skin damage caused by cetrimide. Dodecyl trimethyl ammonium bromide (DTAB) can induce erythema on human skin after 8 consecutive days of application on volunteer's forearm at 7.5% during 20 min (Wilhelm, K. P., et al. 1994). Apart from cetrimide, BenzAlkonium Chloride (BAC) and Stearyl Trimethyl Ammonium Chloride (STAC) were also found to possess higher irritation potential according to human patch test score (Lee, J. K., et al. 2000).

For zwitterionic surfactants, Cocoamidopropyl Betaine (CAPB) was compared to SDS and BAC, when applied to skin and CAPB induced less epidermal water loss than SDS (Berardesca, E., et al. 1990). However, CAPB was reported to have higher irritation potential than poly ethylene glycol (non-ionic surfactant) when cytotoxicity assays were carried out using human keratinocytes (Korting, H. C., 1994).

Basically, non-ionic surfactants were classified to have no irritancy potential. A most used non-ionic surfactant Tween 20 was reported by different groups. At 20 mM, it can neither induce significant trans-epidermal water loss nor change in erythema after 24 h occlusive exposure. Experiments on an *in vitro* EpidDerm™ skin model confirmed that 10% v/v Tween 20 isn't irritant (Kidd, D. A., et al. 2007). Other non-ionic surfactants, Brij 35, Tween 40 and Tween 60 were less toxic/ irritating compared to a series of cationics (Roccal, MAC, Emcol E607S...), anionics (Richonol A, Richonol T, Bioterge AS40) and amphoteric (Emery 6748A, Miranol C2M SF) (North-Root, H., et al. 1982). It is worth mentioning that the sugar-based surfactant, Alkyl polyglucoside, was found to induce no significant skin irritation even when it is applied onto human skin at concentration of 2% for 24h, which demonstrated the improvement in reduction of skin irritation achieved by development of novel detergents (Löffler, H., & Happle, R. 2003).

3. Cytotoxicity

Cytotoxicity defines the degree to which an agent possesses a specific destructive action on certain cells or the possession of such action (Dorland's Medical Dictionary for Health Consumers. 2007). For decades, surfactants' cytotoxicity against different cells (fibroblasts, keratinocytes) in distinguished models (2D models, 3D models) has been reported by various research groups (Arechabala, B., et al. 1999; Grant, R. L., et al. 1992; Vian, L., et al. 1995; Korting, H. C., et al. 1994; Yang, W., & Acosta, D. 1994). Evaluating surfactants' *in vitro* cytotoxicity is a simple and, to some extent, reliable way to predict their *in vivo* irritancy potential (Vian, L., et al. 1995; Tachon, P., et al. 1989) and this also helps to reduce animal tests with regards of the 3Rs principles (Replacement, Reduction and Refinement) which has already been embedded in national and international legislation regulating the use of animals in scientific procedures (Registration, Evaluation, Authorisation and Restriction of Chemicals, REACH. <http://ec.europa.eu>).

3.1. Cell structure

Eukaryotic cell is cell with a distinct, membrane surrounded nucleus. The structure of animal cells (eukaryotic cell) is presented in figure 18, some of the principle organelles' functions are presented in Table 6. Human body consists of about 200 types of different cells, each type of cell has its unique size, shape and biological function such as generation of energy, oxygen transportation, absorption of food. Together they maintain the whole human body.

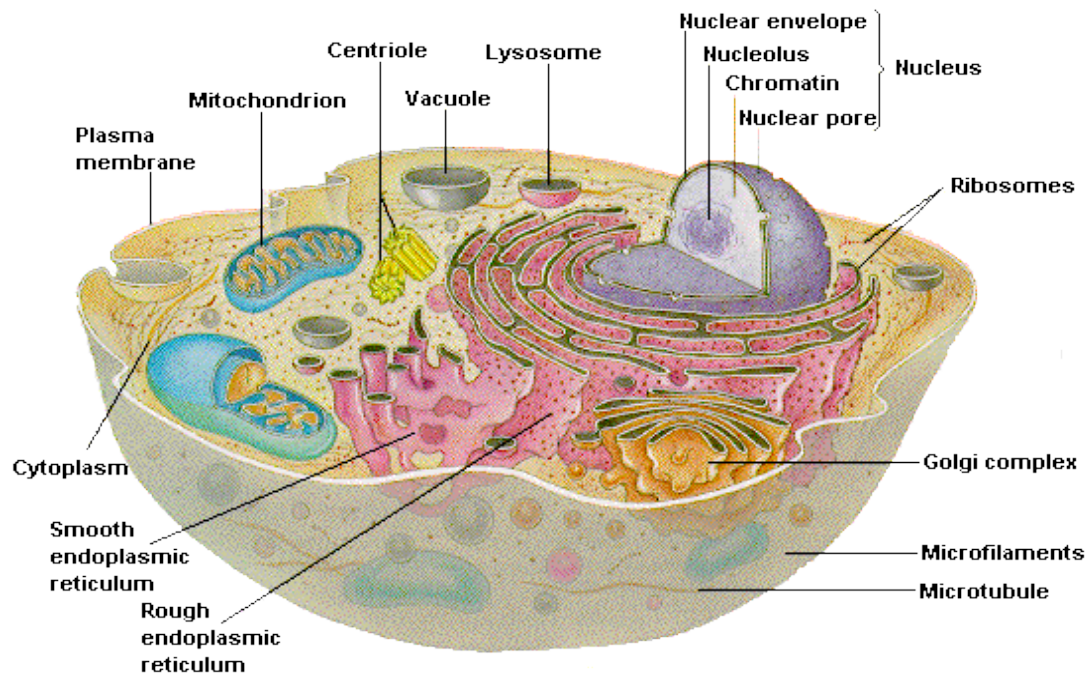


Figure 18: Anatomy of animal cell (<http://people.eku.edu/ritchisong/301notes1.htm>).

Table 6: Eukaryotic cell organelles and their functions (Adapted from <http://primarysourcescells.weebly.com/structure-and-functon-of-a-anmal-cell.html>; Lieberman, M., et al. 2006)

Organelle	Functions
● Cell membrane	Forms the outer covering of the cell, and is semi permeable
● Cytoplasm	Gel-like matrix where all the other cell organelles are expelled inside the cell
● Nucleus	Contains the hereditary material DNA and directs the activities of the cell
● Nucleolus	Structure within the nucleus and helps in synthesis of ribosomes
● Vacuole	Storage, transportation, helps to maintain homeostasis
● Endoplasmic Reticulum	Network of membranes composed of rough and smooth endoplasmic reticulum
● Golgi complex	Responsible for storing, packaging of cellular products
● Lysosomes	Enzyme sacs, digest cellular wastes
● Mitochondria	Site for cellular respiration and producers of energy
● Ribosomes	Made of RNA and proteins, sites for protein
● Microtubules	Hollow rods, function primarily as support and shape to the cell
● Centrioles	Organize the microtubules assembly during cell division
● Microfilament	Action in cytokinesis, amoeboid movement, and changes in cell shape

Eukaryotic cell behaviors include cell proliferation, migration, death... These behaviors can be regulated when chemical molecules are applied. For cytotoxicity evaluation specifically, it refers to the effects of chemical agents on cell proliferation and cell viability.

3.2. Cell cycle

The cell cycle (cell-division cycle) is the life cycle of a dividing cell. For most eukaryotes, cell cycle contains 2 gap phases (G₁, G₂), S phase and M phase (Figure 19).

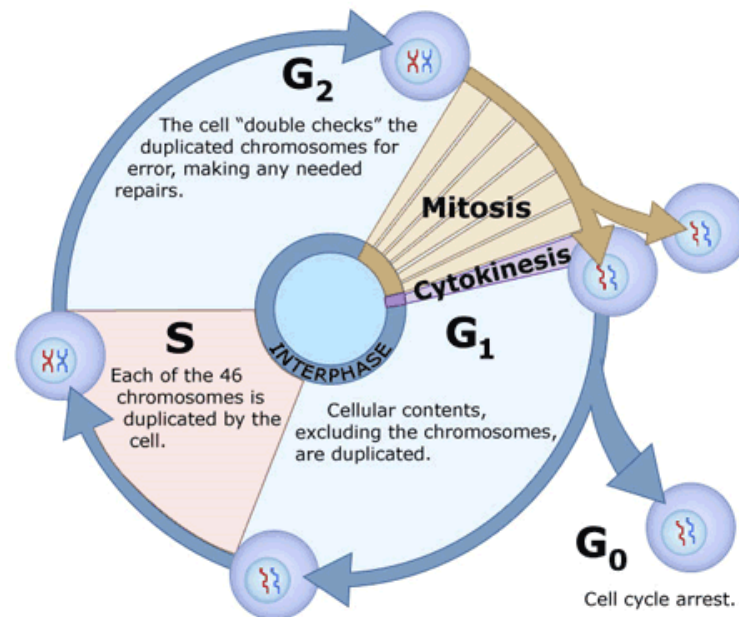


Figure 19: Schema of human cell cycle (*The cell cycle, mitosis and meiosis* <http://www2.le.ac.uk>).

G₁, S and G₂ phases together construct the interphase, which occupies approximately 80% of total time in cell cycle. During interphase, the cell grows and increases in size, stores energy and duplicates its chromosomes for cell mitosis (Alberts, B., et al. 1995). More specifically, after cell division, G₁ phase occurs firstly, protein supply and the number of organelles (mitochondria, ribosomes etc...) rise up. S phase starts when chromosomes in cells start their duplication: at the end of S phase, new strands of DNA identical to the original ones are synthesized. G₂ phase is the gap between S phase and M phase. During this period, doubled chromosomes are checked and repaired again to ensure correct cell division. Finally, in M phase, doubled chromosomes are divided into two parallel groups (mitosis) and then cell cytoplasm is separated to produce two daughter cells (cytokinesis). Apart from the 4 phases mentioned above, G₀ phase represents a quiescent state where neither cell division nor preparation of division is undergoing.

3.3. Cell death: apoptosis, necrosis, autophagy and cornification.

l) Apoptosis

Apoptosis is the process of Programmed Cell Death (PCD) that may occur in multicellular organisms (Green, D. R. 2011). It is considered as a vital component of various processes including normal cell turnover, proper development and functioning of the immune system, hormone-dependent atrophy, embryonic development and chemical-induced cell death (Elmore, S. 2007). Cells going through apoptosis can be characterized by nuclear fragmentation, condensation, chromosomal DNA fragmentation, blebbing and cell shrinkage, cells will eventually break into several apoptotic bodies with functional organelles (Figure 20). During the process, cell membrane maintains its integrity, no intracellular contents are released. In most cases, broken apoptotic bodies will be recognized and cleared out by phagocytes (Gewies, A. 2003). In some other conditions, when there are no phagocytes (*in vitro* culture conditions) or apoptotic cell bodies are not cleared out fast enough (in a solid organ etc...), apoptotic cells undergo secondary necrosis and become permeable. This results in releasing of damage associated molecular patterns and induces inflammation (Kono, H., & Rock, K. L. 2008).

l) Necrosis

Necrosis, on the contrary, is often considered as a form of passive cell death compared to apoptosis. In this case, it is caused by extracellular factors such as toxins, infection or trauma that result in the unregulated digestion of cell components. Cells going through the process of necrosis are characterized by a gain in cell volume (oncosis), swelling of organelles, plasma membrane rupture and subsequent loss of intracellular contents (Kroemer, G., et al. 2009) (Figure 20). Since the cytoplasmic contents of necrotic cells which include lysosomal enzymes will eventually be released to extracellular environment, they can always cause inflammatory response. In recent studies, however, necrosis serving as a form of cell death in physiological processes or regulated events was discovered. It is believed that in some cases, necrosis can be also regarded as a form of programmed cell death (Proskuryakov, S. Y., et al. 2003). For example, cell necrosis was found to contribute to normal cell loss in mammalian small intestine together with cell apoptosis (Mayhew, T. M., et al. 1999). Another example concerns the loss of interdigital cells in the mouse embryo, a paradigm of programmed cell death. When apoptosis was inhibited genetically or by drugs, interdigital cell death, although delayed, can still proceed due to necrosis pathway (Chautan, M., et al. 1999). These results demonstrate that necrosis can occur both during pathological processes and normal processes (Proskuryakov, S. Y., et al. 2003).

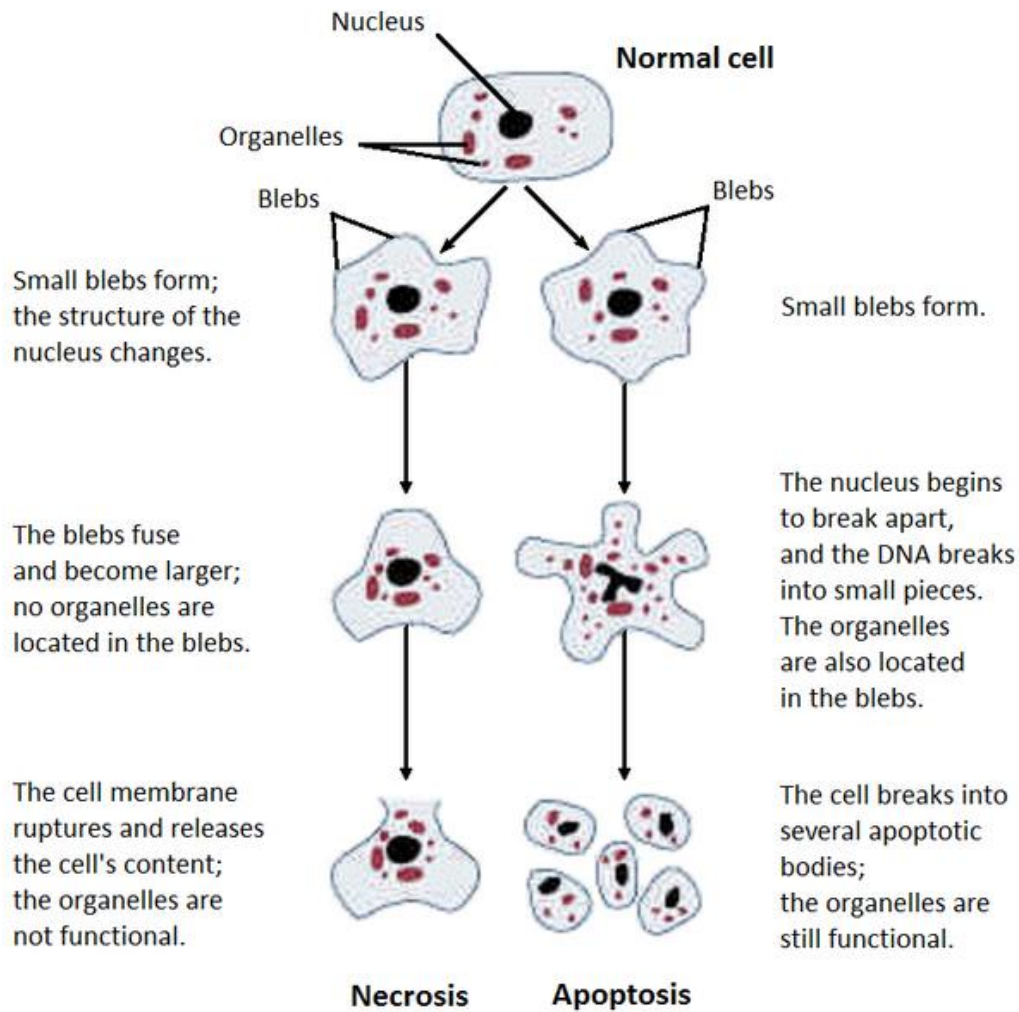


Figure 20: Structure changes of cells undergoing apoptosis or necrosis (Goodlett, C. R., & Horn, K. H. 2001).

II) Autophagy

Autophagy is a catabolic process involving the degradation of cell's own components through lysosomal machinery. It is an essential process to maintain a balance between the synthesis, degradation and subsequent recycling of cellular products (Chen, G. G., & Lai, P. B. 2009). In general, autophagy is characterized by sequestration of bulk cytoplasm and organelles in double or multimembrane autophagic vesicles, and their delivery to and subsequent degradation by the cell's own lysosomal system (Gozuacik, D., & Kimchi, A. 2004). The breakdown products following autophagy can be reused by surrounding cell system to produce new proteins or to generate energy (Rabinowitz, J. D., & White, E. 2010). It is a very important process to maintain cells' survival under low nutrition conditions and fight against different diseases such as cancer, neurodegeneration, bacterial and viral infection... (Gozuacik, D., & Kimchi, A. 2004; Sarkar, S. 2013). Autophagy can be classified into 3 types, macro-autophagy, micro-autophagy and chaperone-mediated autophagy. Among them, macro-autophagy involves engulfment of cytoplasmic materials (proteins and organelles) by a double isolation membrane, formation of autophagosome by vesicle elongation, docking and fusion between

autophagosome to form autolysosome and digestion of autophagic cargo by lysosomal proteases (Figure 21).

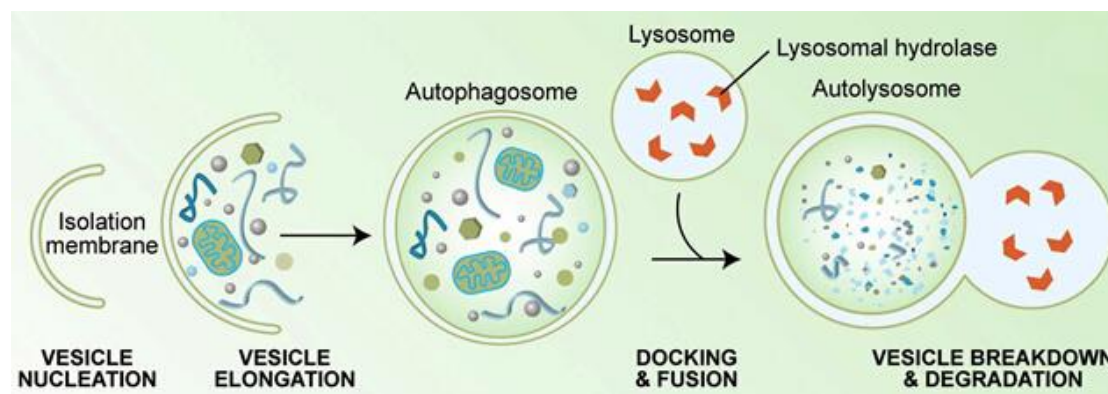


Figure 21: Schema of macro-autophagy process (<http://medschool.umaryland.edu/fadenlab/autophagy.asp>).

III) Cornification

Cornification is one specific type of programmed cell death in epidermal keratinocytes so as to form the outmost skin barrier. It comprises three key elements: the replacement of intracellular organelles and intracellular content by a compact proteinaceous cytoskeleton, the cross-linking of proteins at the cell periphery to form a cornified cell envelope, the linkage of corneocytes into a multicellular, functional but biologically dead structure (Eckhart, L., et al. 2013).

3.4. Surfactant-induced cytotoxicity

As a result of regulations to reduce use of animals in biological experiments, more and more test methods have been developed to assess cytotoxicity of chemical agents against *in vitro* models. Simple cell models are easy to establish, they often give out reproducible results and can help to reduce expenses in the early stages of risk evaluation. Therefore, surfactant cytotoxicities on different cells has been reported by various groups. Some of them are believed to correspond with surfactant *in vitro* toxicity effect, other preliminary cytotoxicity results can be used as references for later experiments.

The neutral red uptake (NRU) bioassay has been used to measure the cytotoxicity effects of about 30 surfactants on rabbit cornea derived SIRC cell line (Roguet, R., et al. 1992): they observed a cytotoxicity effects of surfactants in the order of cationic, anionic, amphoteric, non-ionic (from most cytotoxic to least cytotoxic). The results correlate well with *in vivo* results. They believe this method is effective for predicting eye irritancy without the use of animals. In a test concerning primary cultures of rabbit corneal epithelial cells, methods of morphological observation, NRU and mitochondrial 3-(4,5-dimethylthiazol-2-yl)-2,5-diphenyl tetrazolium bromide (MTT) reduction were used to detect the cytotoxicities of different surfactants (Grant, R. L., et al. 1992). Results indicated the cytotoxicity levels of different surfactants (cytotoxicity: cationic > anionic or amphoteric > non-ionic). They also found that the Lactate DeHydrogenase

(LDH) leakage test is suitable for prolonged cell injury assessment. Tests on other cell lines, such as mouse fibroblasts L929, were carried out by Vian, L., et al. (1992). However, they didn't observe a marked correlation between *in vivo* ocular irritancy data with NRU/MTT/total protein content determination (TPC) tests of 20 surfactants. The cytotoxicity of different surfactant-single walled carbon nanotube conjugates on human astrocytoma cells were evaluated by phase contrast and epifluorescence microscopy observation (Dong, L., et al. 2009). They discovered that the conjugates' cytotoxicity is based on the surfactants component. Specifically, SDS and Sodium DodecylBenzene Sulfonate (SDBS) are believed to be toxic to cells and their correspondent conjugates with carbon nanotubes presented high cytotoxicity.

The mechanisms of surfactant induced cytotoxicity are not quite clear yet, but the possible interactions between surfactant and cell membrane are believed to play an important role in cell death. The matrix of the plasma membrane of mammalian cells is organized as lipid bilayer consists of phospholipids, sphingolipids, glycolipids and cholesterol. Proteins serving as receptors and transporters are embedded in this bilayer for cell function. In this context, surfactant molecules with amphiphilic properties can influence membrane integrity through binding to different sites of membrane or enclosing lipids in micelles. The situation when cell membrane is exposed to increasing concentration of surfactant was explained (Jones, M. N. 1992) (Figure 22). Surfactant will firstly bind to the membrane bilayer due to their hydrophobic affinity until a saturation state is reached. With addition of surfactant to a concentration higher than its CMC, cell membrane lyses, leading to disruption and solubilization concomitant the formation of lipid-protein-surfactant complexes. At sufficient high concentration, lipids in the complexes will move to surfactant micelles, an equilibration is then established between protein-surfactant complexes, lipid-surfactant micelles and surfactant micelles. In others' research works (Partearroyo, M. A., et al. 1990), two distinct mechanisms to induce cell death by surfactant have been discussed, at low surfactant concentrations, incorporation of surfactant monomers into the cell membranes can impair their barrier function; at high concentrations near the CMC, the bilayer-micelle transition may take place and cause lysis of cell membrane.

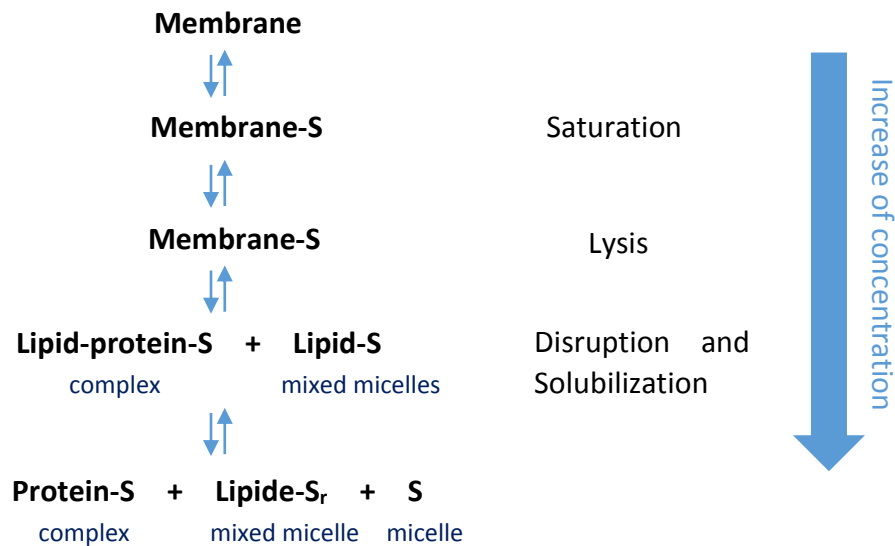


Figure 22: Schematic representation of the sequence of events arising on exposure of a bio-membrane to increasing amounts of surfactant, *S*: surfactant (Adapted from Jones, M. N. 1992).

Apart from influence of surfactant on cell bilayer, some of them possess ability to denature proteins. It is generally believed that non-ionic surfactants do not denature proteins whereas anionic and cationic surfactants do so at very low concentrations, often well below their CMC (Otzen, D. 2011). Among them, SDS is a typical surfactant denaturant, when considering the minimal concentration to denature proteins, it is 500-1000 times more effective than commonly used denaturant urea or guanidinium chloride (Magdassi, S. (Ed.). 1996). The mechanism of surfactant-globular protein interaction was studied (Figure 23). Firstly, ionic surfactant molecules bind their head group to the ionic sites of the protein, which may induce protein unfolding and exposition of many more hydrophobic binding sites previously buried in the core of the tertiary structure. The saturation of all potential binding sites is generally completed as the free surfactant concentration approaches the CMC (Jones, M. N. 1992; Dickinson, E. (Ed.). 1991).

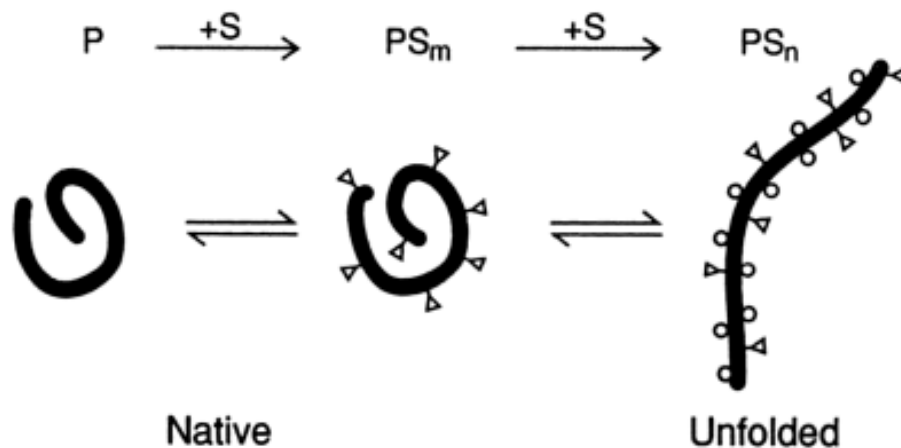


Figure 23: The binding of surfactant ligands S to the native state of a protein P and surfactant induced unfolding. S : surfactant, S_m : surfactant bound to ionic site of protein, S_n : surfactant bound to hydrophobic site of protein (Dickinson, E. (Ed.). 1991).

4. *In vitro* models for skin related cytotoxicity or irritation tests

Tests on *in vivo* animals have long been used as means to predict chemicals' potential damage to human health. These methods, however, are at the expense of animal welfare. With regard to the rise of ethical and scientific concerns, there is a great need to develop alternative *in vitro* test methods to prevent or minimize experiments on animals and to screen large quantity of new chemicals prior to further more complexed tests. In these circumstances, the European Union Reference Laboratory for alternatives to Animal testing (EURL-ECVAM) has been established in 2011 so as to validate new methods which Reduce, Refine or Replace (3R) the use of animals for safety testing and efficacy/ potency testing of chemicals, biologicals and vaccines (<https://eurl-ecvam.jrc.ec.europa.eu>). In the meantime, different methods have been developed by organizations and laboratories worldwide and their results were compared with *in vivo* data.

4.1. Primary and continuous cell cultures

There are 2 types of cell cultures. Primary cell culture refers to the maintenance of growth of cells derived directly from parental tissues by mechanical or enzymatic dissociation. In this condition, primary cells have a finite life span and are very heterogeneous in the beginning of culture. On the contrary, cell lines have at least one passage, which means transfer of cells from one culture vessel to another one. For example, primary cells undergoing subculture through cell passage are then called cell line. Cell lines can either be finite or infinite. Finite cell lines can only go through limited passage whereas infinite cell lines can be propagated indefinitely because they are transformed cells, tumor cells or become tumor cells after specific treatment (i.e.: separation of spontaneous or induced mutated cells; introduction of gene to deregulate the cell cycle, expression of proteins for cell immortality).

For maintenance of cells, two culture models are used. Monolayer cultures usually refer to cells that need to attach to the bottom of culture vessel in order to grow and proliferate. Suspension cultures are mainly used for cells from blood system such as lymphocytes.

4.2. 2D cell models

Adherent cells grown on substrates such as glass or polystyrene, forming single cell monolayer in 2 dimensional surface is known as 2D cell models. 2D cell culture models are relatively easy to establish compared to more complexed *in vitro* or *in vivo* models. Tests on these models are usually less expensive, easier to manipulate, faster and can present reproducible results. Therefore, they are often used for cytotoxicity tests, drug screening or cell based bioassays in early stages of research works.

For skin related cytotoxicity tests, fibroblasts and keratinocytes are the most used cells because they are the major cells in dermis and epidermis. Human fibroblasts, either under the form of primary cells or cell lines have been cultured for the cytotoxicity evaluation of surfactants, resins, nanoparticles, metal salts, etc... (Geurtsen, W., et al. 1998; Tian, F., et al. 2006; Ding, L., et al. 2005; Rothenberg, M. E., et al. 1989; Cooper, M. L., et al. 1991; Anane, R., & Creppy, E. E. 2001). Similarly, keratinocytes cultured in 2D conditions are proven technique for preliminary skin irritation tests (Shvedova, A., et al. 2003; Kumar KC, S., & Müller, K. 1999; Ball, N., et al. 1996; Cooper, M. L., et al. 1991).

For animal cells, an immortal cell line - L929 (mouse connective tissue fibroblast cells) is broadly chosen. It is the cell line recommended by ECVAM for basal cytotoxicity assay (<http://ecvam-dbalm.jrc.ec.europa.eu/beta/index.cfm/methodsAndProtocols/index>) and is considered in validated methods to assess acute systemic toxicity (City, H. R. C. 2000). Indeed, L929 cells have been used to study the cytotoxicity of different surfactants (Tween 20, Span 20, CTAB etc...), nanoparticles (molybdenum nanoparticles...) and ions (Pb, Cu, Ni, Co, Zn...) (Vian, L., et al. 1995; Siddiqui, M. A., et al. 2015; Okazaki, Y., & Gotoh, E. 2013).

4.3. 3D cell models

2D cell models, despite their pivotal role in understanding of various biological activity, have multitude inadequacies, especially with respect to their inability to emulate *in vivo* conditions and providing physiological relevance (Sanyal, S. <http://www.corning.com>). More specifically, 2D cell models can not represent the native morphology of cells in tissues and their cell-cell or cell-extracellular matrix (ECM) interactions are strictly limited (Zang, R., et al. 2012). These limitations result in poor predictive power of preclinical cell-based drug and toxicity screening assays. Therefore, 3D cell models have been developed to fill the gap between 2D models and *in vivo* models. Generally speaking, 3D culture models can be grouped into the study of organotypic explant cultures, cell spheroids, cells cultured in scaffold and tissue-engineered models (Pampaloni, F., et al. 2007; Rosenstein, J. M., et al. 2003).

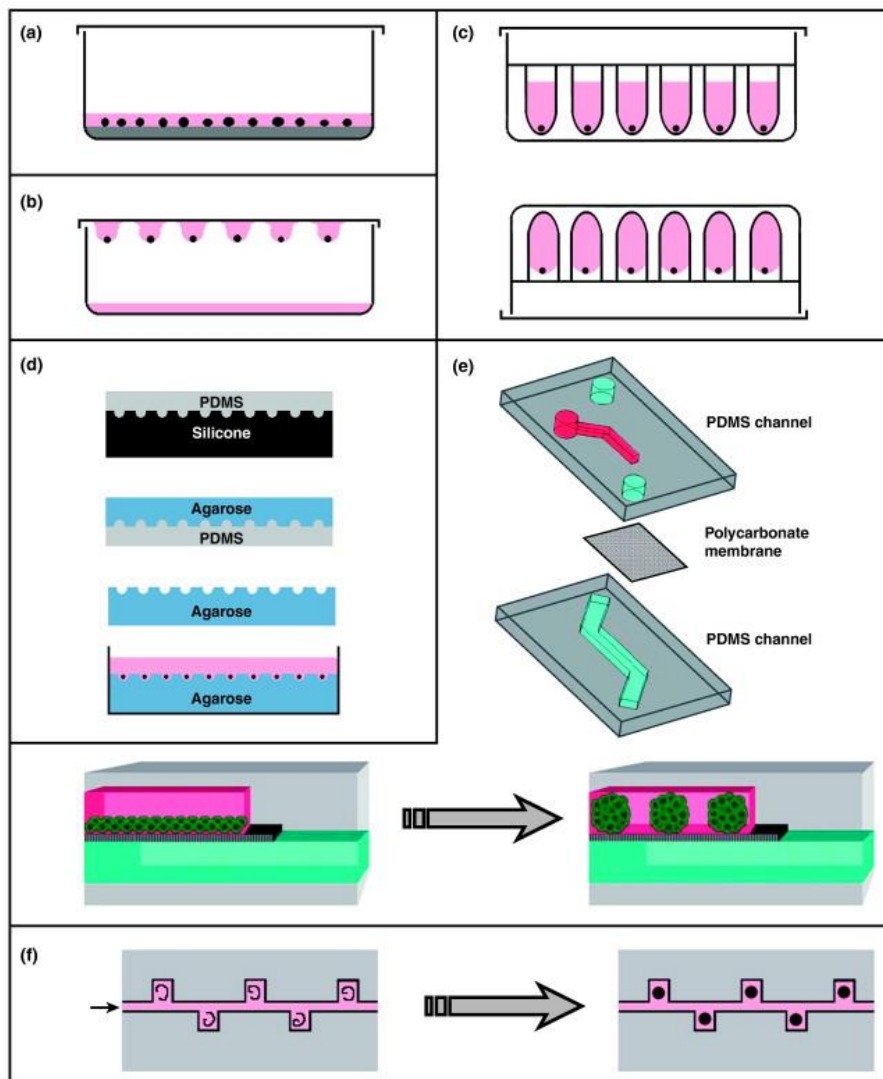
I) Organotypic explant cultures

Organotypic explant fills the gap between dissociated cell culture systems and *in vivo* animal models. It allows the study of cells *in situ* compared to dissociated cell culture, in the meantime, it can be more efficient (in terms of time and resources) and controllable (in terms of microenvironment) than *in vivo* studies. Organotypic explant cultures are used when an absolute requirement for tissue-specific information is needed (Bull, N., et al. 2011; Haycock, J. W. 2011). A common application of this culture model is the explant of brain or neuron to study their physiology (Woodward, M. N., et al. 2000). These models are also widely used in skin related tested. To assess skin irritation, animal or human skin explants are cultured in an air-liquid interface and exposed to testing chemicals for a short period. The leakage of intracellular enzymes (for example, aspartate aminotransferase, alanine aminotransferase, lactate dehydrogenase) or release of various hydroxy fatty acids (13-HODE, 9-HODE, 12-HETE or 15-HETE) can be used to provide endpoints for the evaluation of skin toxic (Van de Sandt, J., et al. 1999). To maintain this culture model, environmental factors such as temperature, culture medium, culture substrates, O₂ level and pH should be precisely controlled. Main advantages of these models are that the cells within are well differentiated and the organ architecture is maintained (Haycock, J. W. 2011).

Disadvantages of these models include limited recording time for each individual organ and variation of test results when comparing experiments performed on different days.

II) Cellular spheroids

Cellular spheroids are simple 3D models that can be generated from a wide range of cell types without scaffolds. Techniques to create cellular spheroids include liquid overlay technique (LOT), hanging drop technique, microwell hanging drop technique, antiadhesive substrate technique and microfluidic spheroid formation. Their principles are presented in Figure 24.



TRENDS in Biotechnology

Figure 24: Spheroid fabrication methods: a) liquid overlay technique; b) hanging drop technique; c) microwell hanging drop technique; d) microwell array from micropatterned agarose wells; e,f) microfluidic spheroid formation. PDMS (Polydimethylsiloxane) (Fennema, E., et al. 2013).

Liquid overlay/ cell suspension culture: by stirring large volume of culture medium, cellular aggregates can be formed in the suspension. Hanging drop method: cell aggregates will form automatically in drops hanging from a surface. Microwell arrays: this method refers to formation of cellular aggregates in round-bottom nonadherent wells or plan surface (for example, formation of cellular aggregates onto plan/ round-bottom agarose substrate). Microfluidic: different microfluidic channels are used to promote the formation of cellular aggregates (Fennema, E., et al. 2013).

Main advantage of cellular spheroid models compared to cell cultured in 2D surface is that this model includes 3 dimensional cell-cell interactions and better mimic *in vivo* situations. However, since no ECM components like collagen, elastin, proteoglycans are used in these models, the cell-ECMs interaction are weaker than *in vivo* models. More importantly, these

models are not suitable for our purpose of establishing a skin-like cell culture models where collagen gel is an important component in the dermal layer.

III) Cells cultured in scaffold

To study the cytotoxicity of chemicals against fibroblasts, the main cells in dermal layer, a simple but effective 3D model has been established. In this model, fibroblasts are completely surrounded by collagen gel, which forms a 3D fibrous network (Cukierman, E., et al. 2002). This model not only preserves the mechanical properties that mimic connective tissues *in vivo* by cell-cell and cell-ECM interactions, but also enhances cellular signal transduction than in monolayer cell models (Grinnell, F. 2000; Cukierman, E., et al. 2002). Therefore, it is an ideal model for study the cellular response to different stimulations (Awang, M. A., et al. 2014). More importantly, this fibroblasts embedded into collagen gel system can activate keratinocyte outgrowth onto it, thus creates the possibility of modeling skin of both dermal and epidermal layers (Tuan, T. L., et al. 1994). In other models, matrix can also be formed by natural derived polymer materials such as fibrin, fibroin, glycosaminoglycans (GAGs) hydrogel or by synthetic polymers such as poly(glycolic acid) (PGA), poly(lactic acid)(PLA), each of them provide unique mechanical and biological properties for 3D cell culture (Haycock, J. W. (Ed.). 2011).

The systems of cells cultured in scaffold enable both 3 dimensional cell-cell interactions and cell-ECM interactions. They are good model for skin-related cytotoxicity tests.

IV) Tissue engineering: reconstituted human epidermis

Tissue engineering is an interdisciplinary field that applies the principles of engineering and life sciences toward the development of biological substitutes that restore, maintain, or improve function or a whole organ (Vacanti, J. P., & Langer, R. 1999). Besides their medical applications, tissue engineered cell cultures can be used as validated models for *in vitro* physiological studies. Investigation of dermal, epidermal cell behaviors in a condition similar to their *in vivo* environment is becoming more and more important in recent years for the aim to reduce animals used in experiments. To understand chemicals' effects against human skin, tissue engineered cell culture models with distinct complexity were developed.

Stratum corneum serving as skin barrier plays an important role when assessing the effects of chemicals on its inside cells. Although *in vitro* tests with monolayer keratinocytes or fibroblasts have shown a good correlation with the irritating effects observed *in vivo*, the concentrations inducing irritation in these cell cultures are usually several orders of magnitude lower than those which induce irritation *in vivo* (Van de Sandt, J., et al. 1999). This situation promoted the development of human skin equivalent or reconstructed human skin models, where differentiated keratinocytes at air-liquid interface resemble human skin to a large extent. Commercially available human skin equivalents are produced by different companies such as the EpiDerm™ of Mattek, Leiden epidermal skin model of Biomimiq and SkinEthic of L'Oréal (Figure 25) (<http://www.mattek.com>; <http://www.biomimiq.com>;

<http://www.episkin.com>). In these three models, normal human keratinocytes are cultured on an inert polycarbonate filter with a chemically defined medium. Different laboratories have also succeeded in creating differentiated keratinocytes on support like fibroblasts embedded collagen gel (full thickness human skin equivalent) or fibroblasts gown on a nylon mesh, see Table 7. (Bell, E., et al. 1991; <http://www.episkin.com>; Contard, P., et al. 1993).

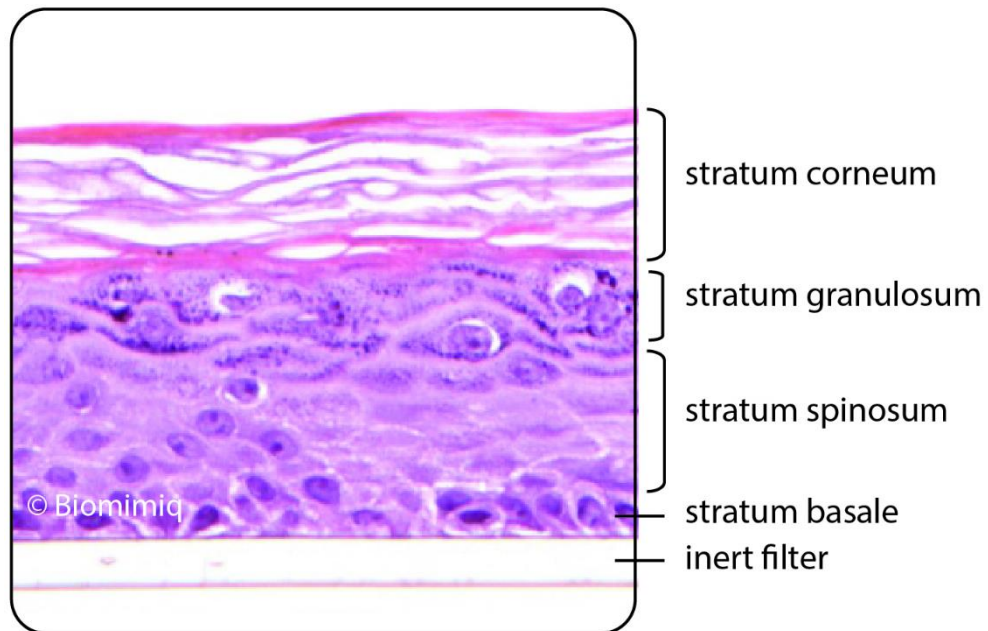


Figure 25: Leiden epidermal skin model (<http://www.biomimiq.com>).

Table 7: Reconstituted human epidermis by different companies and research groups.

Company/ Research groups	Name	Cells	Substrate
Mattek	EpiDerm™	Keratinocytes	Inert polycarbonate filter
Biomimiq	Leiden epidermal skin model	Keratinocytes	Inert polycarbonate filter
L'Oréal	SkinEthic	Keratinocytes	Inert polycarbonate filter
Bell, E., et al. 1991;	N.A	Keratinocytes	Collagen gel embedded with fibroblasts
Mattek	EpidermFT	Keratinocytes	Collagen gel embedded with fibroblasts
Contard, P., et al. 1993	N.A	Keratinocytes	Nylon mesh with fibroblasts

C) Objectives

As presented in Chapter I, novel sugar-based non-ionic surfactants are of great potential as substitutes of currently used petrol-derived surfactants. They have shown interesting surface-active properties and synthesis of these surfactants with renewable natural building blocks can reduce the use of hazardous substances. Some sugar-based surfactants are reported to have relatively higher biodegradability and less toxicity to different organisms. More importantly, a number of sugar-based surfactants are identified to have weak cytotoxicity effect against human cells and are non-irritants, they may therefore be applied in detergent productions, cosmetic formulations, food industries, pharmaceutical researches... In this context, to the aim of valorizing biomass-derived surfactants, our objectives can be grouped into three major parts.

1. Pre-selection of synthesized sugar-based surfactants and their physico-chemical properties.

Different molecules, containing a hydrocarbon chain linked to a glucose or maltose head through an amide functional group are synthesized. These sugar-based surfactants, characterized by gradual structure modifications, will be firstly distinguished according to their solubility and ability to reduce surface tension of water solutions. After first-step selection, potential candidates with high water solubility and strong ability to reduce water surface tension will be synthesized in larger quantities. Their surface-active properties, CMCs, Krafft points and self-assembling properties will be characterized. Their behavior in both water and in culture medium will be investigated.

2. Establishment of cell/ tissue models and surfactant's cytotoxicity/ irritant effects on those models.

To predict effects of surfactants on cells/ tissues of human skin (potential application), three *in vitro* models will be used: 2D cell culture model (L929 cell monolayer), 3D cell culture model (L929 cells embedded into collagen gel) and 3D tissue culture model (reconstituted human epidermis). Cytotoxicity effects of surfactants on the 3 models will be evaluated by different methods and compared. The irritancy potential of surfactants on reconstituted human epidermis will also be assessed.

3. Analysis of results, relationship between structures/ physico-chemical properties of surfactants and their cytotoxicity.

According to the results obtained from experiments, the possible relationship between structure/ physico-chemical properties of surfactants and their cytotoxicity will be evaluated and compared to previous published work.

Chapter II: Materials and Methods

A) Materials

Materials used are listed in Table 8:

Table 8: Materials used in experiments and their origins (part 1).

Origin	Product
Corning Life Sciences, France	Costar® Cell culture plates 6 well, 24 well and 96 well. Falcon® 75cm ² cell culture Flasks,
eBioscience, France	Human IL-1alpha Platinum ELISA.
Enso Lifescience, France	Hecameg® (purity: ≥99%).
Laboratoire de Glycochimie, des Antimicrobiens et des Agroressources of Université de Picardie Jules Verne, France	Glu1amideOC8, Glu1amideOC10, Glu1amideC8, Glu1amideC10, Glu6amideC8, Glu6amideC10, Glu6amideC8', Glu6amideC10', Mal1amideC8, Mal1amideC10.
Life Technologies, France	0.25 % Typsin-EDTA, Click-iT® EdU Alexa Fluor® 488 Imaging kit, DMEM (Dulbecco's modified Eagle's medium), FBS (fetal bovine serum), Gibco® Collagenase Type I, HBSS (Hank's Balanced Salt Solution), L-glutamine 100X, MEM 10X, Penicillin/ Streptomycin 100X.
MARIENFELD-superior, Germany	Malassez hemocytomer.
MATTEK, Slovakia	EpiDerm™ EPI-200-SIT kit (Human Skin Equivalent).
Promega, France	MTS (3-(4,5-dimethylthiazol-2-yl)-5-(3-carboxymethoxyphenyl)-2-(4-sulfophenyl)-2H-tetrazolium) assay kit (CellTiter® 96 Aqueous One Solution Cell Proliferation Assay).
RAL Diagnostics, France	Eosin Y (yellow).

Table 8: Materials used in experiments and their origins (part 2).

Sigma-Aldrich, France	Bovine Serum Albumin lyophilized powder ($\geq 98\%$), Collagen I solution from bovine skin, DAPI, ECACC Cell Lines - L929 mouse fibroblasts, Ethanol, EUKITT [®] mount medium, Formaldehyde solution ($\geq 36.5\%$ in H ₂ O), Hematoxylin Sodium dodecyl sulfate (98%), Trypan blue solution, Tween [®] 20 ($\geq 97\%$).
Thermo Scientific, France	Nunc [™] Polycarbonate Membrane Inserts in 6 dishes, Superfrost [™] Ultra Plus Adhesion Slideslide.
VWR Chemicals, Australia	O.C.T. Compound

The complete DMEM was prepared as follows: 90% v/v DMEM, 10% v/v FBS, 100 U/mL penicillin, 100 $\mu\text{g}/\text{mL}$ streptomycin and 2mM L-glutamine.

B) Sugar-based surfactants and their physico-chemical properties, pre-selection of surfactants for biological tests

1. Synthesis of sugar-based surfactants

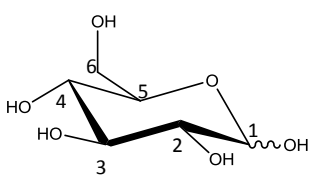
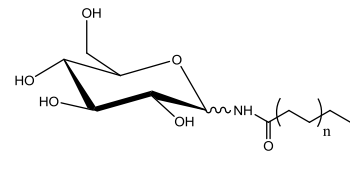
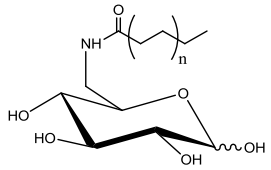
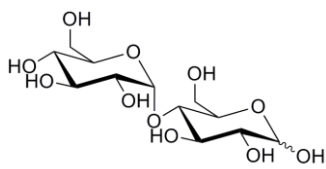
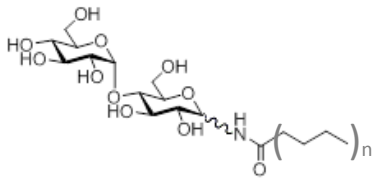
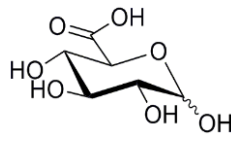
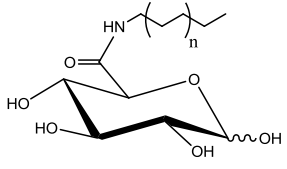
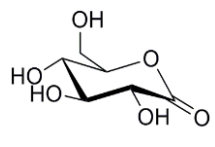
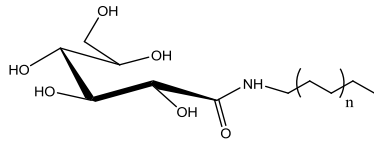
Sugar-based surfactants were synthesized and provided by the partner of the AMPHISKIN project (Miao Yong, post-doctoral fellow, Laboratoire LG2A, UPJV, Amiens). The synthesis will be briefly presented below for each family of molecule studied. The details of optimized syntheses are presented in Appendix 1.

Sugar-based surfactants (glycolipids derivatives) belonging to different families and characterized by structural variability were chosen in order to investigate possible relationships between structural elements and functional properties. 10 different molecules, containing a hydrocarbon chain linked to a glucose or maltose head through an amide functional group, and belonging to three families, which syntheses are already described in the literature, were identified (Table 9):

- I) N-acyl amino-glucose or amino-maltose derivatives substituted in position C-1 and N-acyl amino-glucose derivatives substituted in position C-6, all bearing C8 or C10 alkyl chains
- II) Glucuronamide derivatives substituted with a C8 or C10 hydrocarbon chain
- III) Gluconamide derivatives substituted with a C8 or C10 hydrocarbon chain

These surfactants were first provided in small quantity for preliminary analysis (batch 1). Afterwards, selected surfactants were synthesized in larger quantity, their physico-chemical properties and biological effects were evaluated (batch 2).

Table 9: Families of synthesized sugar-based surfactants.

Substrate	Position	Junction	Hydrocarbon Chain		Developed formula
			C8	C10	
 D-Glucose	1	NHC(O)R	C8	C10	
	6	NHC(O)R	C8	C10	
 D-Maltose	1	NHC(O)R	C8	C10	
 D-Glucuronic acid	6	C(O)NHR	C8	C10	
 D-Gluconolactone	1	C(O)NHR	C8	C10	

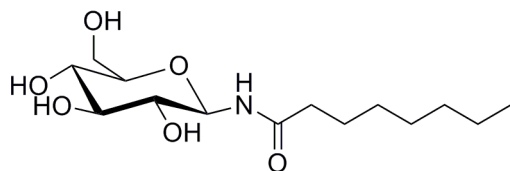
As seen in Table 9, these synthesized molecules can be classified according to 4 parameters. I) Length of carbon chain, these molecules possess either a C8 chain or a C10 chain; II) position of junction, carbon chain is attached to 1' end or 6' end of its corresponding sugar head through an amide group; III) orientation of amide group, carbohydrate scaffold or alky chain bears the carbonyl of amide group; IV) type of sugar head, these molecules carry either

glucose head or maltose head. Their synthesis routes are briefly described below.

1.1. *N*-acyl amino glucose and maltose derivatives substituted in position 1:

I) *N*-Octanoyl- β -D-glucopyranosylamine

Abbreviation: Glu1amideC8

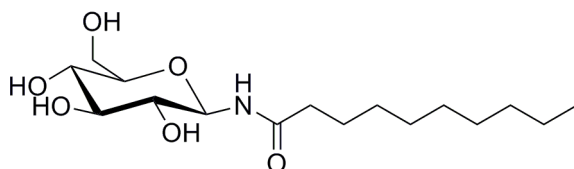


CAS: 134403-86-4

MW: 305.37

II) *N*-Decanoyl- β -D-glucopyranosylamine

Abbreviation: Glu1amideC10

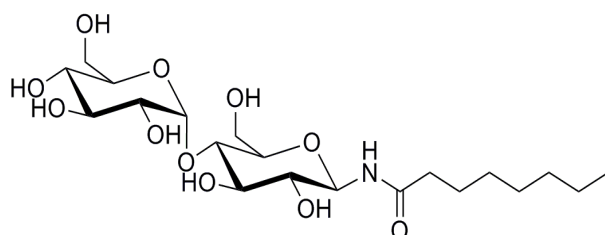


CAS: 101442-68-6

MW: 333,42

III) *N*-Octanoyl -4-*O*- α -D-glucopyranosyl- β -D-glucopyranosylamine

Abbreviation: Mal1amideC8

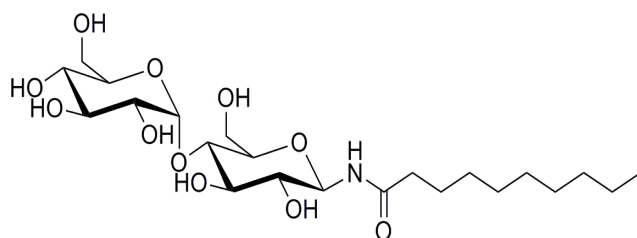


CAS: 161296-88-4

MW: 467,51

IV) *N*-decanoyl -4-*O*- α -D-glucopyranosyl- β -D-glucopyranosylamine

Abbreviation: Mal1amideC10



CAS: 161296-89-5

MW: 495,56

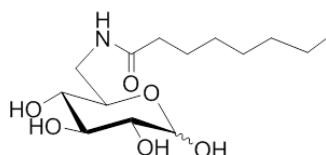
The synthesis of these four derivatives follows the same pathway. It involves a 2-step procedure similar to the one described by Lubineau, A., Augé, J., & Drouillat, B. (1995). In the first step, glucosylamine and maltosylamine derivatives are obtained by substituting the anomeric hydroxyl group of D-glucose and D-maltose with an amino group. In a second step, the amino derivative reacts with octanoyl or decanoyl chloride in order to graft the alkyl chain

to the polar head group. After evaporation of the solvent (MeOH), the products are purified by reverse C18 phase flash chromatography or on a silica gel column (CH₂Cl₂/MeOH:4/1). The purity of the products (estimated higher than 95%) was verified by ¹H and ¹³C RMN. No trace of other potentially amphiphilic carbon bearing molecules was detected.

1.2. N-acyl amino glucose derivatives substituted in position 6:

I) 6-deoxy-6-octanamido-D-glucopyranose

Abbreviation: Glu6amide C8'

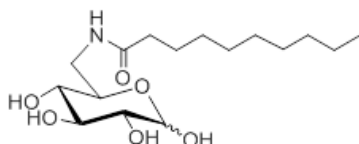


CAS: 189503-43-3

MW: 305.37

II) 6-deoxy-6-decanamido-D-glucopyranose

Abbreviation:



Glu6amideC10'

CAS: 916461-03-5

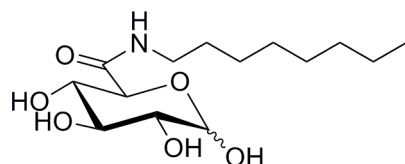
MW: 333.4

The obtention of an alkylcarboxamide group in position 6 is much more challenging than in position 1. The synthesis is long and required 6 steps starting with D-glucose as the substrate (see Appendix 1) in order to selectively substitute the hydroxyl group in position 6 (the hydroxyl group in position 1 has to be protected). It involves 6-azido-6-deoxy-1,2-*O*-isopropylidene- α -D-glucopyranose as a key intermediate. The reaction product was purified on a silica gel column (CH₂Cl₂ / MeOH 8.5:1.5) to give a white solid. The purity (estimated higher than 95%) was verified by ¹H and ¹³C RMN. The synthesis (with different steps) and amphiphilic properties of the octyl derivative were first described by Maunier, V., et al. (1997).

1.3. Glucuronamide derivatives:

I) N-octyl-D-glucopyranuronamide

Abbreviation: Glu6amideC8



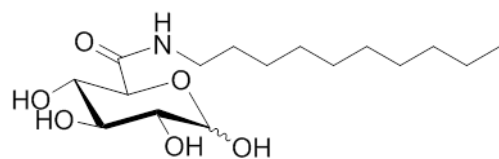
CAS: 78798-01-3

MW: 305.37

CAS : 1263382-58-6 (β derivative)

II) N-decyl-D-glucopyranuronamide

Abbreviation: Glu6amideC10



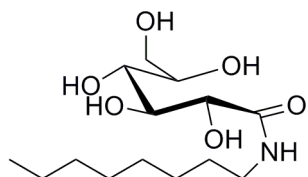
CAS: 885120-77-4 MW: 333.42

The product is obtained after three successive reactions as described by Laurent et al (Laurent, P., et al. 2011). In a first step, glucuronic acid reacts with acetic anhydride in presence of iodide to give peracetate glucuronic anhydride as a white solid after recrystallization in hexane. In a second step, the alkyl chain is introduced by reaction of the peracetate glucuronic anhydride with octylamine or decylamine. Deacetylation occurs in the third step and the products are purified on a silica column (CH₂Cl₂/MeOH:4/1). The purity (estimated higher than 95%) was verified by ¹H and ¹³C RMN.

1.4. Gluconamide derivatives:

I) N-octyl-D-gluconamide

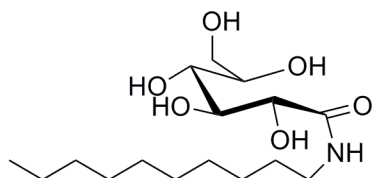
Abbreviation : Glu1amideOC8



CAS: 18375-61-6 MW: 307,38

II) N-decyl-D-gluconamide

Abbreviation : Glu1amideOC10



CAS: 18375-62-7 MW: 335,44

The alkyl gluconamide derivatives were obtained by an easy one step reaction involving D-gluconolactone and an equimolar amount of 1-aminooctane (or 1-aminodecane) in methanol at 45°C. The solvent was then evaporated, and a white solid was obtained after drying under vacuum. The purity (estimated higher than 95%) was verified by ¹H and ¹³C RMN. The amphiphilic properties and ability of these compounds to associate as cylindrical fibers are related in several publications (Piispanen, P. S. 2004; Fuhrhop, J. H., et al. 1990).

2. Selection of standard surfactants

Tween 20 and Hecameg were used as standard non-ionic surfactants during different processes of experiments. Their structures are presented in Figure 26. Tween 20 (polyoxyethylene (20) sorbitan monolaurate) is used as emulsifier and detergent in a broad range of domestic, scientific and pharmacological applications. Hecameg (6-O-(N-Heptylcarbamoyl)-methyl- α -D-glucopyranoside) is a glucose-based surfactant which has a

similar structure compared to synthesized surfactants mentioned above. It is often used to extract, purify and stabilize proteins or to solubilize lipids in biological related research work (Ruiz, M. B., et al. 1994).

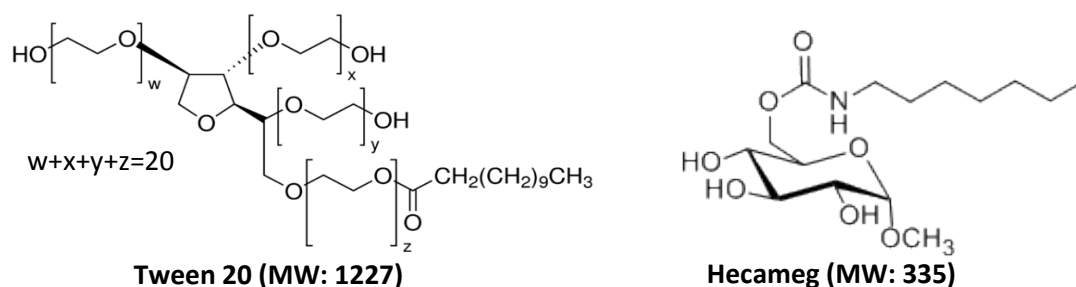


Figure 26: Structure of commercially available standard surfactants.

3. HLB of surfactants

Hydrophile-lipophile balance of surfactants were calculated so as to estimate their amphiphilic properties in solutions. According to Griffin's method previously described in Chapter I, A-5:

$$HLB = 20 \times \frac{M_h}{M}$$

M_h is the molecular mass of the hydrophilic part of surfactant and M is the molecular mass of the whole surfactant.

4. Solubility of surfactants

Solubility of surfactant in water was evaluated. Surfactant with a relatively high solubility and the ability to form micelles in solutions has potential to be applied in cosmetic, pharmaceutical and food industries where its surface-active and self-assembling properties are used to stabilize mixed systems, encapsulate substances for drug delivery or to improve texture of food...

Surfactants from batch 1 were used for preliminary tests, the purpose was to classify them into two groups: surfactants with relatively high solubility (higher than 0.5 g/L) and surfactants with relatively low solubility (lower than 0.5 g/L). In the test, surfactant (0.05 g) was firstly added into 5 mL water to form 10 g/L solution or suspension. After 10 min of ultrasonic homogenization and overnight equilibration at room temperature or at 37°C, the clarity of solutions was observed visually. For surfactant that was not be able to be totally dissolved at this concentration, more water was added into the mixture to dilute it. After the dilution, surfactant-water mixture was again treated by 10 min of ultrasonic homogenization and overnight equilibration at room temperature or at 37°C, a clarity examination was then carried out. The minimum concentration used for surfactant in water during the test was 0.5 g/L, below which the clarity of surfactant-water mixture can hardly be confirmed visually.

Surfactants from batch 2, as described previously, were provided in larger quantity. Therefore, solubility of pre-selected surfactants in batch 2 (according to results from batch 1) were tested more precisely. The solubility of surfactant from batch 2 was evaluated by the same method in a wider range of concentrations. The starting concentration was 50 g/L (60 g/L for Mal1amideC8) and minimum concentration was 1 g/L instead of 0.5 g/L (because all pre-selected surfactants showed solubility higher than 1 g/L). This time, solubility of surfactant was also verified with UV/VIS spectrometer by measuring the absorbance of surfactant-eosin mixed water solution at 518nm (detailed procedure is described in Chapter II, B-8).

5. Measurement of Krafft point

The Krafft point of surfactant can be determined by measuring the melting temperature of its hydrated crystal (Shinoda, K., et al. 1989). According to the example (Figure 27), two methods can be used to determine the transition temperature in the obtained DSC thermograms (Matsuki, H., et al. 1996). The first one is to determine the intersection of the horizontal baseline and the initial slope of the peak in the DSC curve, the second one is to take the peak temperature of the curve as transition temperature. In our experiment, the first method was used.

Concerning the experiment, surfactant solutions (50 g/L) were prepared after 10 min ultrasonic homogenization and overnight equilibration at 37°C. The solutions were then cooled down to 4°C to form crystal precipitates. The melting process of hydrated surfactant crystals was then monitored by Micro DSCVII CS Evol (SETARAM, France) in the range from 4°C to 45°C with the heating rate was 0.5°C /min to define the Krafft points.

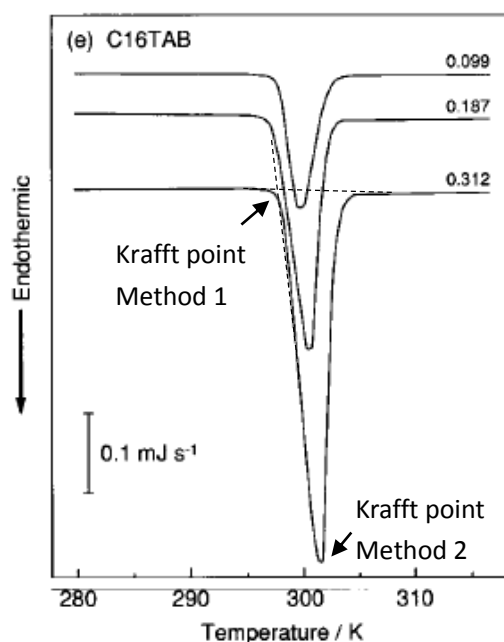


Figure 27: Krafft point of C16TAB determined by DSC by heating C16TAB-water mixture above its CMC, the concentrations are shown in mol/kg (Adapted from Matsuki, H., et al. 1996).

6. Surface active properties of surfactants

In order to understand surfactant's surface active properties in water as well as in culture medium used for cell models, surface tensions of surfactant solutions (water, complete DMEM without fetal bovine serum or complete DMEM) were measured as a function of surfactant concentrations by Wilhelmy plate method at 37°C using KRÜSS Processor Tensiometer K100 (KRÜSS, Germany), $n=1$ due to limited sample quantity. Measurements were repeated two or three times, in water and/ or DMEM medium (repeatability was not systematic due to limited sample quantity).

The Wilhelmy plate method is a frequent used technique to measure interfacial tension (Figure 28). In the method, a platinum/ filter paper/ glass plate is oriented perpendicular to the liquid/ air or liquid/ liquid interface. The weight of plate and the liquid formed on the plate due to interfacial tension is recorded by a microbalance hanging the plate. In an air/ liquid interface, assuming that the contact angle θ between liquid and plate is 0 (for platinum, filter paper or glass plate), the total force measured by microbalance can be described in the equation below:

$$F = W_{plate} + \gamma L \cos\theta$$

Where W_{plate} is the weight (unit: N) of the plate, L is the wetted perimeter of the plate ($2l + 2d$) (unit: m), γ is the surface tension (unit: N/m) between liquid and air.

The liquid/ air surface tension can then be determined:

$$\gamma = \frac{F - W_{plate}}{L \cos\theta} = \frac{F - W_{plate}}{L}$$

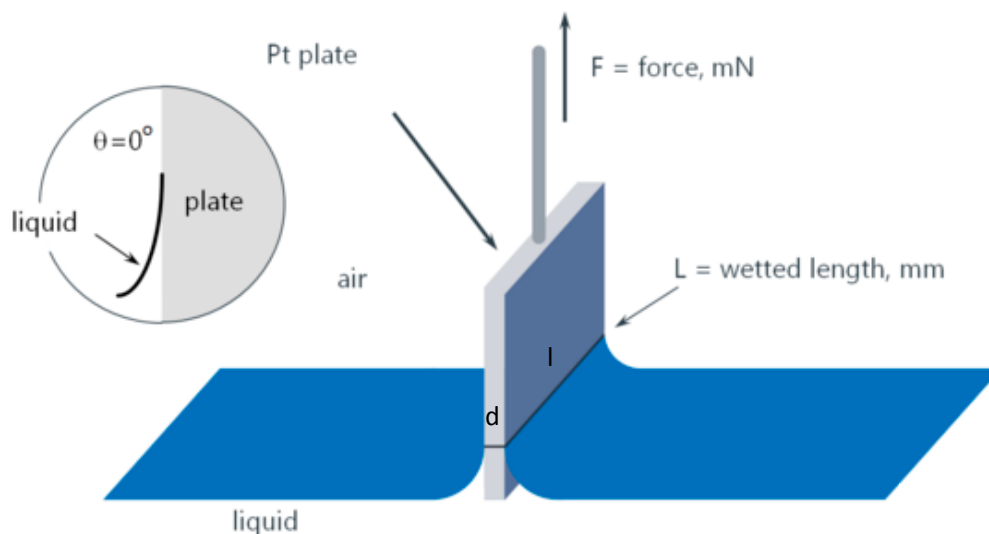


Figure 28: Schematic of Wilhelmy plate method (Adapted from <http://www.kruss.de>).

7. Adsorption of surfactant molecules at air/water interface

Adsorption of surfactant molecules at air/water interface can be determined by results from surface tension measurement. According to an approximation of Gibbs equation, for non-ionic surfactant in a diluted solution:

$$d\gamma = -\Gamma RT d\ln c = -2.303\Gamma RT d\log c$$

Where γ is the surface tension (unit: N/m), R is ideal gas constant ($R=8.314$ J/mol.K), T is the system temperature (unit: K), Γ is the surface excess concentration (unit: mol/m²) of surfactant molecules, c is the surfactant concentration in solution (unit: mol/m³).

Therefore, maximal surface excess concentration at CMC can be calculated:

$$\Gamma_{max} = -\frac{1}{2.303 RT} \frac{d\gamma_{cmc}}{d\log C_{cmc}}$$

Actually, the surface excess concentration Γ is the difference between the interfacial concentration Γ_I and the concentration at a virtual interface in the interior of the volume phase Γ_V .

$$\Gamma = \Gamma_I - \Gamma_V$$

However, as the surface excess concentration in surfactants is very much greater than Γ_V , this is usually equated with the interfacial concentration (<http://www.kruss.de>). Therefore, the minimum surface area occupied by each surfactant (A_{min}) at their CMC can be determined:

$$A_{min} = \frac{1}{\Gamma_{max} N_0}$$

Where N_0 is the Avogadro number (6.023×10^{23} molecule/mol) (Attwood, D. 2012).

8. Determination of Critical Micellar Concentrations (CMC)

Several techniques can be used to determine the CMCs of surfactants (Chapter I, A-3). Indirect methods are generally used to identify the presence of micelles as some properties of the solution undergoes some changes. The most commonly used one is to investigate the surface tension variation as a function of concentration. The surface tension will reach a minimum value at the CMC (Figure 29). However, this observation alone is not enough to prove the presence of micelles as it arise mainly from the appearance of a new phase in the solution (molecules aggregates as micelles, or precipitate in solid form) depending if the temperature is above or below the Krafft point.

When the surfactant solubility is high enough (temperature higher than its Krafft point), the

CMC of the surfactant can be determined at the intersection point in the curve when the surface tension reaches a minimum plateau value (Figure 29).

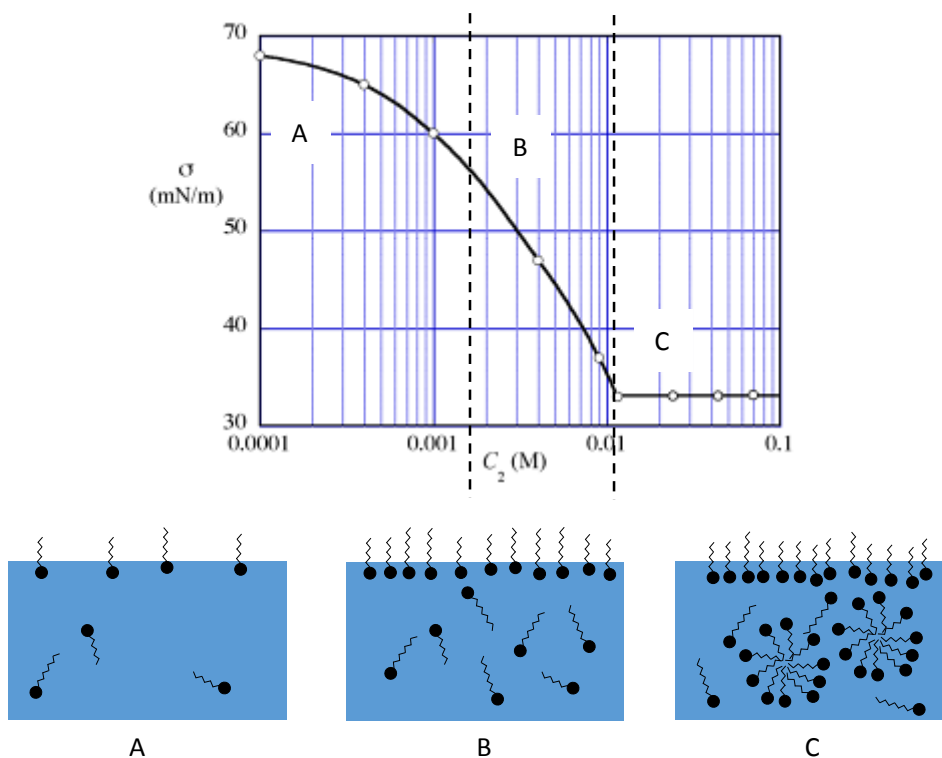


Figure 29: Schematic of surface tension behavior of aqueous surfactant solutions and behaviors of surfactant molecules in solutions (Adapted from Berg, J.C. 2010).

Complementary methods can be undertaken to confirm the presence of micelles. According to the dye solubilization method, probe UV-absorbing molecules are characterized by an absorption spectrum which depends of the polarity of their environment. For instance, Eosin Y will be characterized by a maximum absorbance at 518 nm below the CMC when the molecules are surrounded by water (in a polar environment). Above the CMC, the incorporation of Eosin Y within the micelles (in an apolar environment) will induce a shift to 542 nm in maximum absorbance. A decrease in absorbance measured at 518 nm can therefore reflect the appearance of micelles in solution (Figure 30) (Patist, A., et al. 2000; Suradkar, Y. R., & Bhagwat, S. S. 2006).

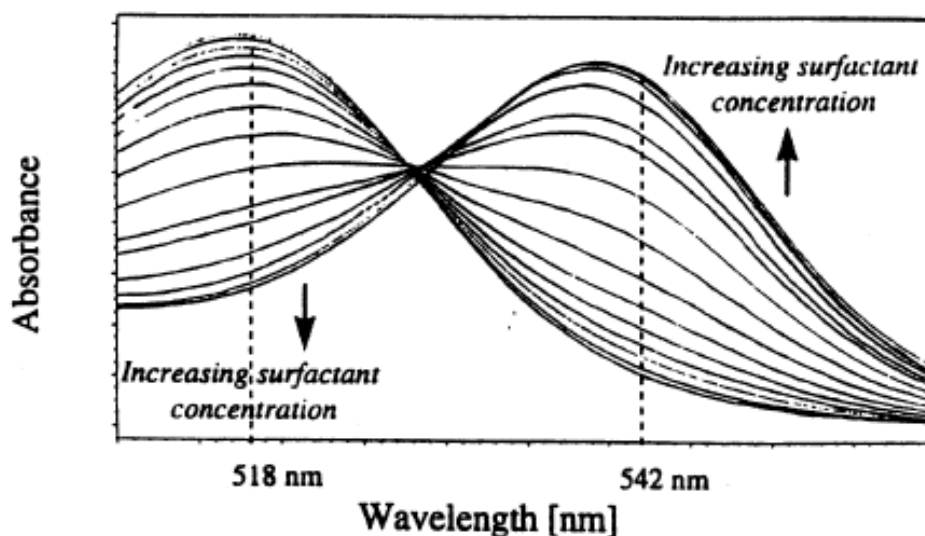


Figure 30: Ultraviolet-visible absorbance spectrum of eosin Y in aqueous surfactant solution. The wavelength maximum (λ_{max}) shifts from 518nm in the absence of surfactant to 538 nm as the surfactant concentration increases. The rise is most significant at 542 nm and the decrease is most significant at 518 nm. The increase and decrease of absorbance are only significant at concentrations higher than CMC of surfactants (Patist, A., et al. 2000).

In the experiments, surfactant solutions (5 mL) of varying concentrations were prepared at 37°C and 0.5 mL of 0.17 mM Eosin Y solution was added into each solution. Absorbance at 518nm of these mixed solutions was measured using UV/VIS spectrometer (Lambda 12, PerkinElmer, German).

9. Self-assembling properties of surfactants

Within the Amphiskin project of GENESYS program, we had the opportunity to subcontract a few SAXS experiments to the research team NANO (Mélanie Emo, Marie-José Stébé) from the Laboratoire Structure et Réactivité des Systèmes Moléculaires Complexes (UMR CNRS 7565) of the Université de Lorraine. The experimental conditions in which the experiments were performed are described in Appendix 2.

Small angle X-Ray scattering (SAXS) data were collected on a SAXS instrument (SAXSess mc2, Anton Paar, Austria), using line-collimation system. This instrument is attached to a ID 3003 laboratory X-Ray generator (General Electric) equipped with a sealed X-Ray tube (PANalytical, $\lambda_{Cu K\alpha} = 0.1542$ nm) operating at 40 kV and 50 mA. Several mirrors and a block collimator provide a monochromatic primary beam with very low background. A translucent beam stop allows the measurement of an attenuated primary beam at $q=0$.

Samples were put in a Special glass capillary (outer diameter 1.5mm), before being placed inside an evacuated sample chamber at the desired temperature (with a temperature-controlled sample holder unit (TCS 120, Anton Paar), and exposed to X-ray beam for 1 hour 30

minutes (for SAXS measurements) or 15 minutes (for WAXS measurements). Scattering of X-Ray beam was recorded by a CCD detector for SAXS measurements, at 309 mm distance from sample or by an image plate (IP) detection system Cyclone (Perkin-Elmer) for WAXS measurements, at 261.2 mm distance from sample.

Using SAXSQuant software (Anton Paar), the 2D image was integrated into one-dimensional scattering intensities $I(q)$ as a function of the magnitude of the scattering vector $q = (4\pi/\lambda) \sin(\theta)$, where 2θ is the total scattering angle. All data were corrected for the background scattering from the capillary and for slit-smearing effects by a desmearing procedure from SAXSQuant software.

C) Establishment of cell/ tissue models and cytotoxicity/ irritancy tests

1. Cells/ tissues used in tests

1.1. L929 cells (cultured)

Fibroblasts L929 were chosen to evaluate the biological effect of surfactants since it is a cost-effective, reliable standard cell line and has been used by many research groups for cytotoxicity and biocompatibility tests (Vian, L., et al. et al. 1995; Memisoglu-Bilensoy, E., et al. 2006; Colomer, A., et al. 2012). Furthermore, fibroblasts are the major cells in dermal layer, they are ideal cells for skin related experiments.

L929 cells (passage 15-40) were cultured in 75 cm² Falcon® cell culture flasks using complete DMEM as culture medium and maintained in a humid atmosphere at 37°C with 5% CO₂. Cells were diluted and seeded into new flasks each 2 or 3 days. 0.25% Trypsin-EDTA treatment for 5 min at 37°C was used to detach cells in each passage.

1.2. EpiDerm™ – Reconstituted Human Epidermis (purchased)

Normal (non-transformed) human keratinocytes in the form of reconstituted human epidermis were chosen for cytotoxicity/ irritancy tests. Keratinocyte is the major cell in epidermal layer of skin, well differentiated keratinocyte cultured on insert are suitable for skin-related tests (Genno, M., et al. 1998; Botham, P. A., et al. 1998; Costin, G. E., et al. 2009; Jang, Y. S., et al. 2012). Corresponding commercially available models (EpiDerm™) are validated by EURL-ECVAM (European Union Reference Laboratory for alternatives to animal testing) as alternatives to *in vivo* skin irritation tests (Botham, P. A., Earl, L. K., et al.).

2. 2D cell models

I) Model 1

L929 cells (10000 cells/ cm² or 5200 cells/cm²) were seeded into each well of Costar® Cell culture plates (6 or 24 well) together with 4 mL or 2 mL complete DMEM as culture medium, surfactants were immediately added into each well to form solutions with different concentrations. After 48 h of culture at 37°C with 5% CO₂ in a humid incubator, cytotoxicity tests were carried out (Figure 31).

II) Model 2 (monolayer model)

L929 cells (5000 cells/cm² or 2600 cells/cm²) were seeded into each well of Costar® Cell culture plates 6 or 24 well together with 4 or 2 mL complete DMEM. After 24 h of incubation at 37°C

with 5% CO₂ in a humid incubator, cells attached to the bottom of culture plate and form monolayer. Surfactants in fresh culture medium with different concentrations (from 0 – 1000 µg/mL) were then added. After another 48 h of incubation, cytotoxicity tests were conducted (Figure 31).

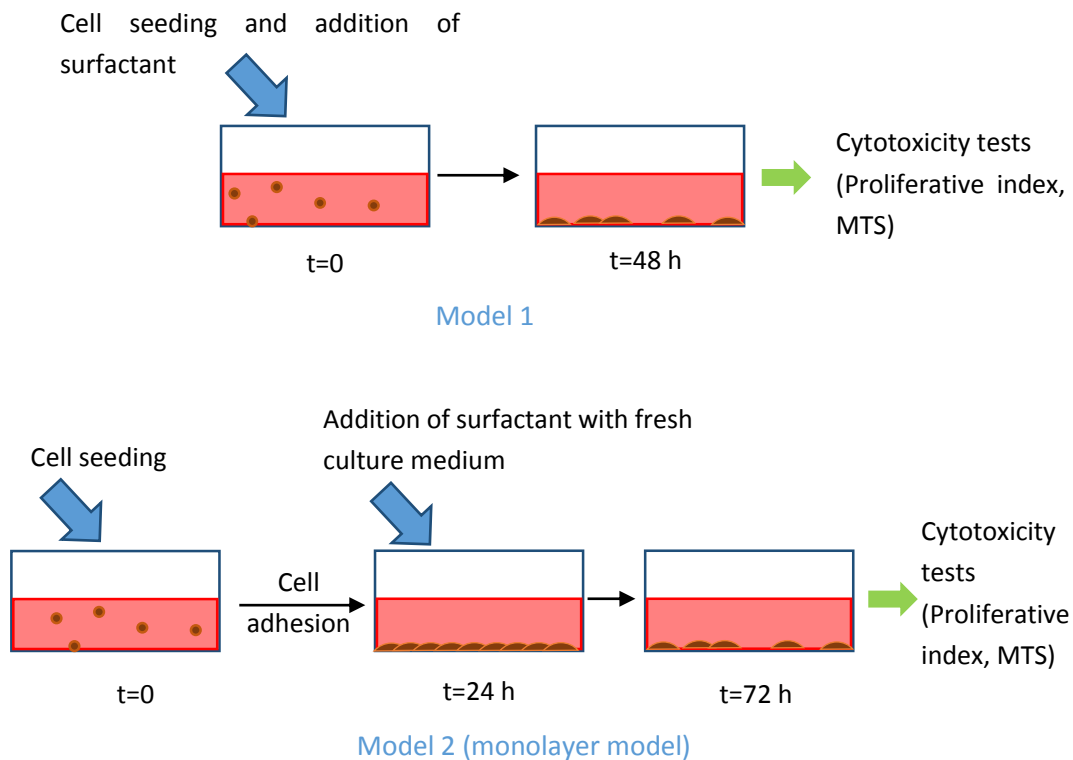


Figure 31 : Schematic of 2D cell culture models and test procedure.

2.1. Cell morphology

Cell morphology of model 2 (monolayer models) were observed by microscope. Cells were firstly cultured for 24 h, then treated with surfactant for 48h, photos were taken.

2.2. Tests on 2D cell models

1) Cell proliferative index

Trypan blue is a stain used for cell counting. Live L929 cells with intact cell membranes are not colored since trypan blue is not absorbed inside. However, when cells are dead, trypan blue can enter the cells and color them in blue.

After exposure to surfactants, cell culture medium was removed, cells were detached from each well by 1 mL 0.25% Trypsin-EDTA treatment at 37°C for 5min. The trypsin activity was then inhibited by adding 1 mL FBS into each well. Number of living and dead cells were counted using Malassez hemocytometer after Trypan blue staining. Cell proliferative index

and viability were calculated according to the equation below:

$$\text{Proliferative Index} = \frac{\text{number of living cells after treatment}}{\text{number of seeded cells}}$$

Cell viability in each condition was also calculated:

$$\text{Viability} = \frac{\text{number of living cells after treatment}}{\text{total cell number after treatment}}$$

II) Cell metabolic activity (MTS test)

The MTS compound (3-(4,5-dimethylthiazol-2-yl)-5-(3-carboxymethoxyphenyl)-2-(4-sulfophenyl)-2H-tetrazolium) is derived from tetrazolium and can be bio-reduced by cell mitochondrial activity into a colorful formazan that are soluble into cell/ tissue culture medium. This conversion is presumably accomplished by NADPH or NADH produce by dehydrogenase enzymes in metabolically active cells (<https://france.promega.com/>). The quantity of formazan formed is proportional to metabolic active cells in culture medium and can be measured by absorbance at 490 nm in a plate reader.

To conduct the MTS test, MTS solution (100 μ L) was added into 2 mL culture medium of each well after cell treatment. After 4h of incubation at 37°C, 3 times 100 μ L culture medium from each well was transferred into cell culture plate 96 well. Optical density of samples was read by Bio-Rad Model 680 microplate reader at 490 nm. Possible interactions between MTS and tested molecules can induce false positive, so molecules dissolved in culture medium without cells were also tested by the MTS based assay and their optical density values were subtracted from test results (Figure 32). Optical absorbance % which is proportional to Cell metabolic activity was calculated and normalized according to model without surfactants:

Optical Absorbance %

$$= \frac{\text{optical absorbance of sample} - \text{optical absorbance of sample without cells}}{\text{optical absorbance of negative control} - \text{optical absorbance of negative control without cells}}$$

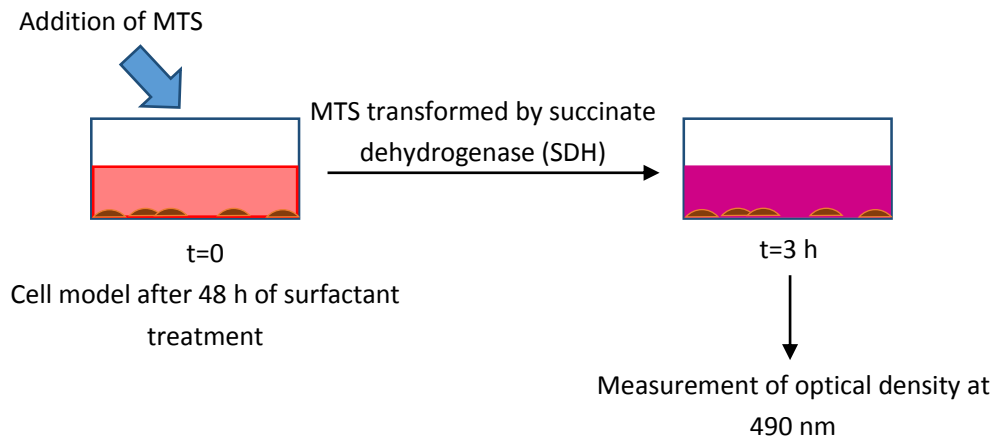


Figure 32: Schematic of MTS based assay.

3. 3D cell model

3.1. Establishment and treatment of 3D cell model

3D cell culture model was constructed using type I collagen solution from bovine skin and L929 cells in Nunc™ Polycarbonate Membrane Inserts (6 dishes). Type I collagen can spontaneously form a triple helix scaffold at neutral pH and 37°C, thus creates the 3D matrix for cell growth.

In 3D cell culture model, neutral collagen solution without cells were firstly prepared on ice. Original collagen solution was diluted from 6 mg/mL to 1.2 mg/mL by adding MEM 10X, Penicillin/ streptomycin 100X, L-Glutamine 100X and sterile water. The mixed solution was neutralized by NaOH (1N), color change of phenol red from yellow to red in solution was used to monitor the pH (~7.2). 1 mL neutral collagen solution was then added into each of the 6 inserts of Nunc™ culture plate and incubated at 37°C to allow polymerization of collagen. After 1h, when collagen gel without cells in insert was formed, freshly prepared neutral collagen solution with L929 cells (100000 cells/ mL) was added upon the existing collagen gel and incubated for another 1h. 5 mL complete DMEM was added in each well of Nunc™ culture plate to complete the 3D culture model (Figure 33).

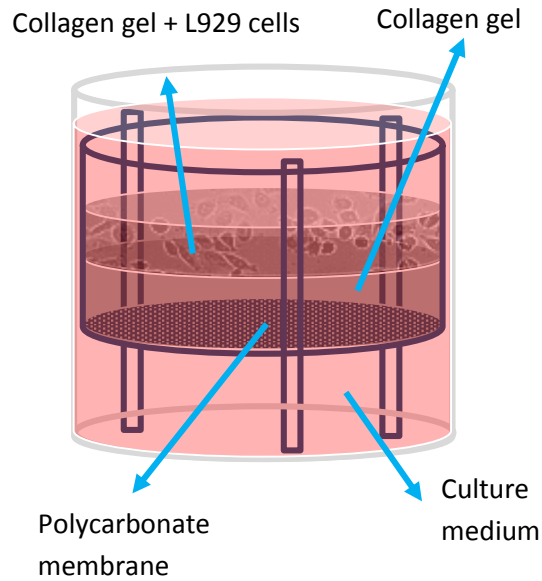


Figure 33: Schematic of 3D cell culture model.

To test influence of surfactants, the 3D cell culture model was firstly incubated at 37°C with 5% CO₂ for 96 h, then surfactants were added into the culture wells together with fresh culture medium. Cytotoxicity tests were carried out 48 h later (Figure 34).

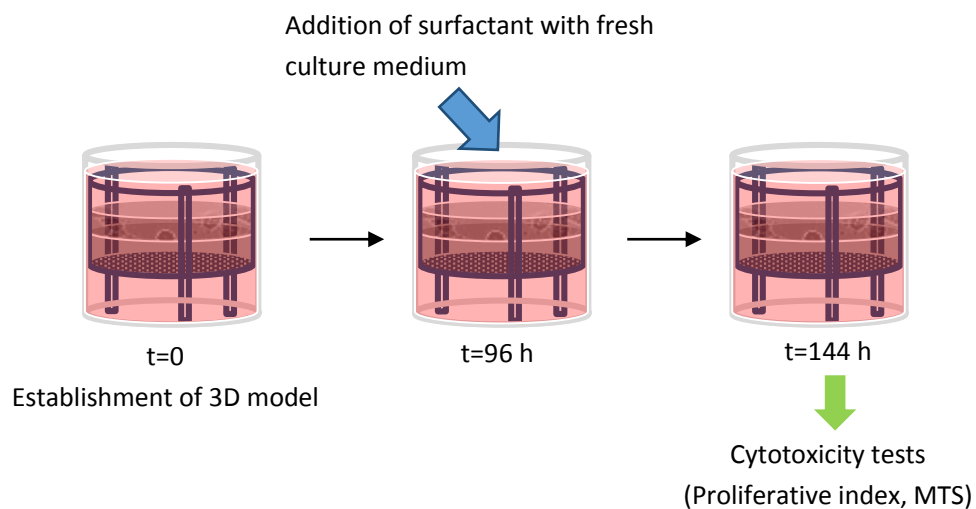


Figure 34: Schematic surfactant treatment on 3D cell culture model.

3.2. Histology of 3D cell models

Paraffin section of sample was prepared. Collagen gel with cells after 144 h of incubation without surfactant treatment was carefully harvested and fixed by formalin for 24 h at 4°C. After fixation, sample was dehydrated in 70%, 95%, 100% alcohol for 30 min consecutively. Sample was then immersed in toluene for 2 times (each during 1 h) followed by liquid paraffin treatment at 62°C for 24 h. Next, paraffin block containing sample was prepared in a cuboid mould at room temperature. Sample was cross-sectioned at 8 µm of thickness by Semi-

automated rotary microtome Leica RM2245 (USA) and then fastened to microscope slide by glycerin-albumin solution.

Hematoxylin and Eosin stain was used for histology of samples. Paraffin section was immersed in toluene twice for 10 min. Then the section was treated with 100%, 95%, 70% alcohol each for 5 min. After 10 min of wash in water, DNA/RNA of cells in sample were stained violet by hematoxylin during 5 min of treatment in hematoxylin solution. After washing the paraffin section thoroughly by water, proteins in cytoplasm of sample cells were stained red by eosin during 2 min of treatment in eosin solution. Sample was then washed by water, dehydrated and cleaned by consecutive treatment in 70%, 95%, 100% alcohol and toluene. Paraffin sections were then mounted by EUKITT® mount medium together with coverslip. Photos of sample were taken through light microscope.

3.3. Tests on 3D cell model

I) Cell proliferative index, 3D

After surfactant exposure, the culture medium was removed. Collagen gel containing L929 cells was degraded by 2 mL reconstitute collagenase solution (200 U/mL collagenase in HBSS) after 4 h interaction at 37°C. Dissociated L929 cells were then collected and counted using Malassez hemocytometer after Trypan blue staining. Cell proliferative index and viability were calculated.

II) Cell metabolic activity (MTS test), 3D

MTS solution (200 µL) was added into 5 mL of culture medium of each well after surfactant treatment. After 2 h of incubation at 37°C, 3 times 100 µL culture medium from each well was transferred into cell culture plate 96 well. Optical density of samples was read by Bio-Rad Model 680 microplate reader at 490 nm. To eliminate possible false positive, surfactants dissolved in culture medium in the 3D culture model without cells were tested by MTS test and their optical density values were subtracted from normal tests results. Metabolic activity related optical absorbance was then calculated:

$$\text{Optical Absorbance \%} = \frac{\text{optical absorbance of sample} - \text{optical absorbance of sample without cells}}{\text{optical absorbance of negative control} - \text{optical absorbance of negative control without cells}}$$

4. 3D tissue model

4.1. Conditioning and treatment of 3D tissue model

Reconstituted Human Epidermis (RHE) models (EpiDerm™ EPI-200-SIT kit) were purchased (Figure 35). This model consists of normal human epithelial keratinocytes, which have been cultured at air/liquid interface to form a multilayered, highly skin-like structure on specially

prepared permeable cell culture inserts (GENNO, M., et al. 1998).

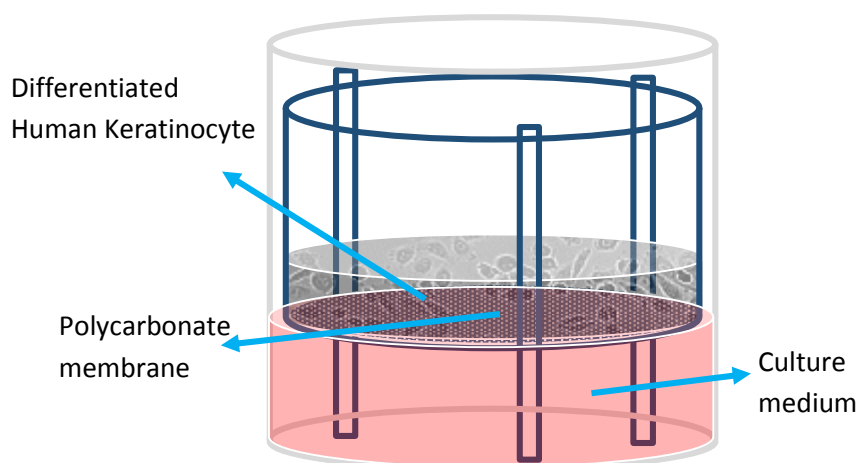


Figure 35: Schematic of RHE model.

Upon receipt of EpiDerm™ EPI-200-SIT kit, every insert containing the tissue was moved from its original 24-well plate to each well of Falcon® cell culture 6-well plates containing 0.9 mL culture medium provided in the kit. After 1 h of pre-incubation at 37°C with 5% CO₂, insert was moved to a new culture well containing 0.9 mL culture medium followed by overnight incubation for tissue conditioning.

After tissue conditioning, inserts with tissues were placed into new 6-well plates containing 0.9 mL culture medium in each well. Surfactant dissolved in PBS (30 µL, 1000 µg/mL), negative control (30 µL PBS), positive control (30 µL, 5% m/v SDS in PBS) were applied on top of each tissue separately, nylon meshes provided in the kit were used to cover the tissue surface and guarantee the spreading of liquid. After 48 h of exposure (for ELISA, both 24 h and 48 of exposure were conducted), nylon meshes on tissues were removed, tissues in inserts were washed thoroughly with PBS. Cytotoxicity/ irritancy tests were conducted (Figure 36). It should be noted that 48 h (or 24 h) of surfactant exposure is much longer than recommended 1 h of exposure in ECVAM validated skin irritation test using the same tissue model (<http://www.mattek.com>).

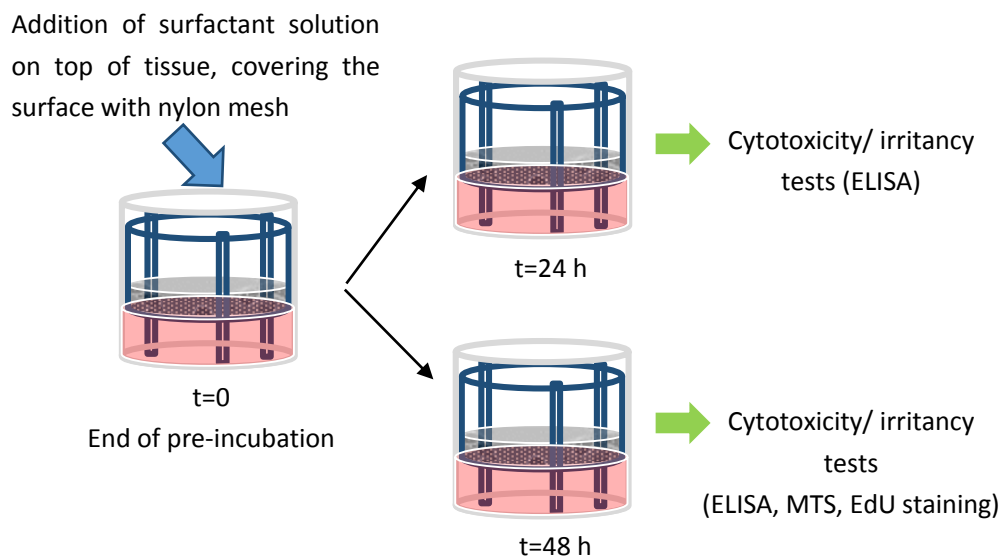


Figure 36: Schematic of surfactant treatment on RHE model.

4.2. Histology of RHE models

Hematoxylin and Eosin stained paraffin section of sample was prepared as described in (Chapter II, C-3) after tissue conditioning and treatment.

4.3. Cytotoxicity/ irritancy tests on RHE models

I) Cell metabolic activity (MTS test), RHE

HBSS solution (300 μ L) containing MTS (0.2 mg/mL) was added into each well of Costar 24-well plates. EpiDerm™ in inserts after treatment and wash were then transferred into these wells and incubated at 37°C for 3 h. Three times 100 μ L culture medium from each well was transferred into cell culture plate 96 well. Optical density of samples was read by Bio-Rad Model 680 microplate reader at 490 nm. Metabolic activity related optical absorbance of cells in RHE model was calculated:

Optical Absorbance %

$$= \frac{\text{optical absorbance of sample} - \text{optical absorbance of HBSS solution containing MTS}}{\text{optical absorbance of negative control} - \text{optical absorbance of HBSS solution containing MTS}}$$

II) Irritancy potential of surfactants (IL-1 α Enzyme Linked Immunosorbent Assay (ELISA)), RHE

The interleukin-1 α (IL-1 α) is an important cytokine which can be secreted by keratinocytes and is involved in inflammatory reactions in human skin (Bigler, C. F., et al. 1992). Therefore, release of IL-1 α in culture medium can be regarded as an indication of inflammation reaction in RHE model.

To quantify IL-1 α in culture medium, Human IL-1alpha Platinum ELISA kit was used. Principles of this ELISA is presented in Figure 37. An anti-human IL-1 α coating antibody is firstly adsorbed onto microwells. Human IL-1 α present in the sample or standard binds to antibodies adsorbed to the microwells. A biotin-conjugated anti-human IL-1 α is added and binds to human IL-1 α captured by the first antibody. Following incubation, unbound biotin-conjugated anti-human IL-1 α antibody is removed during a wash step. Streptavidin-HRP is added and binds to the biotin-conjugated anti-human IL-1 α antibody. Following incubation unbound streptavidin-HRP is removed during a wash step, and substrate solution reactive with HRP is added to the wells. A colored product is formed in proportion to the amount of human IL-1 α present in the sample or standard. The reaction is terminated by addition of acid and absorbance is measured at 450 nm. A standard curve is prepared from 7 human IL-1 α standard dilutions and human IL-1 α sample concentration determined (<http://www.ebioscience.com>).

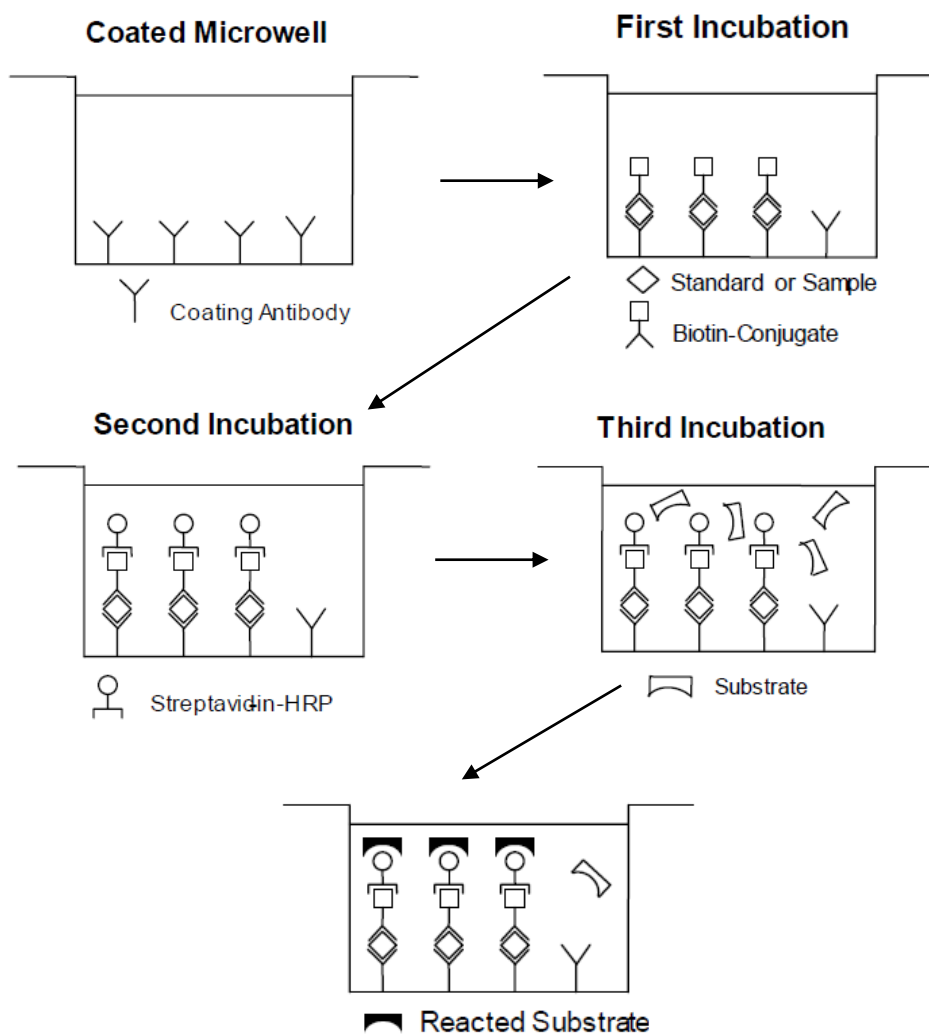


Figure 37: Principles of IL-1 α ELISA (Adapted from <http://www.ebioscience.com>).

By using the materials provided in the Human IL-1alpha Platinum ELISA kit, microwell strips were firstly washed by wash buffer for 3 times and dried. Standard human IL-1 α dilutions (100 μ L, from 0 to 100 μ g/mL) were added to standard wells. Samples of culture medium (100 μ L)

after surfactant treatment were added to sample wells. Then, prepared biotin-conjugate (50 μL) were added to all wells. All the microwell strips were covered with an adhesive film and incubated at room temperature for 2 hours. After the incubation, each microwell strip was washed by wash buffer for 4 times. Streptavidin-HRP (100 μL) was added into microwell strip and incubated at room temperature for 1 h. Microwell strips were then again washed thoroughly for 4 times by wash buffer. TMB substrate solution (100 μL) was pipetted into each well. The microwell strips were incubated at room temperature for about 10 min, exposure to intense light was inhibited by aluminum foil. Color was developed during this process, and the enzyme reaction was then stopped by pipetting 100 μL stop solution (H_2SO_4 (2N)) into each well. Optical absorbance of samples was measured by Bio-Rad Model 680 microplate reader at 450 nm.

Standard curve by plotting the mean absorbance for each standard concentration on the ordinate against the human IL-1 α concentration on the abscissa was drawn. A 5-parameter curve is used to fit the points of the graph and an equation for IL-1 α concentration dependent absorption is created. The equation was then used to determine IL-1 α concentration in each sample.

III) Percentage of proliferating cells in basal layer (EdU-DAPI double staining), reconstituted human epidermis model

Cell health can be assessed by measuring its ability to proliferate. In Click-iT[®] EdU Alexa Fluor[®] 488 Imaging kit, EdU (5-ethynyl-2'-deoxyuridine) is a nucleoside analog of thymidine and is incorporated into DNA during active DNA synthesis. Detection is based on a click reaction, a copper-catalyzed covalent reaction between an azide and an alkyne. In this application, the EdU contains the alkyne and the alexa Fluor contains the azide. After reaction, proliferating cells will emit green fluorescence under an excitation light at 450-490 nm.

DAPI (4',6-diamidino-2-phenylindole) is a fluorescent stain that can bind to A-T rich regions in DNA. It can be used to stain both live and fixed live cells and emit a blue fluorescent after excitation at 512-542 nm.

To conduct the EdU-DAPI immunostaining assay, sample after 48 h of surfactants treatment was firstly incubated in culture medium containing 10 μM EdU for 4 h to allow incorporation of EdU into DNA during DNA synthesis in proliferating cells. Then frozen-section of samples were prepared.

RHE tissue was carefully removed from its culture inserts and immersed into 2 M sucrose overnight at 4°C to displace water from cellular spaces. Sample was then blotted to remove excess sucrose solution and embedded in OCT compound through a flash freezing procedure (sample was immersed into OCT in a cylinder mould and placed upon the upper surface of liquid nitrogen for about 5 min). Fresh-frozen tissue sections at 5 μm thickness were then cut onto superfrost[™] Ultra Plus slides by Cryostat LEICA CM3050 S (France).

Tissue on slide was fully covered and fixed by 100 μ L 3.7% formaldehyde by incubation at room temperature for 15 min. The fixation media was then removed, sample was washed twice by 3% BSA in PBS and permeabilized by 100 μ L 0.5% Triton[®] X-100 for 20 min at room temperature. Permeabilization buffer was removed, slide containing the sample was again washed twice by 3% BSA in PBS. Click-iT[®] reaction cocktail (100 μ L) prepared from the assay kit was added upon tissue section. Sample was incubated at room temperature for 30 min and protected from light. Reaction cocktail was removed, sample was washed by 3% BSA in PBS twice. To conduct the DAPI staining, DAPI solution (100 μ L) was applied onto each tissue section and incubated at room temperature for 30 min. Afterwards, DAPI solution was removed; sample was washed 3 times by 3% BSA in PBS and mounted by Mowiol[®] 4-88 mounting medium with coverslip.

EdU-DAPI double staining image was obtained by Leica DMI6000 epifluorescence microscope with an exciting light at 450-490 nm and 512-542 nm respectively. To calculate the percentage of proliferating cells in basal layer, three 3D cell culture tissue segments with 300 μ m length were chosen randomly from the photos of double stained tissue, number of proliferating cells and total cells in their basal layer were counted.

5. Statistical analysis

A statistical analysis has been realized for all the biological-related tests. The values are average of 3-9 points. Results are presented as average with standard derivation. For comparison with negative control, the difference between test result and negative control is examined by Mann-Whitney test (nonparametric test). All the analysis data was obtained by software InStat3 (GraphPad, USA).

Chapter III: Results and Discussions

A) Reception of synthesized molecules

Sugar-based surfactants were synthesized and provided by the partners of the AMPHISKIN project (Laboratoire LG2A, UPJV, Amiens), as described in Chapter II, B-1, in different batches. Synthesized molecules with their quantity and corresponding batch are presented in Tables 10 and 11 (molecules comprising a hydrocarbon chain with respectively 8 and 10 carbons). Molecules from the first batch were used for preliminary physico-chemical analysis. Then, pre-selected molecules were synthesized in larger quantity and characterized for surface-active properties and in multi-scale biological models.

Table 10: Structures of synthesized surfactants with C8 hydrocarbon chain.

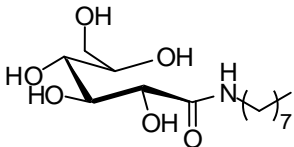
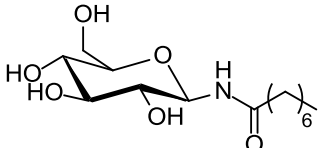
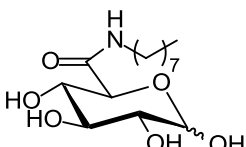
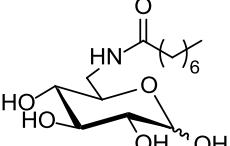
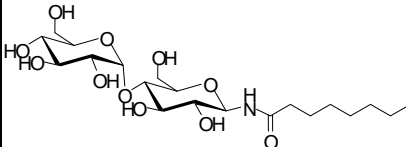
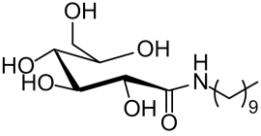
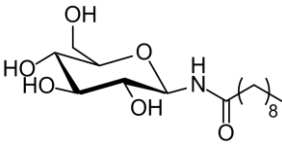
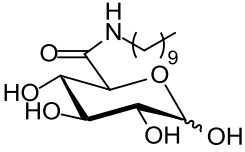
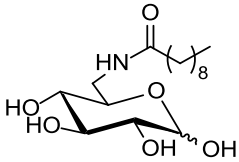
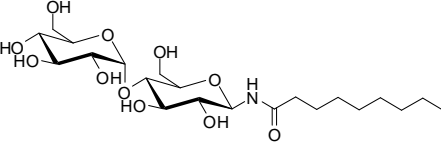
Molecules with C8 Hydrocarbon Chain	Molecular weight g/mol	Batch 1	Batch 2
<p>Glu1amideOC8</p> 	307	1g white powder	8g white powder
<p>Glu1amideC8</p> 	305	1g yellowish aggregates	8g white powder
<p>Glu6amideC8</p> 	305	1g yellowish aggregates	5.6 g yellowish powder
<p>Glu6amideC8'</p> 	305	0.7g white powder	6.4 g white powder
<p>Mal1amideC8</p> 	467	0.4 g white aggregates	4g white powder

Table 11: Structures of synthesized surfactants with C10 hydrocarbon chain.

Molecules with C10 Hydrocarbon Chain	Molecular weight g/mol	Batch 1	Batch 2
<p>Glu1amideOC10</p> 	335	1g white powder	-
<p>Glu1amideC10</p> 	333	1g yellowish-white aggregates	-
<p>Glu6amideC10</p> 	333	1g off-white powder	-
<p>Glu6amideC10'</p> 	333	0.6g off-white powder	-
<p>Mal1amideC10</p> 	495	0.7 g white-reddish aggregates	-

B) Physico-chemical properties of surfactants

1. HLB of synthesized and standard surfactants

HLB values are linked to surfactant solubility and can be used to estimate their potential domain of applications. Therefore, for synthesized and standard molecules, their HLB values are calculated and presented in Table 12. Griffin's method is taken for the calculation rather than Davies' method. Because group number of some hydrophilic/ hydrophobic groups are still lacking in Davies' method (for example, the amide group), a further estimation is needed to obtain a proper group number for these groups. In regards with the calculation, take Glu6amideC8 and Glu6amideC8' for example:

$$\text{HLB}(\text{Glu6amideC8}) = 20 * \frac{192 \text{ (molar mass of glucopyranuronamide)}}{305 \text{ (total molar mass of molecule)}} = 12.6$$

$$\text{HLB}(\text{Glu6amideC8}') = 20 * \frac{206 \text{ (molar mass of 6 - amino - D - glucopyranose)}}{305 \text{ (total molar mass of molecule)}} = 13.5$$

Table 12: HLB values of synthesized and standards surfactant calculated by Griffin's method.

Molecule	HLB (Griffin's method)
Glu1amideOC8	12.6
Glu1amideOC10	11.6
Glu1amideC8	13.5
Glu1amideC10	12.4
Glu6amideC8	12.6
Glu6amideC10	11.5
Glu6amideC8'	13.5
Glu6amideC10'	12.4
Mal1amideC8	15.8
Mal1amideC10	14.9
Tween 20	17.0
Hecameg	14.0

In reference, the HLB of Glu1amideOC8 has been calculated by Piispanen, P. S., et al. (2004) through Griffin's method. They obtain a value of 11.7. It is lower than our value of 12.6. The difference is attributed to the way of how the molecule is divided into hydrophilic/ hydrophobic moieties. In our calculation, amide linker is considered as hydrophilic moiety while in Piispanen's work, it is included as hydrophobic group. A most commonly used HLB value of Tween 20 is calculated according the equation below:

$$\text{HLB} = 20 \left(1 - \frac{S}{A}\right)$$

Wherein: S=saponification number of the ester; A=acid number of the acid (these two numbers require experiment assessment). HLB of Tween 20 by the method is 16.7 (Griffin, W. C. 1955), which is close to our result of 17 calculated directly from Tween 20's chemical structure.

According to surfactants' properties classified by their HLB in Table 3 (Chapter I, A-5), surfactant with a HLB of 8-13 is considered water dispersible or water soluble, HLB of 13 or above is water soluble. As is presented in Table 12, synthetic molecules possess HLB values between 11 and 16, therefore, it is worth investigating their solubility in aqueous systems.

2. Preliminary tests – estimation of water solubility of surfactants from batch 1 and their ability to lower surface tension of water

In the first batch, provided during the first year of the project, all surfactants were supplied in small amount (less than 1 g) in order to firstly verify their water solubility and their ability to lower surface tension of water solutions.

After the solubility tests described in chapter II, B-4, synthesized surfactants from batch 1 were divided into two groups: I) Solubility higher than 0.5 g/L at 37°C (Glu1amideC8, Glu6amideC8, Glu6amideC8' and Mal1amideC8); II) solubility lower than 0.5 g/L at 37°C (Glu1amideOC8, Glu1amideOC10, Glu1amideC10, Glu6amideC10, Glu6amideC10' and Mal1amideC10), the solubility is not sufficient to further investigate their physico-chemical properties and cytotoxicity in details.

To obtain preliminary results of surfactants' surface-active properties, surfactants were added into water or into complete DMEM solutions progressively at 37°C and stirred until non-soluble aggregates are formed. After filtration, saturated surfactant solutions were prepared. Their surface tensions were measured by Wilhelmy plate method and presented in Figure 38 (Glu6amideC8', Glu6amideC10', Mal1amideC8 and Mal1amideC10 were not tested due to limited sample quantity).

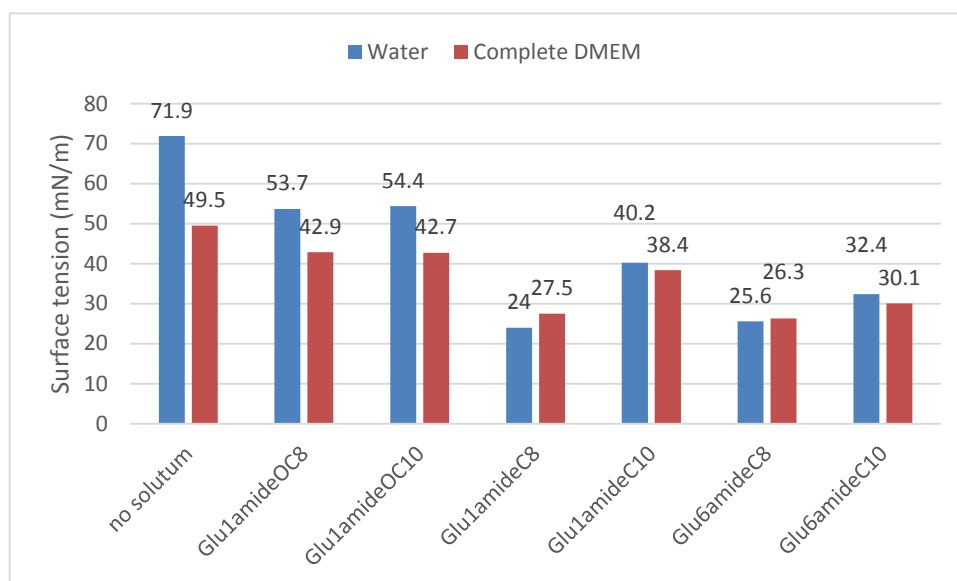


Figure 38: Surface tensions of saturated surfactant solutions in water/ complete DMEM at 37°C.

The exact concentration of each surfactant solution is unknown after filtration, but the results revealed their surface-active properties. Considering that Minimal surface tension of Tween 20 and Hecameg aqueous solutions are reported to be 33 mN/m at 30 °C and 32 mN/m at 25°C (Plusquellec, D., et al. 1989; Maunier, V., et al. 1997). If we take the value of 35 mN/m as a reference value, the ability of synthesized surfactants to lower surface tension of water/ complete DMEM solutions can be classified into two groups. I) Minimum surface tension is higher than 35 mN/m (Glu1amideOC8, Glu1amideOC10, Glu1amideC10); II) Minimum surface tension is lower than 35 mN/m (Glu1amideC8, Glu6amideC8).

By combining the results of solubility and surface-active properties, surfactant with relatively higher solubility and stronger ability to lower the surface tension (Glu1amideC8, Glu6amideC8) were chosen and synthesized in larger quantity for more complexed tests (Table 13). For Glu6amideC8', Glu6amideC10', Mal1amideC8 and Mal1amideC10, although their surface active properties were not measured in the preliminary testing, Glu6amideC8' and Mal1amideC8 were still chosen due to their higher solubility.

Table 13: solubility of synthesized surfactants and minimum surface tension of saturated surfactant water solutions (37°C).

	Solubility (< 0.5 g/L)	Solubility (> 0.5 g/L)
Minimum surface tension (< 35 mN/m)	Glu6amideC10	Glu1amideC8 Glu6amideC8
Minimum surface tension (>35 mN/m)	Glu1amideOC8 Glu1amideOC10 Glu1amideC10	

3. Solubility of standard surfactants and pre-selected surfactants in batch 2

Solubility of synthesized surfactants from batch 2 and of standard surfactants was estimated by naked eye observation as described in Chapter II, B-4, results are presented in Table 14.

Table 14: a) solubility of synthesized molecules from batch 2 and b) solubility of standard surfactants.

a. Molecule (provided in batch 2)	Solubility (room temperature) (g/L)	Solubility (room temperature) (mmol/L)	Solubility (T=37°C) (g/L)	Solubility (T=37°C) (mmol/L)
Glu1amideC8	5 – 10	16 - 33	> 50	> 164
Glu6amideC8	1 – 2	3 - 6	1 - 2	3 – 6
Glu6amideC8'	5 - 10	16 - 33	> 50	> 164
Mal1amideC8	> 60	> 128	> 60	> 128

b. Molecule (standard)	Solubility (room temperature) (g/L)	Solubility (room temperature) (mmol/L)	Solubility (T=37°C) (g/L)	Solubility (T=37°C) (mmol/L)
Tween 20	> 100	> 81	> 100	> 81
Hecameg	> 100	> 298	> 100	> 298

The dash mark is used to represent the solubility of surfactant within two concentrations. For example, 5 g/L - 10 g/L means that the solubility of surfactant is between 5 g/L and 10 g/L.

For synthesized molecules at room temperature, a general trend is that molecule with longer carbon chain are less soluble compared to their analog with shorter carbon chain (comparison within the same batch), it can be explained that molecule with longer carbon chain is more hydrophobic. The trend is also reflected by HLB value of each molecule, when two molecule with same sugar head are compared, the one with higher HLB is more soluble. Concerning the influence of sugar unit of molecule on its solubility, molecule with maltose head is more soluble than molecule with glucose head (for example, solubility: Mal1amideC8>Glu1amideC8), this result was predicted by HLB values by the fact that maltose group (2 glucose unit) is more hydrophilic than a single glucose group.

Temperature were found to alter the solubility of several surfactants. When test temperature was raised from room temperature (approximately 25°C) to 37°C, solubility of these molecules (Glu1amideC8, Glu6amideC8') increases significantly. One general explanation is that the higher temperature provides water system with increased kinetic energy and break apart the solute molecules that are held together by intermolecular attractions (exception: ethoxylated surfactants in water will reach their cloud point and become turbid with increase of temperature). Concerning synthesized surfactants, such an increase of solubility for Glu1amideC8 and Glu6amideC8' could possibly be attributed to their Krafft point values which

may be between room temperature and 37°C. As seen in Chapter I, A-4, Krafft point is the minimum temperature above which surfactant have the ability to form micelles in solutions. When the temperature rises from below Krafft point to above it, a sudden increase of surfactant's solubility can be observed. Therefore, it is worth investigating the exact Krafft point of our synthesized surfactant to figure out their conformation at 37°C. This is the temperature at which we will evaluated cytotoxicity of surfactant on cells/ tissues.

4. Comparison between batch 1 and batch 2

Results obtained with compounds from batch 1 and batch 2 were most of the time consistent except that:

- I) Glu1amideOC8, which showed different solubility in water (less than 0.5 g/L in batch 1 and between 5-10 g/L in batch 2, room temperature). A reference value mentions 1.2 g/L at room temperature (Piispanen, P. S., et al. 2004). This compound was not selected for further experiments due to the relatively high surface tension of its water solution obtained. Further analysis of the 2 batches will be undertaken in order to understand the origin of the discrepancy.
- II) Surface tensions of saturated solutions of Glu1amideC8 compound are different from 2 batches. For Glu1amideC8 from batch 1, the minimum surface tension in water was 24 mN/m (Figure 38) while for Glu1amideC8 from batch 2, it was 33 mN/m at 37°C (date will be shown in Chapter III, Figure 43). We also noticed a different appearance of the two samples: batch 1 had yellowish aggregates whereas batch 2 was a white powder. Very little amount of impurity could be the reason for surface tension difference.

Therefore, for further tests, all samples used were from batch 2 to ensure reproducibility.

5. Krafft point determination

In our tests, Glu1amideC8, Glu6amideC8' and Glu6amideC8 displayed limited solubility in water at room temperature. However, at 37°C, Glu1amideC8 and Glu6amideC8' showed a much higher solubility. To understand the reason for this increase of solubility (increase of kinetic energy or overcome of Krafft point), the Krafft point of surfactant was measured by following the heat flow during the melting process of their hydrated crystals (Van Doren, H. A. 1996; Tsujii, K., & Mino, J. 1978) using DSC (Figure 39). The DSC results show the Krafft points of Glu1amideC8 was at 30°C and of Glu6amideC8' at 32°C, this confirms their ability to form micelles at 37°C. Maunier, V., et al. (1997) have also estimated the Krafft point of Glu6amideC8' by slow heating of its aqueous mixtures, they obtained a value of 41°C, it is the temperature at which the surfactant's aqueous mixture becomes clear. The Krafft point determined by Maunier actually corresponds to the upper limit of our absorption peak of Glu6amideC8' in DSC analysis, at this temperature, the fusion process is completed.

During our experiment, no Krafft point in the range from 4°C to 45°C for Glu6amideC8 was detected. This result is in agreement with what was observed in the previous tests, where

Glu6amideC8 showed low solubility at both room temperature and at 37°C. For the three surfactants, Mal1amideC8, Tween 20 and Hecameg, no solubility problems were encountered during the test and their Krafft points may be below room temperature.

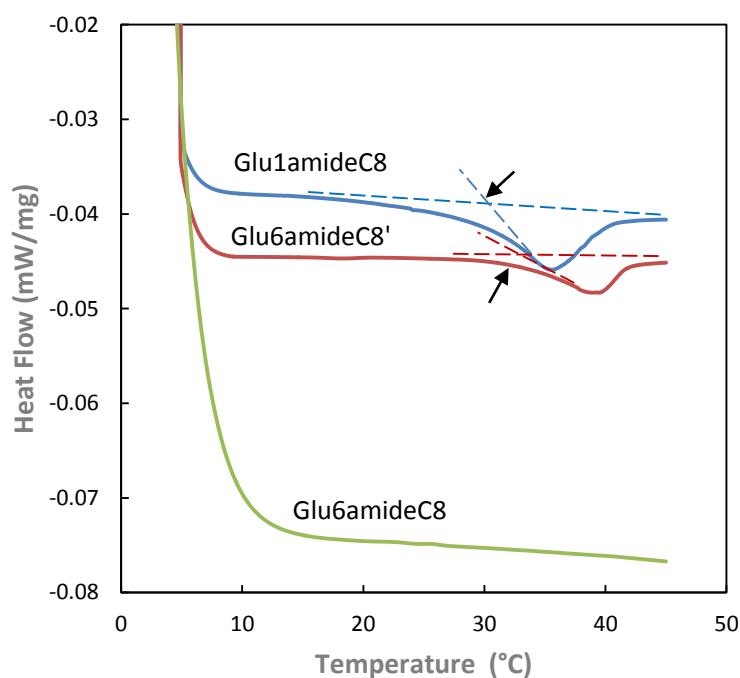


Figure 39: DSC curves obtained for Glu1amideC8, Glu6amideC8 and Glu6amideC8' hydrated crystals. Heating rate is 0.5°C. Arrows point out the Krafft point of surfactant.

6. Surface-active properties of surfactants and their CMCs in water

6.1. Surface tensions of surfactants solutions in water

Surfactants adsorb at the air-water interface to minimize the contact of their hydrophobic part with water. When their concentration increases, the surface becomes progressively saturated with surfactant molecules, and the surface tension of the solution decreases until it reaches a minimum value. Usually, above this concentration, the surface tension is almost constant. If the temperature is above the Krafft point of the surfactant, then the concentration at which the surface tension has attained its minimum value corresponds to their Critical Micellar Concentration (CMC). In other cases, the surfactant has reached its limit solubility in water and precipitates in solid form at higher concentration. It is important for many applications to determine the conformation of surfactant molecules in solutions, more precisely, whether surfactant molecules are in form of monomers (below CMC), in form of micelles (above CMC) or in form of a solid suspension.

Surface tensions of 4 synthetic sugar-based surfactants and 2 standard surfactants measured by Wilhelmy plate method in water solutions at 37°C are presented in Figure 40.

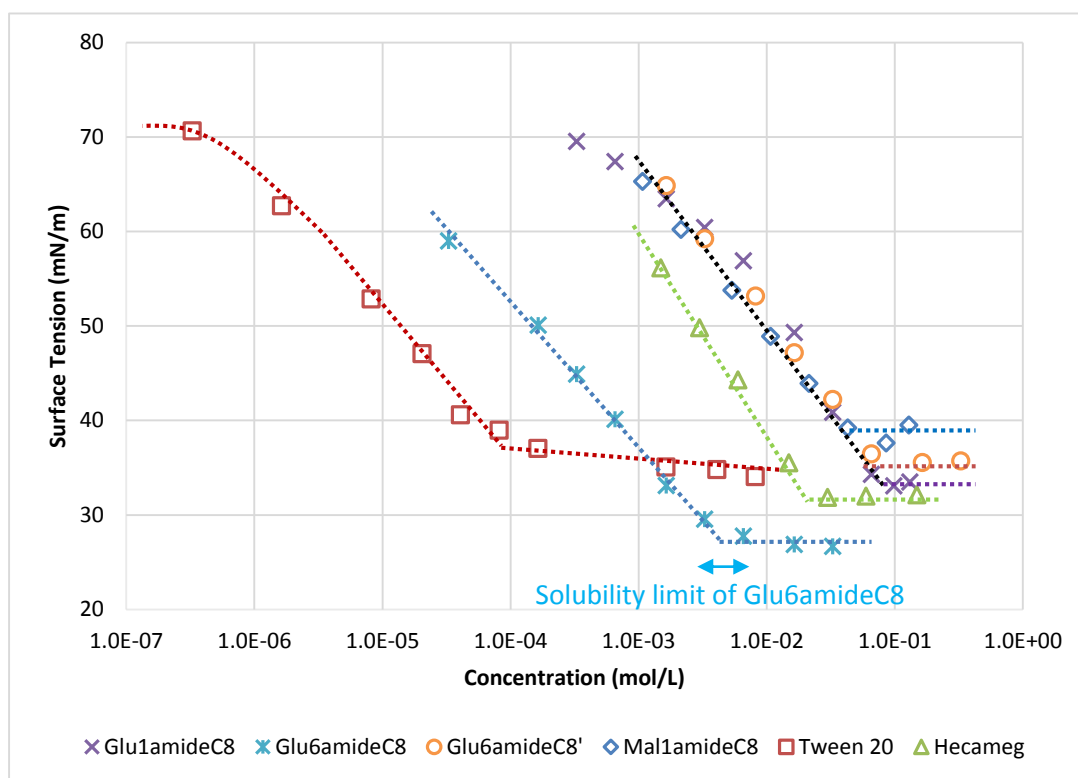


Figure 40: Surface tensions of surfactants in water solutions at 37°C (Solubility limit of Glu6amideC8 determined visually is pointed out, some points of Glu1amideC8, Glu6amideC8' and Mal1amideC8 are represented by only one curve for the purpose of readability).

Glu6amideC8 displays the strongest surface-active property at 37°C, by lowering the surface tension down to 26.6 mN/m at its solubility limit (between 3 mmol/L and 6 mmol/L). This result is in accordance with published report of a minimal surface tension of 24.4 mN/m for Glu6amideC8 water solution (Laurent, P., et al. 2011). Other surfactants, Glu1amideC8, Glu6amideC8' and Mal1amideC8, all reduced the surface tension to a comparable level as Tween 20 and Hecameg. Their minimal surface tension were 33 mN/m (Glu1amideC8), 35 mN/m (Glu6amideC8'), 39mN/m (Mal1amideC8), 34 mN/m (Tween 20) and 31 mN/m (Hecameg), respectively. The results of Glu1amideC8 were found to be similar to study of Brennerhenaff, C., et al. (1993) where the surface tension was be reduced to ~30 mN/m at 25°C. Glu6amideC8' was reported to achieve a minimum surface tension of 33 mN/m at 70°C (Maunier, V., et al. 1997). Minimal surface tension of Tween 20 and Hecameg aqueous solutions are reported to be 33 mN/m at 30 °C and 32 mN/m at 25°C (Plusquellec, D., et al. 1989; Maunier, V., et al. 1997), respectively. It should be noted that, Glu6amideC8 reached its solubility limit between 3 mmol/L and 6 mmol/L. All the surface tension values above this concentration are actually measured in turbid solutions of Glu6amideC8.

The minimal surface tension curve was reached at concentrations (reported in Table 15) which were interpreted as CMCs when the surfactant is completely soluble in water above this concentration. When the solution becomes turbid at this particular concentration, the related concentration was noted CMC*. Further experiments were performed by dye solubilization (see paragraph II of this section) in order to confirm the interpretation of this critical

concentration as a CMC value.

Table 15: CMCs of surfactants determined by surface tension measurement.

Surfactant	Subphase: water
	CMC by surface tension method (mmol/L)
Glu1amideC8	70
Glu6amideC8	4 (CMC*)
Glu6amideC8'	65
Mal1amideC8	60
Tween 20	0.08
Hecameg	20

CMC*: concentration to reach minimum surface tension when surfactant was not soluble.

Similar values were found in product information sheet for Tween 20 (0.06 mmol/L, 20°C - 25°C) and Hecameg (19.5 mmol/L, room temperature) or in the literature: Glu1amideC8 (80 mmol/L, 37°C), Glu6amideC8' (55 mmol/L, 70°C) and Mal1amideC8 (51 mmol/L, 20°C) (Brennerhenoff C., 1993; Maunier, V., et al. 1997; Lubineau, A., Augé, J., & Drouillat, B. 1995). For Glu6amideC8, which we have observed a solubility limit and a CMC* at 4 mmol/L, Laurent, P., et al. (2011) reported a CMC at 3.3 mmol/L at 20°C.

6.2. CMCs of surfactant by dye solubilization method

Since the apparition of plateau in surface tension curves can either due to presence of new phase (micelles) or due to limitation of solubility (no more free monomers can contribute to the surface pressure), dye solubilization experiments were performed to further clarify surfactants behavior at their CMCs (CMC* for Glu6amideC8).

Synthesized sugar-based surfactants Glu1amideC8 and Glu8amideC8' displayed Krafft points at 30°C and 32°C respectively. Dye solubilization method was carried out both below (room temperature) and above (37°C) their Krafft points so as to display the difference of measured absorbance (Figure 41). If micelles are formed in the solution, the absorbance (518 nm) tends to decrease as is described in Chapter II, B-8.

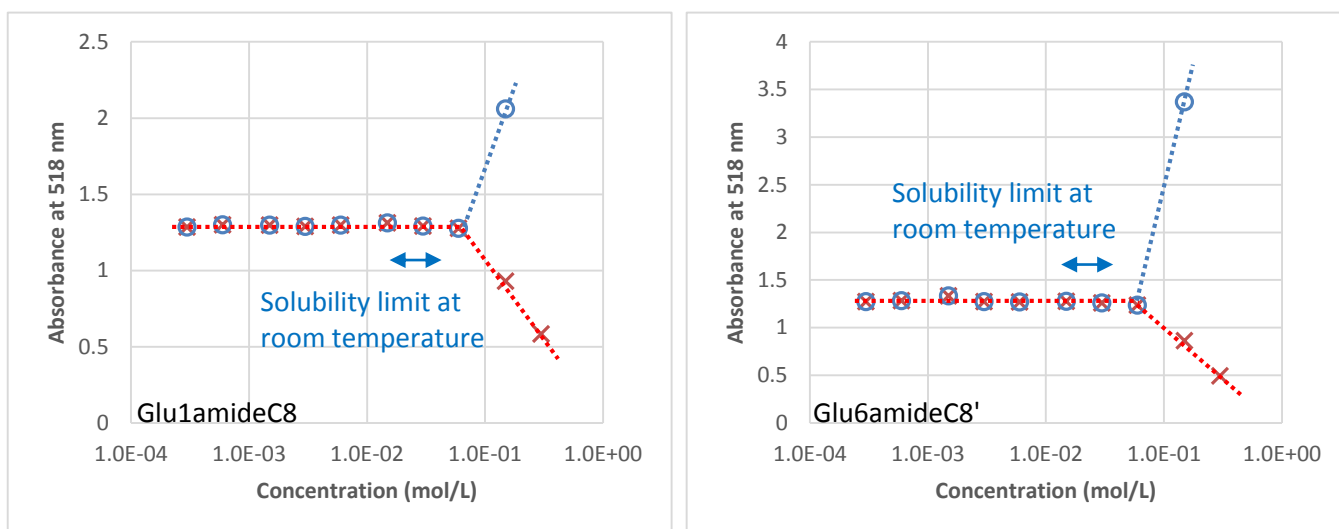


Figure 41: Absorbance (518 nm) of Eosin Y-surfactant mixed solution at room temperature (○) and at 37°C (×), concentration of Eosin Y is fixed at 0.17 mmol/L. The solubility limit was determined previously by visual observation.

A clear difference of absorbance between tests at room temperature and at 37°C can be seen according to Figure 41. At room temperature, solubility of Glu1amideC8 and Glu6amideC8' is both limited between 16-33 mmol/L by visual observation. At concentrations slightly higher than their solubility limit, insoluble particles appear in the mixture, but it is still not enough to induce significant change of light absorbance at 518 nm. However, when the concentrations of surfactants increase to over ~60 mmol/L (about 2 times higher than their solubility limit), light passing through the suspensions with insoluble aggregates is scattered and the measured optical absorbance increases. In this case, no micelles were formed. At 37°C, however, an opposite trends are observed at concentration higher than ~60 mmol/L (in this case, the surfactant solutions were still clear), the optical absorbance at 518 nm of solutions decreases. This is due to incorporation of Eosin Y molecules into surfactant micelles in the solution. The results are in agreement with the fact that Glu1amideC8 and Glu6amideC8' both possess Krafft points between room temperature and 37°C, revealing that they are more soluble and can form micelles at 37°C.

In general, UV absorption experiments reveal an increase of absorption when the solubility limit is reached. It shows a clear distinction between surfactant solution below and above the Krafft point compared to surface tension measurement.

For other synthesized surfactants and standard surfactants, their water solutions were characterized by dye solubilization method at 37°C. Results are presented in Figure 42, solubility limit of Glu6amideC8 determined visually is pointed out.

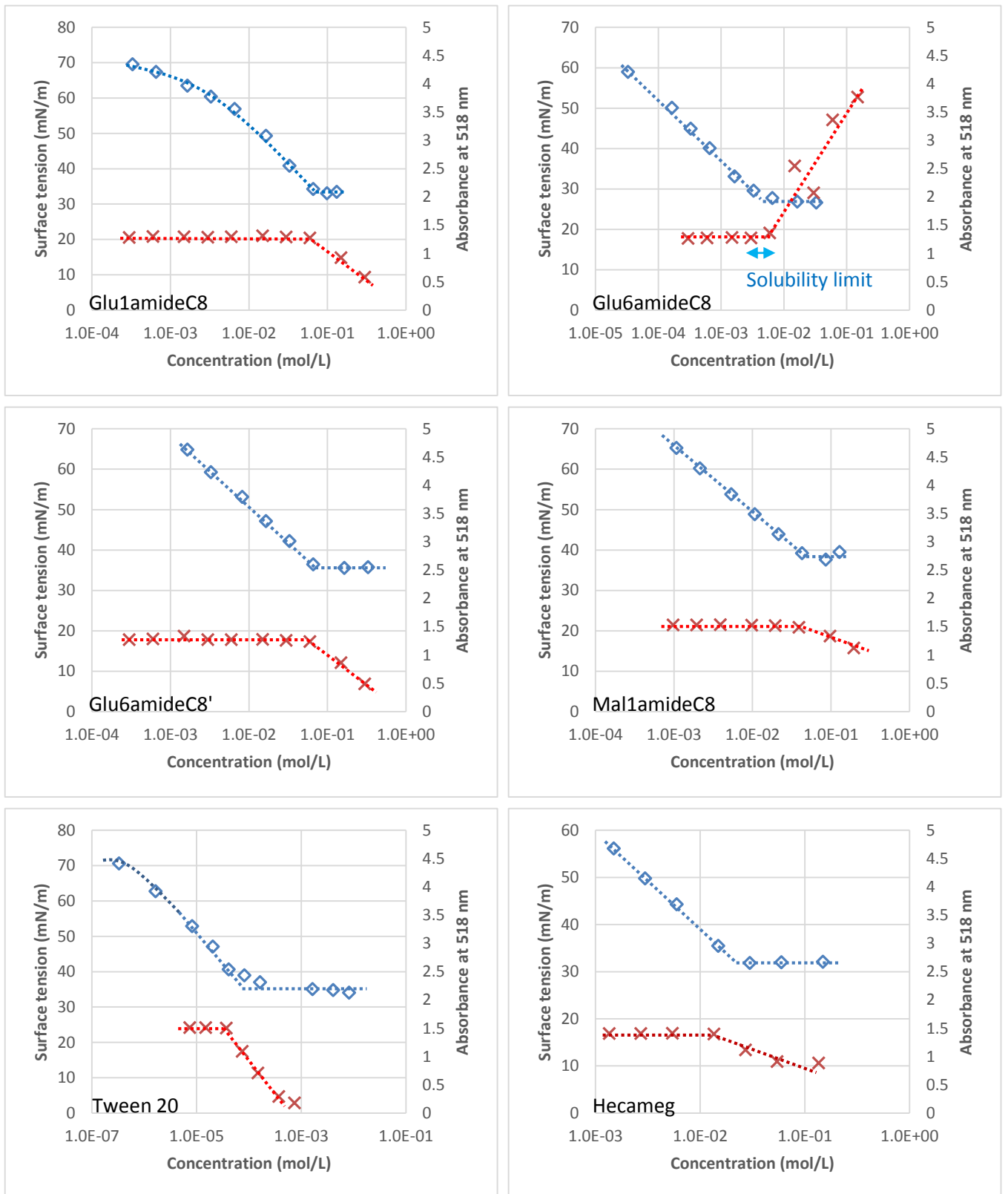


Figure 42: Surface tension (◇) of surfactant solutions and optical absorbance at 518 nm (×) of Eosin Y-surfactant mixed solutions, concentration of Eosin Y is fixed at 0.17 mmol/L. Solubility limit is determined visually.

Absorbance of Eosin Y in surfactant solution decreases near the concentration where

minimum surface tension are obtained for Tween 20, Hecameg, Glu1amideC8, Glu6amideC8', Mal1amideC8. However, for Glu6amideC8, the optical absorbance at 518 nm increases dramatically showing the presence of non-soluble Glu6amideC8 aggregates in the solution (as is also observed for Glu1amideC8 and Glu6amideC8' at room temperature as seen in Figure 42). It indicated that no micelles were formed under this condition and insoluble particles are suspended in solution. CMCs for surfactants determined by two methods are listed in Table 16.

Table 16: CMC of surfactant in water solution determined by surface tension and dye solubilization, $T=37^{\circ}\text{C}$.

Surfactant	Subphase: water	
	CMC by surface tension method (mmol/L)	CMC by dye solubilization method (mmol/L)
Glu1amideC8	70	65
Glu6amideC8	4 (CMC*)	N.A
Glu6amideC8'	65	70
Mal1amideC8	60	50
Tween 20	0.08	0.04
Hecameg	20	15

CMC*: concentration to reach minimum surface tension when surfactant was not soluble.

As can be seen from the results, CMCs determined by surface tension method and by dye solubilization method showed a consistency.

7. Maximal surface excess concentration and minimum surface area of surfactants in water solutions

According to the surface tension measurement, the maximal surface excess concentration Γ_{max} and the minimum surface area occupied by each surfactant A_{min} were calculated and presented in Table 17 (methods are presented in Chapter II, B-7).

Table 17: Calculated surface excess concentration and surface area occupied by molecule.

Molecule	Γ_{max} ($\mu\text{mol/L}$)	A_{min} (\AA^2)
Glu1amideC8	3.39	48.9
Glu6amideC8	2.91	57.2
Glu6amideC8'	3.01	55.1
Mal1amideC8	2.62	63.5
Tween 20	2.86	58.1
Hecameg	3.36	49.4

Corresponding results of some molecules are reported by others, Glu6amideC8 ($A_{min}=25 \text{\AA}^2$, 20°C), Glu6amideC8' ($A_{min}=57 \text{\AA}^2$, 70°C), Tween 20 ($\Gamma_{max}=3.57 \mu\text{mol/L}$, $A_{min}=46.5 \text{\AA}^2$, 30°C),

Hecameg ($A_{\min}=49 \text{ \AA}^2$, 70°C ; $A_{\min}=41 \text{ \AA}^2$, 21°C) (Laurent, P., et al. 2011; Maunier, V., et al. 1997; Niño, M. R. R., & Patino, J. R. 1998). Some of the results (Glu6amideC8, Tween 20) are remote from what we obtained. There are several possibilities. I) The exact composition of each sample. For example, the α/β glycopyranosides ratio for Glu6amideC8 synthesized by Laurent, P. is 36/64 (in DMSO), while in our case, the ratio has not been investigated. The stereochemical structure of molecules can influence their adsorption behavior at liquid-air interface. II) Test temperature, A_{\min} may increase with test temperature due to thermodynamic perturbation. III) There is some imprecision in the determination of A_{\min} from the slope of the surface tension curves.

8. Self-assembling properties of surfactant in water

Another way to assess the presence of micelles in solution is to perform Small-angle X-ray scattering experiments (SAXS), which were conducted on a few samples by Mélanie Emo and Marie-José Stébé from the SRSMC laboratory of the Université de Lorraine (Nancy). SAXS is a non-destructive technique allowing the investigation of nanostructures ranging from 1nm to about 200nm. Scattering intensity curves $I(q)$ will reveal the presence of scattering objects in solution. Analysis of the curves and confrontation between models and experimental results will confirm the existence (or not) of micelles and give information about their size and shape, as well as their internal structure. Indeed, the electron-density difference between the hydrophobic and hydrophilic parts of the surfactant provides information on the repartition of both fragments in the micelle (core-shell structure). In order to obtain sufficient intensity, rather concentrated solutions are needed. In this study, 50 g/L (5% wt/vol) solutions of Glu6amideC8' surfactant were investigated both at room temperature and at 45°C in order to evidence the change of structure from below to above the Krafft point of the surfactant (32°C). For comparison purposes, 50 g/L solutions of Hecameg were also studied at room temperature. The analysis of the results was performed by the SRSMC laboratory in Nancy on the basis of their previous work (see for instance Emo, M., et al. 2013; May Masnou, A., et al. 2012).

At 45°C , the scattering intensity curve of the Glu6amideC8' solution shows a maximum at around 2.3 nm^{-1} . This maximum, being above 1 nm^{-1} , does not arise from inter-particle effects but is consistent with the presence of isolated micelles in the solution (form factor). Analysis by Generalized Indirect Fourier Transformation (GIFT) gives the pair-distance distribution function reflecting the structural features of the systems. It reveals the presence of almost spherical micelles (slightly ellipsoidal) with a maximum diameter of 5.5 nm. The micelles are characterized by an inhomogeneous repartition of electronic density typical of core-shell micelles. The radius of the internal core is around 1.2-1.3 nm (Figure 43). More results will be found in Appendix 2.

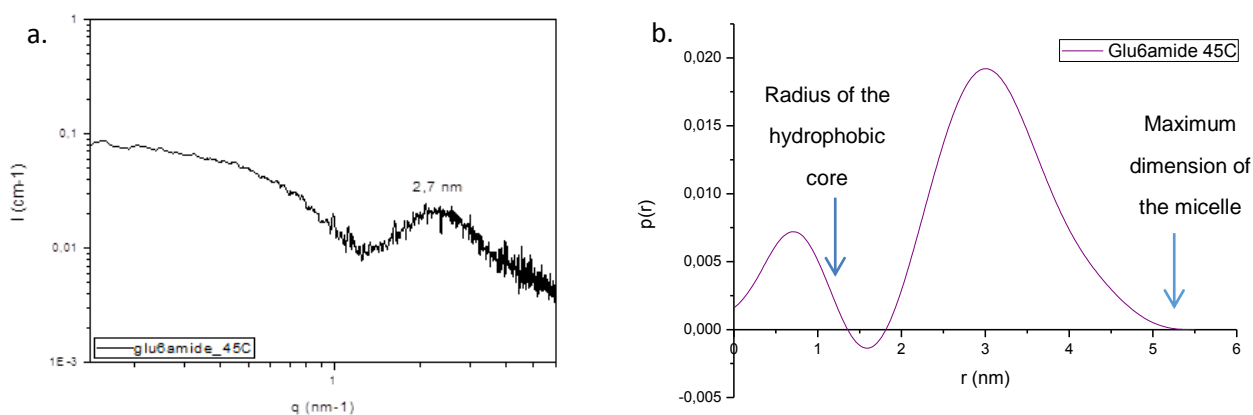


Figure 43: a) Experimental SAXS spectrum of 50 g/L Glu6amideC8' in water at 45°C, b) Pair-distance distribution function obtained by GIFT analysis showing the characteristic dimensions of the micelle.

When placed at 25°C, the 5% Glu6amideC8' sample crystallized rapidly and the structure formed is radically different from the one observed at 45°C. Characteristic distances being much smaller in the crystal than in micelles, WAXS/SAXS experiments were performed, showing the presence of a L β phase, consisting of a stack of bilayers, in which the alkyl chains are in a solid phase (May Masnou, A., et al. 2012) (see Appendix 2).

A solution of Hecameg of the same concentration (50 g/L in water) was analyzed at 25°C. The variation of scattering intensity looks rather similar to what was obtained for Glu6amideC8', although the absolute value of intensity is significantly higher in the case of Hecameg, and is typical of a micellar solution (Figure 44). However, the GIFT analysis evidence a pair-distribution function with quite different features. The long tail at high values of r reveals of an elongated cylindrical particle (May, Masnou, et al. 2012). The micelle has a core shell cylindrical structure of maximum length about 14 nm with a radius of the hydrophobic core of around 3.9-4.0 nm.

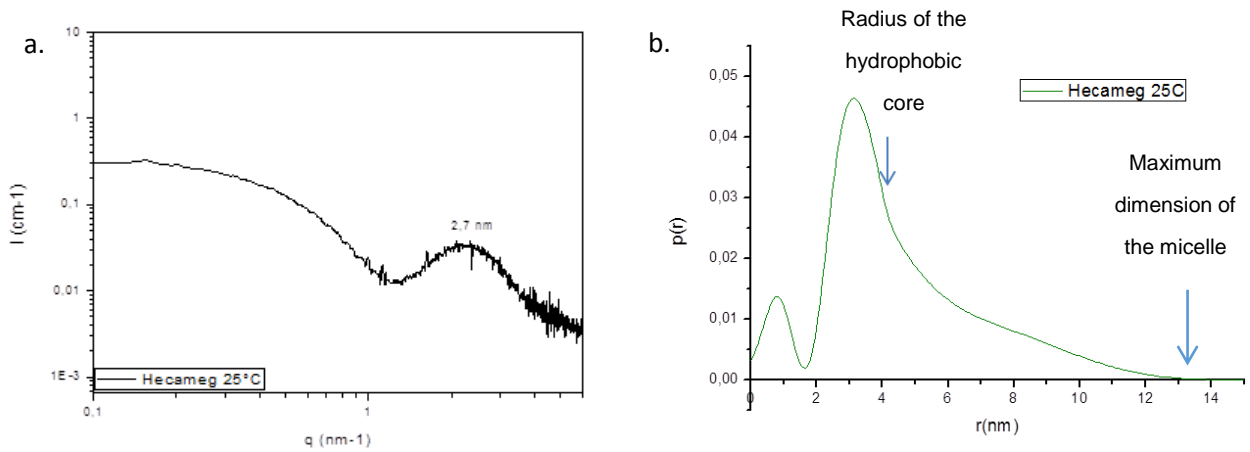


Figure 44: a) Experimental SAXS spectrum of 50 g/L Hecameg in water at 25°C, b) Pair-distance distribution function obtained by GIFT analysis showing the characteristic dimensions of the micelle.

9. Surface tensions of surfactants in complete DMEM without Fetal Bovine Serum

In order to understand surfactant's behavior in culture medium, surface tensions of surfactants in complete DMEM without addition of fetal bovine serum have been compared with their values in water, results are presented in Figure 45.

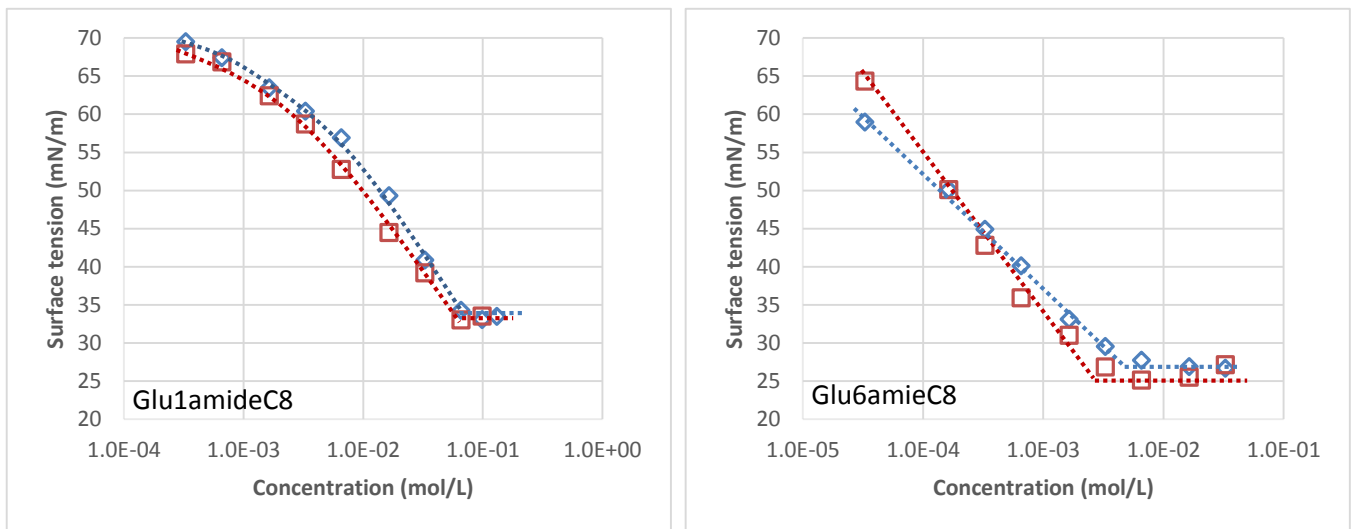


Figure 45: Surface tensions of surfactant in water (\diamond) and in complete DMEM (no FBS) (\square), $T=37^\circ\text{C}$ (part 1).

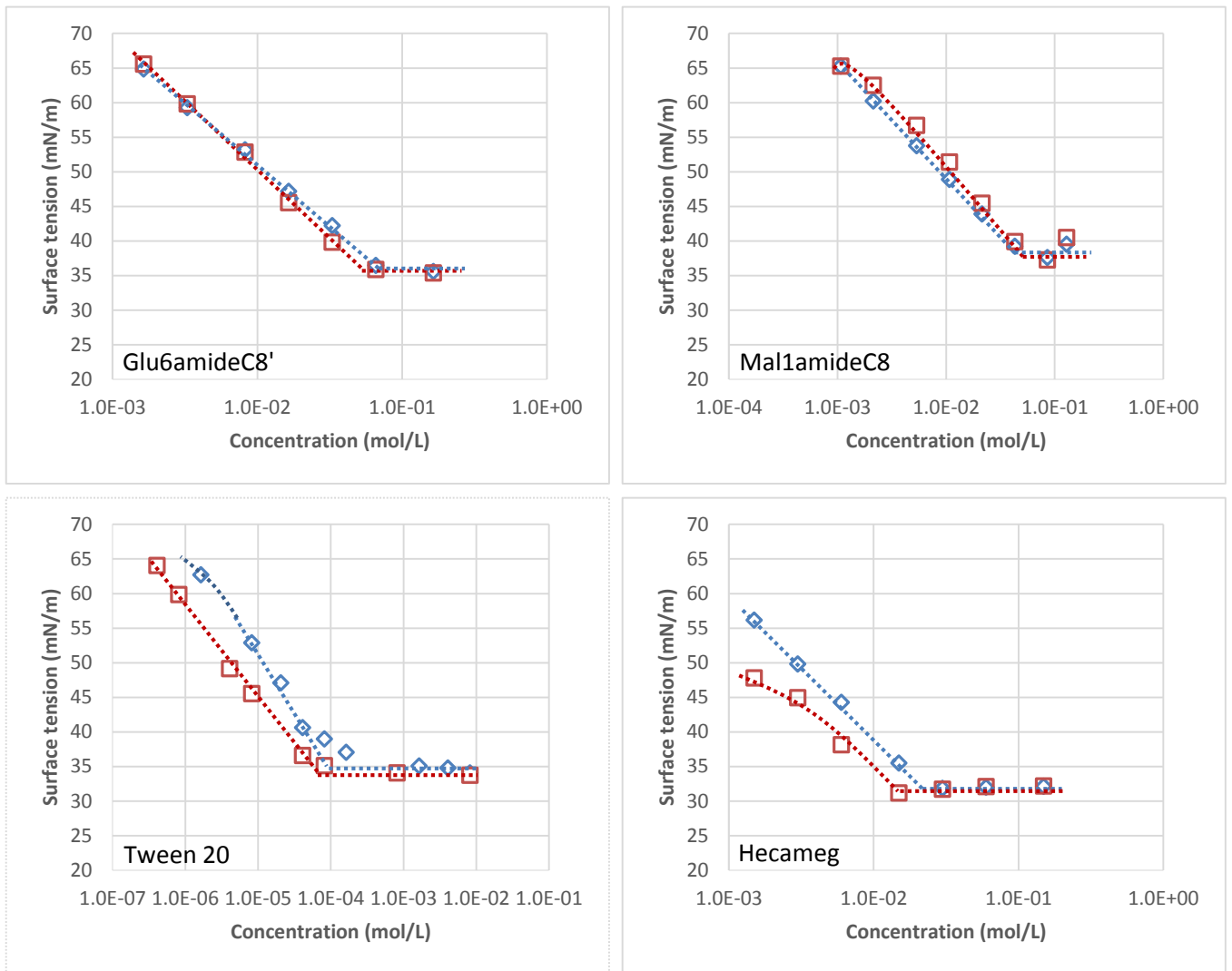


Figure 45: Surface tensions of surfactant in water (\diamond) and in complete DMEM (no FBS) (\square), $T=37^{\circ}\text{C}$ (part 2).

Surface tensions of water and complete DMEM (no FBS) when no surfactant is added are 72 mN/m and 69 mN/m respectively. The surface tension curves obtained for each surfactant in two solutions are close to each other, indicating that the adsorption behavior of surfactant molecules at air/ liquid interface in these two solutions are similar. No significant interaction between surfactant and molecules in complete DMEM (no FBS) is observed.

10.Surface tensions of surfactants in complete DMEM (with Fetal Bovine Serum)

Surface tensions of surfactant in complete DMEM (FBS was added in the solution) were studied and compared to the values in complete DMEM (no FBS). Results are presented in Figure 46.

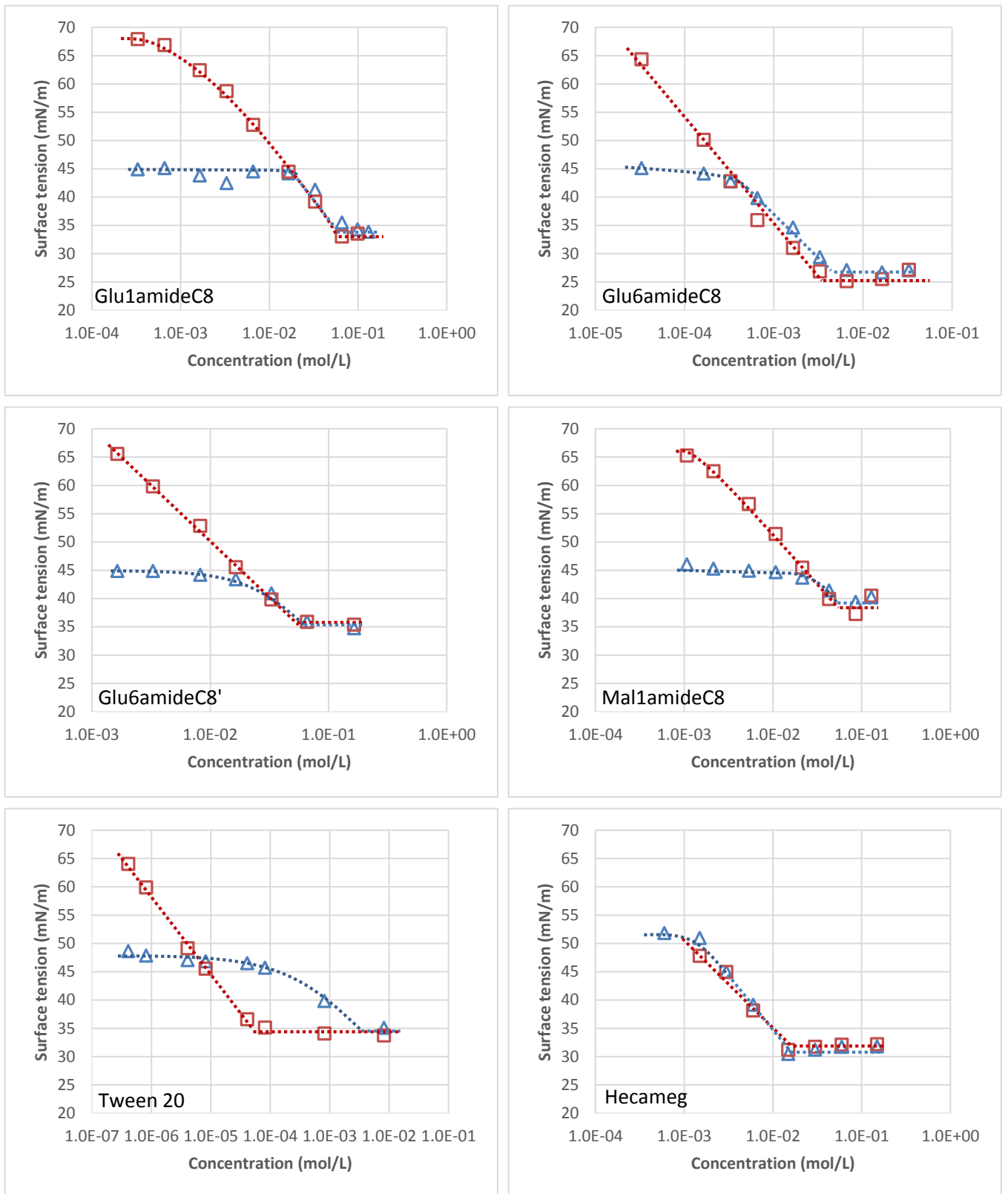


Figure 46: Surface tensions of surfactant in complete DMEM (Δ) and in complete DMEM (no FBS) (\square), $T=37^{\circ}\text{C}$.

The surface tension of complete DMEM and complete DMEM (no FBS) at 37°C are 49 mN/m and 69 mN/m respectively. As seen from the Figure 46, in complete DMEM solution, surface

tensions of solutions start to drop from ~ 49 mN/m instead of 72 mN/m (the case in water solutions). At low concentrations, surface tension of complete DMEM solution slightly decreases from ~ 49 mN/m to ~ 44 mN/m. At higher concentrations, two different phenomena are observed for tested surfactants. I) Curve 1 (surface tension in complete DMEM) meets and then follows the same variations as curve 2 (surface tension in complete DMEM (no FBS)), they reach a same minimum surface tension and CMC (CMC* for Glu6amideC8) in the end. II) Curve 1 intersects with curve 2, they finally reach a same minimum surface tension, but curve 1 presents a higher CMC than curve 2.

Through the comparison, it can be concluded that the decrease of surface tension at low surfactant concentration is mainly caused by addition of FBS in complete DMEM. Actually, the ability of Bovine Serum Albumin (BSA) that can be found in FBS to lower surface tension of water has been reported. At concentration between 100 ppm and 10000 ppm (1.5 $\mu\text{mol/L}$ to 150 $\mu\text{mol/L}$), BSA can move to air/ liquid interface and BSA water solution exhibit a surface tension of 51 mN/m (McClellan, S. J., & Franses, E. I. 2003).

Actually, the results observed can be explained by the model of Lucassen-Reynders, E. H. (1994). Large surfactant molecules (BSA in the case) existing at the air/ liquid interface can be replaced by added smaller surfactant molecules (synthetic surfactants, Tween 20 or Hecameg) (Figure 47). During the process, the total surface coverage increases and surface tension drops slowly, when large surfactant molecules are completely displaced from the interface, the surface tension of solution is solely monitored by concentration of surfactant with smaller molecule.

For Tween 20 – BSA mixture specifically, Niño, M. R. R., & Patino, J. R. (1998) described their behavior in aqueous solutions. Tween 20 and BSA interact at interface and in the bulk phase, at low Tween 20 concentration, BSA serves as the major component to reduce surface tension. With addition of Tween 20 in the intermediate region, it can either bound to BSA in the solution or replace BSA at the interface, the two behaviors happen spontaneously, which results in a slow decrease of surface tension. At higher concentration, when the bounding site on BSA are saturated, added Tween 20 can move freely to the interface and replace BSA, this is demonstrated by a rapid decrease of surface tension. Therefore, higher Tween 20 concentration is needed to obtain the minimum surface tension in complete DMEM can attribute to interactions between Tween 20 and BSA in bulk solution.

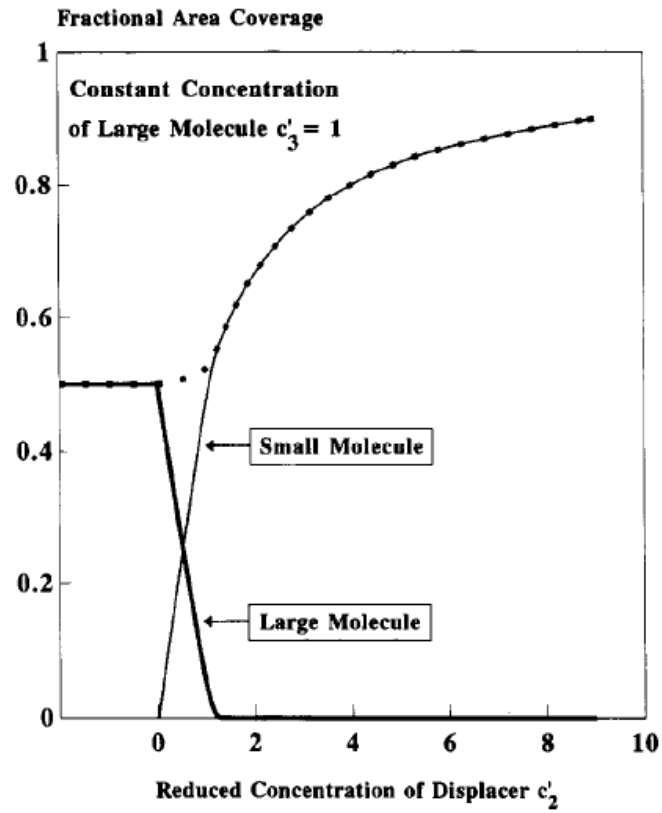


Figure 47: Displacement of macromolecule by small surfactant molecule at fixed concentration of macromolecule, c_3 ; broken line: total surface coverage. (Results calculated and presented by Lucassen-Reynders, E. H. 1994).

C) Cytotoxic/ irritant effects of synthesized surfactants on multi-scale cell/ tissue models

The physico-chemical properties of surfactants have been characterized and synthesized surfactants presented interesting surface-active properties. To explore their potential applications in domains such as cosmetic, pharmaceutical industries, it is important to understand their effects on human skin which is often exposed. Therefore, multi-scale cell/ tissue models have been established to test the potential cytotoxic/ irritant effects of synthesized surfactants.

1. Selection of 2D cell culture models for cytotoxicity tests

L929 fibroblasts were used because it is the standard cell line recommended for cytotoxicity test and always give out reproducible results (see Chapter II, C-1). In order to select a proper 2D cell culture model for cytotoxicity tests, two 2D cell culture models were firstly established and compared. In the first 2D cell culture model, standard surfactant Tween 20 was added in the culture medium right after cell seeding (Model 1). For the second 2D cell culture model, cells were seeded into culture plate and were left to grow for 24 h, a cell monolayer was hence formed, then, Tween 20 was applied (Model 2). Cytotoxicity tests were carried out after 48 h of surfactant treatment.

Cytotoxicity of surfactants against L929 cells in these 2 models was evaluated by proliferative index of cells (Figure 48). After treatment, living and dead cells were distinguished by trypan blue staining and the proliferative index was calculated as described in Chapter II, C-2. In the experiment, 24-well culture plates were used, densities of cells seeded in Model 1 and Model 2 are 10000 cells/ cm² and 5000 cells/ cm² respectively.

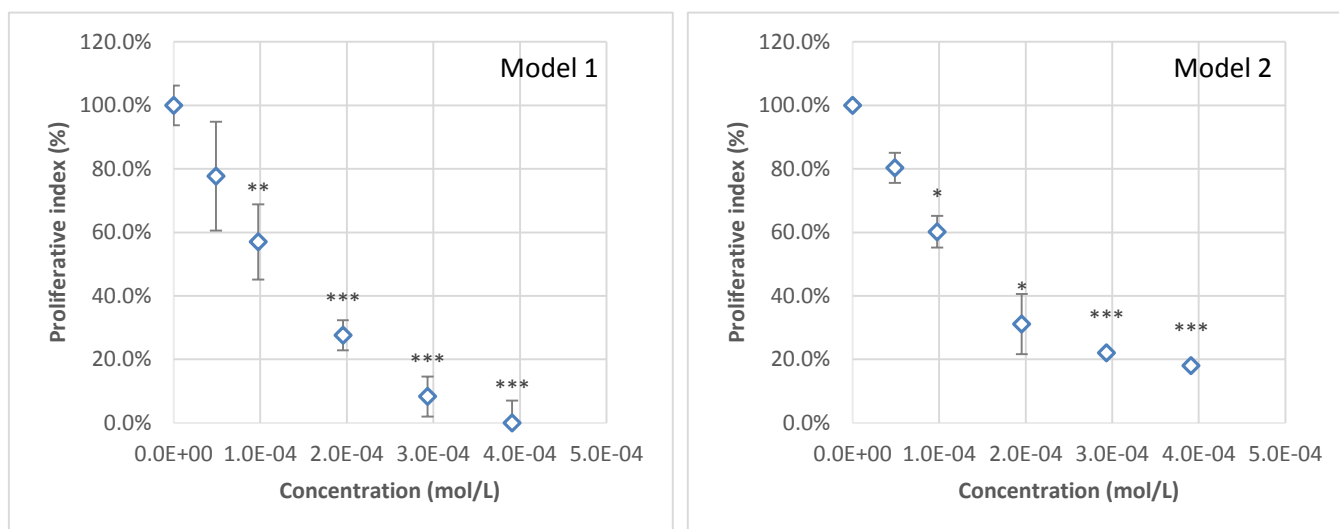


Figure 48: Proliferative index (◆) of L929 cells cultured in Model 1 and Model 2 treated with Tween 20 for 48 h (Model 1: Tween 20 was added right after seeding of cells; Model 2: Tween 20 was added after 24 h of cell culture in spread cells), results were normalized according to cell culture models without treatment. (n=6 per group for proliferative index; n=9 per group for metabolic activity, data are presented as mean with SD, *p<0.05, **p<0.01, ***p<0.001 (Mann-Whitney test) as compared to negative control).

Addition of Tween 20 significantly reduce the proliferative index of cells to a low level compared to negative control. Meanwhile, in Model 1, Tween 20 showed a relatively higher cytotoxicity against L929 cells than in monolayer models. The IC₅₀ values are 9.9×10^{-5} mol/L (Model 1) and 1.4×10^{-4} mol/L (Model 2) respectively. When Tween 20 was already dissolved in the culture medium, the surfactant may inhibit the adhesion of cells onto the bottom of culture plate due to its surface-active properties, therefore, fewer cells can proceed to the normal cell cycle and proliferate. On the contrary, when a cell monolayer was already formed, Tween 20 only affects cells at their exposed membrane, a lower cytotoxicity was thus observed. For most of the case in industrial applications, surfactants affect only existing cell matrix, the Model 2 (monolayer model) better mimic the situation and thus was used as standard 2D model for following tests.

2. Influence of surfactant on cell morphology in Model 2 (monolayer model)

Studying the morphology change of L929 cells after exposure to surfactants can help to understand the cytotoxicity effect. Hereby 4 pictures of 2D cell culture models treated with Glu1amideC8 and Glu6amideC8 within the range from 0.16 mmol/L to 2.3 mmol/L were chosen as representative samples to illustrate the morphology change. For other surfactants, similar trends were observed in a different range of concentrations. The tested concentrations are all below the surfactants' corresponding CMCs (CMC* for Glu6amideC8, CMC* here means the solubility limit of Glu6amideC8) in complete DMEM, which means that surfactant molecules are in form of monomers in culture medium.

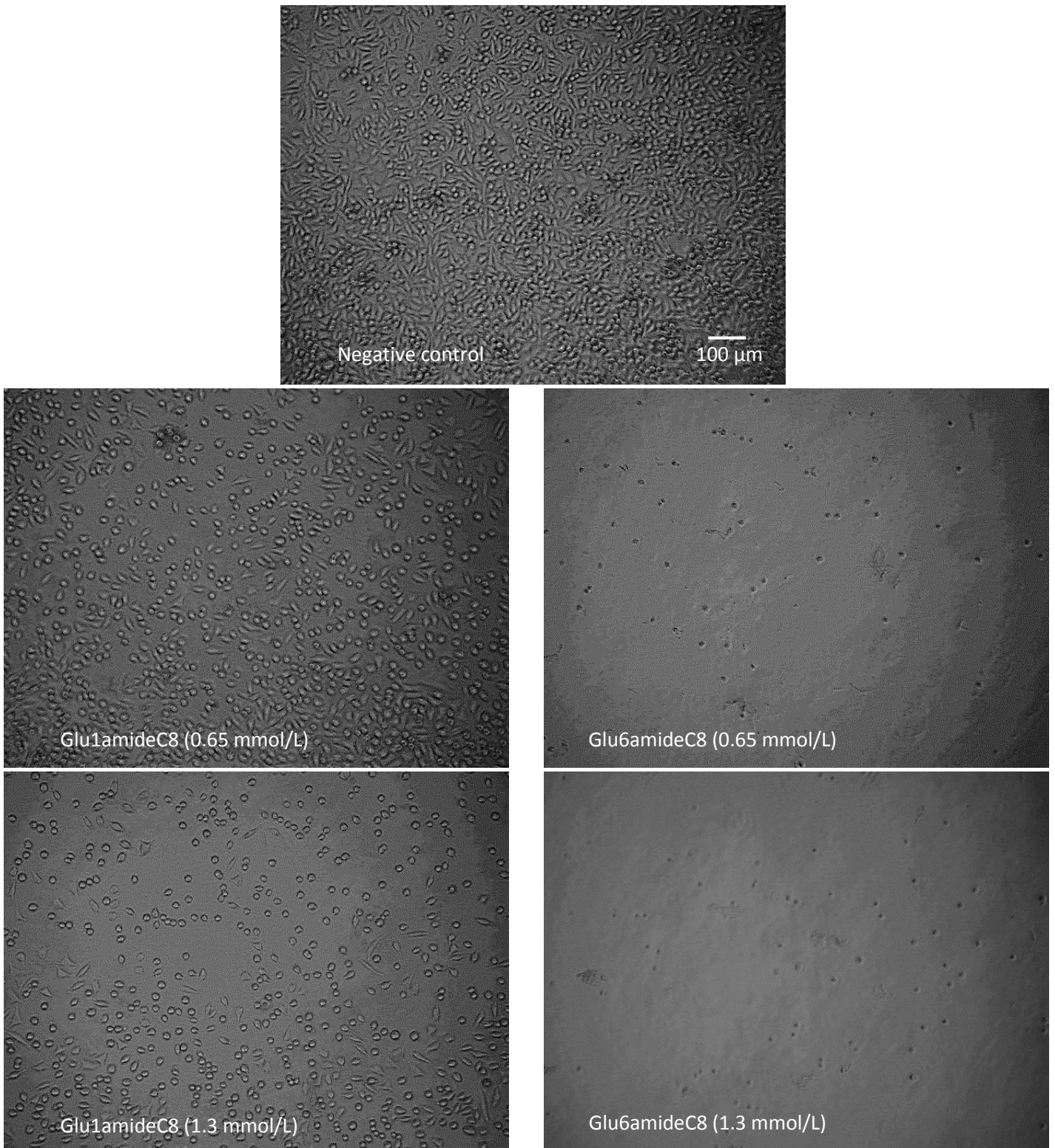


Figure 49: Morphology of L929 cells cultured in Model 2 (monolayer model) treated with surfactants for 48 h.

As seen in Figure 49, with the increase of surfactant concentration, density of L929 cells cultured in 2D cell culture model reduces accordingly. In negative control, when no surfactant is added into culture medium, the majority of cells are spindle-shaped and adhere at the bottom surface of culture plate, the morphology represents L929 fibroblasts undergoing

normal culture condition. At concentration of 0.65 mmol/L, a decrease of cell density can be seen, besides, more than half of the living cells have started rounding up, which indicates a gradual detachment of the cells from the culture plate. At higher concentration (1.3 mmol/L), even more living cells become spherical-shaped and total cell number continues to decrease. For 2D cell culture model treated with Glu6maideC8 at 0.65 mmol/L and 1.3 mmol/L, no living cells can be observed (at the bottom of culture plate or floating in the culture medium), suggesting they are possibly destructed.

3. Cytotoxicity of surfactants on monolayer cell culture models

In previous tests, surfactants reduce cell density and change their morphology. The relationship of cytotoxicity effect of surfactants and their concentrations is still unclear. To obtain quantitative results of surfactant cytotoxicity, L929 cells cultured in monolayer models were characterized by their proliferative index and metabolic activity after 48 h of surfactants treatment.

Proliferative index and metabolic activity of L929 cells cultured in monolayer models treated with synthesized surfactants and standard surfactants are presented in Figure 50 and Figure 51, results are all normalized according to negative control.

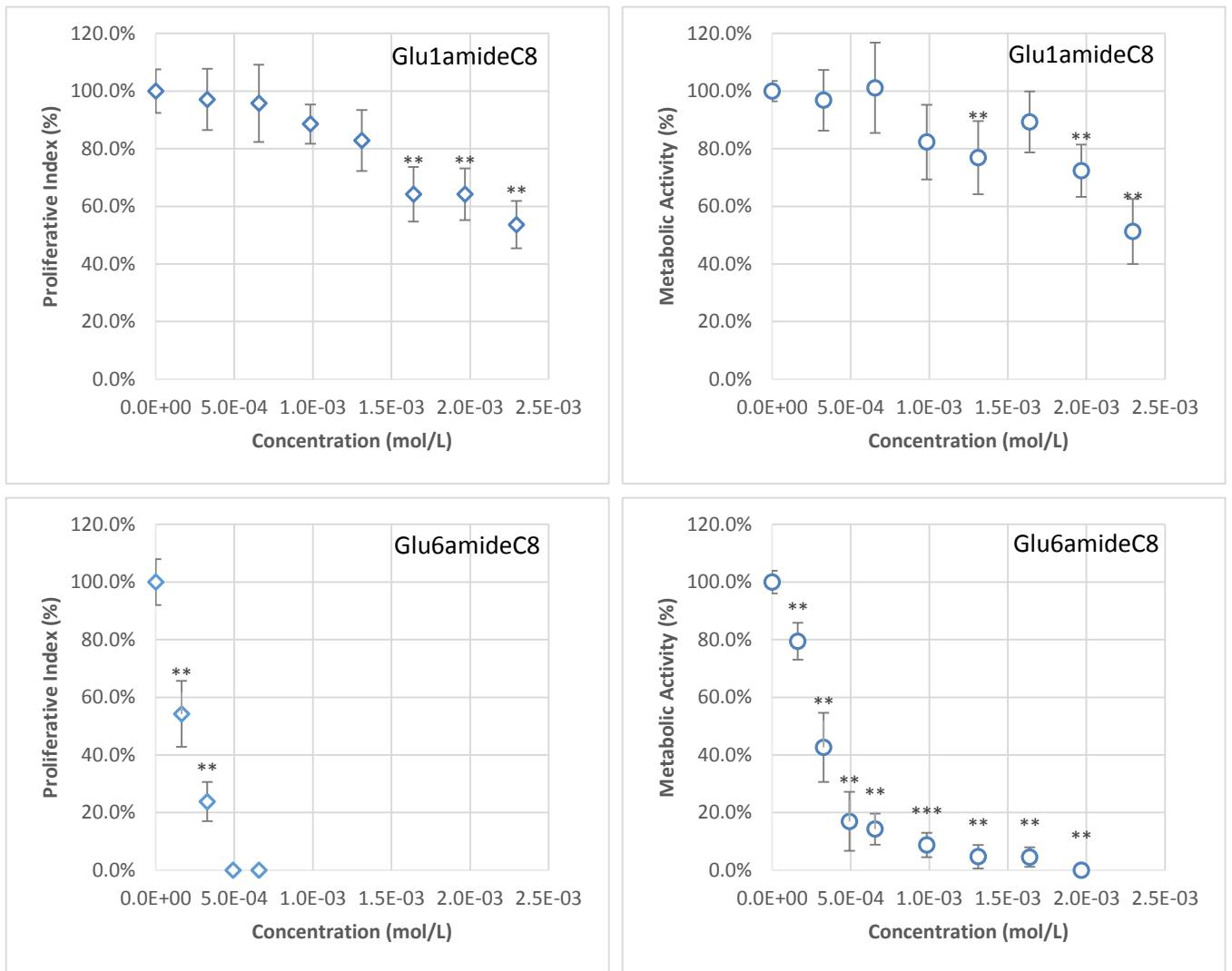


Figure 50: Normalized proliferative index (◊) and metabolic activity (○) of L929 cells cultured in monolayer model for 24 h and then treated with synthesized surfactants for 48 h. (n=5 per group, data are presented as mean with SD, *p<0.05, **p<0.01, ***p<0.001 (Mann-Whitney test) as compared to negative control) (part 1).

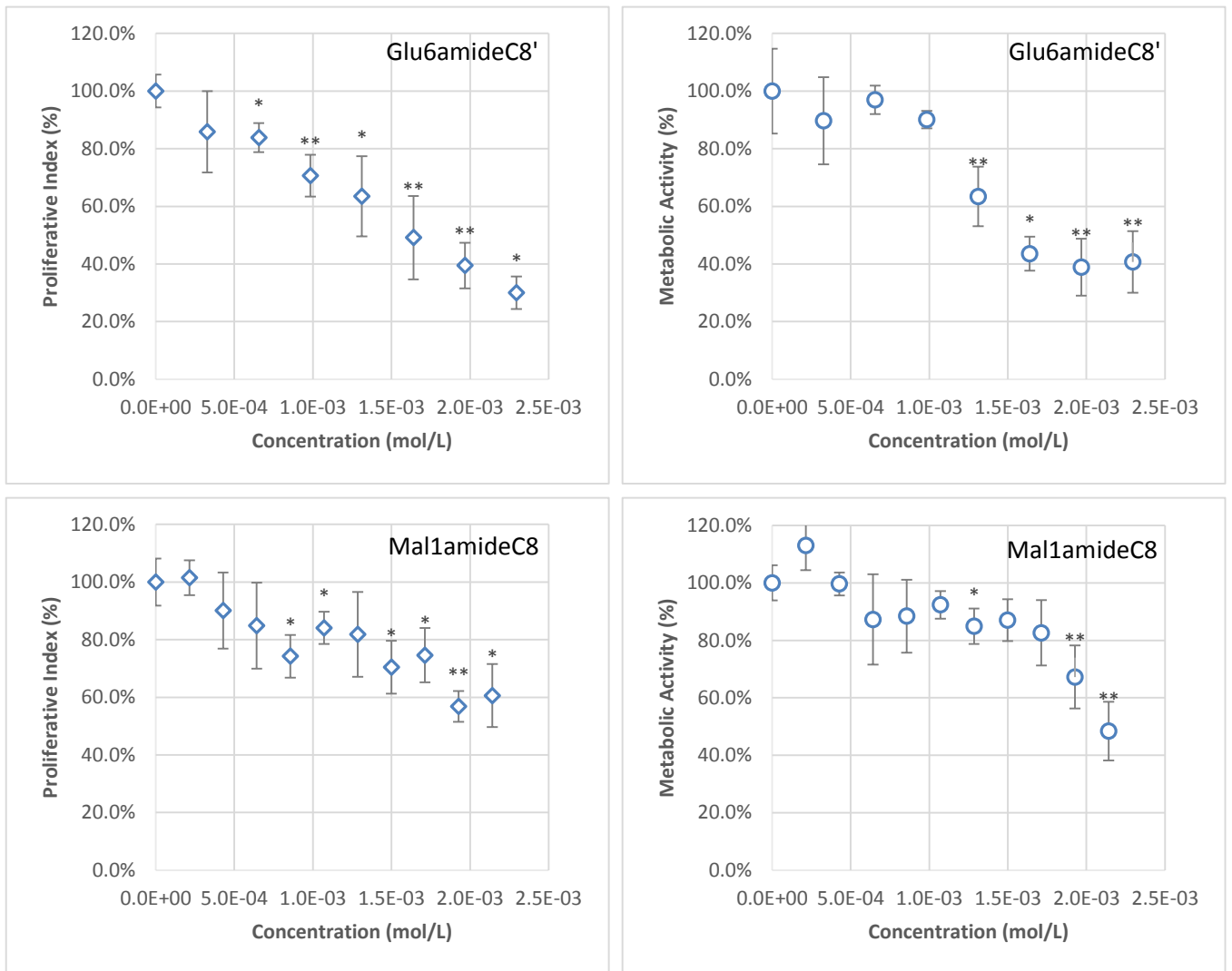


Figure 50: Normalized proliferative index (◊) and metabolic activity (●) of L929 cells cultured in monolayer model for 24 h and then treated with synthesized surfactants for 48 h. (n=5 per group, data are presented as mean with SD, *p<0.05, **p<0.01, ***p<0.001 (Mann-Whitney test) as compared to negative control) (part 2).

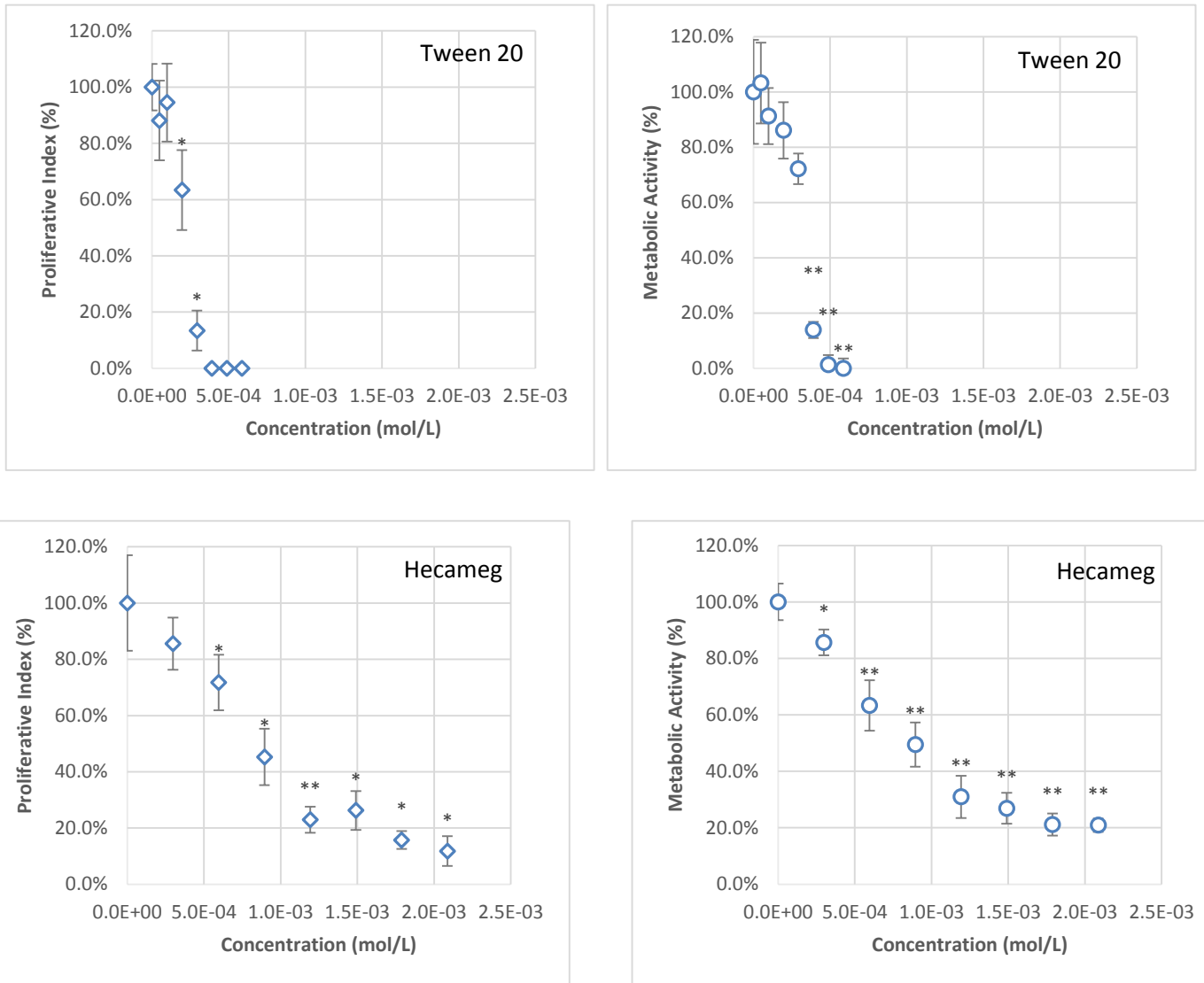


Figure 51: Normalized proliferative index (\diamond) and metabolic activity (\circ) of L929 cells cultured in monolayer model for 24 h and then treated with standard surfactants for 48 h. ($n=5$ per group, data are presented as mean with SD, $*p<0.05$, $**p<0.01$, $***p<0.001$ (Mann-Whitney test) as compared to negative control).

Results from proliferative index and metabolic activity of cells showed a similar trend for each surfactant, indicating a consistency between two methods. Glu6amideC8 and Tween 20 reduce the proliferative index of L929 cells in 2D models to 0 at concentration near 0.5 mmol/L, and they present relatively higher cytotoxicity compared to other surfactants (Glu1amideC8, Glu6amideC8', Mal1amideC8 and Hecameg). On the contrary, for Glu1amideC8 and Mal1amideC8, at the concentration near 2 mmol/L, the proliferative index or metabolic activity of L929 cells are still above 50%. To quantify the cytotoxicity of surfactants, their IC50s (half maximum inhibition concentration) against L929 cells were estimated and presented in Table 18.

Table 18: IC50 of surfactant against L929 cells determined by cell proliferative index or cell metabolic activity in monolayer model.

Surfactant	IC50 determined by proliferative index (mmol/L)	IC50 determined by metabolic activity (mmol/L)
Glu1amideC8	>2.3	>2.3
Glu6amideC8	0.20	0.31
Glu6amideC8'	1.6	1.5
Mal1amideC8	>2.1	2.0
Tween 20	0.19	0.29
Hecameg	0.81	0.86

Table 18 shows that the values of IC50 obtained by the two methods are close. Previous cytotoxicity experiments on cultured L929 cells have showed IC50 values of Tween 20 at 0.51 mmol/L (Neutral Red Uptake assay, 24 h exposure) and 0.31 mmol/L (Total protein Content test, 24 h exposure) respectively (Vian, L., et al. 1995), which are comparable to our results. Table 18 indicates that the three surfactants, Glu1amideC8, Glu6amideC8' and Mal1amideC8, are less toxic against L929 cells than Tween 20 or Hecameg. It is interesting to note that, the Glu6amideC8, regardless of its same molar mass and chemical compositions with Glu6amideC8', show a much higher cytotoxicity. It is possible that a subtle difference in the direction of amide group in Glu6amideC8' and Glu6amideC8 structures may be a factor to induce their different cytotoxicity.

Cell viability calculated after trypan blue coloration can help to quantify the amount of living cells compared to amount of total cells after surfactant treatment. Cell viabilities at 3 typical surfactant concentrations are presented in Table 19 (the lowest test concentration, the moderate test concentration and the highest test concentration).

Table 19: Cell viability after 24 h of growth followed by 48 h of surfactant treatment and their corresponding proliferative index in 2D cell culture model.

Surfactant	C ₁ mmol/L	V ₁ %	PI ₁ %	C ₂ mmol/L	V ₂ %	PI ₂ %	C ₃ mmol/L	V ₃ %	PI ₃ %
Glu1amideC8	0.33	98 ± 2	97 ± 11	1.3	97 ± 3	83 ± 11	2.3	99 ± 3	54 ± 8
Glu6amideC8	0.16	98 ± 3	54 ± 11	0.33	94 ± 6	24 ± 7	0.66	0	0
Glu6amideC8'	0.33	99 ± 2	86 ± 14	1.3	99 ± 1	64 ± 14	2.3	100	30 ± 6
Mal1amideC8	0.21	99 ± 2	102 ± 6	1.1	98 ± 2	84 ± 6	2.1	98 ± 3	61 ± 11
Tween 20	0.049	96 ± 3	88 ± 14	0.20	89 ± 7	63 ± 14	0.59	0	0
Hecameg	0.30	99 ± 2	86 ± 9	1.2	98 ± 4	23 ± 4	2.1	90 ± 10	12 ± 5

Values are presented as average ± std. C₁, C₂, C₃: concentration of surfactant; V₁, V₂, V₃: viability of cells; PI₁, PI₂, PI₃: normalized proliferative index of cells.

It is believed that the viability for cells is overestimated. According to the calculated results, viability of cells is always above ~90% as long as there are living cells at the bottom of culture

plate, these values are independent of type and concentration of surfactants. Actually, few dead cells were visible during the experiments although a sharp diminution of living cell number was observed, which indicated that a large number of dead cells was totally destructed (Altman, S. A., et al. 1993).

The non-normalized proliferative index of cells (number of living cells after treatment/ number of seeded cells) is used to characterize the inhibition ability of surfactants on cell proliferation. Proliferative index higher than 1 means that the cytotoxicity effect of surfactant is not enough to inhibit the increase of cell numbers; on the contrary, proliferative index lower than 1 means that the cell proliferation is greatly inhibited, cells are dying with surfactant treatment and total cell number decreases. Non-normalized proliferative index at 3 typical concentrations (the lowest test concentration, the moderate test concentration and the highest test concentration) are presented in Table 20.

Table 20: Non-normalized proliferative index after 24 h of growth and then 48 h of surfactant treatment in 2D cell culture models.

Surfactant	C ₁ mmol/L	nPI ₁	C ₂ mmol/L	nPI ₂	C ₃ mmol/L	nPI ₃
Glu1amideC8	0.33	11 ± 1.2	1.3	10 ± 1.2	2.3	6 ± 1.0
Glu6amideC8	0.16	11 ± 2.2	0.33	5 ± 1.4	0.66	0
Glu6amideC8'	0.33	17 ± 2.8	1.3	12 ± 2.7	2.3	6 ± 1.1
Mal1amideC8	0.21	11 ± 0.6	1.1	9 ± 0.6	2.1	6 ± 1.2
Tween 20	0.049	6 ± 0.9	0.20	4 ± 0.9	0.59	0
Hecameg	0.30	10 ± 1.1	1.2	3 ± 0.6	2.1	1 ± 0.6

Values are presented as average ± std. C₁, C₂, C₃: concentration of surfactant; nPI₁, nPI₂, nPI₃: non-normalized proliferative index of cells.

For Glu6amideC8 and Tween 20, at their highest test concentrations, cell proliferative index are zero, which means the two surfactants inhibit the growth and induce death of L929 cells at 0.66 mmol/L (Glu6amideC8) and 0.59 mmol/L (Tween 20) respectively. For other surfactants, the non-normalized proliferative index are above 1, cell number increases compared to the number of seeded cells. However, it should be noted that, cells were cultured for 24 h to form monolayer prior to surfactant treatment, therefore, the calculated non-normalized proliferative index cannot uniquely reflect the effects of surfactant treatment. For example, cells can firstly proliferated for 24 h, reaching a larger cell population, then, after surfactant treatment, cell numbers fall back but it was still higher than number of seeded cells. In this case, surfactant inhibits cell proliferation but the calculated non-normalized proliferative index is still above 1. In Table 20, a non-normalized proliferative index of 1 ± 0.6 after 24 h of cell growth and 48 h Hecameg treatment at 0.21 mmol/L can possibly be attributed to this condition.

Due to model limitations (limited cell-cell/ cell-ECM interactions...), cytotoxicity tests in 2D cell culture models are not sufficient to evaluate these surfactants, therefore, more complexed

models need to be established.

4. Establishment and characterization of L929 cells in 3D cell culture model

To characterize the cytotoxicity of synthesized surfactant, 2D models are cost-effective and easy to establish. Nevertheless, in 2D models, cells are restricted on plan surface and are all exposed to surfactant during treatment. 3D cell culture model includes the effect of Extra Cellular Matrix (ECM) on cells' response against chemical exposure and is more relevant to *in vivo* situations. In the context, model of L929 cells embedded in collagen gel and incubated in culture insert was prepared to produce physiologically similar environment to human dermis.

Hematoxylin and Eosin staining was used to label the nucleus and cytoplasm of cells in 3D model. Morphology of L929 cells cultured in 3D cell culture model after 6 days (144 h) of incubation is presented in Figure 52.

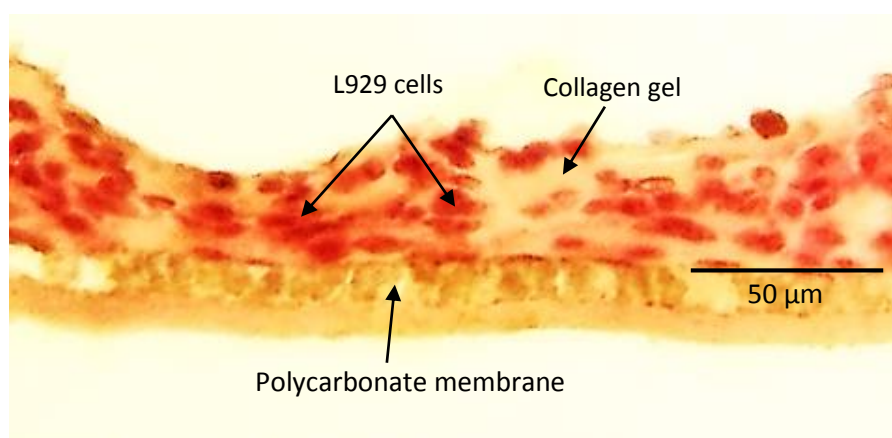


Figure 52: H&E stained paraffin section of L929 cells cultured in 3D cell culture model.

According to the protocol described previously, right after the construction of model, a collagen gel layer without cells lays between the membrane of insert and gel layer containing cells. However, after 144 h of incubation, as can be seen from the Figure 52, collagen gel function as a scaffold of the system and cells are distributed homogenously inside it. The cell-cell interaction and ECM interaction happen both horizontally and vertically. In this model, culture plate is filled with culture medium, it can penetrate into inner collagen gel either through the insert membrane or through the upper surface.

3D cell culture model allows cells to adhere to its matrix, enhancing three dimensional biophysical and biochemical interactions within them. It also possesses proper porosity, permeability and mechanical stability. All these properties make it a more suitable model for *in vitro* cytotoxicity evaluation than 2D models.

5. Cytotoxicity of surfactants on 3D cell culture models

Results obtained from 2D cell culture models helped to characterize surfactants' direct cytotoxicity effect against L929 cells. In 3D models, cells were cultured in a more complexed environment. Cell-cell, cell-ECM interactions, penetration of surfactant into the cell cluster, adsorption of surfactant onto collagen gel may all influence the measured cytotoxicity. Therefore, the exact effects of surfactants against cells in 3D models are worth investigating.

Cytotoxicity of surfactants was characterized by proliferative index and metabolic activity of L929 cells after treatment. Results are presented in Figures 53 and 54.

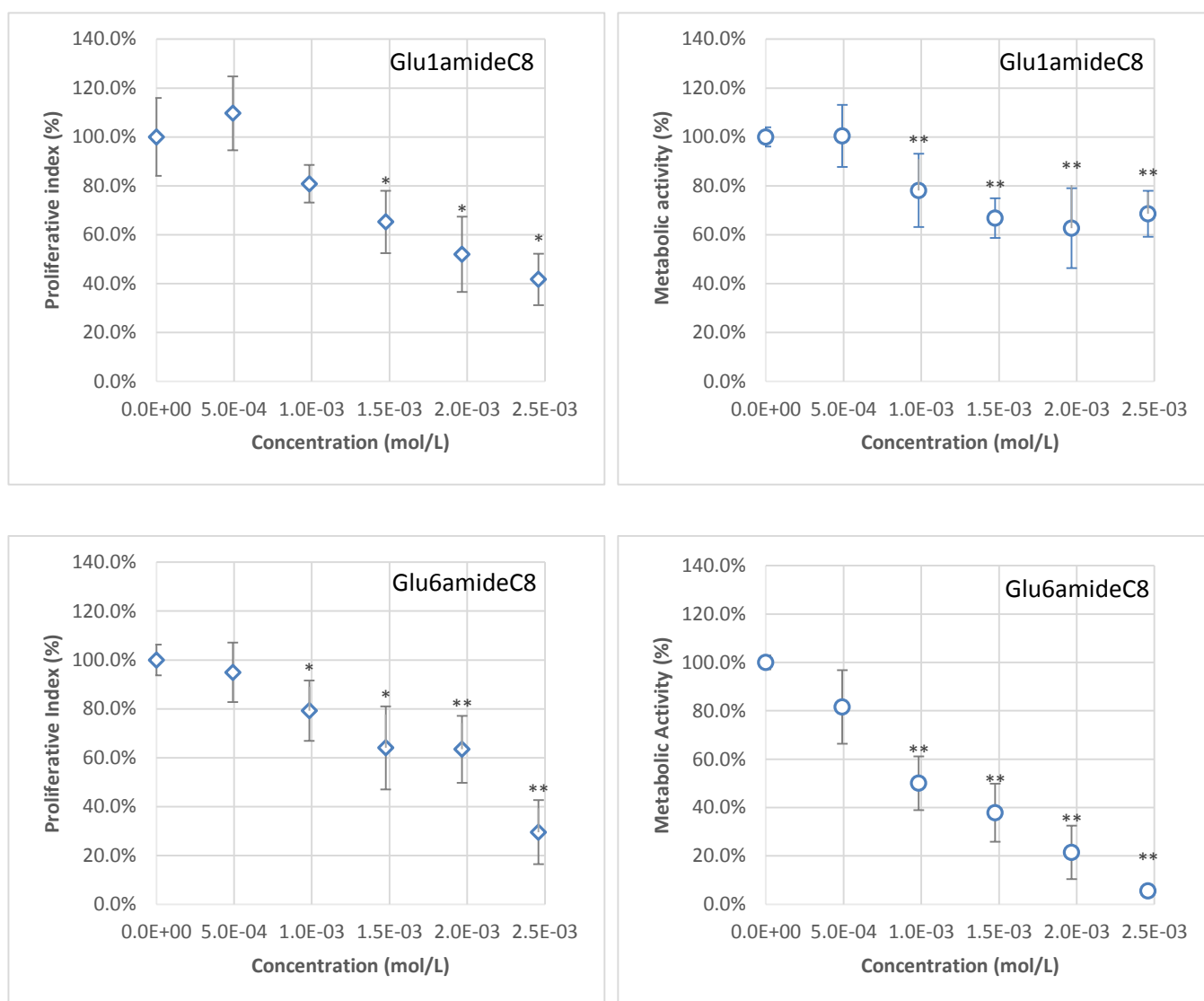


Figure 53: Normalized proliferative index (◆) and metabolic activity (○) of L929 cells cultured for 96 h in 3D cell culture model and then treated with synthesized surfactants for 48 h. (n=5 per group, data are presented as mean with SD, *p<0.05, **p<0.01, ***p<0.001 (Mann-Whitney test) as compared to negative control) (part 1).

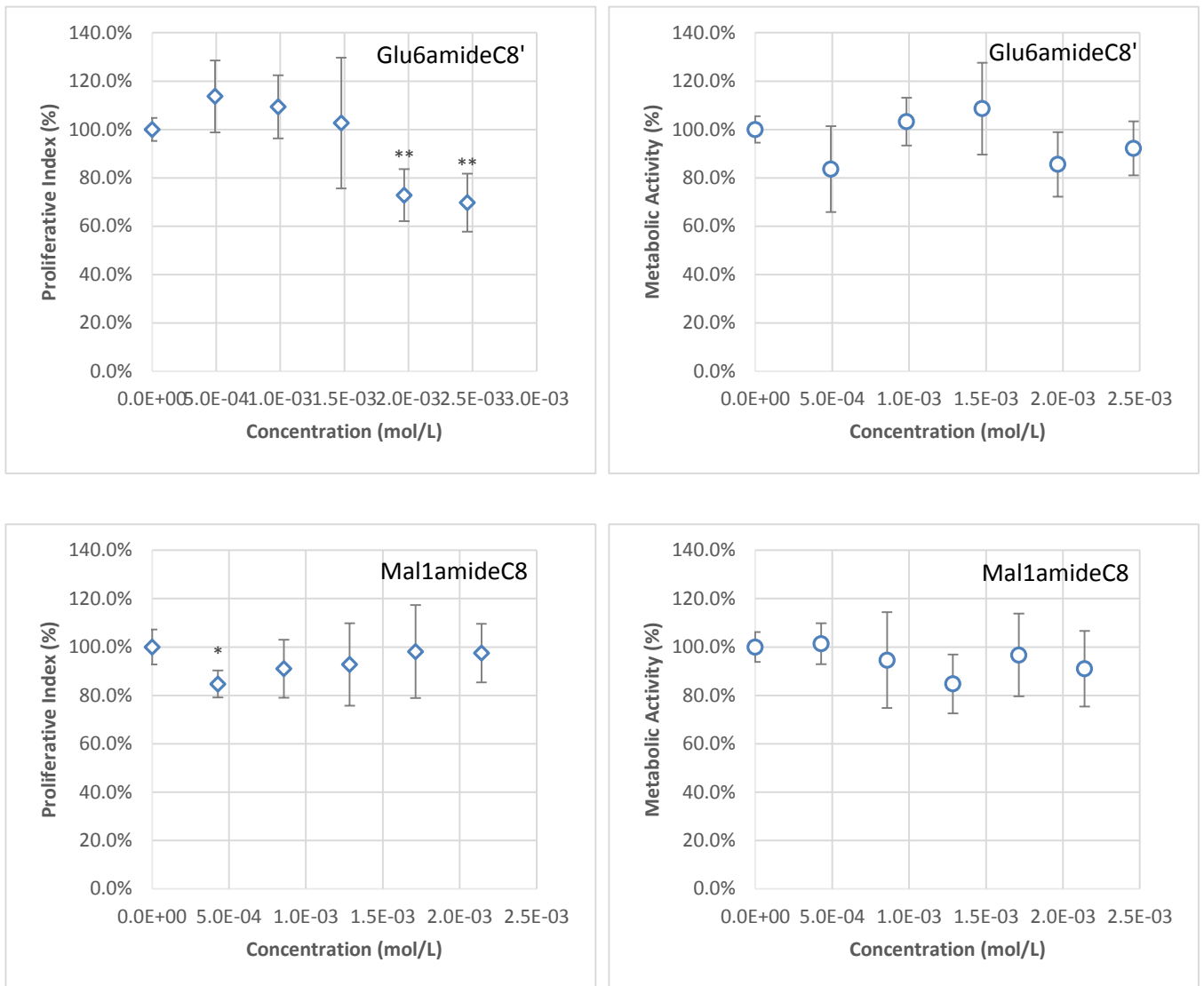


Figure 53: Normalized proliferative index (◆) and metabolic activity (○) of L929 cells cultured for 96 h in 3D cell culture model and then treated with synthesized surfactants for 48 h. (n=5 per group, data are presented as mean with SD, *p<0.05, **p<0.01, ***p<0.001 (Mann-Whitney test) as compared to negative control) (part 2).

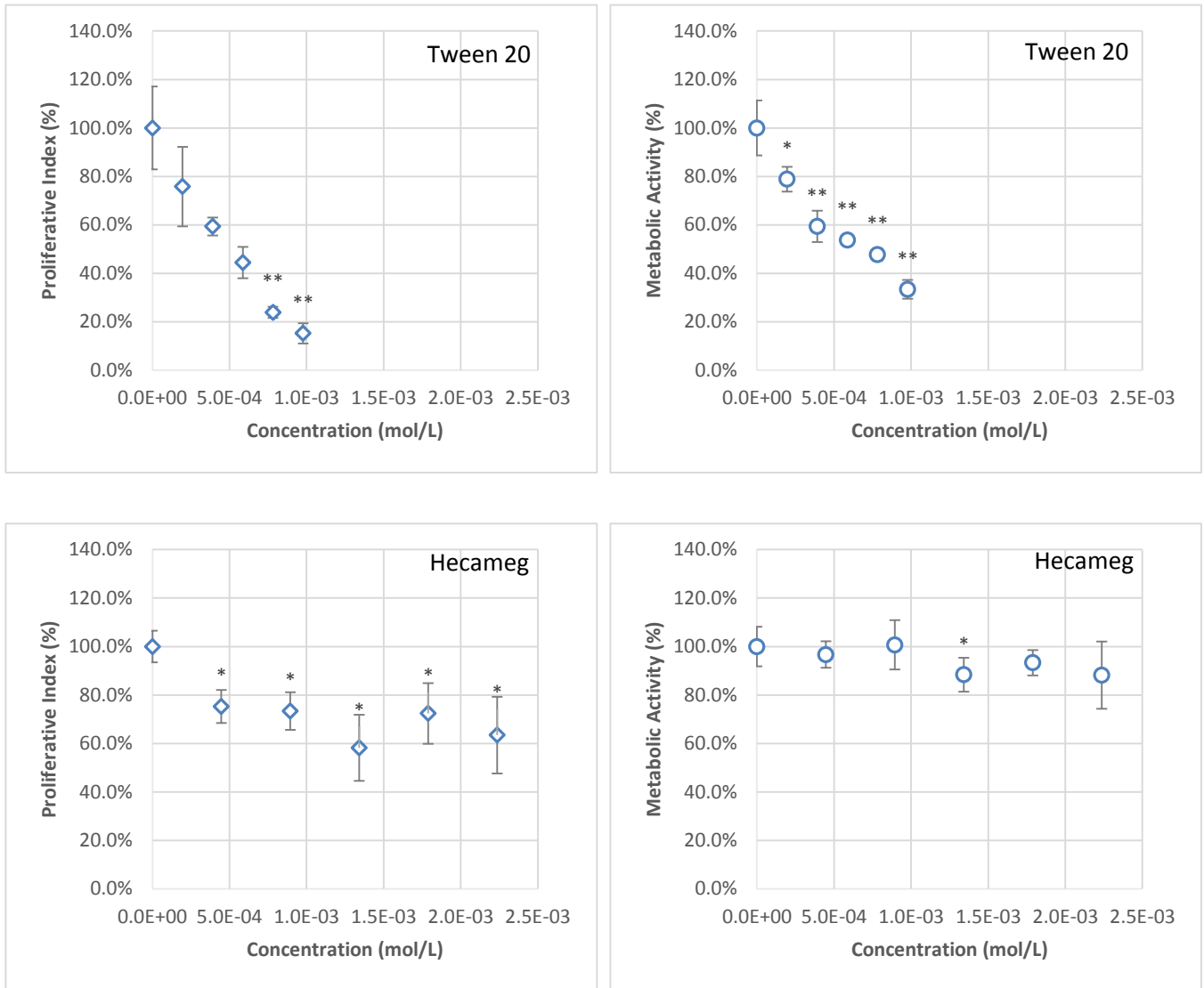


Figure 54: Normalized proliferative index (◆) and metabolic activity (○) of L929 cells cultured for 96 h in 3D cell culture model and then treated with standard surfactants for 48 h. (n=5 per group, data are presented as mean with SD, *p<0.05, **p<0.01, ***p<0.001 (Mann-Whitney test) as compared to negative control).

Corresponding IC50s of surfactants in 3D cell culture models are presented and compared to that obtained in monolayer models in Table 21.

Table 21: Comparison of cytotoxicity of surfactants against L929 cells cultured in 2D and 3D models.

Surfactant	IC50 determined by proliferative index (mmol/L)		IC50 determined by metabolic activity (mmol/L)	
	2D	3D	2D	3D
Glu1amideC8	>2.3	2.3	>2.3	>2.3
Glu6amideC8	0.20	1.9	0.31	1.0
Glu6amideC8'	1.6	>2.4	1.5	>2.4
Mal1amideC8	>2.1	>2.1	2.0	>2.1
Tween 20	0.19	0.45	0.29	0.60
Hecameg	0.81	>2.2	0.86	>2.2

Results from 3D model showed a similar trend compared to monolayer model, proliferative index and metabolic activity of cells decrease with the addition of surfactants. Tween 20, Glu6amideC8 are still more cytotoxic than other surfactants. However, a decrease of cytotoxicity in 3D models were observed according to both proliferative index and metabolic activity of cells. For Glu6amideC8, Glu6amideC8', Tween 20 and Hecameg, their IC50s are higher in 3D models than in monolayer models, which means they are less cytotoxic in 3D models.

To interpret the different cytotoxicities observed in 2D and 3D models, several factors need to be considered.

l) Penetration of surfactants and assay agent (MTS)

It is believed that the penetration of surfactants or assay agent (MTS) into the collagen gel is quick in our model and their effect on cytotoxicity results are negligible. In other works, effort has been made to study the diffusion of Alamar Blue (AB) solution in to collagen gel without cells. Collagen solution of 2.5 mg/mL was prepared and incubated to allow gelation and formation of the collagen fibers. Absorbance of AB solution in the well containing collagen gel and without collagen gel (negative control) at 570 nm was measured and compared. Results demonstrated that the absorbance of AB solution added in well with collagen gel is 76%, 74% and 75% after 1h, 2h and 3h of incubation compared to the value of negative control. It reflects that the dye from AB solution can diffuse quickly through the collagen gels and reach a equilibration. Besides, the concentration of AB solution is proven to be diluted by the collagen gel (Bonnier, F., et al. 2015). In our study, the concentration of collagen solution is 1.2 mg/mL, which is even lower than that in Bonnier's test, therefore, the penetration of surfactants or test agent (MTS) is not considered a major problem influencing the results. Moreover, cytotoxicity of surfactants measured by cell proliferative index and MTS test are similar. The consistency of results also indicates the negligible penetration difficulty for MTS in the tests.

II) Dilution effect of collagen gel.

In the study of Bonnier, F., et al. (2015), viability of HeLa cells cultured on 2D substratum and in 3D collagen (type I from rat tendons) matrix was characterized by Alamar Blue (AB) assay and flow cytometry assay. The AB assay showed that cells cultured in 3D conditions are less viable to that in 2D conditions. However, the flow cytometry assay indicates that cell viability is considered similar in both culture conditions. The difference can be interpreted by the dilution effect of collagen gels in 3D model on AB solutions. Since the collagen gel is mostly water, the volume of collagen needs to be considered when tested substances are applied on the model. In our tests, 1 mL collagen solution without cells and 2 mL collagen solution with cells were added successively in the culture insert to form collagen matrix. During the process of surfactant exposure, 5 mL culture medium containing surfactant was used. The total volume of collagen solution (3 mL) can have an important effect on dilution of surfactant solution in culture medium (5 mL). Therefore, the real surfactant concentrations in 3D models are probably lower than what are presented in Figures 53 and 54. The IC50s of surfactants by considering their 'real concentration' should be lower than that are presented in Table 21. However, even the dilution effect of collagen matrix is counted in for the cytotoxicity assay, they still cannot fully explain the difference of cytotoxicity effect between 2D and 3D models. For example, supposing that 3 mL collagen solution that we used has a same dilution effect as water (which is overestimated), all the surfactant concentrations presented in 3D models should be multiplied by a correction index of 5/8. The corresponding IC50s of surfactants can be 0.20 mmol/L in 2D condition and 1.2 mmol/L in 3D condition (Glu6amideC8), 0.19 mmol/L in 2D condition and 0.28 mmol/L in 3D condition (Tween 20). There are still gaps between the cytotoxicity in 2D and 3D conditions. Therefore, other factors should also be taken into consideration to explain the different cytotoxicity.

III) Possible adsorption of surfactant molecules on collagen gel.

The binding of nonionic surfactants to collagen previously treated with anionic surfactant through the hydrophobic effect has been reported (Maldonado, F., et al. 1990). The authors have observed a sequential adsorption of anionic surfactant (SDS, 1st stage) and ALOE85 (2nd stage) on bovine collagen hide powder at 25°C. They believe that anionic surfactant can firstly bind to collagen protein (primary adsorption) that would be ionic and hydrophobic in character. The primary adsorption can then provoke a strengthening or a development of the hydrophobic regions neighboring the bonding sites, which would favor the adsorption of non-ionic surfactant (secondary adsorption). In their tests, no adsorption of non-ionic surfactant on non-treated bovine hide powder was observed, nevertheless, in our 3D cell culture models, more factors need to be considered. The porosity in collagen matrix can greatly increase its surface/volume ratio and thus expose more interaction sites to surfactant molecules in culture medium and the hydrophobic affinity between our synthesized/ standard surfactant and collagen can possibly lead to their binding. Besides, the culture medium contains more than 20 components (amino acids, vitamins, inorganic salts, FBS etc...), the presence of amphiphiles and ionic compounds may also favor the adsorption of non-ionic surfactant onto collagen matrix. Therefore, the possibility of adsorption onto collagen gel cannot be excluded.

IV) Microenvironment regulated cell phenotype

In the 3D cell culture models, cells are connect to each other and to the ECM after 4 days of incubation. These interactions not only control the shape and orientation of cells but can also directly regulate cellular functions, including migration, differentiation, proliferation, and the expression of different genes (Eckes, B., et al. 2000). Concerning cell growth, it has been reported that it can be regulated by ECM, direct cell-cell contacts, density of cell culture, mechanical forces as well as growth factors. There is also a report indicating that human fibroblasts plated on cell or tissue-derived 3D matrices form distinct integrin structures and have higher proliferation rates than cells grown in 2D culture (Cukierman, E., et al. 2001). In consideration of these factors, cells cultured in 3D model have distinct phenotype compared to 2D model. Their responses to surfactant treatment could be different. For example, total cellular viability of human dermal fibroblasts or HaCaT (transformed keratinocytes) cells cultured in a 3D cell culture system (using non-woven viscose rayon Azowipes® as scaffold) are found to be higher than in 2D cell culture model against silver nitrate treatment. In the same report, the cytotoxicity induced by hydrogen peroxide tested in 3D culture human dermal fibroblasts is also lower than in 2D model (Sun, T., et al. 2006). These results are in agreement with what we have observed in the 2 models, indicating that change of microenvironment can influence cell phenotype.

As described for cytotoxicity evaluation in 2D cell culture models, cell viability calculated after trypan blue coloration can also help to quantify the amount of living cells compared to amount of total cells in 3D cell culture models after surfactant treatment. Cell viability at 3 typical surfactant concentrations are presented in Table 22 (the lowest test concentration, the moderate test concentration and the highest test concentration).

Table 22: Cell viability after 96 h of growth followed by 48 h of surfactant treatment and their corresponding proliferative index in 3D cell culture model.

Surfactant	C ₁ mmol/L	V ₁ %	PI ₁ %	C ₂ mmol/L	V ₂ %	PI ₂ %	C ₃ mmol/L	V ₃ %	PI ₃ %
Glu1amideC8	0.49	98 ± 1	109 ± 15	1.5	98 ± 1	65 ± 13	2.5	97 ± 1	42 ± 11
Glu6amideC8	0.49	99 ± 1	95 ± 12	1.5	99 ± 1	64 ± 17	2.5	44 ± 26	29 ± 13
Glu6amideC8'	0.49	94 ± 7	114 ± 15	1.5	98 ± 1	103 ± 27	2.5	75 ± 20	70 ± 12
Mal1amideC8	0.43	98 ± 1	85 ± 6	1.3	99 ± 1	93 ± 17	2.1	99 ± 1	97 ± 12
Tween 20	0.20	99 ± 1	76 ± 16	0.59	79 ± 4	44 ± 6	0.98	44 ± 6	15 ± 4
Hecameg	0.45	99 ± 1	75 ± 7	1.3	98 ± 1	58 ± 14	2.2	98 ± 2	63 ± 16

Values are presented as average ± std. C₁, C₂, C₃: concentration of surfactant; V₁, V₂, V₃: viability of cells; PI₁, PI₂, PI₃: normalized proliferative index of cells.

Viability results between 2D and 3D cell culture models can be discussed. In 2D cell culture models, the viability of cells are always above ~90% as long as there are living cells in the culture plate, which indicates that dead cells are quickly destructed and cannot be observed using microscope. However, in 3D cell culture models, the calculated cell viability drops down

when cell proliferative index decreases. For example, in 3D cell culture models, cell viability treated with Tween 20 at concentration of 0.20 mmol/L is 99% and the corresponding cell proliferative index remains relatively high (76%). When Tween 20 concentration increases to 0.59 mmol/L, cell proliferative index decreases to 44% and cell viability decreases to 79% accordingly. If the concentration of Tween 20 continues to augment (0.98 mmol/L), cell proliferative index equals 15% and cell viability drops to 44%. The correlation between cell viability and cell proliferative index can be observed for Glu6amideC8 and Tween 20 treated models.

As is described previously, in 2D cell culture models, few dead cells can be found due to cell destruction. In 3D cell culture models, dead cells still maintain part of their physical structure after surfactant treatment and can thus be counted. One hypothesis is that dead cells are maintained by cell cluster and ECM in 3D cell culture models and cannot be destructed quickly.

The non-normalized proliferative index of cells (number of living cells after treatment/ number of seeded cells) was used to characterize the inhibition ability of surfactant on proliferation of cells. Similar to the calculation conducted for 2D cell culture models, non-normalized proliferative index of cells at 3 typical concentrations (the lowest test concentration, the moderate test concentration and the highest test concentration) of surfactant treatment in 3D cell culture models are presented in Table 23.

Table 23: Non-normalized cell proliferative index after 96 h of growth and then 48 h of surfactant treatment in 3D cell culture models.

Surfactant	C ₁ mmol/L	nPI ₁	C ₂ mmol/L	nPI ₂	C ₃ mmol/L	nPI ₃
Glu1amideC8	0.49	6 ± 1.0	1.5	4 ± 0.8	2.5	3 ± 0.7
Glu6amideC8	0.49	7 ± 0.9	1.5	5 ± 1.3	2.5	2 ± 1.0
Glu6amideC8'	0.49	8 ± 1.1	1.5	7 ± 1.9	2.5	5 ± 0.8
Mal1amideC8	0.43	8 ± 0.6	1.3	9 ± 1.7	2.1	9 ± 1.2
Tween 20	0.20	6 ± 1.3	0.59	3 ± 0.5	0.98	1 ± 0.3
Hecameg	0.30	7 ± 0.6	0.12	5 ± 1.3	0.21	6 ± 1.5

Values are presented as average ± std. C₁, C₂, C₃: concentration of surfactant; nPI₁, nPI₂, nPI₃: non-normalized proliferative index of cells.

In 3D cell culture models, 3 factors can contribute to the final non-normalized proliferative index of cells. I) During the 3D cell culture model establishment, collagen solution should be neutralized by NaOH, this process is monitored by color change of phenol red and the exact proper pH (~7.2) for cell growth can hardly be achieved. Actually, during the first 96 h of cells incubation in 3D models, total cell number firstly decreases from ~2×10⁵ to ~1×10⁵ (0-2 day) then gradually increases (Figure 55). The decrease of cell number can be attribute to improper pH for cell growth and the need for cells to adapt to 3D cell culture environment. II) During the incubation process, 4 days of incubation prior to surfactant treatment can greatly increase cell numbers (~10⁶) compared to number of seeded cells (~2×10⁵). III) Surfactant with higher

cytotoxicity can significantly reduce the total cell number after 48 h of treatment (For example, Tween 20 at 0.98 mmol/L can reduce the proliferative index to $15\pm 4\%$ compared to negative control). In considering of these 3 factors, the effects of surfactants on cells (more precisely, whether they can inhibit cell growth or not) cannot be determined solely by compare the cell non-proliferative index (calculated from number of seeded cells) between 1 as we did for 2D models.

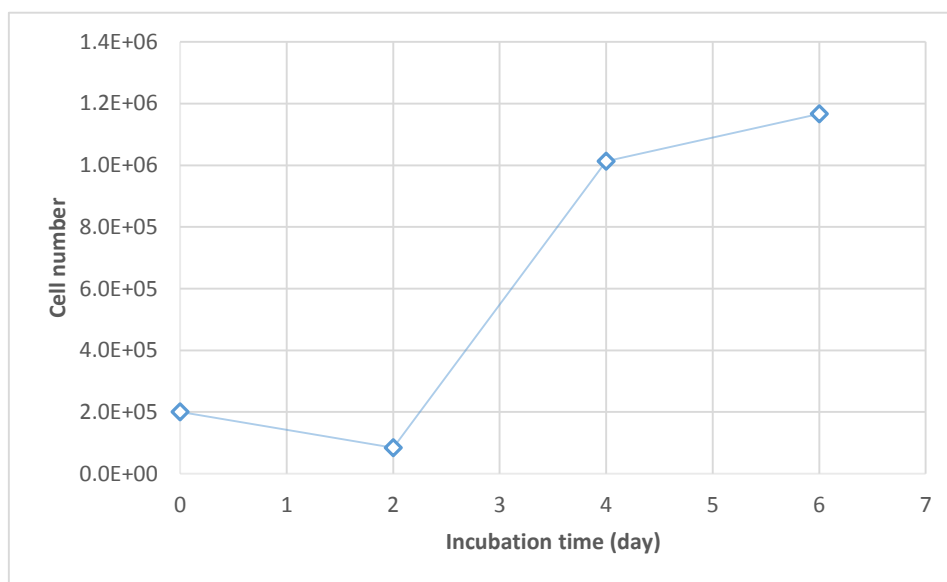


Figure 55: L929 cell growth curve in 3D cell culture model ($n=2$).

6. Morphology of 3D tissue model: Reconstituted Human Epidermis

In 2D and 3D cell culture models, L929 cells (mouse fibroblasts) were used for cytotoxicity tests. One of our goal was to study the response of fibroblasts in dermal layer of skin to surfactants. Lineage cells such as L929 have helped us to classify the cytotoxicity level of synthesized and standard surfactants. However, to fully understand the effects of surfactants on human skin, their interaction with epidermal layer also needs to be studied. Epidermis is the first skin layer exposed to chemical agents in daily life and surfactant can affect cells in dermis only if they have penetrated through epidermis. In regarding to surfactants' possible hazard to epidermis, they may cause perturbation of stratum corneum, death of keratinocytes, irritation, alteration of proliferation etc.... In our research, EpiDerm™ tissue was chosen as standard 3D tissue model for tests. It is a commercially available product with unsurpassed long-term tissue reproducibility and has been used for decades by different research facilities.

Figure 56 shows cross-section of EpiDerm™ tissue model.

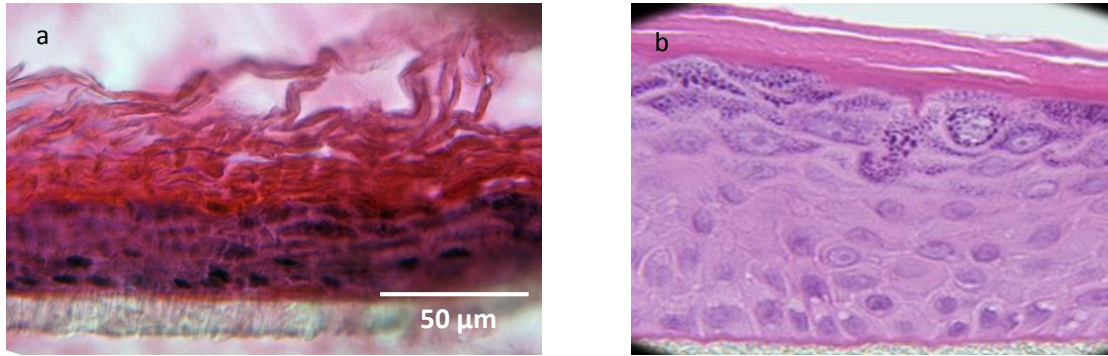
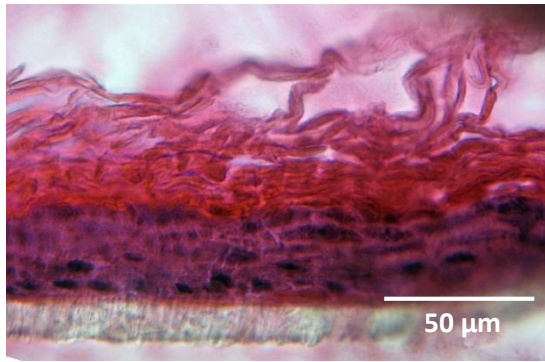


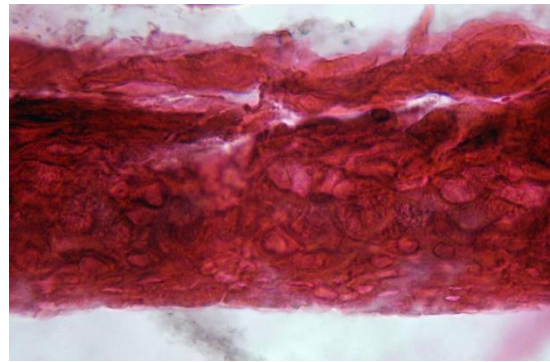
Figure 56: a) H&E stained paraffin section of EpiDerm™ tissue model after conditioning and 48 h of PBS treatment (negative control); b) cross-section of EpiDerm™ tissue model provided by MATTEK (no available scale) (<http://mattek.com>).

This model is produced from normal epithelial keratinocytes, cells are cultured on polycarbonate membrane in cell culture inserts and are exposed to liquid-air interface. As can be seen from the Figure 56, keratinocytes are highly differentiated to form the following layers; one basal layer adjacent to the insert membrane, spinous layer upon it, granular layer where cells lose their nuclei/ cytoplasm and cornified layer at the upper surface of the tissue (air-liquid interface). Ultrastructurally, this in-vitro model is closely similar to human epidermis and is good for dermal toxicology or irritancy study.

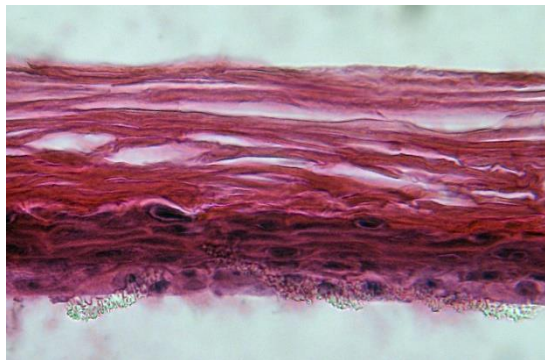
EpiDerm™ tissues were treated with synthesized and standard surfactants using an adapted protocol as described in Chapter II, C-4. As a first step, we compared the morphology of the tissues after 48 h of treatment to detect early signs of tissular effects such as apoptotic cells or tissues disruption (Figure 57). The tissue sections were therefore stained by hematoxylin and eosin staining to detect keratinocytes' nucleus stained in violet/ black.



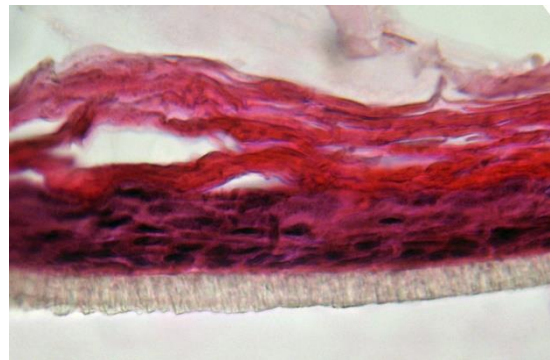
PBS



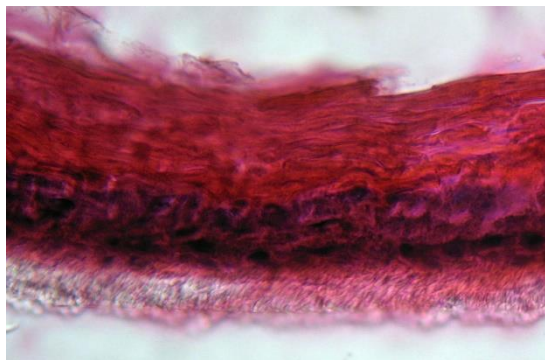
5% SDS



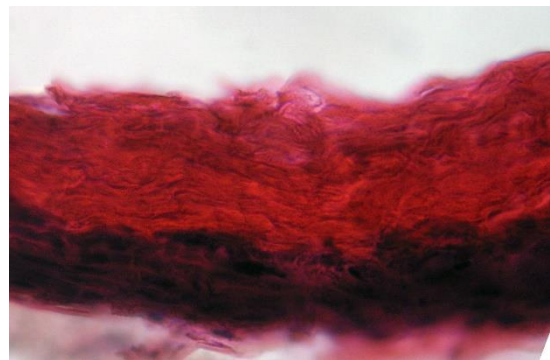
Glu1amideC8 (1000 µg/mL)



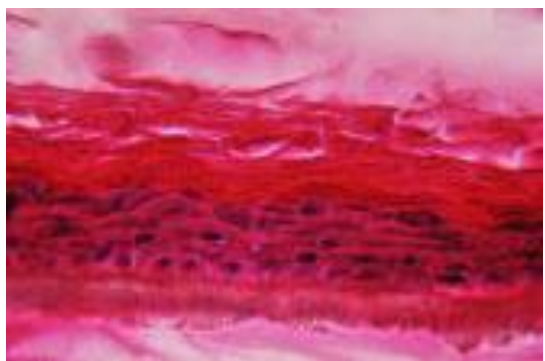
Glu6amideC8 (1000 µg/mL)



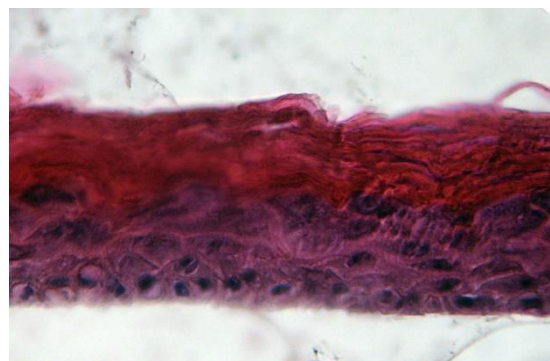
Glu6amideC8' (1000 µg/mL)



Mal1amideC8 (1000 µg/mL)



Tween 20 (1000 µg/mL)



Hecameg (1000 µg/mL)

Figure 57: Hematoxylin and Eosin staining of paraffin section of EpiDerm™ tissues treated with PBS or surfactants in PBS solutions (48h).

In our experiments, PBS treated tissue was used as negative control and 5% SDS in PBS solution was used as positive control. From the Figures 57, the keratinocytes can be seen clearly in the tissue treated with PBS, Glu1amideC8, Glu6amideC8, Glu6amideC8', Tween 20 and Hecameg. For Mal1amideC8 treated tissue, the whole layer adjacent to the insert membrane is colored in black, and no separated keratinocyte can be observed, although the presence of cell nucleus at the basal layer of the tissue can be distinguished. This might be an artifact created by the staining itself. For PBS, Glu1amideC8, Glu6amideC8, Glu6amideC8, Glu6amideC8', Mal1amideC8, Tween 20 and Hecameg treated tissues, corneocytes in the cornified layer at the surface of tissue are stained only in red by eosin. No violet/ black dots can be observed in this layer, which is in accordance with the fact that corneocytes are cells without nucleus. For 5% SDS treated tissue, its morphology is completely different as compared to tissues treated with other surfactants (the stratum corneum is disrupted), cells seems all dead and no stained nucleus can be found throughout the tissue. Actually, the ability of SDS to bind to stratum corneum proteins and denature them have been reported (Ananthapadmanabhan, K. P., et al. 1996). SDS is therefore believed to be able to induce skin barrier perturbation, penetrate into the epidermis and cause cell death (Imokawa, G., et al. 1975; Ghosh, S., & Blankschtein, D. 2007; Newby, C. S., et al. 2000).

Tests on 3D tissue models clearly showed that except for SDS, all synthesized and standard surfactants cause no significant morphological changes in the tissue during 48 h of topical application. This is different from what is observed in 2D or 3D L929 cell culture models, at concentration even lower than 1000 µg/mL, where Glu6amideC8 and Tween 20 can both induce more than 50% cell death compared to negative control. The difference between those models can be explained by two facts: I) The cell types, in 2D and 3D models, L929 fibroblasts were used while in 3D tissue models, human keratinocytes were the examined cells, their tolerance to surfactants might be different. II) The tissue structure, stratum corneum served as barrier against topically applied surfactant solutions, surfactant cannot penetrate into inner layers of epidermis and induce no observable morphological alterations. Therefore, different models were actually used to represent direct/ indirect influence of surfactant molecules on cells in epidermis or dermis layers.

7. Cytotoxicity of surfactants on EpiDerm™ tissues

In the previous experiment, the limited effect of surfactants on morphology of EpiDerm™ tissue has been confirmed. Still, study on surfactant-induced cytotoxicity is necessary to quantify their effects on keratinocytes in 3D tissue models by measuring the cell metabolic activity (Figure 58).

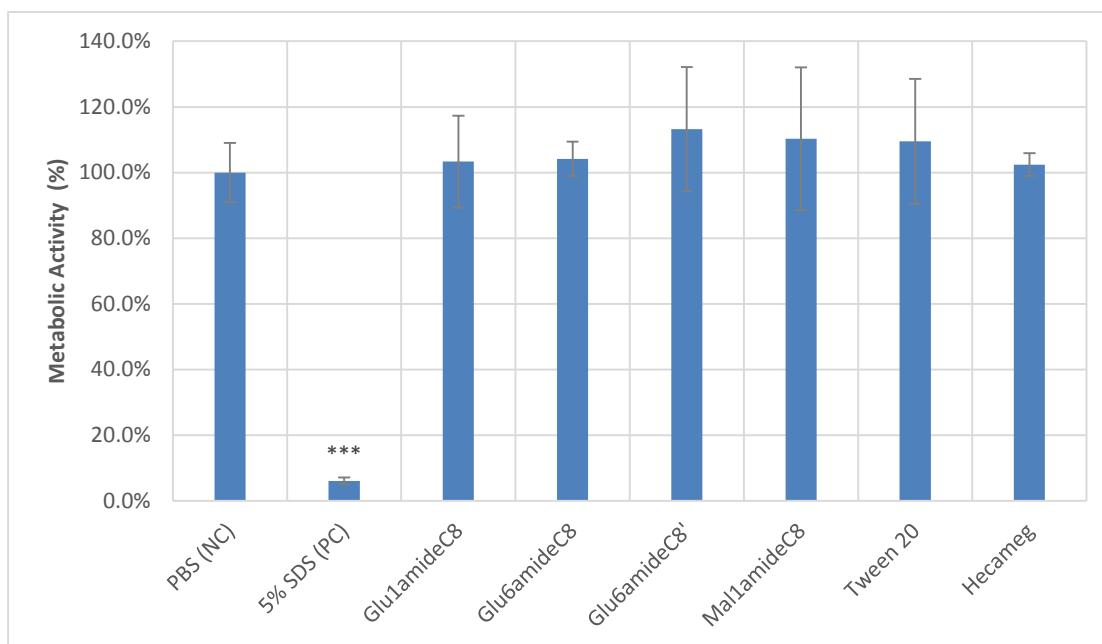


Figure 58: Metabolic activity of human keratinocyte in EpiDerm™ tissue treated with 30 μ L PBS or 30 μ L surfactant in PBS solutions (SDS 5% m/v; Glu1amideC8, Glu6amideC8, Glu6amide8', Mal1amideC8, Tween 20 and Hecameg, 1000 μ g/mL). (n=5 per group, data are presented as mean with SD, ***p<0.001 (Mann-Whitney test) as compared to negative control).

As seen from the Figure 58, only 5% SDS reduces the metabolic activity of cells significantly. This reduction as compared to PBS treated tissue is of 93.9%. For other surfactants, no significant difference was observed when their effects on EpiDerm™ are compared to negative control, indicating no cytotoxicity effect of these surfactants on the model. In Table 24, we described the metabolic activity of L929 fibroblasts in 2D/ 3D models or human keratinocytes in EpiDerm™ models as compared to negative control after 48 h of exposure to surfactants.

Table 24: Maximum surfactant concentrations used in different models and corresponding cell metabolic activity.

Surfactant	2D cell culture model		3D cell culture model		3D tissue culture model	
	Concentration (μ g /mL)	Metabolic activity %	Concentration (μ g /mL)	Metabolic activity %	Concentration (μ g /mL)	Metabolic activity %
Glu1amideC8	700	51	750	69	1000	103
Glu6amideC8	600	0	750	6	1000	104
Glu6amideC8'	700	41	750	92	1000	113
Mal1amideC8	1000	48	1000	91	1000	110
Tween 20	720	0	1200	33	1000	109
Hecameg	700	21	750	88	1000	102

For each surfactant, only the result obtained by applying its highest concentration is presented, units are all transferred to μ g/mL in the Table.

From 2D cell culture model, 3D cell culture model to 3D tissue culture model, the detected cytotoxicity of surfactant continues to decrease. In these experiments, cells still maintain full metabolic activity at higher surfactant concentrations in the 3D tissue culture models than in 2D and 3D cell culture models. This may result from various resistance between different types of cells. More importantly, stratum corneum in EpiDerm™ tissue serves, like in native tissues, as the main barrier to inhibit the penetration of surfactants and protects keratinocytes at the basal/ spinous layer. It helps maintaining the overall metabolic activity of cells in the model. Actually, the ability of surfactant vesicles to penetrate through stratum corneum and to induce skin irritation has been reported by several research groups (Froebe, C. L., et al. 1990; Hofland, H. E. J., et al. 1991; Roguet, R., et al. 1994). It seems that in our experiment, the surfactant concentrations were not high enough (all concentrations are under their CMCs except for SDS and Tween 20) to provoke measurable changes by MTS test.

8. Irritancy potential of surfactants tested on EpiDerm™ tissue

As described above, cell metabolic activity in 3D tissue culture model are not influenced by synthesized and standard surfactants up to 1000 µg/ mL. Further study was carried out to find out if surfactants could induce an irritation response in the 3D tissue culture model.

To this aim, we measured by ELISA after 24 h and 48 h, the concentration of pro-inflammation cytokine, IL-1α detected in culture medium after being synthesized by keratinocytes (Figure 59).

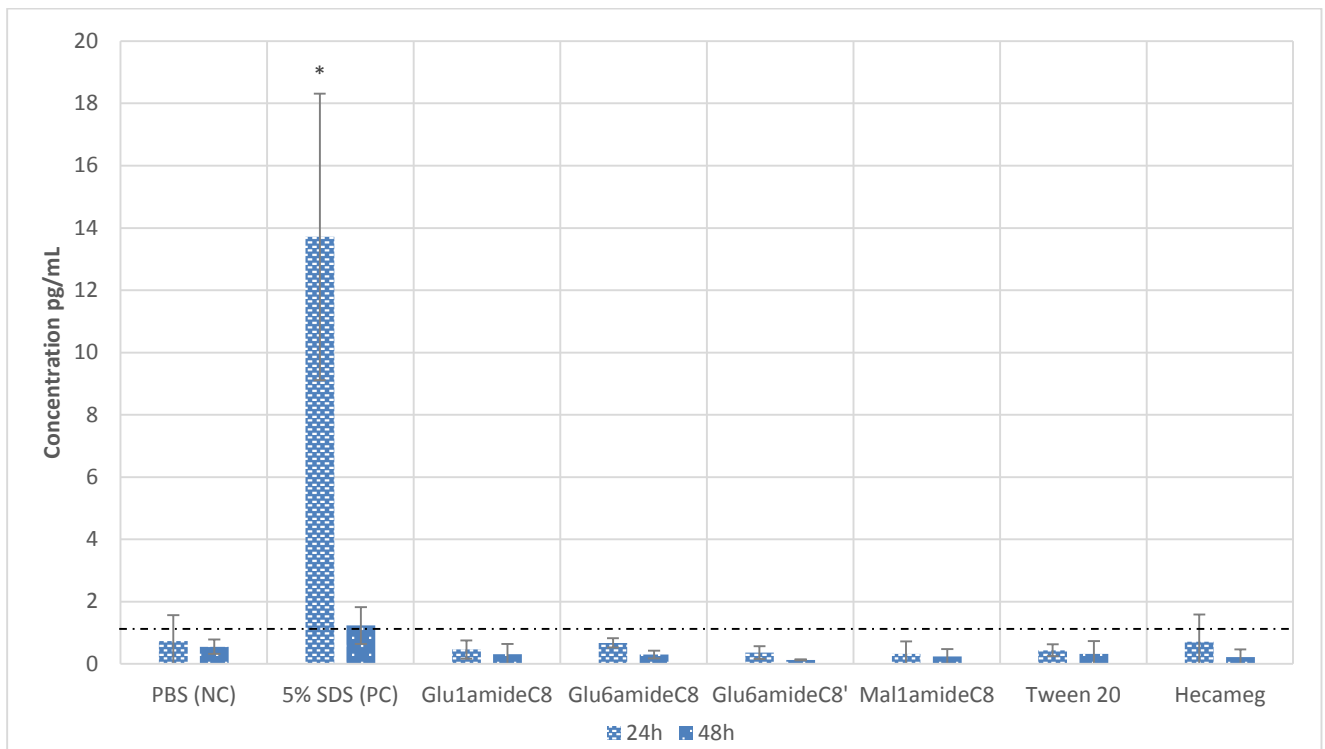


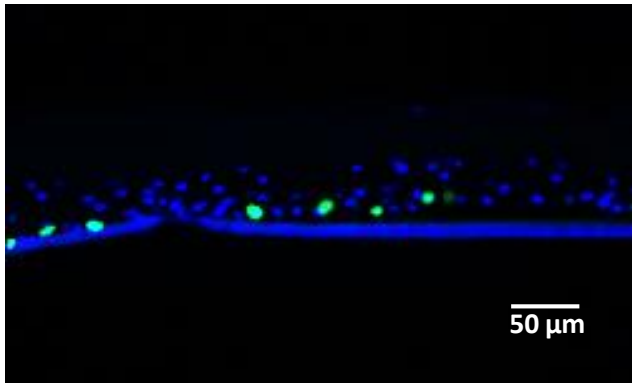
Figure 59: IL-1 α concentration in culture medium for EpiDerm™ tissue treated with topical exposure of 30 μ L PBS or 30 μ L surfactant in PBS solutions (SDS 5% m/v; Glu1amideC8, Glu6amideC8, Glu6amideC8', Mal1amideC8, Tween 20 and Hecameg, 1000 μ g/mL). (n=5 per group, data are presented as mean with SD, *p<0.005 (Mann-Whitney test) as compared to negative control. Dotted line represent the sensitivity of the ELISA-1.1 pg/mL).

At both time points, IL-1 α concentrations calculated by comparing with standard curve were below defined test sensitivity (tested surfactants: Glu1amideC8, Glu6amideC8, Gu6amideC8', Mal1amideC8, Tween 20 and Hecameg). According to our previous results from Figure 59, keratinocytes in EpiDerm™ tissue still maintained their metabolic activity after 48 h of treatment by those surfactants. Since no IL-1 α was secreted by active keratinocytes, it can be concluded that no irritation effect was induced by Glu1amideC8, Glu6amideC8, Glu6amideC8', Mal1amideC8, Tween 20 and Hecameg at 1000 μ g/mL during 24 h or 48 h of treatment. For SDS treated tissue, at 24 h, a much higher IL-1 α level was detected compared to negative control, indicating inflammation within the EpiDerm™ tissue. However, the IL-1 α concentration dropped dramatically after another 24 h of treatment. One reason is that few keratinocytes were still active after 48h of treatment (6.1% according to MTS test), no new IL-1 α can be secreted while the existing IL-1 α lost their reaction activity during the process.

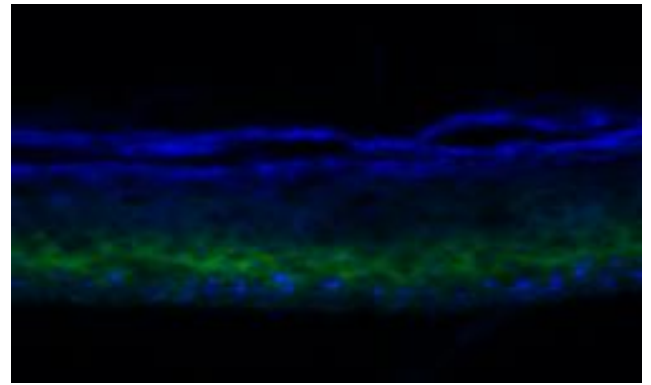
9. Number of proliferating keratinocytes in EpiDerm™ tissues after exposure to surfactants

Some small round keratinocytes in basal layer continually divide and new cells push older ones up toward the surface of the skin, during this process, the keratinocytes undergo multiple stages of differentiation and eventually lose their nucleus and become corneocytes at the surface. To understand in depth the influence of surfactants on 3D cell tissue model, and more specifically, to know whether the ability of keratinocytes to proliferate in basal layer can be

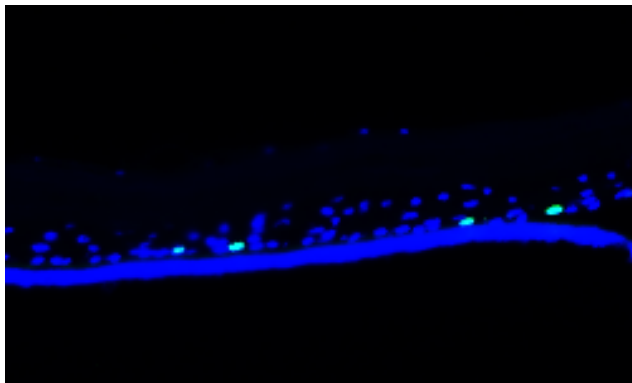
influenced by surfactants. We measured the amount of proliferating cells during a fixed time windows. To this aim, cells undergoing cell cycle during a 4 h time laps were stained using an EdU protocol as described in Chapter II, C-4 (Figure 60).



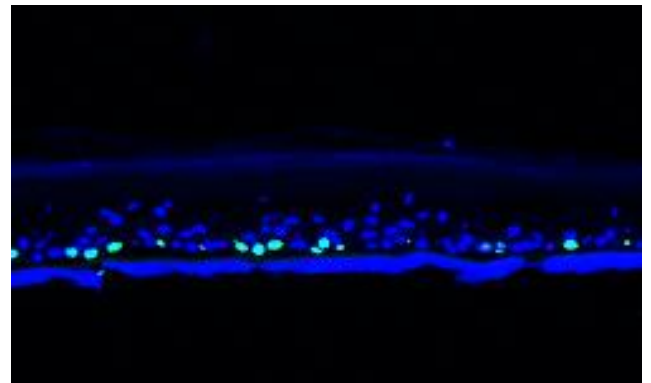
PBS



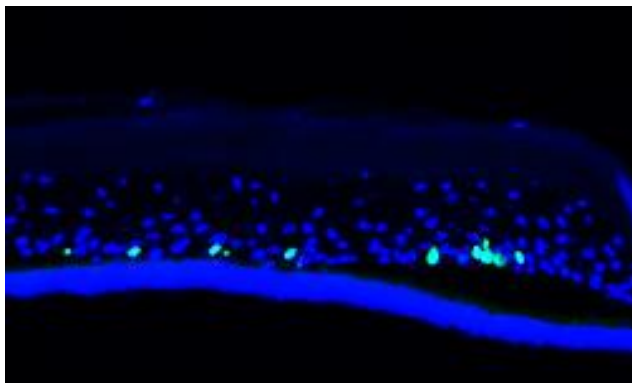
5% SDS



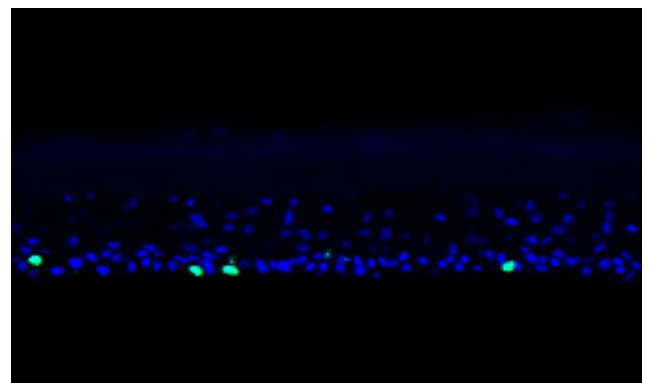
Glu1amideC8 (1000 μg/mL)



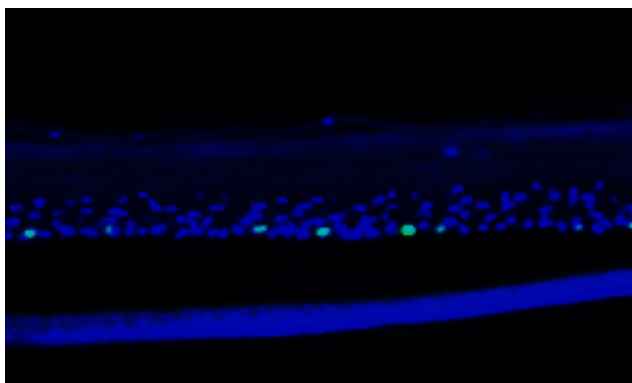
Glu6amideC8 (1000 μg/mL)



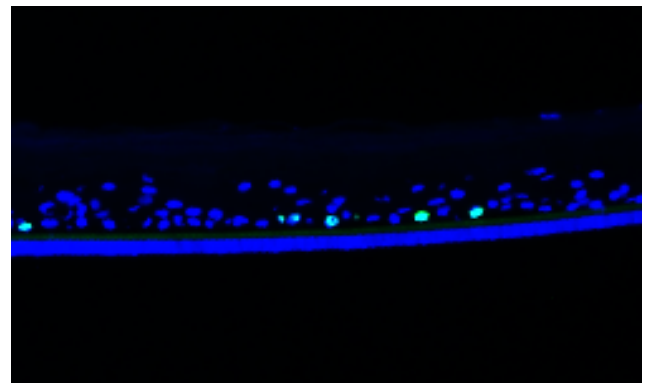
Glu6amideC8' (1000 μg/mL)



Mal1amideC8 (1000 μg/mL)



Tween 20 (1000 μg/mL)



Hecameg (1000 μg/mL)

Figure 60: EdU-DAPI co-staining of cryostat section of EpiDerm™ tissues treated with surfactants (48h).

As shown in the Figure 60, the nucleus of proliferating keratinocytes are labeled by both EdU and DAPI, emitting a green fluorescence under excitation. All keratinocytes' nucleus are stained by DAPI, presenting a blue fluorescence. Keratinocytes in the granular layer and in the cornified layer (top layers of the tissues) have no nucleus, they were therefore not stained. The bright blue line at the bottom of several tissues is the polycarbonate membrane with fluorescent dye residues. SDS treated EpiDerm™ tissue possess neither proliferating nor static cells, the keratinocytes were actually all dead after 48 h of treatment. On the contrary, there are always a small amount of proliferating keratinocytes located at the basal layer of EpiDerm™ tissue in negative control and surfactants treated tissues (Glu1amideC8, Glu6amideC8, Glu6amideC8', Mal1amideC8, Tween 20 and Hecameg), showing that the normal cell activity of EpiDerm™ tissues were not significantly altered.

The number of proliferating cells and total cells in basal layer from each sample were counted and the results presented in Table 25.

Table 25: Amount of proliferating cells in basal layer of EpiDerm™ tissues treated with surfactants.

Surfactants	Total number of counted cells	Proliferating cells %
PBS	84	19.8 ± 5.7
5% SDS	0	0
Glu1amideC8 (1000 µg/mL)	110	12.1 ± 5.5
GLu6amideC8 (1000 µg/mL)	101	24.0 ± 3.2
Glu6amideC8' (1000 µg/mL)	122	25.7 ± 5.5
Mal1amideC8 (1000 µg/mL)	125	19.3 ± 6.0
Tween 20 (1000 µg/mL)	114	21.0 ± 7.0
Hecameg (1000 µg/mL)	100	17.5 ± 5.0

n=5, the difference between value from surfactants treated tissue and PBS treated tissue is considered not significant (Glu1amideC8, Glu6amideC8, Glu6amideC8', Mal1amideC8, Tween 20 and Hecameg) according to Mann-Whitney test.

Since the total number of cells are not sufficient to produce precise results, this is only considered as semi-quantitative analysis. As seen from the Table 25, except for SDS, the percentage of proliferating keratinocytes remains within 12% to 26% after 48 h of surfactant treatment. These values are considered not significantly different from negative control by Mann-Whitney test (In the negative control, the number of proliferating cells occupies 19.8% of total cell number in basal layer). The results indicates that our tested surfactants, when applied topically at the EpiDerm™ for 48 h at 1000 µg/mL, have no significant influence on cell cycles in the model. However, since these are semi-quantitative evaluation, more tests need to do to obtained reliable data.

D) Physico-chemical properties/ Chemical structures of surfactants and their cytotoxicity

In our study, the structure of surfactant can be modified through different synthetic process. Three different models have been established to characterize the cytotoxicity of surfactants. In order to synthesize more sugar-based surfactants with low cytotoxicity for potential applications, it is important to figure out the relationship between the structures of surfactants and their cytotoxicity. By combining obtained results in our tests and analysis of references, several hypothesis can be proposed.

1. Relationship between CMC and cytotoxicity

In previous work by Partearroyo, M. A., et al. (1990), loss of 50% B16 melanoma cells is observed below CMC for surfactants (Triton X-100, Reduced Triton X-100, Octylglucoside etc...), which suggests that the presence of some surfactant monomers in culture medium is enough to influence cell viability. More precisely, the incorporation of monomers can alter significantly the permeability barrier properties of the plasma membrane and induce cell death. This phenomenon was verified in our tests (Table 26). For Glu6amideC8, Glu6amideC8', Tween 20 and Hecameg, their IC50s have been determined in 2D cell culture models and the values are below their corresponding CMCs. It is interesting to notice that, the calculated IC50s of surfactants increase almost linearly with their CMCs (CMC* for Glu6amideC8) (Figure 61), reason for this phenomena still needs to be studied.

Table 26: CMCs in complete DMEM solutions and IC50s against L929 cells culture in 2D models of surfactants, surfactants are listed in the order from the most cytotoxic to the least cytotoxic.

Surfactant	CMC in complete DMEM by surface tension (mmol/L)	IC50 by proliferative index (2D, mmol/L)
Tween 20	4.0	0.19
Glu6amideC8	3.0 (CMC*)	0.20
Hecameg	17	0.81
Glu6amideC8'	65	1.6
Mal1amideC8	67	> 2.1
Glu1amideC8	74	> 2.3

CMC*: concentration to reach minimum surface tension when surfactant was not soluble.

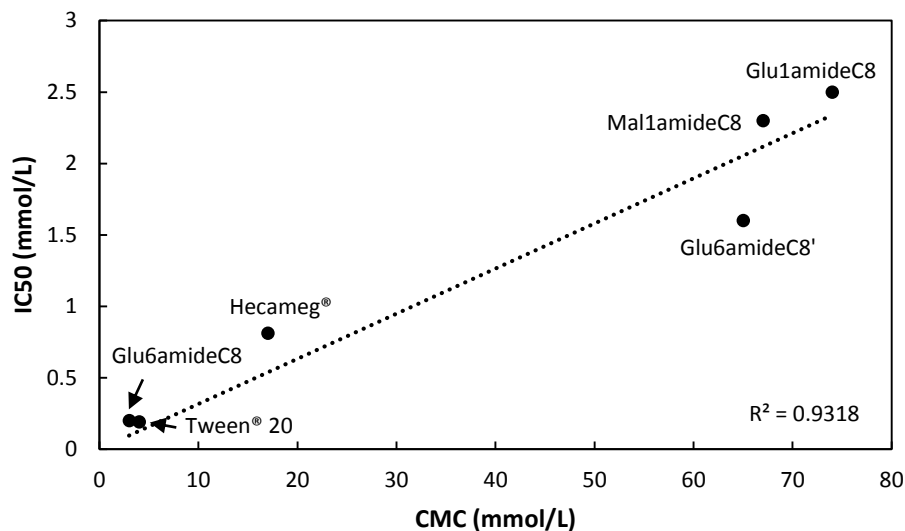


Figure 61: Linear relationship between IC50s and CMCs of observed for tested surfactants in 2D cell culture model, fitted linear regression line with R value is showed (for Glu1amideC8 and Mal1amideC8, their IC50s are estimated according to the tendency of proliferative index curve, corresponding values are 2.4 mmol/L and 2.5 mmol/L respectively).

Among all the three models for cytotoxicity tests (2D cell culture/ 3D cell culture/ 3D tissue culture model), 2D cell culture model is the simplest. Phenomena such as surfactant adsorption on collagen gel (3D cell culture model), dilution effect by collagen gel (3D cell culture model) or surfactant penetration into RHE (3D tissue culture model) do not exist in 2D cell culture model. Therefore, cytotoxicity results from 2D cell culture model reflect well the simple surfactants effect on L929 cells. They are hence used in our discussion for surfactant structure-cytotoxicity relationships.

2. Influence of structural features

2.1. Position of linkage between carbon chain and carbohydrate head

Synthesized molecules, Glu1amideC8 and Glu6amideC8' are of similar structure. For Glu1amideC8, hydrophobic chain is attached to the carbon C-1 of glucose while for Glu6amideC8', the hydrophobic chain is attached to the carbon C-6 of glucose head. A higher cytotoxicity measured for Glu6amideC8' was observed. Similarly, Hecameg and Glu6amideC8 which possess a structure close to Glu6amideC8', with hydrophobic chains linked to carbon C-6 of their glucose heads, also presented higher cytotoxicity than Glu1amideC8.

2.2. Orientation of amide group as linkage between carbohydrate head and carbon tail

It is intriguing to note that, with same molecular weight and similar structure, Glu6amideC8 (carbohydrate scaffold bears the carbonyl of amide group) showed a much higher cytotoxicity in 2D model (IC50=0.2 mmol/L) than Glu6amideC8' (alkyl chain bears the carbonyl of amide

group) ($IC_{50}=1.6$ mmol/L) (structures of Glu6amideC8 and Glu6amideC8' are shown in Figure 62). The mechanism is not yet studied, but several related studies can be found.



Figure 62: Structure of Glu6amideC8 and Glu6amideC8'.

The structure-related surface-active properties between octyl glucuronate (carbohydrate scaffold bears the carbonyl in ester group) and glucose octanoate (alkyl chain bears the carbonyl in ester group) has been investigated (structures are shown in Figure 63) (Razafindralambo, H., et al. 2009).

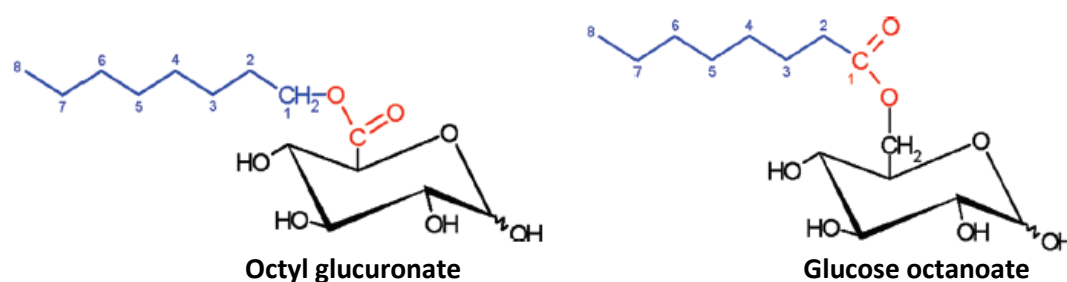


Figure 63: Structure of Octyl glucuronate and Glucose octanoate (Adapted from Razafindralambo, H., et al. 2009; Blecker, C., et al. 2002).

It should be noted that the structure alternation between octyl glucuronate and glucose octanoate is similar compared to our molecules Glu6amideC8 and Glu6amideC8' (carbohydrate scaffold bears the carbonyl or alkyl chain bears the carbonyl). The direction of the ester bond plays a crucial role in the physico-chemical properties of the two molecules at the air-water interface. For instance, in their study, the CMC of Octyl glucuronate is 10.7 mmol/L, which is lower than Glucose octanoate (CMC=19.1 mmol/L). This result are in agreement with ours where Glu6amideC8 has a lower CMC* (3.0 mmol/L) than the CMC (65 mmol/L) of Glu6amideC8' (Figure 62). However, in our results, the CMC* of Glu6amideC8 is much lower than Glu6amideC8', this is presumably due to the difference of properties induced by ester group or amide group. Besides, study has also revealed that octyl glucuronate can adsorb faster at the air-water interface than glucose octanoate (when the surface tension of surfactant solutions were measured by drop volume method, at concentration of 1.63 mmol/L, octyl glucuronate solution reached a stable surface tension after about 5 s whereas glucose

octanoate achieved a stable surface tension after about 23 s). The results are dependent on the steric and energetic constraints of the surfactant molecules toward the air-water interface. In our tests, Glu6amideC8 and Glu6amideC8' possess a very close structure to octyl glucuronate and glucose octanoate respectively. Actually, by substituting the nitrogen in amide group of Glu6amideC8 and Glu6amideC8' by oxygen, they become octyl glucuronate and glucose octanoate respectively. According to our results, the cytotoxicity of Glu6amideC8 is higher than Glu6amideC8' in 2D cell culture models (Glu6amideC8, IC₅₀=0.20 mmol/L; Glu6amideC8', IC₅₀=1.6 mmol/L), one possible explanation is that the Glu6amideC8 can adsorb faster at the cell membrane (which is also a hydrophobic-hydrophilic interface as water-air interface) and cause cell death.

It should be mentioned that, in some cases, the carbonyl of Glu6amideC8 is not considered as part of its carbon chain. Therefore, comparison between Glu6amideC7 and Glu6amideC8' with a same carbon chain length will be necessary.

2.3. Stereochemistry of surfactants

The stereochemistry of the polar headgroup were considered to be able to alter cytotoxicity of carbohydrate surfactants (Li, X., et al. 2009). The cytotoxicity of galactopyranoside is more than 5 times lower than its analog of glucopyranoside surfactant against cultured B16F10 mouse melanoma cell line (examples are listed in Figure 64). The distinct cytotoxicity between these two surfactants with comparable headgroup size and same tail length was believed to originate from the selective interactions of the surfactants with lipid. These interactions impair the function of membrane proteins rather than massive disruption of the phospholipid membrane and provoke apoptosis and/or necrosis of cells. In the case of our synthesized Glu6amideC8 and Glu6amideC8', the selective interactions between lipids in cell membrane and surfactants is a possible explanation for their distinct cytotoxicity. Glu6amideC8 may possess a stronger effect to impair the membrane function and cause cell death.

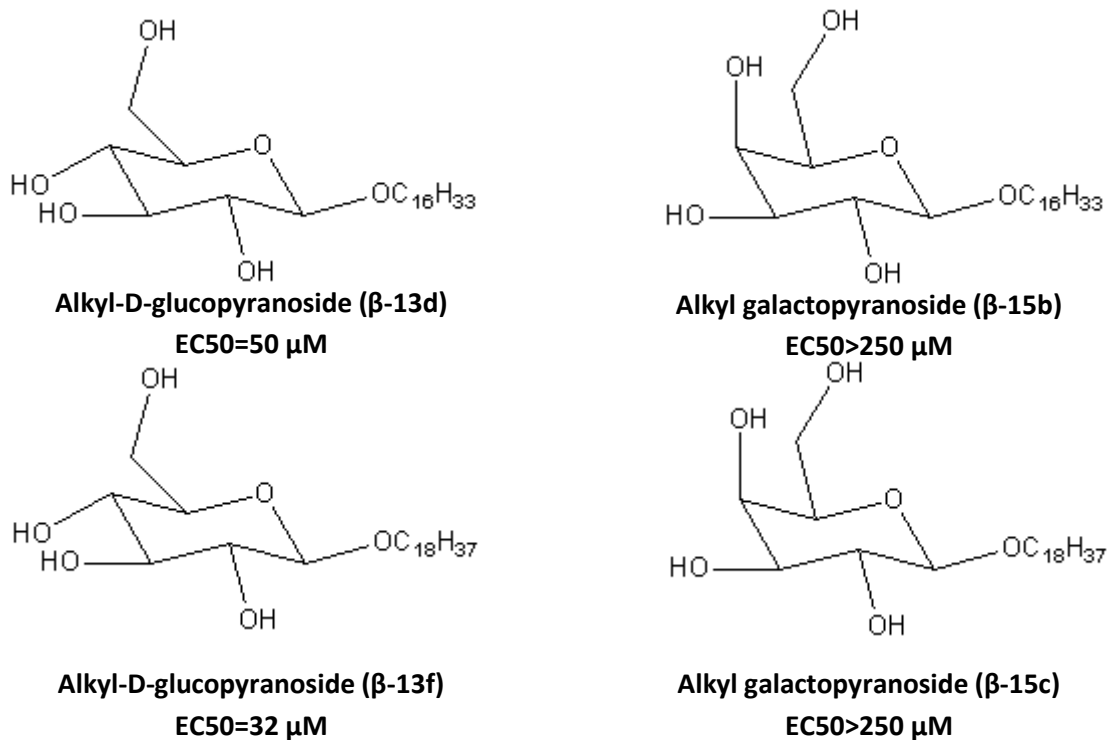


Figure 64 : Structure of Alkyl-D-glucopyranosides and their analog Alkl galactopyranosides. Their corresponding EC₅₀s (the molar concentration which produces 50% of the maximum possible inhibitory response) in B16F10 cell line are presented, values are obtained from MTT-based cytotoxicity test (Adapted from Li, X., et al. 2009).

2.4. Number of glucose units in head group

No significant differences between the cytotoxicity of Glu1amideC8 (glucose head) and Mal1amideC8 (maltose head) were observed in the concentration range of our tests and their surface tension curves are very close (their structures are shown in Figure 66). Cell proliferative index in 2D models treated with those two molecules are 54% at 2.3 mmol/L (Glu1amideC8) and 60% at 2.1 mmol/L (Mal1amideC8) respectively. It indicates that increase number of glucose unit in headgroup of surfactant from 1 to 2 do not alter significantly its cytotoxicity against L929 cells in 2D model.

In the case of different types of headgroups, in others' work, the head-group size of non-ionic polyethyleneoxide-ester surfactant is capable to influence their cytotoxicity against cells. Research has found that the presence of long PEO (polyethyleneoxide) groups (>30 EO units) in PEO-ester surfactant can lead to a decrease of toxicity on Caco-2 cells (colorectal adenocarcinoma cell) by transepithelial electric resistance and mannitol permeability assays (Ekelund, K., et al. 2005) (structure of PEO is shown in Figure 65). The interaction of non-ionic surfactants with membrane phospholipids involves the insertion of the hydrophobic moiety of surfactants into the apolar fatty acid domain of phospholipids. If the effect is strong enough, the surfactant can disturb the organization of membrane and lead to increased permeability and leakage as well as cell death (Cserháti, T. 1995). In the case of PEO, the length of head

effect on 2D cultured human immortalized keratinocyte (HaCaT) viability by MTT assay after 20 h of exposure, their corresponding IC50s are all higher than 1 mmol/L, while for alkyl β -D-xylopyranoside with moderate chain length (C8 and C10), their IC50s are 580 μ mol/L and 165 μ mol/L respectively (Xu, W., et al. 2012) (structures are shown in Figure 67).

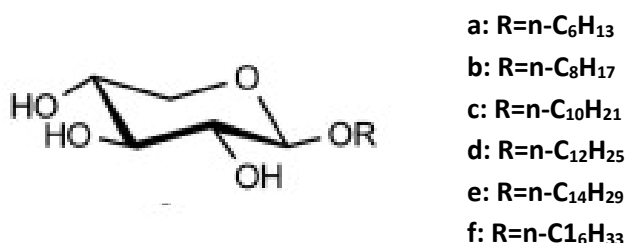


Figure 67 : Structures of hydrocarbon alkyl β -D-xylopyranoside (Adapted from Xu, W., et al. 2012).

Similar results were reported for perfluorinated carboxylic acids. Human colon carcinoma (HCT116) cells were incubated for 24 h then treated for 4/ 24/ 72 h. MTT viability assay indicates that, with the increase of chain length from C6 to C14, the cytotoxicity of perfluorinated carboxylic acids on cells increases, whereas at chain length of C16 and C18, the cytotoxicity start to decrease compared to their C14 analog (Kleszczyński, K., et al. 2007) (structures are shown in Figure 68).

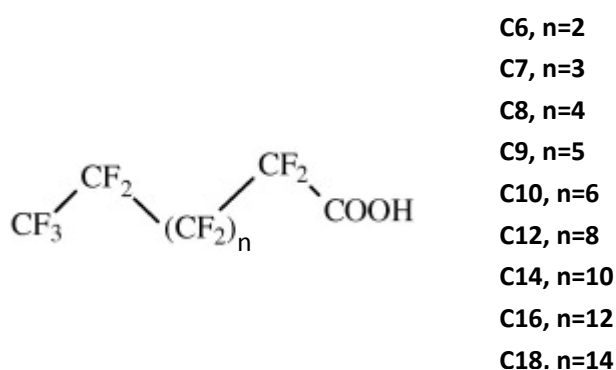


Figure 68 : Structures of perfluorinated carboxylic acids (Adapted from Kleszczyński, K., et al. 2007).

The low cytotoxicity of surfactants with a short hydrophobic tail is likely due to the limited partitioning of these surfactants into the cell membrane. Surfactants with longer carbon chains are more hydrophobic, it will facilitate their partition in the cell bilayer membrane and result in higher cytotoxicity. However, for surfactants with even longer chain, their solubility can be limited due to large hydrophobic moiety, they tend to bind with other proteins (BSA for

example) in culture medium and their diffusion rate through the cell membrane is decreased, those factors can all reduce their cytotoxicity. Balgavý, P., & Devínsky, F. (1996) have discussed the “cut-off” effects in biological activities of surfactants. They believe that in the homologous series of long hydrocarbon chain surface active compounds, their various biological activities increase progressively with increasing chain length up to a critical point, beyond which the compounds cease to be active. Limit aqueous solubility, anomaly in physical properties, different interactions between long chain molecules with proteins and the complex interactions with lipid bilayers can be used to explain the effect.

In this context, by reducing the length of carbon chains to C6 or C4 in our experiments, a weaker surface-active properties are expected, their cytotoxicity against 2D and 3D cell culture models should be less than what we have obtained for C8 surfactants. On the contrary, a low solubility has already been observed when the chain length of surfactants were increased to C10, which limits the application of synthetic surfactants in aqueous systems. To find out a proper chain length for our synthetic surfactant so that it maintains relatively strong surface-active properties as well as low cytotoxicity should be our further work.

Conclusions and Perspectives

Researchers have been working in recent decades to create novel biomass-derived surfactants because a number of them are reported to be more biodegradable and less toxic than traditional ones. Among biomass-derived surfactants, sugar-based molecules are occupying more and more attention, several commercially available products have been developed (alkyl polyglycoside, sucrose esters etc...) and are widely used in domains like food production, detergent production... In the meantime, a large number of potential sugar-based surfactants remains to be explored: their chemical structures can be tailored by synthetic condition, and their properties need to be characterized to fully uncover the potential for applications.

In the AMPHISKIN project, synthesized sugar-based surfactants, with a glucose or maltose derived head group, linked to C8 or C10 chain by amide group were provided. Characterization of these surfactants was conducted both in terms of physico-chemical properties and biological responses. For the aim to study the biological responses of surfactants, three *in vitro* models were established with increased complexity: 1) 2D cell culture model (L929 cells monolayer), 2) 3D cell culture model (L929 cells embedded in collagen gel) and 3) 3D tissue culture model (reconstituted human epidermis). These models helped us to compare the cytotoxicity of surfactants against dermis and epidermis cells in different conditions (direct cytotoxicity against monolayer fibroblast cells, cytotoxicity against fibroblasts cells with the presence of cell-cell/ cell-extracellular matrix interactions or cytotoxic/ irritant effects against differentiated human keratinocytes).

In the experiments, efforts have been made to pre-select surfactants with the highest solubility and strong ability to reduce surface tension of water solutions for further tests: among the synthesized molecules, Glu1amideC8, Glu6amideC8, Glu6amideC8' and Mal1amideC8 were firstly chosen. Their properties were evaluated and compared to standard surfactants (Tween 20 and Hecameg). Surface-tension measurements of these surfactants in water revealed that they all have surface-active properties similar to Tween 20 or Hecameg (all the 4 synthesized sugar-based surfactants can reduce surface tension of water solutions to a level of 25 - 35 mN/m). Moreover, the cytotoxicity results from 2D cell culture model (L929 cells monolayer) and 3D cell culture model (L929 cells embedded in collagen gel) have demonstrated interesting results: Glu1amideC8, Glu6amideC8' and Mal1amideC8 present a lower cytotoxicity than Glu6amideC8, Tween 20 and Hecameg, revealing their potential to be used as safer substitutes of current commercial surfactants.

More tests were carried out to analyze these surfactants. Their CMCs in water were determined both by surface tension method and dye solubilization method. The minimum surface tension of Glu6amideC8 in water solution was obtained at its solubility limit and it is considered to have no CMC (verified by dye solubilization method), for the convenience of discussion, the solubility limit of Glu6amideC8 is therefore denoted as CMC*. CMCs (or CMC*) of surfactants were also determined when they were dissolved in culture medium (complete DMEM) for cell model. The CMCs (CMC*) obtained for surfactants in culture medium were the

same as in water (except for Tween 20, it presented a higher CMC due to its interaction with proteins in the culture medium). A phenomena was observed when the IC50s of surfactants and their CMCs (CMC*) in culture medium were compared. The two parameters showed a linear relationship (IC50s of surfactants increase with their CMCs). To further verify this phenomena, structure of synthesized surfactants need to be modified. For example, more glucose units (from 1 to 20 as too large hydrophilic group will greatly reduce the HLB of surfactants and limit their applications) can be added at the head group of Glu1amideC8, Glu6amideC8 and Glu6amideC8'. Alternatively, the number of carbons in the hydrophobic chain of synthesized surfactants can also be reduced to 6. The CMCs and IC50s of these modified sugar-based surfactants, together with more standards non-ionic surfactants (Alkyl polyglycoside, Alcohol ethoxylates...) against L929 monolayer model will be tested and the relationship between CMCs and IC50s of non-ionic surfactants will then be analyzed with more data.

Self-assembling properties are important for applications of surfactants, therefore, the Krafft points which are the minimum temperature for surfactants to form micelles were measured. Glu1amideC8 and Glu6amideC8' possess Krafft points at 30°C and 32°C respectively, while for other synthesized and standard surfactants, their Krafft points are not within our test range (or do not have a Krafft point). Among them, Glu6amideC8' and Hecameg were chosen to conduct SAXS analysis for their self-assembling properties and results confirmed their ability to form micelles at different temperatures.

The synthesized sugar-based surfactants have potential to be used in various products, their direct contact with human skin is inevitable. For the safety evaluation, the cytotoxic/ irritant effects of surfactants on reconstituted human epidermis models were measured. At concentration of 1000 µg/mL, these surfactants showed neither cytotoxicity nor irritant effects against the epidermis model after 48 h of topical application (much longer than recommended 1 h of application in the standard irritation test), which is presumably due to the presence of corneocytes barrier at the upper most layer of epidermis. Considering the fact that in product such as facial foam, the concentrations of surfactants are often above 1 % w/v (10000 µg/mL). To better understand the effects of surfactants, it would be necessary to tests these synthesized surfactants at higher concentrations and obtain their IC50s on reconstituted human epidermis by MTS assays.

For the purpose to selectively synthesize sugar-based surfactant with desired properties, work has been done to discuss the possible relationship between structures and cytotoxicity of surfactants. These structure alternations are: 1) Position of linkage between carbon chain and carbohydrate head, 2) Orientation of amide group as linkage between carbohydrate head and carbon tail, 3) Stereochemistry of surfactants, 4) Number of glucose units in head group and 5) Number of carbons in hydrophobic moiety. By comparing results from our experiments and from references, hypothesis of structure-relationship were proposed, but more tests will be necessary to verify these hypothesis. In the short term, two major aspects will be considered: 1) Number of glucose units in the head group, in the thesis work, only sugar-based surfactants with 1 glucose unit (glucose head) or 2 glucose units (maltose head) linked to C8 chain were

tested for their cytotoxicity and no significant differences were observed. While according to literature, the modification of head group size of ethoxylated alcohol can change its cytotoxicity. Therefore, it will be interesting to increase the number of glucose units (from 1 to 20 for example) in the head group and figure out if their cytotoxicity effects on L929 2D cell culture model and L929 3D cell culture models will change with structure.

2) Influence of glucose derived precursors on the cytotoxicity of synthesized surfactants. As can be seen from Appendix 1, surfactants with different structures were synthesized from various glucose-derived precursors. For example, we could use Glu1amideC8 (precursor: D-glucose) and Glu6amideC8 (precursor: Glucuronic acid). These molecules can also be tested in 2D cell culture, 3D cell culture models, determined IC50s against L929 cells can be compared to synthesized surfactants. It will be interesting to verify if the cytotoxicity of synthesized surfactants and their corresponding precursors are of the same level.

In the long term, desired surfactants can be synthesized according to the structure-cytotoxicity relationship. Besides, to step closer to applications, surfactant mixtures or surfactants added into various formulations can be tested for foaming/ emulsification/ wetting properties. More importantly, the cytotoxic/ irritant effects of these formulations can be evaluated. These experiments will help to identify possible applications of synthesized sugar-based surfactants in cosmetic, food and pharmaceutical industries.

References

Alberts, B., Bray, D., Lewis, J., Raff, M., Roberts, K., Watson, J. D., & Grimstone, A. V. (1995). *Molecular Biology of the Cell* (3rd edn). Trends in Biochemical Sciences, 20(5), 210-210.

Alexandre, B. S. The skin. <http://www.icsmsu.com>

Altman, S. A., Randers, L., & Rao, G. (1993). Comparison of trypan blue dye exclusion and fluorometric assays for mammalian cell viability determinations. *Biotechnology Progress*, 9(6), 671-674.

Anane, R., & Creppy, E. E. (2001). Lipid peroxidation as pathway of aluminium cytotoxicity in human skin fibroblast cultures: prevention by superoxide dismutase+ catalase and vitamins E and C. *Human & experimental toxicology*, 20(9), 477-481.

Ananthapadmanabhan, K. P., Yu, K. K., Meyers, C. L., & Aronson, M. P. (1996). Binding of surfactants to stratum corneum. *Journal of the Society of Cosmetic Chemists*, 47(4), 185-200.

Arechabala, B., Coiffard, C., Rivalland, P., Coiffard, L. J. M., & de Roeck-Holtzhauer, Y. (1999). Comparison of cytotoxicity of various surfactants tested on normal human fibroblast cultures using the neutral red test, MTT assay and LDH release. *Journal of applied toxicology*, 19(3), 163-165.

Ariyaprakai, S., Limpachoti, T., & Pradipasena, P. (2013). Interfacial and emulsifying properties of sucrose ester in coconut milk emulsions in comparison with Tween. *Food Hydrocolloids*, 30(1), 358-367.

Attwood, D. (2012). *Surfactant systems: their chemistry, pharmacy and biology*. Springer Science & Business Media.

Attwood, D., & Florence, A. T. (2012). *FASTtrack Physical Pharmacy*. Pharmaceutical Press.

Awang, M. A., Abu, B. M., Mh, B. M., Roy, C. S., Rajab, N. F., Wan, K. W., ... & Idrus, R. B. (2014). Cytotoxic evaluation of biomechanically improved crosslinked ovine collagen on human dermal fibroblasts. *Bio-medical materials and engineering*, 24(4), 1715-1724.

Babich, H., Zuckerbraun, H. L., Wurzbarger, B. J., Rubin, Y. L., Borenfreund, E., & Blau, L. (1996). Benzoyl peroxide cytotoxicity evaluated in vitro with the human keratinocyte cell line, RHEK-1. *Toxicology*, 106(1), 187-196.

Baer, H. H., & Madumelu, C. B. (1975). Reactions of α -nitroepoxides. *Carbohydrate Research*, 39(1), C8-C11.

Balgavý, P., & Devínsky, F. (1996). Cut-off effects in biological activities of surfactants. *Advances in colloid and interface science*, 66, 23-63.

Ball, N., Cagen, S., Carrillo, J. C., Certa, H., Eigler, D., Emter, R., ... & Mehling, A. (2011). Evaluating the sensitization potential of surfactants: integrating data from the local lymph node assay, guinea pig maximization test, and in vitro methods in a weight-of-evidence approach. *Regulatory Toxicology and Pharmacology*, 60(3), 389-400.

Balzer, D., & Luders, H. (Eds.). (2000). *Nonionic surfactants: alkyl polyglucosides* (Vol. 91). CRC Press.

Basketter, D. (1999). *Toxicology of contact dermatitis: Allergy, Irritancy and Urticaria*. John Wiley & Sons Inc.

Becker, J. L., & Souza, G. R. (2013). Using space-based investigations to inform cancer research on Earth. *Nature Reviews Cancer*, 13(5), 315-327.

Bell, E., Parenteau, N., Gay, R., Nolte, C., Kemp, P., Bilbo, P., ... & Johnson, E. (1991). The living skin equivalent: its manufacture, its organotypic properties and its responses to irritants. *Toxicology in vitro*, 5(5), 591-596.

Bensouillah. *Aromadermatology*. <http://courses.washington.edu>

Berardesca, E., Fideli, D., Gabba, P., Cespa, M., Raggiosi, G., & Maibach, H. I. (1990). Ranking of surfactant skin irritancy in vivo in man using the plastic occlusion stress test (POST). *Contact dermatitis*, 23(1), 1-5.

Berg, J. C. (2010). *An introduction to interfaces & colloids: the bridge to nanoscience*. World Scientific.

Bergsma, M., Fielden, M. L., & Engberts, J. B. (2001). pH-Dependent aggregation behavior of a sugar-amine gemini surfactant in water: vesicles, micelles, and monolayers of hexane-1, 6-bis (hexadecyl-1'-deoxyglucitylamine). *Journal of colloid and interface science*, 243(2), 491-495.

Bhardwaj, A., & Hartland, S. (1993). Applications of surfactants in petroleum industry. *JOURNAL OF DISPERSION SCIENCE AND TECHNOLOGY*, 14(1), 87-116.

Bidhe, R. M., & Ghosh, S. (2004). Acute and subchronic (28-day) oral toxicity study in rats fed with novel surfactants. *AAPS PharmSci*, 6(2), 7-16.

Bigler, C. F., Norris, D. A., Weston, W. L., & Arend, W. P. (1992). Interleukin-1 receptor antagonist production by human keratinocytes. *Journal of investigative dermatology*, 98(1), 38-44.

Biochem. Assessment of the bio-based products market potential for innovation.

<http://www.biochem-project.eu>.

BIO-TIC. Biobased Surfactant. Summary. <http://www.industrialbiotech-europe.eu>.

Blake-Haskins, J. C., Scala, D., Rhein, L. D., & Robbins, C. R. (1986). Predicting surfactant irritation from the swelling response of a collagen film. *J Soc Cosmet Chem*, 37(4), 199-210.

Blecker, C., Piccicuto, S., Lognay, G., Deroanne, C., Marlier, M., & Paquot, M. (2002). Enzymatically prepared n-alkyl esters of glucuronic acid: the effect of hydrophobic chain length on surface properties. *Journal of colloid and interface science*, 247(2), 424-428.

Bonnier, F., Keating, M. E., Wrobel, T. P., Majzner, K., Baranska, M., Garcia-Munoz, A., ... & Byrne, H. J. (2015). Cell viability assessment using the Alamar blue assay: A comparison of 2D and 3D cell culture models. *Toxicology in vitro*, 29(1), 124-131.

Botham, P. A., Earl, L. K., Fentem, J. H., Roguet, R., & Van De Sandt, J. J. (1998). Alternative methods for skin irritation testing: the current status. *ATLA-NOTTINGHAM*, 26, 195-212.

Brennerhenaff, C., Valdor, J. F., Plusquellec, D., & Wroblewski, H. (1993). Synthesis and characterization of N-octanoyl- β -D-glucosylamine, a new surfactant for membrane studies. *Analytical biochemistry*, 212(1), 117-127.

Brenner-Hénaff, C., Valdor, J. F., Plusquellec, D., & Wróblewski, H. (1993). Thermotropic liquid crystalline properties of some hexuronic acid derivatives bearing a single or two alkyl chains. *Anal. Biochem*, 212, 117.

Buhl, K. J., & Hamilton, S. J. (2000). Acute toxicity of fire-control chemicals, nitrogenous chemicals, and surfactants to rainbow trout. *Transactions of the American Fisheries Society*, 129(2), 408-418.

Bull, N., Johnson, T., & Martin, K. (2011). Organotypic explant culture of adult rat retina for in vitro investigations of neurodegeneration, neuroprotection and cell transplantation. *Protoc* *exch*.

Butenhoff, J. L., Chang, S. C., Ehresman, D. J., & York, R. G. (2009). Evaluation of potential reproductive and developmental toxicity of potassium perfluorohexanesulfonate in Sprague Dawley rats. *Reproductive Toxicology*, 27(3), 331-341.

Carlson, M. A., & Longaker, M. T. (2004). The fibroblast-populated collagen matrix as a model of wound healing: A review of the evidence. *Wound repair and regeneration*, 12(2), 134-147.

Ceresana Market Study: surfactant (2nd edition), <http://www.ceresana.com>

Charaf, U. K., & Hart, G. L. (1991). Phospholipid liposomes/surfactant interactions as predictors of skin irritation. *J Soc Cosmet Chem*, 42(2), 71-86.

Chautan, M., Chazal, G., Cecconi, F., Gruss, P., & Golstein, P. (1999). Interdigital cell death can occur through a necrotic and caspase-independent pathway. *Current biology*, 9(17), 967-51.

Chen, G. G., & Lai, P. B. (2009). *Apoptosis in carcinogenesis and chemotherapy*. Dordrecht, The Netherlands: Springer.

Chou, C. C., Riviere, J. E., & Monteiro-Riviere, N. A. (2003). The cytotoxicity of jet fuel aromatic hydrocarbons and dose-related interleukin-8 release from human epidermal keratinocytes. *Archives of toxicology*, 77(7), 384-391.

City, H. R. C. (2000). *International Workshop on In vitro Methods for Assessing Acute Systemic Toxicity*.

Colin A. Houston (CAH) report, 1997

Colomer, A., Pinazo, A., García, M. T., Mitjans, M., Vinardell, M. P., Infante, M. R., ... & Pérez, L. (2012). pH-sensitive surfactants from lysine: assessment of their cytotoxicity and environmental behavior. *Langmuir*, 28(14), 5900-5912.

Contard, P., Bartel, R. L., Jacobs, L., Perlish, J. S., MacDonald, E. D., Handler, L., ... & Fleischmajer, R. (1993). Culturing keratinocytes and fibroblasts in a three-dimensional mesh results in epidermal differentiation and formation of a basal lamina-anchoring zone. *Journal of investigative dermatology*, 100(1), 35-39.

COOPER, M. L., LAXER, J. A., & HANSBROUGH, J. F. (1991). The cytotoxic effects of commonly used topical antimicrobial agents on human fibroblasts and keratinocytes. *Journal of Trauma and Acute Care Surgery*, 31(6), 775-784.

Corsini, E., & Galli, C. L. (1998). Cytokines and irritant contact dermatitis. *Toxicology letters*, 102, 277-282.

Costin, G. E., Raabe, H. A. N. S., & Curren, R. O. D. G. E. R. (2009). In vitro Safety Testing Strategy for Skin Irritation Using The 3D Reconstructed Human Epidermis. *Rom. J. Biochem*, 46(2), 165-186.

Cowley, N. C., & Farr, P. M. (1992). A dose-response study of irritant reactions to sodium lauryl sulphate in patients with seborrhoeic dermatitis and atopic eczema. *Acta dermato-venereologica*, 72(6), 432-435.

Cruickshank, C. N. D., & Squire, J. R. (1949). Skin Sensitivity to Cetrymide. *British journal of industrial medicine*, 6(3), 164.

Cserháti, T. (1995). Alkyl ethoxylated and alkylphenol ethoxylated nonionic surfactants: interaction with bioactive compounds and biological effects. *Environmental health perspectives*, 103(4), 358.

Cukierman, E., Pankov, R., & Yamada, K. M. (2002). Cell interactions with three-dimensional matrices. *Current opinion in cell biology*, 14(5), 633-640.

Cukierman, E., Pankov, R., Stevens, D. R., & Yamada, K. M. (2001). Taking cell-matrix adhesions to the third dimension. *Science*, 294(5547), 1708-1712.

Cytotoxicity. (n.d.) Dorland's Medical Dictionary for Health Consumers. (2007). Retrieved June 5 2015 from <http://medical-dictionary.thefreedictionary.com/cytotoxicity>

Davies, E., & Hodgson, H. J. (1995). Artificial livers--what's keeping them?. *Gut*, 36(2), 168-170.

Davies, J. T. (1957). A quantitative kinetic theory of emulsion type, I. Physical chemistry of the emulsifying agent. In *Gas/Liquid and Liquid/Liquid Interface. Proceedings of the International Congress of Surface Activity* (pp. 426-438).

Desoize, B., & Jardillier, J. C. (2000). Multicellular resistance: a paradigm for clinical resistance?. *Critical reviews in oncology/hematology*, 36(2), 193-207.

Dickinson, E. (Ed.). (1991). *Food polymers, gels and colloids* (No. 82). Elsevier.

Ding, L., Stilwell, J., Zhang, T., Elboudwarej, O., Jiang, H., Selegue, J. P., ... & Chen, F. F. (2005). Molecular characterization of the cytotoxic mechanism of multiwall carbon nanotubes and nano-onions on human skin fibroblast. *Nano Letters*, 5(12), 2448-2464.

Dobson, K. S., Williams, K. D., & Boriack, C. J. (1993). The preparation of polyglycerol esters suitable as low-caloric fat substitutes. *Journal of the American Oil Chemists Society*, 70(11), 1089-1092.

Dominique, C. (1994). *Synthèse enzymatique de surfactants non ioniques à base d'huile végétale*. PhD thesis, Université de Technologie de Compiègne. 19.

Dong, L., Witkowski, C. M., Craig, M. M., Greenwade, M. M., & Joseph, K. L. (2009). Cytotoxicity effects of different surfactant molecules conjugated to carbon nanotubes on human astrocytoma cells. *Nanoscale research letters*, 4(12), 1517-1523.

Eastoe J. (Ed.). (2002). *Surfactant chemistry*.

Eckes, B., Kessler, D., Aumailley, M., & Krieg, T. (2000, June). Interactions of fibroblasts with the extracellular matrix: implications for the understanding of fibrosis. In *Springer seminars in immunopathology* (Vol. 21, No. 4, pp. 415-429). Springer-Verlag.

Eckhart, L., Lippens, S., Tschachler, E., & Declercq, W. (2013). Cell death by cornification. *Biochimica et Biophysica Acta (BBA)-Molecular Cell Research*, 1833(12), 3471-3480.

Effendy, I., & Maibach, H. I. (1995). Surfactants and experimental irritant contact dermatitis. *Contact dermatitis*, 33(4), 217-225.

Egan, P. A. (1989). Surfactants from biomass. *Chemtech*, 19(12), 758-762.

Eichman, P. (1999). From the Lipid Bilayer to the Fluid Mosaic: A Brief History of Membrane Models. *Resource Center for Sociology, History and Philosophy in Science Teaching-Teachers Network News*, 9(2), 1.

Ekelund, K., Östh, K., Pålhorstorp, C., Björk, E., Ulvenlund, S., & Johansson, F. (2005). Correlation between epithelial toxicity and surfactant structure as derived from the effects of polyethyleneoxide surfactants on caco-2 cell monolayers and pig nasal mucosa. *Journal of pharmaceutical sciences*, 94(4), 730-744.

Elmore, S. (2007). Apoptosis: a review of programmed cell death. *Toxicologic pathology*, 35(4), 495-516.

Emerson, M. F., & Holtzer, A. (1967). On the ionic strength dependence of micelle number. II. *The Journal of physical chemistry*, 71(6), 1898-1907.

Emo, M., Stébé, M. J., Blin, J. L., & Pasc, A. (2013). Metastable micelles and true liquid crystal behaviour of newly designed "catanionic" surfactants. *Soft Matter*, 9(9), 2760-2768.

European Chemicals Agency, <http://echa.europa.eu/>

Farn, R. J. (Ed.). (2008). *Chemistry and technology of surfactants*. John Wiley & Sons.

Farooq, K., & Haque, Z. U. (1992). Effect of sugar esters on the textural properties of nonfat low calorie yogurt. *Journal of Dairy Science*, 75(10), 2676-2680.

Fayed, T. A., Shaaban, M. H., El-Nahass, M. N., & Hassan, F. M. (2014). Hybrid organic-inorganic mesoporous silicates as optical nanosensor for toxic metals detection. *International Journal of Chemical and Applied Biological Sciences*, 1(6), 74.

Fennema, E., Rivron, N., Rouwkema, J., van Blitterswijk, C., & de Boer, J. (2013). Spheroid culture as a tool for creating 3D complex tissues. *Trends in biotechnology*, 31(2), 108-115.

Fiechter, A. (1992). Biosurfactants: moving towards industrial application. *Trends in biotechnology*, 10, 208-217.

Freinkel, R. K., & Woodley, D. T. (Eds.). (2001). *The biology of the skin*. CRC Press.

Friedrich, J., Seidel, C., Ebner, R., & Kunz-Schughart, L. A. (2009). Spheroid-based drug screen: considerations and practical approach. *Nature protocols*, 4(3), 309-324.

Froebe, C. L., Simion, F. A., Rhein, L. D., Cagan, R. H., & Kligman, A. (1990). Stratum corneum lipid removal by surfactants: relation to in vivo irritation. *Dermatology*, 181(4), 277-283.

Fuhrhop, J. H., Svenson, S., Boettcher, C., Rössler, E., & Vieth, H. M. (1990). Long-lived micellar N-alkylaldonamide fiber gels. Solid-state NMR and electron microscopic studies. *Journal of the American Chemical Society*, 112(11), 4307-4312.

Garcia, C., Ball, N., Cagen, S., Carrillo, J. C., Certa, H., Eigler, D., & Mehling, A. (2010). Comparative testing for the identification of skin-sensitizing potentials of nonionic sugar lipid surfactants. *Regulatory Toxicology and Pharmacology*, 58(2), 301-307.

GENNO, M., YAMAMOTO, R., KOJIMA, H., KONISHI, H., & KLAUSNER, M. (1998). Evaluation of a New Alternative to Primary Draize Skin Irritation Testing Using the EpiDerm™ Skin Model. *AATEX (Alternatives to animal testing and experimentation)*, 5, 195-200.

Geurtsen, W., Lehmann, F., Spahl, W., & Leyhausen, G. (1998). Cytotoxicity of 35 dental resin composite monomers/additives in permanent 3T3 and three human primary fibroblast cultures. *Journal of biomedical materials research*, 41(3), 474-480.

Gewies, A. (2003). Introduction to apoptosis. *ApoReview*, 1.

Ghosh, S., & Blankschtein, D. (2007). The role of sodium dodecyl sulfate (SDS) micelles in inducing skin barrier perturbation in the presence. *J. Cosmet. Sci*, 58, 109-133.

Gingell, R., & Lu, C. C. (1991). Acute, subchronic, and reproductive toxicity of a linear alcohol ethoxylate surfactant in the rat. *International Journal of Toxicology*, 10(4), 477-486.

Goodlett, C. R., & Horn, K. H. (2001). Mechanisms of alcohol-induced damage to the developing nervous system. *Alcohol research and Health*, 25(3), 175-184.

Gozuacik, D., & Kimchi, A. (2004). Autophagy as a cell death and tumor suppressor mechanism. *Oncogene*, 23(16), 2891-2906.

Grant, R. L., Yao, C., Gabaldon, D., & Acosta, D. (1992). Evaluation of surfactant cytotoxicity potential by primary cultures of ocular tissues: I. Characterization of rabbit corneal epithelial cells and initial injury and delayed toxicity studies. *Toxicology*, 76(2), 153-176.

Green, D. R. (2011). *Means to an end: apoptosis and other cell death mechanisms*. Cold Spring Harbor Laboratory Press.

Griffin, W. C. (1946). Classification of surface-active agents by "HLB". *J Soc Cosmetic Chemists*, 1, 311-326.

Griffin, W. C. (1955). Calculation of HLB values of non-ionic surfactants. *Am Perfumer Essent Oil Rev*, 65, 26-29.

Griffin, W.C. (1954). Calculation of HLB values of non-ionic surfactants. *J. Soc. Cosmetic Chemists*, 5, 249.

Grinnell, F. (2000). Fibroblast–collagen-matrix contraction: growth-factor signalling and mechanical loading. *Trends in cell biology*, 10(9), 362-365.

Hammond, T. G., & Hammond, J. M. (2001). Optimized suspension culture: the rotating-wall vessel. *American Journal of Physiology-Renal Physiology*, 281(1), F12-F25.

Harding, C. R. (2004). The stratum corneum: structure and function in health and disease. *Dermatologic therapy*, 17(s1), 6-15.

Hato, M., & Shinoda, K. (1973). Krafft points of calcium and sodium dodecylpoly (oxyethylene) sulfates and their mixtures. *The Journal of Physical Chemistry*, 77(3), 378-381.

Haycock, J. W. (2011). 3D cell culture: a review of current approaches and techniques. In *3D Cell Culture* (pp. 1-15). Humana Press.

Heerklotz, H., & Seelig, J. (2000). Titration calorimetry of surfactant–membrane partitioning and membrane solubilization. *Biochimica et Biophysica Acta (BBA)-Biomembranes*, 1508(1), 69-85.

Hofland, H. E. J., Bouwstra, J. A., Ponec, M., Bodde, H. E., Spies, F., Verhoef, J. C., & Junginger, H. E. (1991). Interactions of non-ionic surfactant vesicles with cultured keratinocytes and human skin in vitro: a survey of toxicological aspects and ultrastructural changes in stratum corneum. *Journal of Controlled Release*, 16(1), 155-167.

Holmberg, K. (2001). Natural surfactants. *Current Opinion in Colloid & Interface Science*, 6(2), 148-159.

Huang, S., & Fu, X. (2010). Naturally derived materials-based cell and drug delivery systems in skin regeneration. *Journal of Controlled Release*, 142(2), 149-159.

Imokawa, G., Sumura, K., & Katsumi, M. (1975). Study on skin roughness caused by surfactants: II. Correlation between protein denaturation and skin roughness. *Journal of the American Oil Chemists Society*, 52(12), 484-489.

Inoue, K., Sunakawa, T., & Takayama, S. (1980). Studies of in vitro cell transformation and mutagenicity by surfactants and other compounds. *Food and cosmetics toxicology*, 18(3), 289-296.

International Labour Organization. <http://www.ilo.org>

Isaac, P. C. G., & Jenkins, D. (1958). Biological oxidation of sugar-based detergents. *CHEMISTRY*

& INDUSTRY, (31), 976-977.

Isomaa, B., Reuter, J., & Djupsund, B. M. (1976). The subacute and chronic toxicity of cetyltrimethylammonium bromide (CTAB), a cationic surfactant, in the rat. *Archives of toxicology*, 35(2), 91-96.

Ivanković, T., & Hrenović, J. (2010). Surfactants in the environment. *Arhiv za higijenu rada i toksikologiju*, 61(1), 95-109.

Jang, Y. S., Lee, E. Y., Park, Y. H., Jeong, S. H., Lee, S. G., Kim, Y. R., ... & Son, S. W. (2012). The potential for skin irritation, phototoxicity, and sensitization of ZnO nanoparticles. *Molecular & Cellular Toxicology*, 8(2), 171-177.

Jones, M. N. (1992). Surfactant interactions with biomembranes and proteins. *Chem. Soc. Rev.*, 21(2), 127-136.

Kabanov, A. V., Chekhonin, V. P., Alakhov, V. Y., Batrakova, E. V., Lebedev, A. S., Melik-Nubarov, N. S., ... & Kabanov, V. A. (1989). The neuroleptic activity of haloperidol increases after its solubilization in surfactant micelles: micelles as microcontainers for drug targeting. *FEBS letters*, 258(2), 343-345.

Kanicky, J. R., Lopez-Montilla, J. C., Pandey, S., & Shah, D. (2001). Surface chemistry in the petroleum industry. *Handbook of applied surface and colloid chemistry*, 1, 251-267.

Karlberg, A. T., Bodin, A., & Matura, M. (2003). Allergenic activity of an air-oxidized ethoxylated surfactant. *Contact dermatitis*, 49(5), 241-247.

Khandal, R.K. (2003). Trends in surfactant scene: opportunities and challenges.

Kidd, D. A., Johnson, M., & Clements, J. (2007). Development of an in vitro corrosion/irritation prediction assay using the EpiDerm™ skin model. *Toxicology in vitro*, 21(7), 1292-1297.

Kleszczyński, K., Gardzielewski, P., Mulkiwicz, E., Stepnowski, P., & Składanowski, A. C. (2007). Analysis of structure–cytotoxicity in vitro relationship (SAR) for perfluorinated carboxylic acids. *Toxicology in vitro*, 21(6), 1206-1211.

Kono, H., & Rock, K. L. (2008). How dying cells alert the immune system to danger. *Nature Reviews Immunology*, 8(4), 279-289.

Korting, H. C., Herzinger, T., Hartinger, A., Kerscher, M., Angerpointner, T., & Maibach, H. I. (1994). Discrimination of the irritancy potential of surfactants in vitro by two cytotoxicity assays using normal human keratinocytes, HaCaT cells and 3T3 mouse fibroblasts: correlation with in vivo data from a soap chamber assay. *Journal of dermatological science*, 7(2), 119-129.

Kralova, I., & Sjöblom, J. (2009). Surfactants used in food industry: a review. *Journal of Dispersion Science and Technology*, 30(9), 1363-1383.

Kristin, K., Balzer, D., & Luders, H. (Eds.). (2000). *Nonionic surfactants: alkyl polyglucosides* (Vol. 91). CRC Press.

Kroemer, G., Galluzzi, L., Vandenabeele, P., Abrams, J., Alnemri, E. S., Baehrecke, E. H., ... & Melino, G. (2009). Classification of cell death: recommendations of the Nomenclature Committee on Cell Death 2009. *Cell Death & Differentiation*, 16(1), 3-11.

Kumar KC, S., & Müller, K. (1999). Lichen metabolites. 2. Antiproliferative and cytotoxic activity of gyrophoric, usnic, and diffractaic acid on human keratinocyte growth. *Journal of natural products*, 62(6), 821-823.

Lansdown, A. B. G., & Grasso, P. (1972). PHYSICO-CHEMICAL FACTORS INFLUENCING EPIDERMAL DAMAGE BY SURFACE ACTIVE AGENTS. *British journal of dermatology*, 86(4), 361-378.

Laurent, P., Razafindralambo, H., Wathelet, B., Blecker, C., Wathelet, J. P., & Paquot, M. (2011). Synthesis and surface-active properties of uronic amide derivatives, surfactants from renewable organic raw materials. *Journal of Surfactants and Detergents*, 14(1), 51-63.

Lawrence, M. J. (1994). Surfactant systems: their use in drug delivery. *Chemical Society Reviews*, 23(6), 417-424.

Le, M., Schalkwijk, J., Siegenthaler, G., van de Kerkhof, P. C., Veerkamp, J. H., & van der Valk, P. G. (1996). Changes in keratinocyte differentiation following mild irritation by sodium dodecyl sulphate. *Archives of dermatological research*, 288(11), 684-690.

Lee, J. K., Kim, D. B., Kim, J. I., & Kim, P. Y. (2000). In vitro cytotoxicity tests on cultured human skin fibroblasts to predict skin irritation potential of surfactants. *Toxicology in vitro*, 14(4), 345-349.

Lewis, M. A. (1990). Chronic toxicities of surfactants and detergent builders to algae: a review and risk assessment. *Ecotoxicology and environmental safety*, 20(2), 123-140.

Li, X., Turánek, J., Knötigová, P., Kudláčková, H., Mašek, J., Parkin, S., ... & Lehmler, H. J. (2009). Hydrophobic tail length, degree of fluorination and headgroup stereochemistry are determinants of the biocompatibility of (fluorinated) carbohydrate surfactants. *Colloids and Surfaces B: Biointerfaces*, 73(1), 65-74.

Lieberman, M., Marks, A. D., Smith, C. M., & Marks, D. B. (2006). *Marks' Essential Medical Biochemistry*. Lippincott Williams & Wilkins.

Likhoshev, L. M., Novikova, O. S., & Shibaev, V. N. (2003, April). New Synthesis of β -Glycosylamines of D-Mannose, 2- and 6-Deoxysugars, and D-Glucuronic Acid with the Use of Ammonium Carbamate. In *Doklady Chemistry* (Vol. 389, No. 4, pp. 73-76). MAIK Nauka/Interperiodica.

Liu, J. Y., Hafner, J., Dragieva, G., & Burg, G. (2006). A novel bioreactor microcarrier cell culture system for high yields of proliferating autologous human keratinocytes. *Cell transplantation*, 15(5), 435-443.

Löffler, H., & Happle, R. (2003). Profile of irritant patch testing with detergents: sodium lauryl sulfate, sodium laureth sulfate and alkyl polyglucoside. *Contact Dermatitis*, 48(1), 26-32.

Lubineau, A., Augé, J., & Drouillat, B. (1995). Improved synthesis of glycosylamines and a straightforward preparation of N-acylglycosylamines as carbohydrate-based detergents. *Carbohydrate research*, 266(2), 211-219.

Lucassen-Reynders, E. H. (1994). Competitive adsorption of emulsifiers 1. Theory for adsorption of small and large molecules. *Colloids and Surfaces A: Physicochemical and Engineering Aspects*, 91, 79-88.

Madsen, T., Petersen, G., Seierø, C., & Tørsløv, J. (1996). Biodegradability and aquatic toxicity of glycoside surfactants and a nonionic alcohol ethoxylate. *Journal of the American Oil Chemists' Society*, 73(7), 929-933.

Magdassi, S. (Ed.). (1996). *Surface activity of proteins: chemical and physicochemical modifications*. CRC Press.

Malda, J., & Frondoza, C. G. (2006). Microcarriers in the engineering of cartilage and bone. *Trends in biotechnology*, 24(7), 299-304.

Maldonado, F., Almela, M., Otero, A., & Costa-López, J. (1991). The binding of anionic and nonionic surfactants to collagen through the hydrophobic effect. *Journal of protein chemistry*, 10(2), 189-192.

Mann, R. M., & Bidwell, J. R. (2001). The acute toxicity of agricultural surfactants to the tadpoles of four Australian and two exotic frogs. *Environmental pollution*, 114(2), 195-205.

Markets and Markets report. Surfactants market by product type. <http://marketsandmarkets.com>

Martin, Y., Eldardiri, M., Lawrence-Watt, D. J., & Sharpe, J. R. (2010). Microcarriers and their potential in tissue regeneration. *Tissue Engineering Part B: Reviews*, 17(1), 71-80.

Matsson, M. K., Kronberg, B., & Claesson, P. M. (2004). Adsorption of alkyl polyglucosides on the solid/water interface: equilibrium effects of alkyl chain length and head group

Matsuki, H., Ichikawa, R., Kaneshina, S., Kamaya, H., & Ueda, I. (1996). Differential scanning calorimetric study on the Krafft phenomenon of local anesthetics. *Journal of colloid and interface science*, 181(2), 362-369.

Maunier, V., Boullanger, P., Lafont, D., & Chevalier, Y. (1997). Synthesis and surface-active properties of amphiphilic 6-aminocarbonyl derivatives of D-glucose. *Carbohydrate research*, 299(1), 49-57.

Mayhew, T. M., Myklebust, R., Whybrow, A., & Jenkins, R. (1999). Epithelial integrity, cell death and cell loss in mammalian small intestine. *Histology and histopathology*, 14(1), 257-267.

May Masnou, A., Pasc, A., Stébé, M. J., Gutiérrez González, J. M., Porras Rodríguez, M., & Blin, J. L. (2012). Tailored Jeffamine molecular tools for ordering mesoporous Silica. *Langmuir*, 2012, vol. 28, num. 25, p. 9816-9824.

McClellan, S. J., & Franses, E. I. (2003). Effect of concentration and denaturation on adsorption and surface tension of bovine serum albumin. *Colloids and Surfaces B: Biointerfaces*, 28(1), 63-75.

Memisoglu-Bilensoy, E., Doğan, A. L., & Hincal, A. A. (2006). Cytotoxic evaluation of injectable cyclodextrin nanoparticles. *Journal of pharmacy and pharmacology*, 58(5), 585-589.

Migahed, M. A., & Al-Sabagh, A. M. (2009). Beneficial role of surfactants as corrosion inhibitors in petroleum industry: a review article. *Chemical Engineering Communications*, 196(9), 1054-1075.

Montagnon, B. J., Fanget, B., & Nicolas, A. J. (1980). The large-scale cultivation of VERO cells in micro-carrier culture for virus vaccine production. Preliminary results for killed poliovirus vaccine. *Developments in biological standardization*, 47, 55-64.

Montagnon, B. J., Fanget, B., & Vincent-Falquet, J. C. (1984). Industrial-scale production of inactivated poliovirus vaccine prepared by culture of Vero cells on microcarrier. *Review of Infectious Diseases*, 6(Supplement 2), S341-S344.

Mukerjee, P., & Mysels, K. J. (1971). Critical micelle concentrations of aqueous surfactant systems (No. NSRDS-NBS-36). National Standard reference data system.

Mukerjee, P., Mysels, K., & Kapauan, P. (1967). Counterion specificity in the formation of ionic micelles-size, hydration, and hydrophobic bonding effects. *The Journal of Physical Chemistry*, 71(13), 4166-4175.

Myers, D. (2005). *Surfactant science and technology*. John Wiley & Sons.

Nakamura, Y., Murakami, A., Ohto, Y., Torikai, K., Tanaka, T., & Ohigashi, H. (1998). Suppression of tumor promoter-induced oxidative stress and inflammatory responses in mouse skin by a

superoxide generation inhibitor 1'-acetoxychavicol acetate. *Cancer Research*, 58(21), 4832-4839.

Negm, N. A., & Tawfik, S. M. (2013). Environmentally Friendly Surface Active Agents and Their Applications. *Surfactants in Tribology*, 3, 147.

Newby, C. S., Barr, R. M., Greaves, M. W., & Mallet, A. I. (2000). Cytokine release and cytotoxicity in human keratinocytes and fibroblasts induced by phenols and sodium dodecyl sulfate. *Journal of investigative dermatology*, 115(2), 292-298.

Niño, M. R. R., & Patino, J. R. (1998). Surface tension of bovine serum albumin and tween 20 at the air-aqueous interface. *Journal of the American Oil Chemists' Society*, 75(10), 1241-1248.

Nishikido, N., Kobayashi, H., & Tanaka, M. (1982). Pressure effect on the Krafft points of ionic surfactants. *The Journal of Physical Chemistry*, 86(16), 3170-3172.

North-Root, H., Yackovich, F., Demetrulias, J., Gacula, M., & Heinze, J. E. (1982). Evaluation of an in vitro cell toxicity test using rabbit corneal cells to predict the eye irritation potential of surfactants. *Toxicology Letters*, 14(3), 207-212.

OECD guideline for the testing of chemicals. <http://oecd-ilibrary.com>

Okayama, Y. (2005). Oxidative stress in allergic and inflammatory skin diseases. *Current Drug Targets-Inflammation & Allergy*, 4(4), 517-519.

Okazaki, Y., & Gotoh, E. (2013). Metal ion effects on different types of cell line, metal ion incorporation into L929 and MC3T3-E1 cells, and activation of macrophage-like J774. 1 cells. *Materials Science and Engineering: C*, 33(4), 1993-2001.

Otzen, D. (2011). Protein-surfactant interactions: a tale of many states. *Biochimica et Biophysica Acta (BBA)-Proteins and Proteomics*, 1814(5), 562-591.

Pampaloni, F., Reynaud, E. G., & Stelzer, E. H. (2007). The third dimension bridges the gap between cell culture and live tissue. *Nature reviews Molecular cell biology*, 8(10), 839-845.

Park, J., Rader, L. H., Thomas, G. B., Danoff, E. J., English, D. S., & DeShong, P. (2008). Carbohydrate-functionalized cationic surfactant vesicles: preparation and lectin-binding studies. *Soft Matter*, 4(9), 1916-1921.

Parris, N., Weil, J. K., & Linfield, W. M. (1973). Soap based detergent formulations. V. Amphoteric lime soap dispersing agents. *Journal of the American Oil Chemists Society*, 50(12), 509-512.

Partearroyo, M. A., Ostolaza, H., Goñi, F. M., & Barberá-Guillem, E. (1990). Surfactant-induced cell toxicity and cell lysis: a study using B16 melanoma cells. *Biochemical pharmacology*, 40(6),

1323-1328.

Patist, A., Bhagwat, S. S., Penfield, K. W., Aikens, P., & Shah, D. O. (2000). On the measurement of critical micelle concentrations of pure and technical-grade nonionic surfactants. *Journal of Surfactants and Detergents*, 3(1), 53-58.

Piispanen, P. S., Persson, M., Claesson, P., & Norin, T. (2004). Surface properties of surfactants derived from natural products. Part 1: Syntheses and structure/property relationships—Solubility and emulsification. *Journal of surfactants and detergents*, 7(2), 147-159.

Plusquellec, D., Brenner-Hénaff, C., Léon-Rnaud, P., Duquenoy, S., Lefeuvre, M., & Wróblewski, H. (1994). An efficient acylation of free glycosylamines for the synthesis of N-glycosyl amino acids and N-glycosidic surfactants for membrane studies. *Journal of carbohydrate chemistry*, 13(5), 737-751.

Plusquellec, D., Chevalier, G., Talibart, R., & Wro, H. (1989). Synthesis and characterization of 6-O-(N-heptylcarbamoyl)-methyl- α -D-glucopyranoside, a new surfactant for membrane studies. *Analytical biochemistry*, 179(1), 145-153.

Ponec, M. (1992). In vitro cultured human skin cells as alternatives to animals for skin irritancy screening. *International journal of cosmetic science*, 14(6), 245-264.

Porter, M. R. (Ed.). (1995). *Biodegradability of surfactants*. Springer Science & Business Media.

Proskuryakov, S. Y., Konoplyannikov, A. G., & Gabai, V. L. (2003). Necrosis: a specific form of programmed cell death?. *Experimental cell research*, 283(1), 1-16.

Prottey, C., & Ferguson, T. (1975). Factors which determine the skin irritation potential of soaps and detergents. *J Soc Cosmet Chem*, 26(1), 29-46.

Rabinowitz, J. D., & White, E. (2010). Autophagy and metabolism. *Science*, 330(6009), 1344-1348.

Ramiz, A., Goethals, G., Martin, P., Villa, P., & Godé, P. (2002). Mesophase properties of N-glycidyl (ityl)-amides. *Journal of thermal analysis and calorimetry*, 69(2), 417-426.

Razafindralambo, H., Blecker, C., & Paquot, M. (2011, September). Screening of Basic Properties of Amphiphilic Molecular Structures for Colloidal System Formation and Stability: The Case of Carbohydrate-Based Surfactants. In 239th ACS National Meeting. ACS.

Razafindralambo, H., Blecker, C., Mezdour, S., Deroanne, C., Crowet, J. M., Brasseur, R., ... & Paquot, M. (2009). Impacts of the carbonyl group location of ester bond on interfacial properties of sugar-based surfactants: experimental and computational evidences. *The Journal of Physical Chemistry B*, 113(26), 8872-8877.

Reininger-Mack, A., Thielecke, H., & Robitzki, A. A. (2002). 3D-biohybrid systems: applications in drug screening. *TRENDS in Biotechnology*, 20(2), 56-61.

Rhein, L. D., Simion, F. A., Hill, R. L., Cagan, R. H., Mattai, J. A. I. R. A. J. H., & Maibach, H. I. (1990). Human cutaneous response to a mixed surfactant system: role of solution phenomena in controlling surfactant irritation. *Dermatology*, 180(1), 18-23.

Rogerson, A., Cummings, J., Willmott, N., & Florence, A. T. (1988). The distribution of doxorubicin in mice following administration in niosomes. *Journal of pharmacy and pharmacology*, 40(5), 337-342.

Roguet, R., Cohen, C., Dossou, K. G., & Rougier, A. (1994). Episkin, a reconstituted human epidermis for assessing in vitro the irritancy of topically applied compounds. *Toxicology in vitro*, 8(2), 283-291.

Roguet, R., Dossou, K. G., & Rougier, A. (1992). Prediction of eye irritation potential of surfactants using the SIRC-NRU cytotoxicity test. *Alternatives to laboratory animals: ATLA*.

Rosen, M. J., & Kunjappu, J. T. (2012). *Surfactants and interfacial phenomena*. John Wiley & Sons.

Rosenstein, J. M., Mani, N., Khaibullina, A., & Krum, J. M. (2003). Neurotrophic effects of vascular endothelial growth factor on organotypic cortical explants and primary cortical neurons. *The Journal of neuroscience*, 23(35), 11036-11044.

Rosette, C., & Karin, M. (1996). Ultraviolet light and osmotic stress: activation of the JNK cascade through multiple growth factor and cytokine receptors. *Science*, 274(5290), 1194-1197.

Rothenberg, M. E., Petersen, J. E. A. N. N. I. N. E., Stevens, R. L., Silberstein, D. S., McKenzie, D. T., Austen, K. F., & Owen, W. F. (1989). IL-5-dependent conversion of normodense human eosinophils to the hypodense phenotype uses 3T3 fibroblasts for enhanced viability, accelerated hypodensity, and sustained antibody-dependent cytotoxicity. *The Journal of Immunology*, 143(7), 2311-2316.

Ruiz, M. B., Prado, A., Goñi, F. M., & Alonso, A. (1994). An assessment of the biochemical applications of the non-ionic surfactant Hecameg. *Biochimica et Biophysica Acta (BBA)-Biomembranes*, 1193(2), 301-306.

Sandbacka, M., Christianson, I., & Isomaa, B. (2000). The acute toxicity of surfactants on fish cells, *Daphnia magna* and fish—a comparative study. *Toxicology in vitro*, 14(1), 61-68.

Sanyal, S. Culture and assay systems used for 3D cell culture. <http://www.corning.com>

Sarkar, S. (2013). Chemical screening platforms for autophagy drug discovery to identify therapeutic candidates for Huntington's disease and other neurodegenerative disorders. *Drug Discovery Today: Technologies*,10(1), e137-e144.

Schick, M. J. (Ed.). (1987). *Nonionic Surfactants: Physical Chemistry*. CRC Press.

Schott, H., & Han, S. K. (1976). Effect of inorganic additives on solutions of nonionic surfactants IV: Krafft points. *Journal of pharmaceutical sciences*,65(7), 979-981.

Schramm, L. L. (Ed.). (2000). *Surfactants: fundamentals and applications in the petroleum industry*. Cambridge University Press.

Schramm, L. L., Stasiuk, E. N., & Marangoni, D. G. (2003). 2 Surfactants and their applications. *Annual Reports Section " C"(Physical Chemistry)*, 99, 3-48.

Shimizu, H. (2007). Shimizu's textbook of dermatology (pp. 42-48). Hokkaido University.

Shinoda, K., Nakagawa, T., & Tamamushi, B. I. (2013). *Colloidal surfactants: some physicochemical properties* (Vol. 12). Elsevier.

Shinoda, K., Yamaguchi, N., & Carlsson, A. (1989). Physical meaning of the Krafft point: observation of melting phenomenon of hydrated solid surfactant at the Krafft point. *The Journal of Physical Chemistry*, 93(20), 7216-7218.

Shvedova, A., Castranova, V., Kisin, E., Schwegler-Berry, D., Murray, A., Gandelsman, V., ... & Baron, P. (2003). Exposure to carbon nanotube material: assessment of nanotube cytotoxicity using human keratinocyte cells. *Journal of toxicology and environmental health Part A*, 66(20),

Siddiqui, M. A., Saquib, Q., Ahamed, M., Farshori, N. N., Ahmad, J., Wahab, R., ... & Pant, A. B. (2015). Molybdenum nanoparticles-induced cytotoxicity, oxidative stress, G2/M arrest, and DNA damage in mouse skin fibroblast cells (L929). *Colloids and Surfaces B: Biointerfaces*, 125, 73-81.

Simion, F. A., Warscjewski, D., & Zyzyck, L. A. (1990). U.S. Patent No. 4,923,635. Washington, DC: U.S. Patent and Trademark Office.

Stadler, J. C., Delker, D. A., Malley, L. A., Frame, S. R., Everds, N. E., Mylchreest, E., ... & Buck, R. C. (2008). Subchronic, Reproductive, and Developmental Toxicity of a Fluorotelomer-Based Urethane Polymeric Product*. *Drug and chemical toxicology*, 31(3), 317-337.

Stasiuk, E. N., & Schramm, L. L. (1996). The temperature dependence of the critical micelle concentrations of foam-forming surfactants. *Journal of colloid and interface science*, 178(1), 324-333.

Steber, J., Guhl, W., Stelter, N., & Schrbder, F. R. (2008). 11. Ecological Evaluation of Alkyl

Polyglycosides. Alkyl Polyglycosides: Technology, Properties, Applications, 177.

Stefanska, B. J., Falkowski, L. S., & Borowski, E. (1982). U.S. Patent No. 4,351,937. Washington, DC: U.S. Patent and Trademark Office.

Stubenrauch, C. (2001). Sugar surfactants—aggregation, interfacial, and adsorption phenomena. *Current opinion in colloid & interface science*, 6(2), 160-170.

Sun, T., Jackson, S., Haycock, J. W., & MacNeil, S. (2006). Culture of skin cells in 3D rather than 2D improves their ability to survive exposure to cytotoxic agents. *Journal of biotechnology*, 122(3), 372-381.

Suradkar, Y. R., & Bhagwat, S. S. (2006). CMC determination of an odd carbon chain surfactant (C13E20) mixed with other surfactants using a spectrophotometric technique. *Journal of Chemical & Engineering Data*, 51(6), 2026-2031.

Tachon, P., Cotovio, J., Dossou, K. G., & Prunieras, M. (1989). Assessment of surfactant cytotoxicity: comparison with the Draize eye test. *International journal of cosmetic science*, 11(5), 233-243.

Talmage, S. S. (1994). Environmental and human safety of major surfactants: alcohol ethoxylates and alkylphenol ethoxylates. CRC Press.

Tian, F., Cui, D., Schwarz, H., Estrada, G. G., & Kobayashi, H. (2006). Cytotoxicity of single-wall carbon nanotubes on human fibroblasts. *Toxicology in vitro*, 20(7), 1202-1212.

Timmins, N. E., & Nielsen, L. K. (2007). Generation of multicellular tumor spheroids by the hanging-drop method. In *Tissue Engineering* (pp. 141-151). Humana Press.

Tsuji, K., & Mino, J. (1978). Krafft point depression of some zwitterionic surfactants by inorganic salts. *The Journal of Physical Chemistry*, 82(14), 1610-1614.

Tuan, T. L., Keller, L. C., Sun, D., Nimni, M. E., & Cheung, D. (1994). Dermal fibroblasts activate keratinocyte outgrowth on collagen gels. *Journal of cell science*, 107(8), 2285-2289.

Tung, Y. C., Hsiao, A. Y., Allen, S. G., Torisawa, Y. S., Ho, M., & Takayama, S. (2011). High-throughput 3D spheroid culture and drug testing using a 384 hanging drop array. *Analyst*, 136(3), 473-478.

Uchegbu, I. F., Double, J. A., Turton, J. A., & Florence, A. T. (1995). Distribution, metabolism and tumoricidal activity of doxorubicin administered in sorbitan monostearate (Span 60) niosomes in the mouse. *Pharmaceutical research*, 12(7), 1019-1024.

United Nations, Economic Commission for Europe, <http://www.unece.org>

Vacanti, J. P., & Langer, R. (1999). Tissue engineering: the design and fabrication of living replacement devices for surgical reconstruction and transplantation. *The Lancet*, 354, S32-S34.

Van de Sandt, J., Roguet, R., Cohen, C., Esdaile, D., Ponc, M., Corsini, E., ... & Fartasch, M. (1999). The use of human keratinocytes and human skin models for predicting skin irritation. *ATLA-NOTTINGHAM-*, 27, 723-744

Van Doren, H. A. (1996). Tailor-made carbohydrate surfactants? Systematic investigations into structure-property relationships of N-Acyl N-Alkyl 1-Amino-1-Deoxy-D-Glucitols. *Carbohydrates as Organic Raw Materials III*, 255-272.

Van Os, N. M. (Ed.). (1997). *Nonionic surfactants: organic chemistry* (Vol. 72). CRC Press.

Van Smeden, J., Janssens, M., Gooris, G. S., & Bouwstra, J. A. (2014). The important role of stratum corneum lipids for the cutaneous barrier function. *Biochimica et Biophysica Acta (BBA)-Molecular and Cell Biology of Lipids*, 1841(3), 295-313.

Vian, L., Vincent, J., Maurin, J., Fabre, I., Giroux, J., & Cano, J. P. (1995). Comparison of three in vitro cytotoxicity assays for estimating surfactant ocular irritation. *Toxicology in vitro*, 9(2), 185-190.

Voigt, M., Schauer, M., Schaefer, D. J., Andree, C., Horch, R., & Stark, G. B. (1999). Cultured epidermal keratinocytes on a microspherical transport system are feasible to reconstitute the epidermis in full-thickness wounds. *Tissue engineering*, 5(6), 563-572.

Welss, T., Basketter, D. A., & Schröder, K. R. (2004). In vitro skin irritation: facts and future. State of the art review of mechanisms and models. *Toxicology in vitro*, 18(3), 231-243.

Weuthen, M., Kawa, R., Hill, K., & Ansmann, A. (1995). Long chain alkyl polyglycosides—a new generation of emulsifiers. *Lipid/Fett*, 97(6), 209-211.

Wiles, M., Williams, J., Ahmad, K. A., & Ahmad, K. (2010). *Essentials of Dermatology for Chiropractors*. Jones & Bartlett Learning.

Wilhelm, K. P., Cua, A. B., Wolff, H. H., & Maibach, H. I. (1993). Surfactant-induced stratum corneum hydration in vivo: prediction of the irritation potential of anionic surfactants. *Journal of investigative dermatology*, 101(3), 310-315.

Wilhelm, K. P., Freitag, G., & Wolff, H. H. (1994). Surfactant-induced skin irritation and skin repair: evaluation of a cumulative human irritation model by noninvasive techniques. *Journal of the American Academy of Dermatology*, 31(6), 981-987.p

Willing, A., Messinger, H., & Aulumann, W. (2004). Ecology and toxicology of alkyl polyglycosides. *Handbook of detergents part B: environmental impact*.

Wong, S. F., Choi, Y. Y., Kim, D. S., Chung, B. G., & Lee, S. H. (2011). Concave microwell based size-controllable hepatosphere as a three-dimensional liver tissue model. *Biomaterials*, 32(32), 8087-8096.

Woodward, M. N., Kenny, S. E., Vaillant, C., Lloyd, D. A., & Edgar, D. H. (2000). Time-dependent effects of endothelin-3 on enteric nervous system development in an organ culture model of Hirschsprung's disease. *Journal of pediatric surgery*, 35(1), 25-29.

Wu, S. C., Liu, C. C., & Lian, W. C. (2004). Optimization of microcarrier cell culture process for the inactivated enterovirus type 71 vaccine development. *Vaccine*, 22(29), 3858-3864.

Xu, W., Osei-Prempeh, G., Lema, C., Oldham, E. D., Aguilera, R. J., Parkin, S., ... & Lehmler, H. J. (2012). Synthesis, thermal properties, and cytotoxicity evaluation of hydrocarbon and fluorocarbon alkyl β -D-xylopyranoside surfactants. *Carbohydrate research*, 349, 12-23.

Yam, J., Booman, K. A., Broddle, W., Geiger, L., Heinze, J. E., Lin, Y. J., ... & Wright, G. A. (1984). Surfactants: A survey of short-term genotoxicity testing. *Food and Chemical Toxicology*, 22(9), 761-769.

Yang, W., & Acosta, D. (1994). Cytotoxicity potential of surfactant mixtures evaluated by primary cultures of rabbit corneal epithelial cells. *Toxicology letters*, 70(3), 309-318.

Zang, R., Li, D., Tang, I. C., Wang, J., & Yang, S. T. (2012). Cell-based assays in high-throughput screening for drug discovery. *International Journal of Biotechnology for Wellness Industries*, 1(1), 31-51.

Zavodnik, I. B., Zaborowski, A., Niekurzak, A., & Bryszewska, M. (1997). Effect of free fatty acids on erythrocyte morphology and membrane fluidity. *IUBMB Life*, 42(1), 123-133.

Zhao, J., Lahiri-Chatterjee, M., Sharma, Y., & Agarwal, R. (2000). Inhibitory effect of a flavonoid antioxidant silymarin on benzoyl peroxide-induced tumor promotion, oxidative stress and inflammatory responses in SENCAR mouse skin. *Carcinogenesis*, 21(4), 811-816.

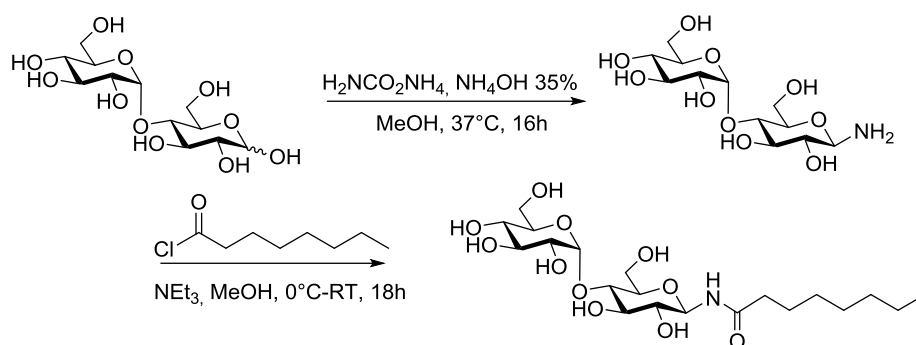
Appendix

Appendix I

Detailed optimized synthesis procedures of the sugar-based surfactant investigated for their physico-chemical properties and biological effects

(Data provided by our partner laboratory LG2A, UPJV, Amiens)

N-Octanoyl-4-O- α -D-glucopyranosyl- β -D-glucopyranosylamine (Mal1amideC8) C₂₀H₃₇NO₁₁ [CAS: 161296-88-4]



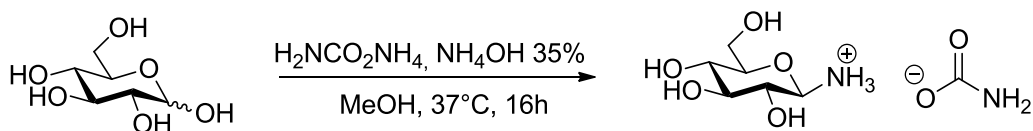
Step 1: Following the procedure described by Likhosherstov (Likhosherstov, L. M., et al. 2003), 12 g of maltose (1eq.) and 5.2 g of $\text{H}_2\text{NCOONH}_4$ were solubilized in NH_4OH 35% (32 mL), then MeOH (72 mL) was added. The mixture was stirred at 37°C for 16h. Isopropanol (120 mL) was then added and the solution maintained at 0°C for 16h. The supernatant was removed and MeOH (100 mL) and isopropanol (100 mL) were added to the crude product, the mixture was triturated until the obtaining of a precipitate of maltosylamine. After filtration and drying under reduced pressure, 12.5 g of maltosylamine were isolated (88% yield). According to Lubineau, A., et al. (1995), the chemical shift of the anomeric carbon is at 85.19 ppm (83.21 for the carbamate form).

Step 2: 1.2 g of β -maltosylamine were dissolved in MeOH (300 mL), and triethylamine (2.36 mL, 5 eq.) was added. The mixture was stirred at 0°C for 2h then 3.6 mL (6 eq.) of octanoyl chloride were added and the stirring was maintained for 18h at °C. The solvent was evaporated and the crude N-octanoyl- β -maltosylamine was purified by reverse C18 phase flash chromatography, as a white solid in 49% yield (806 mg).

The procedure reported by Lubineau, A., et al. (1995), using 1:2 H₂O-EtOH, Na₂CO₃ gave a similar yield (50%). Another multi step procedure (Park et al, 2008) described the synthesis of N-octanoyl- β -maltosylamine via a reaction sequence: peracetylation, azidation, reduction of the azide and acylation followed by a deacetylation. This compound was obtained in 41% yield in 4 steps. The synthesis of this family is also described in other publications of Plusquellec, D., et al. 1994; Brenner-Hénaff, C., et al. 1993.

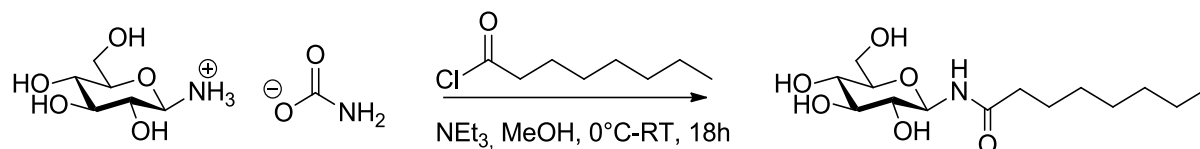
N-Octanoyl-β-D-glucopyranosylamine (Glu1amideC8) $C_{14}H_{27}NO_6$ [CAS: 134403-86-4]

Step 1:



D-(+)-glucose (10g; 55.5 mmol) and ammonium carbamate (8.7 g; 111.4 mmol) were dissolved into 35% aqueous ammonia (28 ml). Methanol was added (112 ml) and the reaction mixture was stirred at 37°C for 18h. Then isopropanol (100 ml) was added and the mixture was stored at low temperature (0-4°C) for 16 h. The supernatant was removed and methanol (100 ml) and isopropanol (100 ml) were added. The remaining viscous oil was then triturated until a precipitate is obtained. After filtration, a white solid (11.5g; 82%) is obtained which has been dried under reduced pressure.

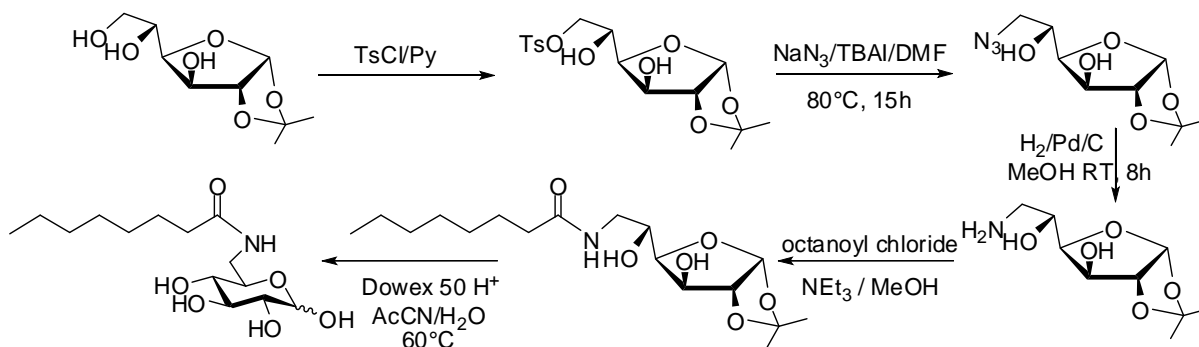
Step 2:



The previous white solid (670 mg; 2.8 mmol) was dissolved in methanol (170 ml) and triethylamine (2.6 ml; 14 mmol) was added. The reaction was then stirred at 0°C for 2h and octanoyl chloride (3.8 ml; 16.8 mmol) was added. The reaction mixture was stirred between 0° and 25°C for 16h. Ion exchange resins were then added (30 g; Dowex® 50WX8 H+) and the mixture was stirred at room temperature for 3h. After filtration, the solvent was removed under vacuum and the residue was purified on silica gel ($CH_2Cl_2/MeOH$: 4/1). A white solid is obtained (700 mg; 60%).

The procedure reported by Lubineau, A., et al. (1995), using 1:2 H₂O-EtOH, Na₂CO₃ gave a similar yield (50%).

6-deoxy-6-octanamido-D-glucose (Glu6amideC8') $C_{14}H_{27}NO_6$ [CAS: 189503-43-3]



Step 1: A solution of TsCl (5.2 g, 27 mmol) in dry pyridine (30 mL) was slowly added to a

solution of 1,2-*O*-isopropylidene- α -D-glucofuranose (4.0 g, 18 mmol) in dry pyridine (30 mL). The reaction was then magnetically stirred 2 h at 0°C and 14 h at room temperature. After evaporation of pyridine, the reaction was dissolved in CH₂Cl₂ (100 mL) and then washed with 1% HCl solution (2 x 100 mL) and then with a saturated NaHCO₃ solution (100 mL). The reaction mixture was purified on silica gel chromatography (cyclohexane / AcOEt 1:1) to give 1,2-*O*-isopropylidene-6-*O*-tosyl- α -D-glucofuranose (4.8 g, 71%) as a solid.

Step 2: A solution of 1,2-*O*-isopropylidene-6-*O*-tosyl- α -D-glucofuranose (4.0 g, 10.7 mmol), NaN₃ (1.4 g, 21.4 mmol) and TBAI (15 mg) in dry DMF (60 mL) under Ar atmosphere was magnetically stirred 15 h at 80°C. After evaporation of DMF, the reaction mixture was purified on silica gel chromatography (cyclohexane / AcOEt 1:1) to give 6-azido-6-deoxy-1,2-*O*-isopropylidene- α -D-glucofuranose (2.1 g, 81%).

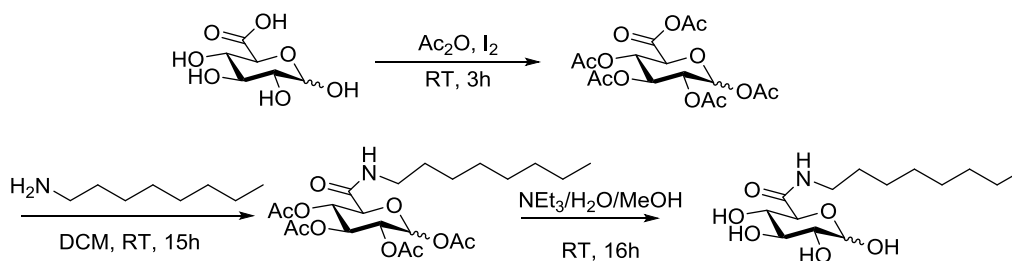
Step 3: A solution of 6-azido-6-deoxy-1,2-*O*-isopropylidene- α -D-glucofuranose (1.5 g, 6.12 mmol) in MeOH (100 mL) was hydrogenated 8 h on a H-cube apparatus using a 10% Pd/C cartridge. After evaporation of MeOH, the reaction mixture was purified on silica gel chromatography (CH₂Cl₂ / MeOH 9:1) to give 6-amino-6-deoxy-1,2-*O*-isopropylidene- α -D-glucofuranose (1.1 g, 82% CAS Registry Number 24384-87-0).

Step 4: A solution of 6-amino-6-deoxy-1,2-*O*-isopropylidene- α -D-glucofuranose (1.1 g, 5.0 mmol) and triethylamine (3.4 mL, 25 mmol) in MeOH (300 mL) was cooled in an ice bath. Octanoyl chloride (15.1 mL, 30 mmol) was added in two portions and the reaction was stirred for 16 h. After evaporation of MeOH, the reaction mixture was purified on silica gel chromatography (CH₂Cl₂ / MeOH 9:1) to give 6-octanamido-6-deoxy-1,2-*O*-isopropylidene- α -D-glucofuranose (1.18 g, 65% CAS Registry Number 487027-37-2).

Step 5: Water (80 mL) was added to a solution of 6-octanamido-6-deoxy-1,2-*O*-isopropylidene- α -D-glucofuranose (1.18 g, 3.4 mmol) in acetonitrile (120 mL). Then Dowex 50 H⁺ (2.0 g) was added to the solution and the reaction stirred at 60°C for 3 h. After filtration and evaporation the reaction mixture was purified on silica gel chromatography (CH₂Cl₂ / MeOH 8.5:1.5) to give 6-octanamido-6-deoxy-D-glucose (600 mg, 58%) as a white solid.

The synthesis and amphiphilic properties of this derivative were first described by Maunier, V., et al. (1997). It involved a different synthesis path. Synthesis similar to the one involved here with different experimental conditions is described in the paper of Ramiz, A., et al. (2002), together with mesophase properties of the compounds. In particular, tetrabutylammonium iodide was used in the step 2, and during step 3, the reduction was made in presence of triphenylphosphine. Some of the intermediates (the amino derivative obtained after step 3) are described in another publication (Baer, H.H., et al. 1975).

***N*-octyl- β -D-glucopyranuronamide (Glu6amideC8) C₁₄H₂₇NO₆ [CAS: 1263382-58-6] or *N*-octyl-D-glucuronamide [CAS: 78798-01-3]**



Glucuronic acid (3g) was dissolved in acetic anhydride (45 mL), and 210 mg of iodide was added, the suspension was first sonicated until the complete solubilization of GlcA, and the solution was stirred at RT for 3h. Acetic anhydride was evaporated and the crude product was diluted in DCM (20 mL), then washed with aqueous $\text{Na}_2\text{S}_2\text{O}_3$ followed by a NaCl saturated solution. The organic phase was dried and concentrated to afford the peracetate glucuronic anhydride as a white solid which was recrystallized in n-hexane; Yield : 80% (5.05 g). This latter (1g) was then dissolved in DCM (25 mL) and octylamine (615 mL; 1.5 eq.) was added dropwise. The mixture was stirred at RT for 15h, and solvent was evaporated, the crude product was purified on silica gel to give the corresponding tetraacetate *N*-octyl- β -D-glucopyranuronamide in 70% yield (822 mg). The deacetylation was carried out in a mixture of 8/1/1 MeOH/ H_2O / NEt_3 for 16h. After evaporation of the solvent, the crude *N*-octyl- β -D-glucopyranuronamide was purified by chromatography and gave the corresponding glucuronamide in 80% yield (417 mg). The overall yield is 45%.

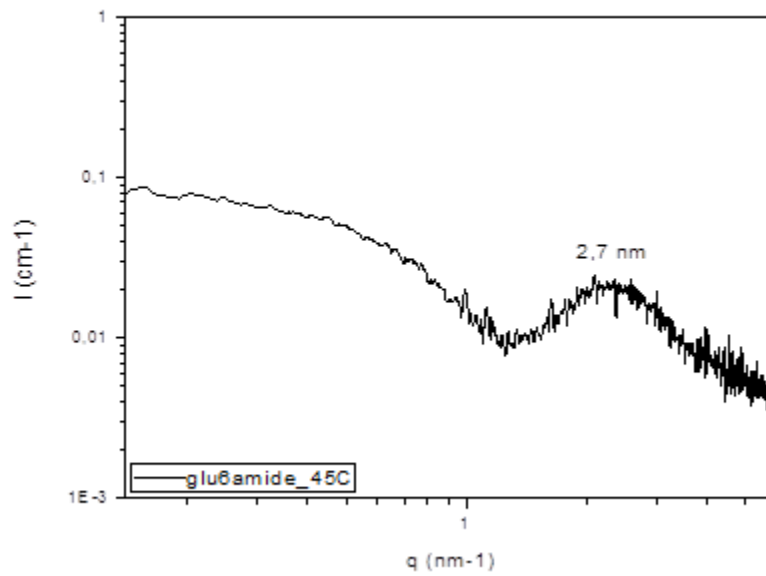
Laurent, P., et al. (2011) reported the synthesis of *N*-octyl- β -D-glucopyranuronamide in 32% yield following the same three successive reactions. The yield reached 40% and 52% when a peptide coupling or an activation of the carboxylic acid with oxalic chloride were used respectively. Amphiphilic properties of *N*-octyl-D-glucuronamide are discussed by Razafindralambo, H., et al. (2011). *N*-octyl-D-glucuronamide is also involved in a patent dealing with the preparation of *N*-Glycosyl derivatives of anthracycline antibiotics Stefanska, B., et al. (1980).

Appendix II

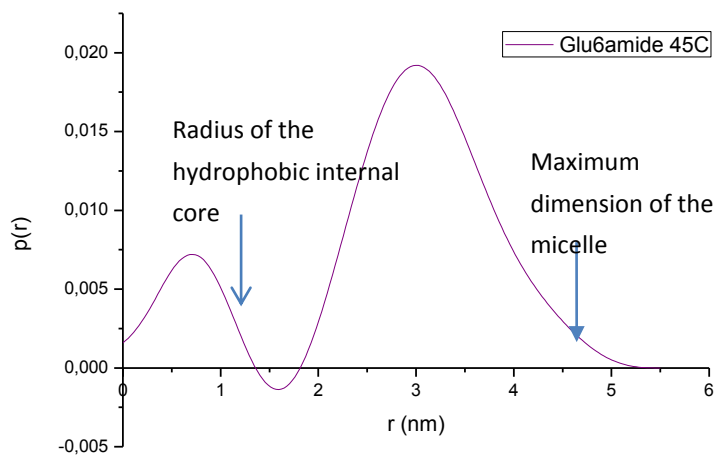
Analysis of the scattering intensities of the Glu6amideC8' samples

(Data provided by the SRSMC Laboratory in the Université de Lorraine)

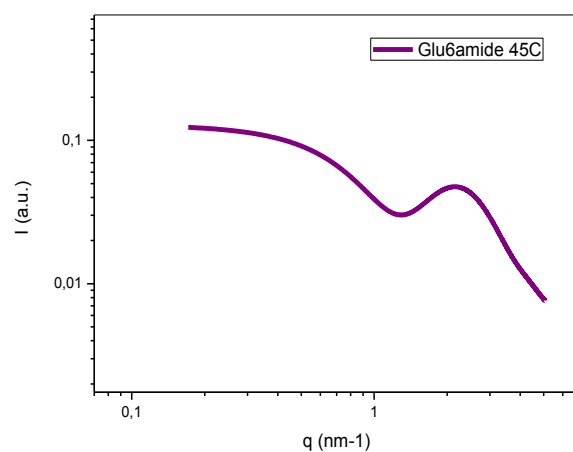
Glu6amideC8



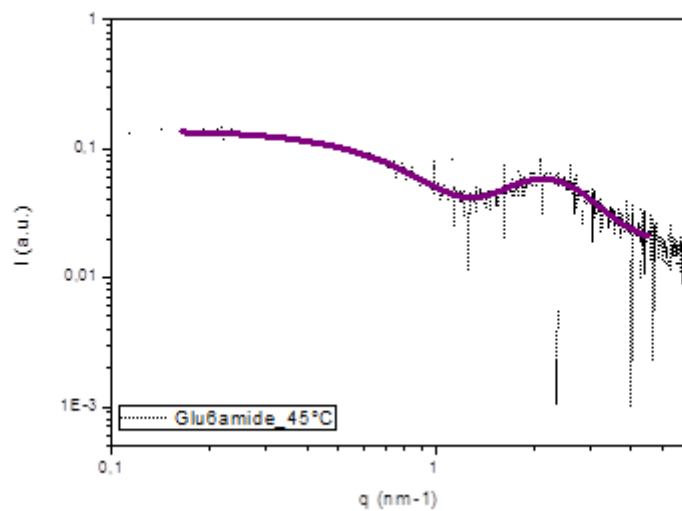
Experimental SAXS spectrum of Glu6amideC8' at 50 g/L concentration in water at $t=45^\circ\text{C}$.



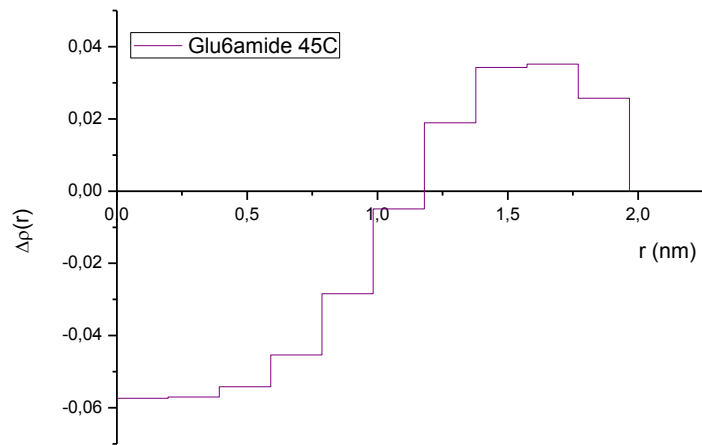
Pair distance distribution function obtained with GIFT analysis.



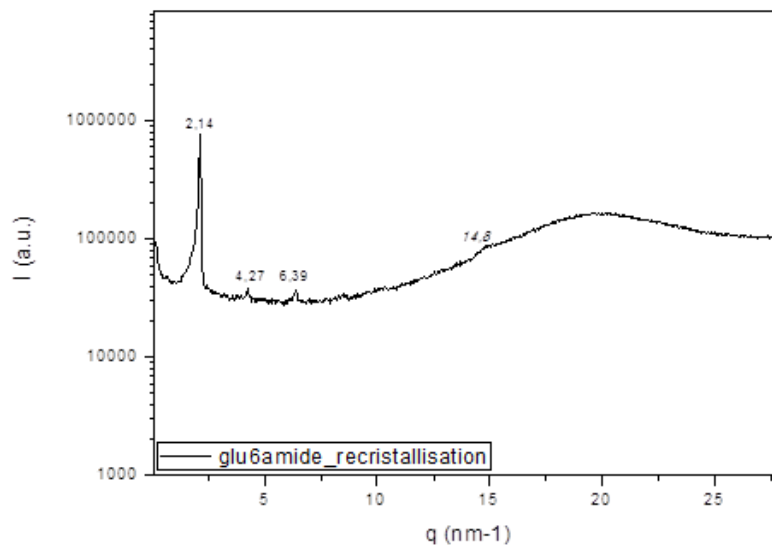
Calculated (GIFT) spectra.



Superposition of experimental and calculated (GIFT) spectra.

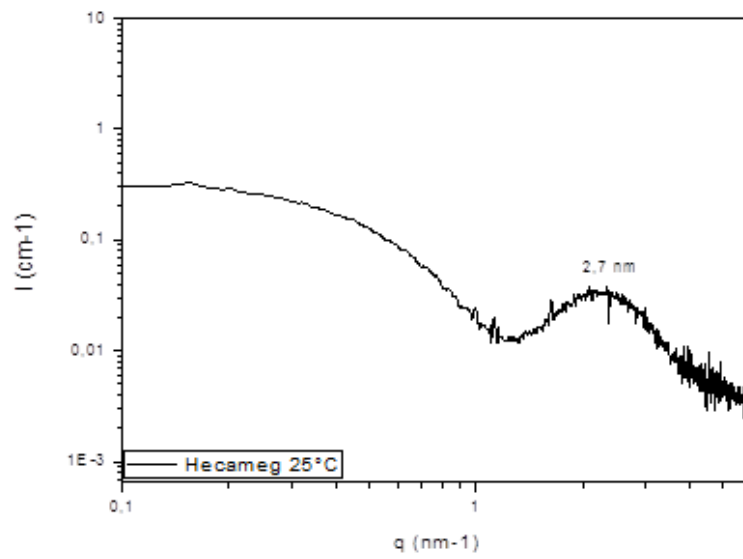


Excess electron density as a function of radial distance.

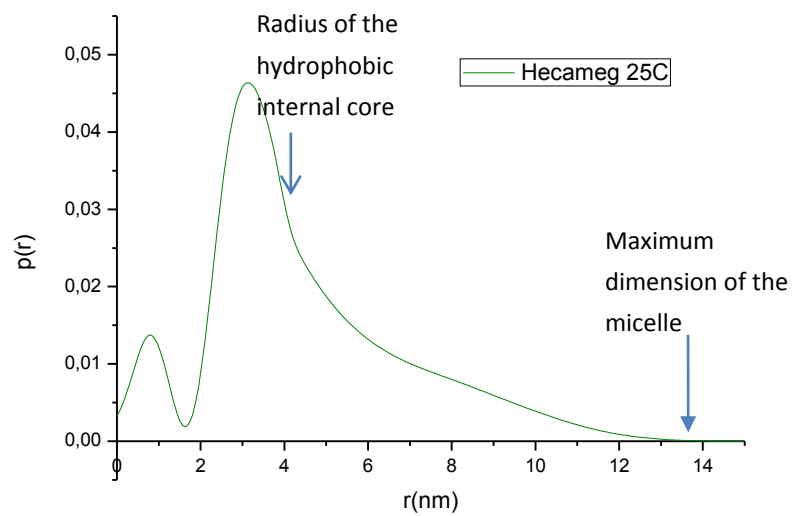


Experimental WAXS/ SAXS spectrum of Glu6amideC8' at a 50 g/L concentration in water at $t=25^\circ\text{C}$.

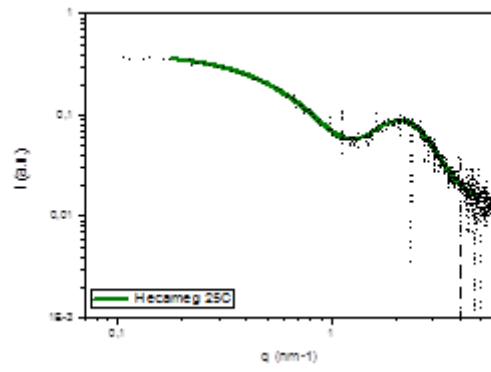
Hecameg



Experimental SAXS spectrum of Hecameg at a 50 g/L concentration in water at $t = 25^\circ\text{C}$.



Pair distance distribution function obtained with GIFT analysis.



Superposition of experimental and calculated (GIFT) spectra.

Appendix III

Publications and communications during the thesis work

Articles in preparation:

Lu Biao, Vayssade Muriel, Miao Yong, Chagnault Vincent, Grand Eric, Wadouachi Anne, Postel Denis, Egles Christophe, Pezron Isabelle. *Physico-chemical properties and cytotoxic effects of sugar-based surfactants: impact of structural variations.*

Lu Biao, Miao Yong, Vayssade Muriel, Pezron Isabelle, Egles Christophe. *Measurement of cytotoxicity and irritancy potential of sugar-based surfactants on skin-related 3D models.*

Oral communication in conference:

Lu Biao, Miao Yong, Chagnault Vincent, Grand Eric, Wadouachi Anne, Postel Denis, Egles Christophe, Pezron Isabelle, Vayssade Muriel. *Evaluation of Cytotoxicity of Biorefinery-derived Amphiphilic Molecules on Multi-scale In-vitro Models.* (15th European Student Solloid Conference. Krakow, POLAND. 8-11 June 2015)

Poster presented in conference:

Lu Biao, Miao Yong, Chagnault Vincent, Wadouachi Anne, Postel Denis, Egles Christophe, Pezron Isabelle, Vayssade Muriel. *Influence of physico-chemical properties of biorefinery derived lipids on their biological effects.* (3rd COSMINNOV. Orléans, FRANCE. 8-9 October 2013)